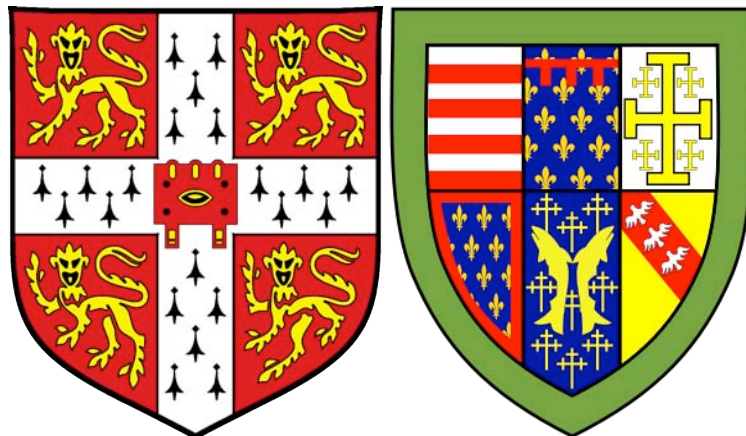


REPROGRAMMING OF T CELLS TO NATURAL KILLER-LIKE CELLS UPON BCL11B DELETION

A Dissertation submitted in fulfilment of the
requirements for the degree of Doctor of Philosophy

By Peng Li



University of Cambridge, Queens' College

The Wellcome Trust Sanger Institute

September 2010

DECLARATION

I hereby declare that this dissertation is the result of my own work and includes nothing which is the outcome of work done in collaboration, except where specially indicated in the text. None of the material presented herein has been submitted previously for the purpose of obtaining another degree. I confirm that this thesis does not exceed 300 single sided pages of double spaced text, or 60,000 words.

Peng Li

For always being there, Dad,

Mum, and Wife

ACKNOWLEDGEMENT

First and foremost, I would like to express my deepest appreciation to my PhD supervisor, Dr Pentao Liu, for his patience and guidance in the projects. It was great to have such an enthusiastic mentor who is always full of creative ideas! I thank him for the challenging projects and the stimulating discussions we had in the lab. I would also like to thank Pentao's lab members, past and present, for their advice, help, and encouragement. Special mention goes to Dr Shannon Burke and Dr Mariaestela Ortiz. Dr Shannon Burke taught me the basis knowledge of immunology, gave me enormous help in experiments, and improved my thesis. In particular, he helped me conduct the killing assays and lymphocyte transfer experiments in this thesis. Dr Mariaestela Ortiz taught me the basic knowledge of haematology and cell cultures and read my thesis. I thank Miss Juexuan Wang for providing a precious Bcl11b reporter mouse used in this thesis. I also thank Dr Song-Choon Lee for instructing me for my molecular biology experiments, Dr Su-Kit Chew, Dr Lia Campos, and Dr Dong Lu for the advice and help they have given me. I thank Yong Yu for taking care of my cells when I wrote my thesis.

Next, I would like to thank the members of the RSF for their excellent technical help in taking care of my mice. I also would like to thank Dr Bee Ling Ng and William Cheng for their help in flow sorting and FACS analysis. Additionally, I thank Dr. David Goulding for taking transmission electronic microscopy images in this thesis.

I was extremely fortunate to have external collaboration with Dr Francesco Colucci and Dr Shannon Burke on natural killer cell studies when they were at Babraham Institute. Their invaluable advice on my project and professional help with my experiments made everything went smoothly. I thank Dr. Xiongfeng Chen from

National Cancer Institute for the microarray analysis in this thesis. I also want to thank Bertie Gottgens and Nicola Wilson from Cambridge Institute for Medical Research for teaching me CHIP assays.

I would love to thank Dr Brian Huntly, my secondary PhD supervisor, who gave me invaluable advice and help on my projects. I also would like to thank my thesis committee, Prof Allan Bradley, Prof Gordon Dougan, and Dr Christine Watson for our valuable meetings and thoughtful suggestions.

Last but not least, I would like to thank my parents Hanguo Li and Yuzhen Liu for their unconditional love and support throughout twenty years of my studies. I would also like to thank my wife, Yao Yao, for her understanding, encouragement, and for always being there to support me in these four years.

REPROGRAMMING OF T CELLS TO NATURAL KILLER-LIKE CELLS UPON BCL11B DELETION

Peng Li

T cells develop in the thymus and play critical roles in immunity. In mice, the transcription factor Bcl11b is required for fetal thymocyte development and for double-positive thymocyte selection. Using a *Bcl11b-tdTomato* knock-in reporter mouse, I found that *Bcl11b* was T-cell-restricted, and was expressed from very early thymocytes to all mature T cells.

To study the functions of Bcl11b in adult T cells, I used a *Bcl11b* conditional knockout mouse strain and demonstrated that Bcl11b was indispensable for early T cell development and for the maintenance of T cell identity. Deletion of Bcl11b caused early T cells to lose their T cell potential and differentiate to natural killer (NK)-like cells in T cell cultures. Similarly, acute loss of Bcl11b in committed and mature T cells resulted in the reprogramming from T cells to induced-T-to-natural killer (ITNK) cells in a cell-autonomous manner. ITNKs derived in vitro and in vivo exhibited many NK cell features, such as expression of NK cell surface markers and lysis of NK tumor targets. In addition, ITNKs derived in vivo were able to prevent the outgrowth of tumour cells in a mouse model.

The gene expression profiles of ITNKs were also similar to that of regular NK cells, and not their parental T cells. ITNKs upregulated NK cell-associated genes while downregulated T cell genes, suggesting that Bcl11b might regulate the T-versus-NK cell fate choice. Furthermore, results from chromatin immunoprecipitation assays confirmed that the canonical Notch signaling directly regulated Bcl11b transcription level.

In summary, I showed that Bcl11b is essential for T cell development and is currently the only known transcription factor critical for the maintenance of T cell identity. Finally, it is believed that human ITNKs may potentially be exploited for therapeutic use in cancer treatments.

LIST OF ABBREVIATIONS

β -gal	β -galactosidase
ACT	Adoptive cell transfer
AGM	Aorta-gonad-mesonephros
AIDS	Acquired immune deficiency syndrome
BAC	Bacteria artificial chromosome
BCA	BioCinchomonic Acid
Bcl	B-cell lymphoma/leukaemia
BCR	B cell receptor
BM	Bone marrow
BSA	Bovine serum albumin
ChIP	Chromatin immunoprecipitation
CKO	Conditional knockout
CLP	Common lymphoid progenitors
CMP	Common myeloid progenitors
COUP-TF	Chicken ovalbumin upstream promoter transcription factor
CRAC	Calcium release-activated Ca^{2+}
CTIP	COUP-TF interacting protein
CTLs	Cytotoxic T lymphocytes
DAG	Diacylglycerol
DMSO	Dimethyl sulfoxide
DN	Double negative ($CD4^{-}CD8^{-}$)
Dox	Doxycyclin
DP	Double positive ($CD4^{+}CD8^{+}$)
dpc	Days post-coitum
eGFP	Enhanced green fluorescent protein
ENU	N-ethyl-N-nitrosourea
ER	Estrogen receptor
ES	Embryonic stem
ETP	Early T cell precursors
FACS	Fluorescent-activated cell sorting
FCS	Fetal calf serum
FDG	Fluorescein di- β -D-galactopyranoside
Flt	Fms-like tyrosine kinase receptor
G-CSF	Granulocyte colony-stimulating factor
GM-CSF	Granulocyte/macrophage colony-stimulating factor
GMP	Granulocyte macrophage progenitors
HD	Huntington's disease
HDAC	Histone deacetylase
HIV	Human immunodeficiency virus
HLA	Human leukocyte antigens
HRP	Horseshoe peroxidase
HSC	Hematopoietic stem cell
IFN	Interferon
IHC	Immunohistochemistry
IL	Interleukin
IRES	Internal ribosome entry site
iPS	Induced pluripotent stem
IP3	Inositol trisphosphate

ISP	Immature single-positive
ITAMs	Immunoreceptor tyrosine-based activation motifs
ITK	Inducible T cell kinase
ITNK	Induced T-to-natural-killer
LAK	Lymphokine-activated killer
LCK	Lymphocyte protein-tyrosine kinase
Lin	Lineage
M-CSF	Macrophage colony-stimulating factor
MEP	Megakaryocyte erythroid progenitors
MHC	Major histocompatibility complex
MTA	Metastasis-associated proteins
NCoR	Nuclear receptor co-repressor
NICD	Notch intracellular domain
NK cells	Natural killer cells
NKP	Natural killer cell precursor
NKT cells	Natural killer T cells
NSC	Neural stem cells
NuRD	Nucleosome remodeling and histone deacetylase
NZB	New Zealand black
OHT	4-hydroxytamoxifen
PAGE	Polyacrylamide gel electrophoresis
PB	PiggyBac
PI	Phosphatidylinositol
PIP2	Phosphatidylinositol 4,5-bisphosphate
PLC γ 1	Phosphorylation of phospholipase C γ 1
polyA	Polyadenylation signal
pre-BCR	pre-B cell receptors
Pre-TCR	Pre-T cell receptors
qRT-PCR	Quantitative real-time reverse transcription PCR
RNAi	RNA interference
RT	Room temperature
SCF	Stem cell factor
SCID	Severe combined immune deficiency
SIRT1	Sirtuin 1
SMRT	Silencing mediator for retinoid and thyroid hormone receptor
SP	Single positive
T-ALL	T-cell adult leukemia/lymphoma
TCR	T cell receptor
tdTomato	Tandem dimmer Tomato
Tet	Tetracycline
TetR	Tet repressor protein
TGF	Transforming growth factor
Th2	T-helper-2
TIL	Tumour-infiltrating lymphocyte
TNF	Tumour necrosis factor
TNKP	T/NK progenitor
TRE	Tetracycline response element
tTA	Tetracycline-controlled transactivator
UTR	Untranslated region
X-gal	5-bromo-4-chloro-3-indolyl- β -D-galactopyranoside

Zap-70
ZFN

Z-chain associated protein kinase
Zinc finger nuclease

TABLE OF CONTENT

Chapter 1	7
INTRODUCTION	7
1.1. Mouse as a genetic tool.....	7
1.1.1. <i>A brief history</i>	7
1.1.2. <i>Genetic manipulation of the mouse genome</i>	7
1.1.3. <i>Using the mouse to study immunity</i>	9
1.2. Conditional knockout (CKO) mice.....	10
1.2.1. <i>CKO technology and its application</i>	10
1.2.2. <i>Inducible Cre systems</i>	12
1.3. Lymphopoiesis.....	13
1.3.1. <i>Haematopoiesis</i>	13
1.3.2. <i>B cell development</i>	14
1.3.3. <i>T cell development</i>	15
1.3.4. <i>TCR signaling</i>	17
1.3.5. <i>NK cell development</i>	18
1.3.6. <i>NKT cell development</i>	19
1.4. Function of Bcl11b	20
1.4.1. <i>Bcl11a</i>	20
1.4.2. <i>Bcl11b in leukemia</i>	21
1.4.3. <i>Bcl11b in early T cell development</i>	22
1.4.4. <i>Bcl11b in mature T cells</i>	23
1.4.5. <i>Bcl11b in other tissues</i>	24
1.4.6. <i>Binding sites of Bcl11b</i>	25

1.5. Thesis projects	26
Chapter 2	28
MATERIAL AND METHODS	28
2.1. Mouse techniques	28
2.1.1. <i>Animal husbandry</i>	28
2.1.2. <i>Tamoxifen administration</i>	29
2.1.3. <i>Intravenous tail vein injection</i>	29
2.2. DNA methods	29
2.2.1. <i>Extraction of DNA from primary cells</i>	29
2.2.2. <i>Extraction of DNA from tissues</i>	30
2.2.3. <i>Genotyping PCR</i>	30
2.2.4. <i>TCR rearrangement PCR</i>	30
2.3. RNA methods	31
2.3.1. <i>Extraction of total RNA from cells</i>	31
2.3.2. <i>First strand cDNA synthesis</i>	32
2.3.3. <i>RT-PCR</i>	32
2.3.4. <i>qRT-PCR</i>	33
2.3.5. <i>Taqman</i>	33
2.3.6. <i>SYBR Green</i>	33
2.4. Protein methods	34
2.4.1. <i>Protein extraction</i>	34
2.4.2. <i>BioCinchomonic Acid (BCA) assay</i>	34
2.4.3. <i>SDS-PAGE</i>	34
2.4.4. <i>Immunoblotting</i>	35
2.4.5. <i>Primary antibody incubation</i>	35

2.4.6. Secondary antibody incubation and detection	35
2.5. Flow cytometry and cell sorting	36
2.5.1. Single cell suspension.....	36
2.5.2. DN thymocytes enrichment.....	36
2.5.3. Staining of cell-surface antigens	37
2.5.4. CD1d stain.....	37
2.5.5. Staining for intracellular antigens	38
2.6. Cell culturing	38
2.6.1. Culture of OP9 and OP9-DL1 stromal cells	38
2.6.2. Culture of T cells	39
2.6.3. Culture of myeloid cells.....	39
2.6.4. Culture of B cells	39
2.6.5. Culture of NK cells	40
2.6.6. Culture of Lymphokine-activated killer (LAK) cells	40
2.6.7. Culture of tumour cell lines.....	40
2.6.8. Activation of unprimed T cells.....	41
2.6.9. OHT treatment in vitro	41
2.7. Gene expression analysis	41
2.8. Chromatin immunoprecipitation.....	41
2.9. Tumour killing assays	42
2.10. Calcium flux	42
Chapter 3.....	43
BCL11B EXPRESSION IN HEMATOPOIETIC LIENAGES	43
3.1. Introduction.....	43
3.1.1. Current knowledge of Bcl11b expression patterns.....	43

3.1.2. Reporter Molecules in Genetically Engineered Mice	43
3.1.3. Purposes of this chapter	44
3.2. Results.....	45
3.2.1. <i>Bcl11b</i> expression in thymocytes.....	45
3.2.2. <i>Bcl11b</i> expression in mature T cells.....	46
3.2.3. <i>Bcl11b</i> expression in other hematopoietic cells.....	47
3.3. Discussion.....	47
3.3.1. <i>Bcl11b</i> is T-cell specific.....	48
3.3.2. Advantages and pitfalls of <i>Bcl11b</i> -tdTomato knock-in mice.....	48
Chapter 4.....	50

BCL11B IS REQUIRED FOR EARLY T CELL

DEVELOPMENT AND MAINTAINANCE OF T CELL IDENTITY

.....	50
4.1. Introduction.....	50
4.1.1. Notch signaling in T cell development	50
4.1.2. Key transcription factors in T cells	51
4.1.3. NK cell-associated genes.....	52
4.1.4. Purposes of this chapter	54
4.2. Results.....	54
4.2.1. <i>Bcl11b</i> transcription regulation in T cells	54
4.2.2. <i>Bcl11b</i> is required for early T cell development	55
4.2.3. <i>Bcl11b</i> is required for committed T cells	57
4.2.4. Reprogramming efficiency from T cells to ITNKs upon <i>Bcl11b</i> ablation	59

4.2.5.	<i>Bcl11b is required in mature T cells</i>	60
4.2.6.	<i>ITNKs detected in Tamoxifen-treated flox/flox mice</i>	61
4.2.7.	<i>Reprogramming from T cells to ITNKs in vivo</i>	63
4.2.8.	<i>Bcl11b is positively regulated by Notch signaling</i>	64
4.3.	Discussion	65
4.3.1.	<i>Deletion of Bcl11b using different Cre systems</i>	66
4.3.2.	<i>Possible factors affecting reprogramming efficiency</i>	67
4.3.3.	<i>“Unconventional NKT cells” in wild type mice</i>	69
4.3.4.	<i>Dynamic balance of ITNKs in vivo</i>	69
Chapter 5		71
CHARACTERIZATION AND APPLICATION OF ITNKs		71
5.1.	Introduction	71
5.1.1.	<i>Cancer immunotherapy</i>	71
5.1.2.	<i>Purposes of this chapter</i>	73
5.2.	Results	73
5.2.1.	<i>Gene expression profile in ITNKs</i>	73
5.2.2.	<i>Characterization of ITNKs derived in vitro</i>	75
5.2.3.	<i>Characterization of ITNKs derived in vivo</i>	76
5.2.4.	<i>Killing ability of ITNK derived in vitro</i>	78
5.2.5.	<i>Killing ability of ITNK derived in vivo</i>	78
5.2.6.	<i>ITNKs prevent tumour expansion in vivo</i>	79
5.3.	Discussion	80
5.3.1.	<i>Potential targets of Bcl11b</i>	80
5.3.2.	<i>Differences between ITNKs derived in vitro and in vivo</i>	81
5.3.3.	<i>Application of ITNKs for tumor killing</i>	82

Chapter 6	84
GENERAL DISCUSSION	84
6.1. Summary	84
6.1.1. <i>Bcl11b</i> expression in T cells.....	84
6.1.2. <i>Bcl11b</i> functions in early T cells	85
6.1.3. <i>Bcl11b</i> functions in committed and mature T cells	86
6.1.4. <i>Bcl11b</i> transcription regulatory networks	88
6.1.5. Potentials of ITNKs in immunotherapy	89
6.2. Significance	89
6.2.1. Novel roles of <i>Bcl11b</i> in the maintenance of T cell identity.....	89
6.2.2. Clinical potential of ITNKs	90
6.3. Future experiments	90
6.3.1. Upstream genes of <i>Bcl11b</i>	91
6.3.2. Downstream genes of <i>Bcl11b</i>	93
6.3.3. Overexpression of <i>Bcl11b</i> in ITNKs and NK cells	94
6.3.4. Reprogramming human T cells to ITNKs.....	94
6.3.5. Testing the tumor-killing ability of human ITNKs.....	95
6.4. Conclusions.....	96
REFERENCES	97

Chapter 1

INTRODUCTION

1.1. *Mouse as a genetic tool*

1.1.1. *A brief history*

Lab mice are invaluable tools in modern biomedical research. Compared to other mammals, the mouse is currently the most commonly used mammalian model organism because of its short generation time, small size and prolificacy in breeding. As a pioneer mouse geneticist, William Ernest Castle carried out the first systematic analysis of Mendelian inheritance and genetic variation in mice (Snell and Reed, 1993). Another important milestone for the study of the mouse is the establishment of inbred mouse strains. A pure genetic background improves the reproducibility of experiments using different individuals from the same mouse strain because they are genetically identical. Currently, all the common inbred strains in the labs have been inbred for at least 80 generations since their original isolation; thus the genomes of all siblings are essentially identical (Silver, 1985). The inbred mouse strains provide invaluable platforms for studying the immune system and modeling human immune disease.

1.1.2. *Genetic manipulation of the mouse genome*

The biggest advantage of using the mouse to study the immune system and to model human disease is the availability of a range of genetic technologies. In 1981, several groups produced transgenic mice by injecting transgenic DNA into mouse

pronuclei (Brinster et al., 1981; Wagner et al., 1981a; Wagner et al., 1981b). DNA introduced into the mouse genome by this method results in stable integration of the transgene into the germline. This technology offers scientists opportunities to perform gain-of-function studies for specific genes in the mouse model. However, there are drawbacks in this technology. Firstly, the injected transgene usually inserts randomly into mouse genome, raising the possibility of disrupting other genes nearby. Secondly, because the nature of this technology is to overexpress injected DNA, it is not suitable to silence a particular gene for loss-of-function studies, which are the gold standard methods for studying gene function, although overexpression of dominant negative forms of some genes can sometimes achieve this purpose. In addition, the copy number of the transgene that integrates into the mouse genome varies, so it is difficult to control the expression level of the transgene (Hickman-Davis and Davis, 2006). Finally, except bacterial artificial chromosome (BAC) transgenes (Antoch et al., 1997), introduced transgenes usually are not large enough to contain all of the *cis*-acting elements that are required for fully regulated expression (Kleinjan and van Heyningen, 2005).

In 1981, pluripotent mouse embryonic stem cells (ES) were isolated from the inner cell mass of 3.5 days post-coitum (dpc) wild type mouse embryos (Evans and Kaufman, 1981; Martin, 1981). Later, it was demonstrated that these ES cells were able to contribute to the germline in chimera mice derived from ES cells, even after genome modification by retrovirus (Bradley et al., 1984; Robertson et al., 1986). Precise manipulation of the mouse genome was achieved by demonstrating that homologous recombination works efficiently in mouse ES cells (Capecchi, 1989; Koller and Smithies, 1989; Smithies et al., 1985; Thomas and Capecchi, 1986). Thus a combination of mouse ES cell manipulation and homologous recombination

technologies gave birth to ‘gene targeting’ and revolutionized mouse genetics. In the near future, it is feasible that all mouse genes will be inactivated individually and phenotypes can be studied in these knockout mice (Guan et al., 2010). These mutant mouse resources will likely shift the current biomedical research paradigm such that comprehensive analyses of genes in many biological processes, including immunity, can be performed.

1.1.3. Using the mouse to study immunity

Because of the similarity between human and the mouse genomes and their development and physiology, the mouse has been instrumental in elucidating key processes in the immune system and revealing molecular mechanisms of immune diseases (Lander et al., 2001; Venter et al., 2001; Waterston et al., 2002). In 1948, George D. Snell began defining and naming the H2 haplotypes, using inbred mouse strain such as DBP/2 and C57BL (Gorer, 1948; Snell, 1951). Later, Marianne and her colleagues derived an inbred mouse strain with spontaneous autoimmune haemolytic anemia and termed it as New Zealand black (NZB) (M. Bielschowsky, 1959). Mice from this strain died with hepatosplenomegaly and jaundice that were seen in human autoimmune haemolytic anemia (Casey, 1966). We learnt precious lessons about the development of the immune system from strains such as *nude*, *scid* (severe combined immune deficiency) and *lpr* with spontaneous mutations, besides NZB (Mak et al., 2001). To accelerate the mutation rate and increase the mutation spectrum, Russell and colleagues at Oak Ridge Laboratories introduced the ethylating chemical N-ethyl-N-nitrosourea (ENU) to produce spontaneous genetic mutations in mouse strains (Russell et al., 1979). These ENU-induced genetic mutant strains were used to reveal many genes regulating the immune system (Nelms and Goodnow, 2001). A drawback with this approach is that it is usually difficult to identify the mutations

causing the defects in these strains because the mutations are random and the mouse genome was, until recently, complicated to sequence. However, this problem will be solved in the future due to the development of next generation sequencing technology (Mardis, 2008).

Thanks to the advent of genetically engineered ‘knockout’ mice, targeted mutations have been introduced to many loci to study functions of these genes in the immunity. In 1990, Smithies’ and Jaenisch’s groups independently generated $\beta 2$ -microglobulin knockout mice in which expression of major histocompatibility complex (MHC) class I molecules was abolished. The mutant mice developed normally but had severely reduced numbers of $CD8^+$ cytotoxic T lymphocytes (CTLs), indicating that MHC class I molecules are required for the selection of MHC-class-I-restricted $CD8^+$ T cells and for antigen recognition by these cells, but not necessary for T cell development (Koller et al., 1990; Zijlstra et al., 1990). In 1991, mice deficient for the T-cell co-receptor, CD8, were generated in Mak’s lab. This study demonstrated that CD8 is essential for the development of $CD8^+$ CTLs but not $CD4^+$ helper T cells (Fung-Leung et al., 1991). Moreover, mice that lack the heavy chain of IgM (μ chain) do not have B cells, showing the importance of this gene and B cell receptor (BCR) for B cell development (Kitamura et al., 1991).

1.2. Conditional knockout (CKO) mice

1.2.1. CKO technology and its application

Analysis of knockout mouse strains has provided fundamental insights into functions of the mouse genome. However, knockout lines of certain genes die *in utero* due to the important roles of these genes in embryos. Consequently, functions of these genes in adult mice cannot be investigated. To overcome this limitation, CKO

approaches have been developed to overcome the embryonic lethality problem and to investigate gene function temporally and spatially using the Cre-loxP system, special type of site-specific recombination (Betz et al., 1996; Glaser et al., 2005; Rajewsky et al., 1996). For example, germline deletion of tumour-suppressor genes *Brcal* and *Pten* leads to early embryonic lethality, the functions of which in T cells could only be demonstrated in CKO strains (Mak et al., 2000; Suzuki et al., 2001). Similarly, *Notch1* and *Gata3* were ablated in adult CKO mice, where T cell development was arrested in early stages, demonstrating the importance of these two genes for T cell development (Pai et al., 2003; Radtke et al., 1999). This could not have been possible in germline knockout mouse strains since *Notch1*- and *Gata3*-deficient mice die at embryonic stages.

Due to the significant differences between the mouse and human genomes, especially in the MHC, it is important to develop mouse models of human disease by replacing large segments of the mouse genome with the wild-type or mutant syntenic region of the human DNA sequence (Wallace et al., 2007). To this end, the Cre-loxP site-specific recombination system has also been used to engineer chromosome segments in mouse to produce humanized mice. For example, the humanized mouse strain where the mouse α globin locus has been replaced with human sequence encoding a mutated α globin locus recapitulates α thalassemia more accurately than the corresponding knock-in mutation in the mouse gene (Wallace et al., 2007).

The procedure for generating CKO mice is essentially the same regardless of the specific targeting strategy (Chan et al., 2007) (Fig. 1.1). Briefly, targeting vectors that contain DNA fragments homologous to the target locus, loxP sites and selectable markers, such as antibiotics resistant genes, are generated in *E. coli* at first. Subsequently, these vectors are transfected into mouse ES cells for homologous

recombination. After drug selection and PCR confirmation, correctly targeted ES cell colonies are identified by either Southern blot analysis or long-range PCR genotyping. These ES cells are expanded and injected into 3.5 dpc blastocysts, which are then re-implanted into the uteri of pseudopregnant surrogate females. Chimeras are subsequently selected from the resulting pups and mated with wild-type mice to check for germ-line transmission of the targeted allele in the F1 offspring. From the F1 offspring, both male and female heterozygotes are selected and mated to produce homozygotes, which are subsequently crossed to different Cre-expressing transgenic mice for temporal and spatial gene deletion. Depending on the nature of the promoter that drives Cre recombinase expression, deletion of targeted gene can occur in specific cells/tissue or in all cells, or at a specific developmental stage (Nagy, 2000).

1.2.2. Inducible Cre systems

It is critical to choose a well-characterized Cre transgenic line that allows the Cre-mediated excision of targeted genes. Consequently, promoters that are used to drive Cre expression need to be carefully validated for its expression levels and specificity to fulfill research purposes (Nagy, 2000). An important improvement to Cre transgenic technology was the development of inducible Cre systems that permit the control of Cre activation, thus allowing temporal deletion of the targeted genes. Currently, there are two widely used inducible Cre systems. One is the tetracycline (Tet)-dependent regulatory system (Tet-off or Tet-on) (Gossen and Bujard, 1992). In the Tet-off system, the tetracycline-controlled transactivator (tTA), a fusion protein binds to the tetracycline response element (TRE) and activates transcription of the target gene, in the absence of the inducer, doxycyclin (Dox) (Takahashi et al., 1986). In contrast, a reverse version of the Tet repressor protein (TetR) known as rtTA binds

the TRE and activates transcription of the target gene only in the presence of Dox in the Tet-on system (Triezenberg et al., 1988).

The other inducible Cre system is the Cre-ERT system, in which the chemical compounds, Tamoxifen (TAM) or its derivative 4-hydroxytamoxifen (OHT) are used to induce Cre expression (Metzger and Chambon, 2001). In the Cre-ERT system, the Cre recombinase is fused to a mutant form of ligand-binding domain of the human estrogen receptor (ER). Once this fusion protein binds to TAM or OHT, but not endogenous estrogen or progesterone, it translocates from cytoplasm to nucleus, activating Cre (Metzger and Chambon, 2001). This Cre-ERT system is widely used in immunology research. For example, using the Cre-ERT system, *Myc* (c-Myc) was also selectively deleted in B cells. The proliferation in response to anti-CD40 plus IL-4 in these *Myc*-deficient B cells was severely impaired, demonstrating the important function of *Myc* in proliferation and apoptosis in mature B cells (de Alboran et al., 2001). However, the induction of Cre expression by Tamoxifen or OHT is not efficient in some tissues such as the brain (Brocard et al., 1997). In this thesis, the Cre-ERT system was used to induce deletion of *Bcl11b* in T cells.

1.3. Lymphopoiesis

1.3.1. Haematopoiesis

Haematopoiesis is the production of blood cellular components, in which hematopoietic cells, including the red blood cells, platelets and white blood cells, are derived from the hematopoietic stem cells (HSCs) (Harrison, 1976). In the mouse, definitive haematopoiesis occurs at 8.0 days postconception (dpc 8) in the yolk sac blood islands, followed by the aorta-gonad-mesonephros (AGM) region, and then migrates to the fetal liver in the mouse embryos (Godin et al., 1995). After birth, the

place of haematopoiesis changes from the fetal liver to the bone marrow (BM), where a specialized microenvironment, the endosteal niche, forms to support haematopoiesis (Godin and Cumano, 2002).

HSCs are composed of long-term HSCs that self-renew for the life of the host, and short-term HSCs that retain self-renewal capacity for approximately 8 weeks (Morrison and Weissman, 1994). Short-term HSCs proliferate and differentiate into multipotent progenitors (MPP): common myeloid progenitors (CMP) and common lymphoid progenitors (CLP). CMP, the progenitors for the myeloerythroid lineages, give rise to granulocyte macrophage progenitors (GMPs) and megakaryocyte erythroid progenitors (MEPs) (Akashi et al., 1999) (Fig. 1.2). GMPs can differentiate towards neutrophils, monocytes, macrophages, eosinophils, basophils, and mast cells, while MEPs generate megakaryocytes and erythrocytes (Iwasaki and Akashi, 2007). In contrast, CLPs are restricted to give rise to T cells, B cells, natural killer (NK) cells, and some dendritic cells, though recent studies suggest that some progenitors derived from CLPs retain myeloid potentials (Bell and Bhandoola, 2008; Kondo et al., 1997; Manz et al., 2001; Wada et al., 2008). However, cell fate can be changed by overexpression or ablation of certain transcription factors in hematopoietic lineages (Graf and Enver, 2009).

1.3.2. B cell development

In the 1950s, the lymphocyte was identified as the cell responsible for both cellular and humoral immunity. Lymphocytes are mainly composed of B cells, T cells and NK cells. B cells and T cells are two arms of the adaptive immune system, which recognizes and has memory for specific pathogens, and subsequently mounts strong attacks each time the pathogen is encountered. B cells produce antibodies against antigens and perform the role of antigen-presenting cells.

In the fetal liver and the bone marrow, CLPs differentiate to B cells under regulation of external cytokines such as Fms-like tyrosine kinase receptor-3 (Flt-3) ligand and Interleukin-7 (IL-7) and endogenous transcription factors including E2A, Ebf1, Bcl11a, and Pax5 (Busslinger, 2004; Liu et al., 2003; Northrup and Allman, 2008). B220 and CD43 are chiefly used to identify pre-pro B cells, the earliest B cell lineage restricted progenitors, although B220 is also expressed in some NK cells (Hardy and Hayakawa, 2001). No, or very few, B220⁺CD43⁺ pre-pro B cells are detected in E2A, EBF1 or Bcl11a mutant mice (Bain et al., 1994; Lin and Grosschedl, 1995; Liu et al., 2003; Zhuang et al., 1994). B cell precursors commit to the B cell lineage by acquiring expression of *Pax5*, which drives CD19 expression in pro-B cells (Busslinger, 2004). Indeed B cell development is arrested at an early pro-B cells stage in *Pax5*-deficient mice (Urbanek et al., 1994). Furthermore, acute loss of Pax5 in pro-B cells causes B cells to lose B cell identity and reprogram to T cells (Mikkola et al., 2002; Rolink et al., 1999). Pro-B cells differentiate to pre-B cells when they start to express pre-B cell receptors (pre-BCR), which enables BCR signaling (Karasuyama et al., 1990; Karasuyama et al., 1993). Pre-B cells finally become mature B cells after they pass the BCR checkpoints (Hardy and Hayakawa, 2001) (Fig. 1.3).

1.3.3. T cell development

T cells were identified as a population of lymphocytes that are derived from the thymus and mediate cellular immunity by Glick (Glick, 1979). T cells recognize antigen peptides that are bound to MHC molecules via their T cell receptors. There are two main subpopulations of T cells: CD4⁺ helper T and CD8⁺ cytotoxic T cells. CD4⁺ T cells recognize MHC II molecule complexes and secrete various cytokines after being activated. Conversely, CD8⁺ T cells recognize MHC class I molecules and exhibit cell-killing activity after activation. AIDS provides a vivid and tragic

illustration of the importance of T cells in immunity. The human immunodeficiency virus (HIV), the causative agent of AIDS, binds to the CD4 molecules. And this infection causes depletion of CD4⁺ T cells in Acquired immune deficiency syndrome (AIDS) patients. Without CD4⁺ T cells, AIDS patients become hypersusceptible to pathogens that inhabit in tissues without much harming, and die of the opportunistic infections (Trono et al., 2010).

T cell development, which happens in the thymus, involves progenitor homing and lineage specification and commitment (Ciofani and Zuniga-Pflucker, 2007; Rothenberg et al., 2008). It also requires the intrathymic microenvironment and interactions among key transcription factors (Anderson et al., 2006; Ciofani and Zuniga-Pflucker, 2007; Rothenberg et al., 2008). In adult mice, CLPs migrate from the bone marrow to the thymus and initiate the program of T cell differentiation (Adolfsson et al., 2005; Yoshida et al., 2006). Progenitors in the thymus lack the T cell receptor (TCR) co-receptors CD4 and CD8, and are therefore referred as double negative (DN) cells (Anderson et al., 1996). The DN population can be further subdivided by the cell surface markers CD117 (c-Kit), CD44, and CD25 (Godfrey et al., 1993). The CD117⁺DN1 (CD44⁺CD25⁻) subsets, also known as early T cell precursors (ETP), are thought to contain multipotent progenitors (Allman et al., 2003; Bell and Bhandoola, 2008; Ikawa et al., 1999; Michie et al., 2000; Wada et al., 2008). T cell specification happens during the transition from ETP to DN2 (CD44⁺CD25⁺) with up-regulation of some key T cell genes, such as *Bcl11b*, *Tcf12* (HEBAIt), *Gata3* and *Notch1*, although NK and myeloid potentials still persist in DN2 cells (Bell and Bhandoola, 2008; Wada et al., 2008) (Taghon et al., 2006; Taghon et al., 2005; Yui and Rothenberg, 2004). ETPs and DN2 thymocytes initiate TCR gene rearrangements, however, they do not exhibit full V(D)J rearrangements or express

any TCR β or TCR $\gamma\delta$ on their cell surface, which are symbols of committed T cells. The non-T cell potentials are lost in the DN3 (CD44⁻CD25⁺) thymocytes. Some DN3 T cells successfully rearrange TCR γ - and δ -chains instead of β -chain and differentiate into $\gamma\delta$ -T cells. The majority of T cells at DN3 stage commit to the $\alpha\beta$ -T cell lineage by further upregulating key T cell genes and shutting down expression of genes that are important for non-T cell lineages (Rothenberg et al., 2008). DN4 (CD44⁻CD25⁻) thymocytes have undergone β -selection after successful TCR β gene rearrangement (Dudley et al., 1994) and have already initiated the process of differentiating to the CD4⁺CD8⁺ double positive (DP) stage (Nikolic-Zugic and Moore, 1989; Petrie et al., 1990). Positive selection of the developing T-cell receptor repertoire occurs in the thymic cortex, whereas events in the medulla purge the system of self-reactive cells. Thymic epithelial-cell microenvironments are crucial for production of T cells and their selection and maintenance during immune responses (Anderson et al., 2006). After positive and negative selection processes, surviving thymocytes migrate to the peripheral lymphoid tissues where the cytokine IL-7 and the constant interaction of T cells with self-peptide MHC play a critical role in T cell maintenance (Takada and Jameson, 2009) (Fig. 1.4).

1.3.4. TCR signaling

TCR is expressed in T cells and is responsible for recognizing antigens bound to MHC molecules. Upon stimulation by antigens, TCR signaling is activated, promoting a number of signaling cascades that ultimately determine cell fate through the regulation of cytokine production, cell survival, proliferation, and differentiation (Marsland and Kopf, 2008). At the beginning of TCR activation, lymphocyte protein-tyrosine kinase (LCK) modulates the phosphorylation of immunoreceptor tyrosine-based activation motifs (ITAMs) on the cytosolic side of the TCR/CD3 complex. ζ -

chain associated protein kinase (Zap-70) is next recruited to the TCR/CD3 complex and becomes activated. Following activation of Zap-70, its downstream scaffold proteins, including SLP-76, are recruited and phosphorylated. Phosphorylation of SLP-76 promotes recruitment of Vav, the adaptor proteins NCK and GADS, and an inducible T cell kinase (ITK) (Qi and August, 2007). ITK then modulate the phosphorylation of phospholipase C γ 1 (PLC γ 1), leading the hydrolysis of phosphatidylinositol 4,5-bisphosphate (PIP2) to produce the second messengers diacylglycerol (DAG) and inositol trisphosphate (IP3) (Burbach et al., 2007). IP3 triggers the release of Ca $^{2+}$ from endoplasmic reticulum, resulting in the entry of extracellular Ca $^{2+}$ into cells through calcium release-activated Ca $^{2+}$ (CRAC) channels (Cronin and Penninger, 2007). Thus calcium flux assays are commonly used to measure TCR activation.

1.3.5. NK cell development

The NK cell was first discovered by Rolf Kiessling in the 1970s, when he found a small population of large granular lymphocytes display cytotoxic activity against a wide range of tumor cells in the absence of any previous immunization with the tumor (Herberman et al., 1975; Kiessling et al., 1975). This population of cells were named "natural killer" because of the initial notion that they did not require prior activation to kill cells. It was later shown that NK cells preferably targeted cells, which expressed low levels of MHC class I molecules, a concept termed as "missing-self" recognition (Kiessling et al., 1978; Kiessling et al., 1976; Oldham, 1983). NK cells constitute an essential component of the innate immune system, which, unlike the adaptive immune system, recognizes and responds to pathogens without requiring prior priming through clonal antigen receptors. Mice with deficiencies in NK stimulatory immunoreceptors such as NKG2D and DNAM-1 are defective in tumor

surveillance in models of spontaneous malignancy (Guerra et al., 2008; Iguchi-Manaka et al., 2008).

NK cell development occurs mainly in BM, although a bipotent T/NK progenitor (TNKPs) containing T- and NK-cell potentials has been identified in mouse fetal liver and fetal thymus (Michie et al., 2000). In BM, CLPs commits to natural killer cell precursors (NKPs), which are defined as Lin⁻ (lineage)CD122⁺NK1.1⁻DX5⁻ (Di Santo and Vosshenrich, 2006). Upon CD122 expression, NKPs lose B-, T- or myeloid-cell potentials and respond to IL-15 stimulation, which promotes NK cell development (Puzanov et al., 1996). Then, NKPs further differentiate into immature NK cells that express NK1.1 in bone marrow and liver (Kim et al., 2002; Takeda et al., 2005). CD94 (KLRD), a membrane protein, covalently associates with five different members of the NKG2 family, except NKG2D (Borrego et al., 2006; Chang et al., 1995). **By acquiring expression of inhibitory NK-cell receptors including members of the Ly49 and CD94-NKG2 family, immature NK cells start to obtain NK-cell self-tolerance. and become mature NK cells that are positively stained for DX5 and CD11b.** Mature NK cells shape their weapons by producing FasL, Trail, Interferon- γ (IFN- γ), perforin and granzymes and circulate in the body as defenders through homeostasis (Colucci et al., 2003). Recently, a small population of NK cells that originate in the thymus was identified. These thymic NK cells express both GATA3 and CD127 (IL-7R α) and have compromised cytotoxicity but considerable cytokine production (Vosshenrich et al., 2006).

1.3.6. NKT cell development

Natural killer T (NKT) cells are a subset of T cells that share some features with NK cells. The majority of NKT cells are defined as CD1d-restricted T cells that

express an invariant TCR combined with a limited, but not invariant, TCR β -chain repertoire (Godfrey et al., 2004). Different subsets of NKT cells have different functions in regulating immune responses. For example, NK1.1⁻ NKT cells produce large amounts of IL-4 and little IFN- γ , while NK1.1⁺ NKT cells produce less IL-4 and more IFN- γ (Benlagha et al., 2002; Pellicci et al., 2002). NKT cells arise in the thymus from a population of DP thymocytes that express a TCR which binds to CD1d plus self-lipid or glycolipid antigen (Bendelac, 1995). CD24, CD44 and NK1.1 are used to define NKT cells at different developmental stages (Benlagha et al., 2005). The earliest NKT cell precursors (CD24⁺CD44^{lo}NK1.1^{lo}) differentiate to highly proliferative NKT progenitors, in which CD24 is later downregulated. These NKT progenitors subsequently expand the NKT cell pool and further differentiate to CD24^{lo}CD44^{hi}NK1.1^{lo} population. Then, this population upregulates NK cell surface markers, such as NK1.1, and become potent producers of IFN- γ (Gadue and Stein, 2002).

1.4. Function of *Bcl11b*

1.4.1. *Bcl11a*

The B-cell lymphoma/leukemia 11 (*Bcl11*) family has two members, *Bcl11a* and *Bcl11b*, both being Kruppel-like C2H2 type zinc finger transcription factors (Satterwhite et al., 2001). *Bcl11a* was first discovered as a retroviral insertion site (*Evi9*) in myeloid leukemia tumours in the BXH-2 mouse (Nakamura et al., 1996) (Nakamura et al., 2000). *Evi9* was later re-named as *Bcl11a* since it was found ectopically expressed in some B cell lymphomas caused by chromosomal translocations (Satterwhite et al., 2001). *Bcl11a* is required for normal lymphoid development. Germline deletion of *Bcl11a* causes neonatal lethality and an absence of

B cells at the earliest B cell development stages (Liu et al., 2003). *Bcl11a* is also expressed in early T cell progenitors and is also important for T cell development (Li et al., 2010) (Tydell et al., 2007). Recipient mice of *Bcl11a*-deficient fetal liver cells develop T cell leukemia (Liu et al., 2003). Recent genome-wide association studies in human have revealed association of the *BCL11A* locus with persistent fetal hemoglobin in the adult (Menzel et al., 2007) (Uda et al., 2008). In the subsequent validation assays, knocking down BCL11A in human primary adult erythroid cells indeed leads to robust HbF expression (Sankaran et al., 2008). Further characterization of *Bcl11a* mutant mice also uncovers the key role of *Bcl11a* in the fetal to adult expression switch of hemoglobin (Sankaran et al., 2008); (Sankaran et al., 2009).

1.4.2. *Bcl11b* in leukemia

Bcl11b is the other member of the *Bcl11* family in the mouse and human genomes. The *Bcl11b* was initially identified as a tumour suppressor gene in T cells was thus named *Rit1* (*radiation-induced tumor suppressor gene 1*) because homozygous deletions and point mutations were located to this locus in a genome-wide allelic loss analysis of γ -ray induced mouse thymic lymphomas (Wakabayashi et al., 2003a) (Matsumoto et al., 1998) (Shinbo et al., 1999).

BCL11B is also found to be involved in human T cell leukemia. A specific cryptic translocation, t(5;14)(q35.1;32.2), present in about one fifth of T-cell adult leukemia/lymphoma (T-ALL) patients, serves to activate expression of HOX11L2 by juxtaposition with strong T cell enhancer elements at the 3' of the BCL11B locus (Bernard et al., 2001; MacLeod et al., 2003; Nagel et al., 2003). Additionally, a novel chromosomal aberration, inv(14)(q11.2q32.31) was reported in T-ALL samples. In this inversion, the 5' part of BCL11B, including exons 1-3, was joined to the TRDD3

segment of the TCR δ locus. Consequently, in-frame transcripts with truncated BCL11B and TCR δ constant region were highly expressed in screened T-ALLs but not in normal T cells (Przybylski et al., 2005). Interestingly, though *BCL11B* is considered as a tumour suppressor gene, it is highly expressed in many human T cell tumour lines and is required for their survival. Suppression of *BCL11B* by RNA interference (RNAi) causes apoptosis of these tumour cells, possibly due to a decrease of a cell-cycle inhibitor, p27, and an anti-apoptotic protein, BCL-xL. This indicates involvement of the mitochondrial apoptotic pathway. In contrast, normal mature T cells remained unaffected within the experimental time period (Grabarczyk et al., 2007; Kamimura et al., 2007a) (Karanam et al., 2010). Therefore, BCL11B could be an attractive therapeutic RNAi target in T-cell malignancies.

1.4.3. *Bcl11b* in early T cell development

Due to the involvement of Bcl11b in mouse thymic lymphoma development (Wakabayashi et al., 2003a), the Bcl11b germline knockout mouse strain was generated in 2003. Loss-of-function studies on Bcl11b in the mouse demonstrated that Bcl11b is required for early T cell development and the survival of T cells. The fact that Bcl11b homozygous mutant knockout mice die in the first few days after birth is likely due to neurological or other uncharacterized defects (Arlotta et al., 2005; Wakabayashi et al., 2003b) (Arlotta et al., 2008). In this *Bcl11b*-deficient strain, T cell development is blocked at the DN2-DN3 stage without obvious defects in other hematopoietic lineages (Wakabayashi et al., 2003b). In *Bcl11b*-deficient thymocytes, V β to D β rearrangements is impaired and contribute the lack of expression of pre-T cell receptors (pre-TCR) complex, which, in turn, leads to the profound apoptosis in the thymocytes. Apoptosis is unlikely to be the main reason for the failure of T cell development upon loss of Bcl11b, because inactivation of p53 in mutant thymocytes

is not sufficient to fully restore the T cell development, even though some immature single-positive (ISP) T cells are indeed detected in *Bcl11b*^{-/-}*p53*^{-/-} embryos (Okazuka et al., 2005). The exact cause of T cell defects in *Bcl11b*-deficient mice thus remained unresolved.

Interestingly, *Bcl11b* haploinsufficiency was demonstrated in thymocyte development. Heterozygous *Bcl11b* mutant mice have fewer thymocytes compared to wild type mice. And these *Bcl11b*^{+/-} thymocytes are much more prone to lymphomagenesis (Kamimura et al., 2007b). Moreover, in γ -irradiated mice, loss of one copy of *Bcl11b* is proposed to promote clonal expansion and differentiation arrest of thymocytes (Go et al., 2010). Nevertheless, it was puzzling that no tumour development has ever been reported in mice transplanted with *Bcl11b* homozygous knockout progenitors from fetal live.

1.4.4. *Bcl11b* in mature T cells

Bcl11b plays a critical role in DP thymocytes by controlling positive selection of both CD4 and CD8 lineages. *Bcl11b*-deficient DP thymocytes are prone to spontaneous apoptosis, possibly due to impaired proximal TCR signaling and attenuated extracellular signal-regulated kinase phosphorylation and calcium flux that are required for initiation of positive selection (Albu et al., 2007). Recently, it was reported that *Bcl11b* represses a gene expression program associated with mature CD4⁺ and CD8⁺ thymocytes, including *Zbtb7b* (Th-POK) and *Runx3* that are important for the development of mature CD4⁺ and CD8⁺ T cells, respectively (Dave et al., 1998; Kastner et al., 2010; Taniuchi et al., 2002). In human CD4⁺ T cells, following activation through TCR, BCL11B promotes *IL2* expression by binding and activating the *IL2* promoter through the US1 site and by enhancing NFKB1 (NF- κ B) activity (Cismasiu et al., 2009; Cismasiu et al., 2006). Downregulation of endogenous

BCL11B reduces the level of expression of IL-2, while overexpression of BCL11B augments IL-2 expression (Cismasiu et al., 2006). In CD8⁺ T cells, Bcl11b plays a role in the antigen-specific clonal expansion and cytolytic effector function of (Zhang et al., 2010).

1.4.5. *Bcl11b* in other tissues

Besides the immune system, Bcl11b is also required in skin, neuron and tooth development (Arlotta et al., 2005; Arlotta et al., 2008; Golonzhka et al., 2007). *Bcl11b* is highly expressed in mouse skin during embryogenesis. In the developing epidermis at late stage of fetal development and in the adult skin, Bcl11b expression decreases and becomes restricted to the proliferating cells of the basal cell layer (Arlotta et al., 2005; Arlotta et al., 2008; Golonzhka et al., 2007). Further analysis indicates that a subset of skin stem cells may express Bcl11b (Golonzhka et al., 2007; Golonzhka et al., 2009a). Analysis of mice with germline deletion of *Bcl11b* shows that Bcl11b is required in skin during development, particularly in keratinocyte proliferation and late differentiation events (Golonzhka et al., 2007; Golonzhka et al., 2009b). Similarly, BCL11B is expressed in human epidermis, and is linked to disease progression and/or maintenance in atopic dermatitis and allergic contact dermatitis patients (Ganguli-Indra et al., 2009).

Bcl11b is crucial for the development of corticospinal motor neurons axonal projections to the spinal cord in vivo (Arlotta et al., 2005). Bcl11b is also indispensable for striatal medium spiny neurons differentiation, striatal patch development, and the establishment of the cellular architecture of the striatum (Arlotta et al., 2008). In humans, BCL11B expression is maintained at high levels in normal adult striatum but significantly decreased in huntington disease (HD) cells. Furthermore, mutant huntington striatal neurons is sensitive to overexpression of

BCL11B, suggesting that sequestration and/or decreased expression of BCL11B is responsible for the deregulation of striatal gene expression and the specificity of pathology that are observed in HD (Desplats et al., 2008).

Bcl11b also participates in the regulation of epithelial cell differentiation during tooth morphogenesis and is highly expressed in ectodermic components of the developing tooth. *Bcl11b*-deficient mice show multiple defects at the bell stage and have abnormal incisors and molars (Golonzhka et al., 2009b).

Bcl11b is among the earliest known genes to be expressed specifically in the embryonic mammary placodes in the mouse. In mammary glands of adult mice, Bcl11b expression is predominantly restricted to basal cells and a small number of luminal progenitors. Deletion of *Bcl11b* in the virgin gland leads to precocious alveologenesis and a basal-to-luminal lineage switch in the basal cells. In contrast, transient overexpression of *Bcl11b* is sufficient to induce expression of basal cell specific genes in luminal cells. Thus, Bcl11b promotes and maintains basal identity, and suppresses the luminal lineage in the mammary gland (unpublished, Song Choon Lee).

1.4.6. Binding sites of Bcl11b

Bcl11b, also termed Ctip2 (COUP-TF interacting protein), was independently isolated for its ability to interact with all members of the chicken ovalbumin upstream promoter transcription factor (COUP-TF) subfamily of orphan nuclear receptors (Avram et al., 2000). COUP-TFs usually mediate transcriptional repression by recruiting nuclear receptor co-repressor (NCoR) and/or silencing mediator for retinoid and thyroid hormone receptor (SMRT) to the template. COUP-TF family members play important roles in pattern formation in the developing nervous systems of *Xenopus* and *Drosophila* (Avram et al., 2000; Mlodzik et al., 1990; van der Wees et

al., 1996). As a COUP-TF-interacting protein, Bcl11b mediates transcriptional repression when tethered to a promoter by interacting with a DNA binding protein, such as ARP1, which is a member of COUP-TF subfamily of orphan nuclear receptors (Avram et al., 2000). BCL11B also directly interact with two metastasis-associated proteins MTA1 and MTA2 (Cismasiu et al., 2005). In HEK293 cells, BCL11B recruits sirtuin 1 (SIRT1), a trichostatin-insensitive, nicotinamide-sensitive class III histone deacetylase, to the promoter region of a reporter gene template (Senawong et al., 2003; Senawong et al., 2005). In addition, BCL11B recruits histone deacetylase (HDAC)1 and HDAC2 to promote local histone H3 deacetylation at the HIV-1 promoter region (Marban et al., 2007).

Bcl11b regulates cell cycle by suppressing cyclin-dependent kinase inhibitors. Bcl11b cooperates with SUV39H1 and histone methylation to silence *Cdkn1a* (p21) (Cherrier et al., 2009), a major cell cycle regulator of the response to DNA damage senescence and tumor suppression (Bunz et al., 1998). Bcl11b also appears to repress another cyclin-dependent kinase inhibitor, *Cdkn1c* (p57KIP2) (Topark-Ngarm et al., 2006), which has the ability to associate with and inhibit the catalytic activity of a number of cyclin-cdk complexes (Cunningham and Roussel, 2001).

1.5. Thesis projects

The work of this thesis is based on the following question: “What will happen to T cells after *Bcl11b* is acutely ablated?” To answer this question, I planned first to identify Bcl11b expression in the T cell compartment in the mouse, and then to characterize its functions at various stages of early T cell development, and in committed and mature T cells.

Currently, Bcl11b expression in T cells is derived primarily from RT-PCR analysis. Whilst being informative, it only measures Bcl11b expression in a

population of T cells at transcription levels but not protein levels. Therefore, the first goal of this project was to use a *Bcl11b* reporter mouse to probe *Bcl11b* expression in hematopoietic lineages, especially in different T cell subsets.

The second goal of this thesis was to study the functions of *Bcl11b* in T cells at different developmental stages and its role during the homeostasis of different T cell subpopulations. Transcription factors involving in T cell development have been extensively studied in the mouse (Carpenter and Bosselut, 2010; Rothenberg et al., 2008; Rothenberg and Taghon, 2005). However, unlike the requirement of *Pax5* in B cells (Cobaleda et al., 2007; Mikkola et al., 2002), none of the characterized transcription factors had been found to be required to guard T cell identity against other hematopoietic lineage potentials. These earlier studies, and the available mouse genetic resources, in particular, the *Bcl11b* conditional knockout mouse and the *Bcl11b* reporter mouse strains prompted me to investigate the roles of *Bcl11b* in T cell.

This thesis is divided into two parts. In the first part, I have characterized the expression of *Bcl11b* in different T cell subsets and in other hematopoietic lineages using the *Bcl11b-tdTomato* knock-in reporter mouse. Then I will present data and analysis on *Bcl11b* loss-of-function studies in T cells at various developmental stages and of different T cell subsets. These functional studies also include generation and characterization of a novel type of cell derived from *Bcl11b*-deficient T cells.

Chapter 2

MATERIAL AND METHODS

2.1. *Mouse techniques*

2.1.1. *Animal husbandry*

All animal experiments were performed in accordance with the UK's 1986 Animals Scientific Procedure Act and local institute ethics committee regulations.

Bcl11b conditional knockout mice were generated by Dr. Pentao Liu. Briefly, *Bcl11b* conditional knockout targeting vector was constructed using recombineering, and the mouse strain *Bcl11b*^{fllox/fllox} was made according to a standard gene targeting approach in ES cells. Then Cre-ERT2;*Bcl11b*^{fllox/fllox} mice were derived from the cross between *Bcl11b*^{fllox/fllox} mice and Cre-ERT2 transgenic mice. Cre-ERT2;*Bcl11b*^{fllox/fllox} mice were in the mixed C57BL/6J and 129S5 genetic background. Most mice were NK1.1+ by flow cytometry, suggesting that they had inherited the C57BL/6 haplotype at the NK gene complex. The *Bcl11b-tdTomato* knock-in mouse strain, in which the *tdTomato* cassette was inserted into the 3' UTR of *Bcl11b*, was generated by Juexuan Wang in Dr. Pentao Liu's lab. *Bcl11b-tdTomato* knock-in mice are in the C57BL/6 genetic background. Both strains in the C57BL/6 and 129S5 genetic background have the H-2b haplotype at the MHC. *Rag2*^{-/-}*Il2rγ*^{-/-} mice that are in the C57BL/6 background were obtained from Francesco Colucci at Babraham Institute.

2.1.2. Tamoxifen administration

1 g of tamoxifen (Sigma) was suspended in 5 ml of ethanol and then dissolved in 50 ml of sunflower oil to obtain a final tamoxifen stock at the concentration of 20 mg/ml. To dissolve the tamoxifen completely, the stock was sonicated on ice for 2 min (at 15 sec interval). 1 mg of tamoxifen in sunflower oil stock (50 μ l) was administered to each mouse by oral route each day for three consecutive days. After administration, mice were provided with food mash and their weights were closely monitored.

2.1.3. Intravenous tail vein injection

Donor cells were counted and re-suspended in PBS solution at a certain concentration for injection. Host mice were initially put under a heat lamp for 5 min to increase blood flow to the tail vein. Then they were transferred to a holding device to allow access to the tail vein. 100 μ l of cell solution was loaded into a small syringe with a 27G needle. The needle was inserted into vein and the 100 μ l cell solution was injected.

2.2. DNA methods

2.2.1. Extraction of DNA from primary cells

Primary cells were initially spun at 300xG for 5 min. Next cell pellets were incubated in 200 μ l of lysis buffer [50 mM Tris (pH 7.5), 25 mM EDTA (pH 8), 100 mM NaCl, 0.5% SDS, and 1mg/mL Proteinase K (added fresh)] at 65⁰C for 2 hours. After adding 200 μ l of isopropanol, the suspension was mixed gently and incubated at -20⁰C for 30 min to precipitate the DNA. The suspension was then spun at 16,000xG

for 10 min and washed twice with 70% ethanol. Finally, the DNA pellet was air dried before re-suspended in an appropriate volume of ddH₂O.

2.2.2. Extraction of DNA from tissues

Tissues (ear or tail biopsies) were incubated in 400 µl of lysis buffer as described above at 65⁰C for 4 hours or overnight. Next, the buffer with tissue was vortexed vigorously and spun at 16,000xG for 10 min. Genomic DNA was precipitated by adding 500 µl of isopropanol into cell lysis buffer. After centrifugation, DNA was washed once with 500 µl of 70% ethanol and air dried before being re-suspended in an appropriate volume of TE buffer.

2.2.3. Genotyping PCR

Extensor Hi-Fidelity PCR Master Mix 2 (Thermo) was used for PCR amplification. 1 ng of DNA template, 1 µl of each primer (10 µM), and 2 µl of PCR-grade water were mixed with 5 µl of the PCR master mix and incubated in PTC-225 PCR machine (Peltier Thermal Cycler) with the following setting: 94⁰C for 2 min, 30 cycles of 94⁰C for 30 sec, 60⁰C for 30 sec and 68⁰C for 30 sec, 68⁰ for 10 min. Primers used here are shown in Table 1.

2.2.4. TCR rearrangement PCR

Extensor Hi-Fidelity PCR Master Mix 2 (Thermo) was used for TCR rearrangement PCR amplification. 10 ng of genomic DNA template, 1 µl of each primer (10 µM) and 2 µl of PCR-grade water were mixed with 5 µl of the PCR master mix and incubated in PTC-225 PCR machine (Peltier Thermal Cycler) with the following setting: 94⁰C for 2 min, 30 cycles of 94⁰C for 30 sec, 60⁰C for 30 sec and 68⁰C for 1 min, 68⁰ for 10 min. 5 µl of PCR product was loaded on 1% agarose gel

TCR rearrangement bands visualization. When further amplification of TCR rearrangement PCR products was necessary, 1-2 μ l of PCR products were purified on the QIAprep spin column (QIAGEN), according to manufacturer's protocols. Finally, 1 μ l of eluted PCR products was used as DNA template to repeat the PCR in the same condition. Primers used here are shown in Table 1.

2.3. RNA methods

2.3.1. Extraction of total RNA from cells

RNA from primary cells was extracted using the RNAqueous-Micro RNA isolation kit according to the manufacturer's protocol (Ambion). Briefly, cells were counted and pelleted by centrifuge at 400xG for 5 min. The supernatant was removed thoroughly by aspiration, and the cell pellet was resuspended in at least 100 μ l of Lysis Solution by vortexing vigorously. Then, 50 μ l of 100% ethanol was added and mixed thoroughly with the lysate. Next, the lysate/ethanol mixture was loaded onto a Micro Filter Cartridge Assembly and centrifuge for 10 sec at 16,000xG. Then the filter was washed with 180 μ l of Wash Solution 1 once and 180 μ l of Wash Solution 2/3 twice. The flow-through was discarded and the filter was centrifuged for 1 min at 16,000 G. The RNA eluted in 10 μ l of preheated Elution Solution. 1/10th volume of 10X DNase I Buffer and 1 μ l of DNase I were added into the RNA sample and mixed gently but thoroughly for DNA elimination. After incubation at 20 min at 37⁰C, the DNase reaction was mixed with 2 μ l of DNase Inactivation Reagent and left at room temperature for 2 min. Finally, the DNase Inactivation Reagent was pelleted and the RNA was transferred to a fresh tube. For RT-PCR or qRT-PCR experiments, RNA quality and quantity was verified using a Nanodrop ND-100 Spectrophotometer

(Thermo Scientific). For gene expression array experiments, RNA quality and quantity was determined using 2100 Bioanalyzer platform (Agilent Technologies).

2.3.2. First strand cDNA synthesis

SuperScript III First-Strand Synthesis System for RT-PCR (Invitrogen) was used for first strand cDNA synthesis from RNA, according to the manufacturer's protocol. In brief, 1-2 μg of RNA was mixed with 1 μl of oligo(dT)₂₀ (50 μM), 1 μl of dNTP mix (10 mM) and DEPC-treated water up to 10 μl . The reaction was incubated at 65⁰C for 5 min and then place on ice for 1 min. Then the following cDNA Synthesis Mix [2 μl of 10X RT buffer, 4 μl of MgCl₂ (25 mM), 2 μl of DDT (0.1 M), 1 μl of RNaseOUT and 1 μl of SuperScript III RT] was prepared and mixed with the reaction gently and incubated for 50 min at 50⁰C. The reactions were terminated at 85⁰C for 5 min and chill on ice. Finally, 1 μl of RNase H was added to the reaction and incubated for 20 min at 37⁰C for RNA elimination.

2.3.3. RT-PCR

RT-PCR was performed on cDNA using primers listed in Table 1. PCR amplification was performed using Extensor Hi-Fidelity PCR Master Mix 2 (Thermo). Similar to genotyping PCR, 1 μl of cDNA (about 10 ng) was used as template. It was mixed with 1 μl of each primer (10 μM) and 2 μl of PCR-grade water were mixed with 5 μl of the PCR master mix and incubated in PTC-225 PCR machine (Peltier Thermal Cycler) with the following setting: 94⁰C for 2 min, 25-30 cycles of 94⁰C for 30 sec, 60⁰C for 30 sec and 68⁰C for 30 sec, 68⁰ for 10 min.

2.3.4. qRT-PCR

Quantitative real-time RT-PCR (qRT-PCR) was used to measure the relative amounts of mRNA expression of gene of interest again β Actin as an internal control. At first, primers were tested for their amplification efficiency. Amount of cDNA samples was determined with a Nanodrop ND-100 Spectrophotometer (Thermo Scientific). The PCR reactions were carried out with either the Taqman or SYBR Green system in an ABI PRISM 7900HT (Applied Biosystems), according to the manufacturer's manuals.

2.3.5. Taqman

50 μ l of cDNA (10 ng/ μ l) was mixed with 12.5 μ l of Absolute QPCR mix (Thermo) with 1 μ l of each primer (10 μ M), 0.5 μ l of probes (0.25 μ M; MWG, Ebersberg, Germany). PCR reactions were conducted in triplicate. Probes were labeled with reported dye (FAM) at the 5' end and the quencher dye TAMRA at the 3' end. Primers and probes used are listed in Table 1.

2.3.6. SYBR Green

50 μ l of cDNA (10 ng/ μ l) was mixed with 12.5 μ l of SYBR GreenER qPCR SuperMix (Invitrogen) with 1 μ l of each primer (10 μ M). PCR reactions were conducted in triplicate. SYBR Green I DNA fluorescent dye was used with high affinity to dsDNA and an excitation wavelength of 488 nm. Primers used are listed in Table 1.

2.4. Protein methods

2.4.1. Protein extraction

Cell pellets were re-suspended in 100-300 μ l of RIPA buffer [50mM Tris (pH 7.4), 1% NP-40, 0.25% sodium deoxycholate, NaCl (150 mM), EDTA (1mM), 1X Cocktail protease inhibitors (Roche), Na_3VO_4 (1mM), and 1 mM NaF] and transferred to a 1.5 ml tube. The lysate was pipetted up and down several times to be dissolved. After boiled at 99⁰C for 5 min, the lysate was chilled on ice for 10 min and spun for 15 min at 16,000xG. Then the supernatant was collected and frozen. Also, 10 μ l of the supernatant was collected in a separate tube for protein concentration assay.

2.4.2. BioCinchomonic Acid (BCA) assay

Bovine Serum Albumin (BSA) (Sigma) was made at required amounts of 0.1 mg, 0.2 mg, 0.5 mg, 1.0 mg and 2.0 mg and used as standards for the assay. The BCA reagents were mixed in a ratio of 50:1 (A:B) respectively, according to manufacturer's protocol. 200 μ l of the reagent mix was added to 5 μ l of standard or sample in a 96-well plate. Samples were diluted in water (from 1:4 to 1:16) before measurement. Each standard or sample was measured for three times. After incubation at room temperature for 20 min, the light absorbance of reactions was measured at a wavelength of 570 nm using a DYNATECH-MR5000 plate reader. The readout of standards was used to plot a graph. Finally, the slope of the graph was used to calculate the concentration of the samples.

2.4.3. SDS-PAGE

The protein samples were diluted to a final concentration of 30 μ g/ml using RIPA buffer and Loading Buffer [125 mM Tris-HCl (pH 6.8), 2.5% SDS, 20%

glycerol, 0.002% Bromophenol blue and 5% b-mercaptoethanol]. After boiling at 95°C for 5 min, samples were chilled on ice for 5 min and then loaded to SDS-PAGE Criterion precast Tris-HCl resolving gels (Biorad). The gels were run at 100 V for 90-120 min at room temperature using Biorad powepac 300 in Running Buffer (3.03 g Tris, 14.4 g Glycine, 1 g SDS and ddH₂O to 1 L).

2.4.4. Immunoblotting

Protein samples were immunoblotted to PVDF membranes (Millipore-immobilon FL) with wet transfer tanks (Biorad), according to the manufacturer's protocols. Briefly, the gels were placed in a cassette facing the PVDF membranes. The concentration of methanol in Transfer Buffer [192 mM Glycine, 25 mM Tris, 0.1% SDS, 5-20 v/v 100% Methanol, pH 8.3) varied depending on the size of proteins of interest. For high molecular weight proteins, transfer buffer with low percentage of methanol was used while for low molecular weight protein that with high percentage of methanol was used. Transfer was performed with electric current applied at 400 mA for 1 hr.

2.4.5. Primary antibody incubation

The PVDA membranes were incubated in blocking solution (5% milk) for 1 hr at room temperature to reduce background signal in the consequent steps. Then primary antibodies were added into blocking solution. All primary antibodies were incubated overnight at 4°C whilst shaking.

2.4.6. Secondary antibody incubation and detection

After the primary antibodies were removed, the membranes were rinsed once with 1X PBS-0.1% Tween (Sigma) (PBST) and incubated in the blocking buffer with the appropriate secondary antibody (1:2000 dilution) for 45 min. The secondary

antibodies used were all conjugated to horseradish peroxidase (HRP) (DAKO). The membrane was then washed twice with 1X PBST for 5 min each to prevent on specific binding. ECL (Amersham) was used as a substrate for the HRP enzyme. The semi-luminescence was detected with Hyper-film (Amersham).

2.5. Flow cytometry and cell sorting

2.5.1. Single cell suspension

Bone marrow cells were flushed out from the femurs using a 26G syringe with fluorescent-activated cell sorting (FACS) Stain Buffer [DPBS (Invitrogen) with 2% FCS (GIBCO)]. Spleen or thymus were placed in FACS Stain Buffer and gently homogenized with a syringe. The red blood cells were removed with ACK lysis buffer (Lonza). Blood was collected into EDTA tubes (Sarstedt). In vitro cultured cells were collected and washed with FACS Stain Buffer. Cells were filtered through a 30 μm mesh to obtain single-cell suspension.

2.5.2. DN thymocytes enrichment

CD4 (L3T4) and CD8 (Ly-2) MicroBeads (Miltenyi Biotec) were used in accordance to the manufacturer's protocols for the enrichment of CD4⁺CD8⁻ population from thymocytes. Briefly, cells were counted and a certain number of cells were pelleted by centrifuge at 300xG for 10 min. The cell pellet was re-suspended in 90 μl of MACS Buffer [PBS pH 7.2, 0.5% BSA and 2 mM EDTA] per 10^7 total cells, after supernatant was completely removed. 5 μl of CD4 and CD8 MicroBeads were mixed with the cells and incubate for 15 min at 4-8⁰C. Cells were washed twice by adding 1-2 mL of MACS Buffer per 10^7 cells and centrifuged at 300xG for 10 min. Cell pellets were resuspended up to 10^8 in 500 μl of MACS Buffer. Then cell

suspension was then applied onto the MACS Separator Column (Miltenyi Biotec). Unlabeled cells that pass through the column were collected and the columns were washed for 3 times. Cells were pelleted by centrifuging the total effluent, re-suspended in FACS Stain Buffer, and stained for cell surface antigens.

2.5.3. Staining of cell-surface antigens

For all cells, Fc receptors were blocked with anti-CD16 (2.4G2) prior to antibody labelling. Antibodies to the following antigens were used: CD3 ϵ (145-2C11), CD4 (L3T4), CD8 α (53-6.7), CD25 (PC61), CD44 (IM7), CD122 (TM- β 1), CD27 (LG.3A10), CD11b (M1/70), CD45.2 (104), TCR β (H57-597), CD117 (2B8), NK1.1 (PK136), CD49b (DX5), NKp46 (29A1.4), Ly49C/I (5E6), Ly49G2 (4D11), Ly49D (4E5). All antibodies were from BD Biosciences or eBioscience. Cells were incubated with antibody for 30 minutes at 4° C before being washed. In some cases, biotinylated antibodies were revealed by incubation with fluorochrome-conjugated streptavidin for a further 20 minutes at 4° C. Cells were washed and resuspended prior to data acquisition using a FACSCalibur (BD Biosciences), LSR II (BD Biosciences) or a FC 500 (Beckman Coulter) with dead cells excluded based on scatter profile or DAPI inclusion. Analysis was performed using FlowJo (Tree Star) software. Sorting was performed using a MoFlo (DAKO) or FACS Aria (BD Biosciences).

2.5.4. CD1d stain

Prior to cell-surface antigen staining, CD1d:Ig proteins (BD Bioscience) were loaded with α -GalCer (Kyowa Hakko Kirin Company) by mixing antigen and CD1d:Ig together in PBS, pH7.2 and incubating at 37° C overnight. 1 μ g of peptide-loaded CD1d:Ig protein was subsequently mixed with 1 μ g of PE-conjugated A85-1

mAb (BD Bioscience) at a ratio of 1:1 of dimmer: A85-1 mAb were incubated for 60 minutes at room temperature (RT) in the dark. Next, 1 μ g of purified mouse IgG1 isotype control mAb A111-3 (BD Bioscience) was added to the staining cocktail and incubated for 30 minutes at room temperature RT in the dark. Finally cells were stained with the prepared stain cocktail, plus any other cell-surface marker-specific antibodies to be used, as described above.

2.5.5. Staining for intracellular antigens

After cell-surface antigen staining, cells were fixed by adding 100 μ l of Fixation Solution (eBioscience), while vortexing the tube. The tube was incubated in the dark at room temperature for 20 min and cells were washed twice with 1 ml of Permeabilization Buffer (eBioscience). Then, cells were resuspended in 100 μ l of Permeabilization Buffer. Fluorochrome-labeled anti-cytokine mouse antibodies were added into tubes and mixed well. After incubation in the dark at room temperature for 20 min, the cell suspension was washed once with 1 ml of Permeabilization Buffer. Cells were resuspended in FACS Stain Buffer and ready for analysis on a flow cytometer.

2.6. Cell culturing

2.6.1. Culture of OP9 and OP9-DL1 stromal cells

OP9 stromal cells were cultured in α -MEM (Sigma) with 10% FCS (heat inactivated at 56⁰C for 30min), 1% penicillin/streptomycin, and 2 mmol/L L-glutamine (Life Technologies). OP9-DL1 stromal cells were cultured in α -MEM (Sigma) with 20% FCS, 1% penicillin/streptomycin, and 2mmol/L L-glutamine (Life Technologies). Cells were passaged every 2 to 3 days by trypsinization (0.25%

trypsin) (Invitrogen). A confluent monolayer (70%-80%) of OP9-DL1 cells was prepared 24 hours prior to co-culture.

2.6.2. Culture of T cells

T cells were co-cultured with OP9-DL1 in T Cell Culture Media [RPMI-1640, 10% FCS, 1% penicillin/streptomycin, and 2 mmol/L L-glutamine, 5 ng/ml Flt-3 ligand, 5 ng/ml IL-7]. Half volume of culture media was replaced with fresh T cell Culture Media every three days. Every week, T cells were disassociated from OP9-DL1 stromal cells by being pipetted gently and passing through 30 μ m mesh, then were transferred to fresh OP9-DL1 culture. All cytokines used in this study were purchased from PeproTech, if not specified otherwise.

2.6.3. Culture of myeloid cells

Myeloid cells were co-cultured with OP9 in Myeloid Cell Culture Media [IMDM, 10% FCS, 1% penicillin/streptomycin, and 2 mmol/L L-glutamine, 5 ng/ml Flt-3 ligand, 1 ng/ml IL-7 and 10 ng/ml IL-3, IL-6, stem cell factor (SCF), and macrophage colony-stimulating factor (M-CSF), granulocyte colony-stimulating factor (G-CSF), and granulocyte/macrophage colony-stimulating factor (GM-CSF)]. Half volume of culture media was replaced with fresh Myeloid Cell Culture Media every three days. Every week, myeloid cells were disassociated from OP9 stromal cells by being pipetted gently and passing through 30 μ m mesh, and were transferred to fresh OP9 culture.

2.6.4. Culture of B cells

B cells were co-cultured with OP9 in B Cell Culture Media [IMDM, 10% FCS, 1% penicillin/streptomycin, and 2 mmol/L L-glutamine, 5 ng/ml Flt-3 ligand, 5 ng/ml IL-7]. Half volume of culture media was replaced with fresh B Cell Culture Media

every three days. Every week, B cells were disassociated from OP9 stromal cells by being pipetted gently and passing through 30 µm mesh, and were transferred to fresh OP9 cultures.

2.6.5. Culture of NK cells

NK cells were co-cultured with OP9 in NK Cell Culture Media [RPMI-1640, 10% FCS, 1% penicillin/streptomycin, and 2 mmol/L L-glutamine, 30 ng/ml IL-15]. Half volume of culture media was replaced with fresh NK Cell Culture Media every three days. Every week, NK cells were disassociated from OP9 stromal cells by being pipetted forcefully and passing through 30 µm mesh, and were transferred to fresh OP9 cultures.

2.6.6. Culture of Lymphokine-activated killer (LAK) cells

Splenic NK cells were enriched using the NK Isolation Kit (Miltenyi) and cultured for 6-9 days at 1×10^6 cells/ml in LAK Culture Media [RPMI 1640 medium containing 10% FCS/50 µM 2-mercaptoethanol/2.0 mM L-glutamine and 100 ng/ml IL-2]. The cells were split every 2 days and supplemented with fresh IL-2. Purity was always >90%. For culturing reprogrammed cells ex vivo, whole splenocytes were cultured without pre-enrichment.

2.6.7. Culture of tumour cell lines

RMA and RMA-s, two mouse lymphoma cell lines were cultured in RMA Culture Media [RPMI 1640 medium containing 5% FCS/50 µM 2-mercaptoethanol /2.0 mM L-glutamine]. B16, a mouse melanoma cell line, was cultured in B16 Culture Media [DMEM medium containing 5% FCS/50 µM 2-mercaptoethanol/2.0 mM L-glutamine]. Cells were passaged every 2 to 3 days by trypsinization (0.25% trypsin) (Invitrogen).

2.6.8. Activation of unprimed T cells

T cells were activated using Dynabeads Mouse T-Activator CD3/CD28 (Invitrogen), according to its protocol. Briefly, 1×10^5 purified T cells were mixed with washed 2 μ l Dynabeads Mouse T-Activator CD3/CD28 to obtain a bead-to-cell ratio of 1:1 in T cell media [RPMI 1640 medium containing 10% FCS/50 μ M 2-mercaptoethanol/2.0 mM L-glutamine and 3 ng/ml hIL-2].

2.6.9. OHT treatment in vitro

Thymocytes or splenocytes were cultured in T Cell Media with 1 μ M OHT (Sigma) at 37⁰C for 48 hrs. After this time, cells were washed and resuspended with fresh media without OHT.

2.7. Gene expression analysis

RNA was extracted using the RNAqueous Micro Kit (Ambion) from FACS sorted cells. Quality and quantity of RNA samples was tested with the Bioanalyzer. Total RNA was amplified using the Illumina Total Prep RNA Amplification Kit (Ambion) according to the manufacturer's instructions. The biotinlated cRNA (1.5 μ g per sample) was applied to Illumina Mouse-6 Expression BeadChips and hybridized overnight at 58⁰C. Chips were washed, detected and scanned according to the manufacture's instruction and the scanner output imported into BeadStudio software (Illumina).

2.8. Chromatin immunoprecipitation

Chromatin immunoprecipitation was performed as previously described (Forsberg et al., 2000). Control IgG and the CSL antibody were purchased from Abcam. Genomic DNA was purified with Qiaquick PCR purification kit (QIAGEN)

and specific genomic DNA regions were quantified by real-time quantitative PCR with Taqman (ABI) or SYBR Green (Invitrogen). Input DNA was used as a standard curve to quantify concentration of DNA recovered after IP. The amount of DNA recovered from each ChIP sample was presented as a relative to the control.

2.9. *Tumour killing assays*

B16F10 melanoma (H-2b), RMA lymphoma and RMA-S lymphoma (H-2b TAP-1-deficient variant) cells were maintained as above. For killing assays, target cells were washed and incubated with 0.1 μCi $\text{Na}_{251}\text{CrO}_4$ (Perkin Elmer) for 45 min at 37° C. The target (T) cells were then washed and added in triplicate to effector (E) cells at the indicated E:T ratio. Plates were incubated for 4 hr at 37° C before the supernatant was tested for chromium release in a scintillation counter. Percent specific lysis was calculated as (experimental release – spontaneous release)/(maximum release – spontaneous release) x 100.

2.10. *Calcium flux*

Briefly, 1×10^6 cells after cell surface antigen staining were re-suspended in 1 ml of Cell Loading Medium (CLM) [RPMI containing 2% FCS]. Next, cells were loaded with Indo-1 (Invitrogen) at a final concentration of 1.5 μM and incubated at 37°C for 45 minutes in the dark. After wash with washing buffer [DMEM containing 2% FCS], cells were gently resuspended in CLM and stored for 1 hour at RT in the dark before flow cytometric analysis.

Chapter 3

BCL11B EXPRESSION IN HEMATOPOIETIC LIENAGES

3.1. *Introduction*

3.1.1. *Current knowledge of Bcl11b expression patterns*

During evolution, a homolog of *Bcl11b* first appeared in cartilaginous fishes. In sea lampreys, a jawless vertebrate, expression of a *Bcl11b* ortholog is specifically detected in VLRA⁺ cells that are similar to T lymphocytes in vertebrates, but not in VLRB⁺ cells that are similar to B lymphocytes in vertebrates (Guo et al., 2009). In bony fish, the *Bcl11b* ortholog is expressed in the thymus and positively regulates *ccr9* expression, which encodes the receptor for ccl25, a novel chemokine expressed in thymic epithelium (Bajoghli et al., 2009). In both the mouse and human, *Bcl11b* is highly expressed in T cells (Bernard et al., 2001; Wakabayashi et al., 2003b). Gene expression studies indicate that expression of many genes important for T cell commitment starts to increase in the transition from DN1 to DN2, with *Bcl11b* being the most drastically upregulated transcription factor (Tydell et al., 2007).

3.1.2. *Reporter Molecules in Genetically Engineered Mice*

Reporter molecules are commonly used in transgenic mice to follow the in vivo gene expression patterns through all developmental stages of the life cycle in all

tissues. The most widely used reporter molecule is the β -galactosidase (β -gal) enzyme of *E. coli* encoded by the *lacZ* gene (Young et al., 1993). However, its staining process usually affects cell viability and sometimes introduces false positive signals in flow cytometry analysis (Abe et al., 1996). Green fluorescent protein (GFP) is another common reporter molecule used in transgenic mice. It is useful for the study of living cells since its expression can be assayed conveniently without any staining processes, though its sensitivity and potential toxicity need to be considered (Hadjantonakis et al., 1998; Huang et al., 2000). Tandem dimer Tomato (tdTomato) provides a useful alternative to enhanced green fluorescent protein (eGFP) for the simultaneous detection of fluorescent protein in histological sections together with fluorescence immunohistochemistry (IHC) (Morris et al., 2010; Shaner et al., 2004). TdTomato is a fluorescent protein with maximum excitation at 554 nm and maximum emission at 581 nm and was used to monitor metastatic progression in live animals (Shaner et al., 2004; Winnard et al., 2006).

3.1.3. Purposes of this chapter

Most Bcl11b expression profiles have been obtained from RT-PCR, northern blot analysis, or RNA anti-sense in situ hybridization. These methods are usually not sensitive enough to detect expression of *Bcl11b* at the single cell level. Using *E. coli lacZ* as a reporter in mice, expression of *Bcl11b* was detected in thymocytes at single cell level (Song Choon Lee, unpublished). However, *lacZ* staining process is time-consuming and can bring false positive signals into analysis by flow cytometry, especially for NK cells, because the substrate, 5-bromo-4-chloro-3-indolyl- β -D-galactopyranoside (X-gal), are likely to react with enzymes in large granules that are abundant in NK cells. Additionally, Bcl11b expression in different hematopoietic lineages such as NK cell, NKT cell, thymic NK cells have not been characterized in

details using the lacZ mice. Therefore I investigated expression pattern of *Bcl11b* in hematopoietic lineage, mainly T cell subsets, using a *Bcl11b-tdTomato* knock-in reporter mouse line in this chapter. As a T cell gene, *Bcl11b* is highly expressed in all T cells throughout T cell development but absent in other hematopoietic cell lineages.

3.2. Results

3.2.1. *Bcl11b* expression in thymocytes

To determine *Bcl11b* expression in T cells at a single cell level, I analyzed *Bcl11b-tdTomato* knock-in mice (*Bcl11b*^{TOM/+}), which were generated by Juexuan Wang in our lab. In this mouse strain, the *tdTomato* cassette was inserted into the 3' untranslated region (UTR) of *Bcl11b*. Hence, the expression of *Bcl11b* can be conveniently studied by detecting fluorescent signals from tdTomato in flow cytometry (Fig. 3.1). The haematopoiesis in *Bcl11b*^{TOM/+} mice was normal, as percentages of B cells (Fig. 3.2A), T cells (Fig. 3.2B) and myeloid lineage cells (Fig. 3.2C) were similar to that of wild type mice. In *Bcl11b*^{TOM/+} mice, flow cytometry analysis showed that *Bcl11b* was expressed in more than 95% of CD4 and CD8 double positive (DP) thymocytes (Fig. 3.3A) and about 85% of CD8 single positive (SP) (Fig. 3.3B) and CD4 SP T thymocytes (Fig. 3.3C). These results are consistent with expression of *Bcl11b* obtained using RT-PCR and direct *Bcl11b* antibody staining (Cismasiu et al., 2006; Tydell et al., 2007), and also confirm that tdTomato signals faithfully recapitulate *Bcl11b* expression.

After depletion of DP and SP T cells, early T cell subsets were defined by expression of CD117, CD44, and CD25 in the lineage negative (Lin⁻) thymocytes (Fig. 3.4A) (Rothenberg et al., 2008). FACS analysis showed that *Bcl11b* was absent in ETP (Fig. 3.4B), which are defined as CD117⁺⁺DN1 and have non-T-cell potentials

including NK, dendritic, and myeloid cell lineages (Rothenberg et al., 2008). *Bcl11b* was only expressed in about 50% of DN2a (CD117⁺DN2) T thymocytes (Fig. 3.4D) which have lost dendritic cell potential, suggesting DN2a population is heterogeneous (Masuda et al., 2007). *Bcl11b* was expressed at relatively lower levels in CD117⁻DN1 thymocytes (Fig. 3.4C), compared to its high expression in DN2b (CD117⁻DN2) (Fig. 3.4E), DN3 (Fig. 3.4F) and DN4 T cells (Fig. 3.4G). The upregulation of *Bcl11b* during transition from ETP to DN2b suggests a critical role of *Bcl11b* in early T cell development (Masuda et al., 2007) (Tydell et al., 2007).

3.2.2. *Bcl11b* expression in mature T cells

T cells migrate from the thymus to secondary lymphoid organs such as the spleen and lymph nodes after maturation. *Bcl11b* was expressed in about 95% of CD8⁺ and CD4⁺ splenic T cells (Fig. 3.5A). In mature T cells, 20% of peripheral activated (CD44⁻CD62L⁺) CD8⁺ T cells (Fig. 3.6A and 3.5B), and 11% of activated (CD44⁻CD62L⁺) CD4⁺ T cells (Fig. 3.6A and 3.5C) had very low levels of *Bcl11b* expression. In contrast, more than 99% of naïve (CD44⁺CD62L⁻) CD8⁺ and CD4⁺ splenic T cells highly expressed *Bcl11b* (Fig. 3.5B and 3.5C). Consistent with FACS analysis, qRT-PCR using RNA from sorted T cells showed that *Bcl11b* expression in activated T cells was two folds lower than that in naïve T cells (Fig. 3.6B). Collectively, the results from both flow cytometry and qRT-PCR suggest that *Bcl11b* may participate in the regulation of T cell activation.

Unlike $\alpha\beta$ -T cells, $\gamma\delta$ -T cells are still found in the *Bcl11b* knockout fetal thymus, indicating that *Bcl11b* is dispensable for fetal $\gamma\delta$ -T cells (Wakabayashi et al., 2003a). However, no studies have been reported about the expression and function of *Bcl11b* in adult $\gamma\delta$ -T cells. Here, using *Bcl11b*^{TOM/+} mice, *Bcl11b* expression was

detected in 90% of adult $\gamma\delta$ -T thymocytes (Fig. 3.7A and 3.7B), suggesting that *Bcl11b* may also be important for adult $\gamma\delta$ -T cells.

Natural killer T (NKT) cells are a subset of T cells that express NK cell surface markers such as NK1.1 and DX5 (Godfrey et al., 2004). The majority of NKT cells are CD1d-restricted and are stained positive for CD3 and CD1d dimer (Fig. 3.7C). 95% of CD1d-restricted NKT cells expressed *Bcl11b* (Fig. 3.7D), indicating that *Bcl11b* could play a role in NKT cells.

3.2.3. *Bcl11b* expression in other hematopoietic cells

NK cell development can be operationally divided into four different stages, which are usually defined using CD122, NK1.1, CD27 and CD11b (Fig. 3.8A) (Di Santo, 2006). During NK cell development, *Bcl11b* was only transiently expressed at low levels in some less mature ($\text{NK1.1}^+\text{CD27}^+\text{CD11b}^-$) NK cells but not in NK progenitors ($\text{CD3}^-\text{CD122}^+\text{NK1.1}^-$) or mature NK cells ($\text{NK1.1}^+\text{CD27}^-\text{CD11b}^+$) (Fig. 3.8B). In contrast, the majority of thymic NK cells, identified by CD127 and Gata3 expression (Vosshenrich et al., 2006), expressed *Bcl11b* (Fig. 3.9A and 3.9B). Therefore *Bcl11b* can be considered as an additional marker to distinguish thymic NK cells from regular NK cells that develop in BM.

In other hematopoietic lineages, *Bcl11b* expression was not detected in B ($\text{B220}^+\text{CD19}^+$) or myeloid cells ($\text{CD11b}^+\text{Gr-1}^+$) (Fig. 3.10). Taken together, the T cell restricted expression of *Bcl11b* further suggests its importance in T cell lineage.

3.3. Discussion

In this chapter, I presented studies on the pattern and dynamics of *Bcl11b* expression in T cell, NK cell and other hematopoietic lineages using a *Bcl11b*-*tdTomato* knock-in reporter mouse. Without intracellular antibody staining, this

mouse strain accurately recapitulated *Bcl11b* expression at a single cell level. *Bcl11b* expression profiles in hematopoietic lineages showed that *Bcl11b* was a T cell specific transcription factor. In T cells, *Bcl11b* expression increased during T cell commitment while decreased after T cell activation, suggesting it may have multiple functions in T cell development and T cell-mediated immunity.

3.3.1. *Bcl11b* is T-cell specific

In the hematopoietic system, *Bcl11b* was absent in B cells, myeloid cells and most NK cells, but highly expressed in T cell lineages. Developmentally, its expression is tightly associated with T cell commitment. Early thymocytes, for example, start to express *Bcl11b* during the transition from ETP to DN2b, at a time when early thymocytes gradually lose non-T-cell potentials, implicating that *Bcl11b* plays an important role in this process. *Bcl11b* expression is maintained at high levels in T cells beyond DN2b stages (Tydell et al., 2007). Therefore, further experiments are required to study function of *Bcl11b* in T cells at different developmental stages. Additionally, using fluorescent tdTomato to mark *Bcl11b*, the *Bcl11b-tdTomato* knock-in reporter mouse is very useful to monitor T cell activities in vivo.

3.3.2. Advantages and pitfalls of *Bcl11b-tdTomato* knock-in mice

It is very helpful to use fluorescent protein knock-in mice to study expression profiles of transcription factors for the two reasons (Nolan et al., 1988). Firstly, the resolution of the gene expression profiles obtained from fluorescent protein reporter mice is at a single cell level. Secondly, the gene expression can be monitored real-time in live cells both in vitro and in vivo, as no fixation or antibody staining is

required. For example, cells that express the tagged gene can be conveniently observed by confocal microscope or sorted in flow cytometry.

Nevertheless, it is important to note that this approach has several pitfalls too. Firstly, it takes enormous time and resources to generate a fluorescent protein knock-in mouse line. Additionally, it is important to decide where to insert the fluorescent gene cassette because the insertion may affect the expression of the tagged gene or genes nearby. For example, in the *Bcl11b-tdTomato* knock-in mouse strain, the tdTomato cassette was inserted into the 3'UTR, where transcriptional and post-transcriptional regulatory machineries may bind, thus might affect *Bcl11b* expression. Moreover, genes encoding fluorescent proteins are separated with targeted genes by IRES in most cases which may interfere with the endogenous gene expression or protein translation (Mohrs et al., 2001). Finally, in the case of extensive post-transcriptional or post-translational regulation of Bcl11b, the tdTomato reporter might not recapitulate the true expression pattern of Bcl11b protein. To solve this problem, the endogenous gene locus maybe engineered so that it produces a fusion protein between the gene product and the fluorescent protein (Feltri et al., 1999; Telling et al., 1997). This approach, however, has its own shortcomings as the fusion protein may lose the activities of one or both proteins or change the original cellular localization of the tagged protein.

Chapter 4

BCL11B IS REQUIRED FOR EARLY T CELL DEVELOPMENT AND MAINTAINANCE OF T CELL IDENTITY

4.1. Introduction

4.1.1. Notch signaling in T cell development

Notch signaling plays a key role in T cell development (Harman et al., 2003; Radtke et al., 2010; Rothenberg et al., 2008). Interactions between Notch1 and its ligands of the Delta and Jagged families trigger the proteolytic cleavage of Notch1 and release its Notch intracellular domain (NICD). Then the NICD translocates from the cytoplasm to the nucleus, where it associates with the DNA-binding protein CSL (Rbpj) to activate genes downstream of Notch signaling (Kopan and Ilagan, 2009). Notch signaling triggers the initiation of the T cell program in hematopoietic progenitor cells. OP9 stromal cells obtain the capacity to induce the differentiation of hematopoietic progenitors into T cells after the Notch ligand Delta-like-1 that activates Notch signaling are forcefully expressed in them (Schmitt and Zuniga-Pflucker, 2002). Overexpression of a constitutively active form of Notch1 in hematopoietic progenitors leads to the development of T cells in the BM and arrested B cell development (Pui et al., 1999). In contrast, deletion of Notch or CSL in the thymus causes the disruption of T cell development and the accumulation of B cells in

the thymus possibly by a cell-extrinsic pathway (Feyerabend et al., 2009; Han et al., 2002; Radtke et al., 1999). Similarly, enforced expression of Dtx1, an antagonist of Notch1, results in B cell development at the expense of T cell development (Izon et al., 2002). Collectively, these studies suggest that Notch signaling controls the T-versus-B cell fate decision in lymphoid progenitors.

Notch signaling is also required to sustain early T cell development (Maillard et al., 2005; Radtke et al., 1999; Rothenberg, 2007). Indeed, loss of Notch signaling in DN1 cells converts them into dendritic cells (Feyerabend et al., 2009). In committed T cells, Notch signaling favors $\alpha\beta$ - versus $\gamma\delta$ -T cell lineage (Washburn et al., 1997; Wolfer et al., 2002), influences CD4 versus CD8 lineage decisions (Fowlkes and Robey, 2002), and regulates T-helper-2 (Th2) cell development partly through Gata3 (Amsen et al., 2009; Ho et al., 2009).

A recent study in *Drosophila* has indeed identified CG6530, the *Drosophila* orthologue of *Bcl11* genes, as a direct downstream target gene of Notch signaling (Krejci et al., 2009). Gene expression analysis in thymocytes reveals that Bcl11b is the most upregulated transcription factor at the transition from ETP to DN2b cell stage, suggesting the potential function of Bcl11b in early T cell development and its possible connection with Notch signaling (Tydell et al., 2007) (David-Fung et al., 2009).

4.1.2. Key transcription factors in T cells

Besides Notch1, other transcription factors also participate in regulating T cell development. For example, the transcriptional repressor Gfi1 is required for the development of early T cell progenitors and the CD4/CD8 lineage decision in the thymus (Yucel et al., 2003). Similarly, the basic helix-loop-helix transcription factor HEBAIt is expressed in pro-T cells and enhances the generation of T cell precursors

(Wang et al., 2006). The zinc finger transcription factor *Zbtb7b* (Th-POK), which appears to be repressed by Runx complexes (Setoguchi et al., 2008), regulates the CD4-versus-CD8 T-cell lineage commitment (He et al., 2008). *Tbx21* (T-bet), a T-box transcription factor, directs Th1 lineage commitment (Szabo et al., 2000). GATA-3 is necessary and sufficient for Th2 cytokine gene expression in CD4⁺ T Cells (Zheng and Flavell, 1997). Eomes, another T-box transcription factor, controls effector CD8⁺ T cell function (Pearce et al., 2003). Despite these advances, no single transcription factor had been identified for T cell lineage commitment and/or identity maintenance.

In the previous chapter, I showed different *Bcl11b* expression levels in T cell subsets. A recent study showed that *Bcl11b* binds to several regions within the *Zbtb7b* locus and possibly regulates differentiation from DP thymocytes to CD4⁺ T cells through *Zbtb7b* (Kastner et al., 2010). Further studies on cross-talk between *Bcl11b* and other T cell transcription factors are required to fully understand the transcription factor network that regulate T cell development and homeostasis.

4.1.3. NK cell-associated genes

Although NK cell developmental pathways are not entirely clear, several transcription factors have been identified as necessary for NK cell development. For example, the helix-loop-helix transcription factor *Id2*, which antagonizes the bHLH E proteins *Tcf3* (E2A) and *Tcf12* (HEB), is essential for full NK cell development since *Id2*-deficient mice exhibit a severe peripheral NK cell deficiency (Ikawa et al., 2001; Yokota et al., 1999). Conversely, forced expression of *Id2* or *Id3* is able to redirect pro-T cells to NK cell differentiation (Fujimoto et al., 2007; Spits et al., 2000). The basic leucine zipper (bZIP) transcription factor *Nfil3* (E4BP4), which acts in a cell-intrinsic manner 'downstream' of the IL-15 receptor and interacts with *Id2*, is

indispensable for the generation of the NK cell lineage. Overexpression of E4bp4 promotes NK cell generation from hematopoietic progenitor cells while a lack of E4bp4 impairs NK cell development and NK cell-mediated cytotoxicity (Gascoyne et al., 2009; Kamizono et al., 2009). Additionally, forced expression of a NK specific transcription factor, Zfp105, promotes differentiation from HSC to the NK cell lineage (Chambers et al., 2007). Additionally, deletion of *Sfp11* (PU.1), *Cbfb* (CBF β) or *Ets1* adversely affects NK cells but this is likely due to their important roles in the lymphoid lineages (Barton et al., 1998; Colucci et al., 2001; Guo et al., 2008).

Besides transcription factors, several molecules including receptors, cytokines, and enzymes are also important for NK cell development and homeostasis. *Il2rb* (CD122), which is one of the receptor subunits for IL-2 and IL-15, is required for NK cell proliferation and differentiation (Waldmann and Tagaya, 1999). *Il2rb*^{-/-} mice exhibited a reduction of peripheral NK cells and absence of NK cytotoxic activity in vitro (Suzuki et al., 1997). The cytokine lymphotoxin α (Lta), is secreted by lymphocytes including NK cells, and is important for NK cells as the number of NK cells is significantly reduced in *Lta*-deficient mice (Kuprash et al., 2002; Wang et al., 2008a; Ware et al., 1992). *Plcg2*, a member of Phosphatidylinositol (PI)-specific phospholipase C- γ enzymes is essential for NK cell cytotoxicity and innate immunity (Caraux et al., 2006; Wilde and Watson, 2001).

It is not known whether *Bcl11b* plays a role in NK cells though it is expressed in DN1 and DN2 thymocytes, which are considered as NK/T progenitors (Bell and Bhandoola, 2008; Wada et al., 2008). In the last chapter, I showed that *Bcl11b* was transiently expressed in some immature NK cells, but was absent in NKPs and mature NK cells. Based on *Bcl11b* expression profiles in T and NK cells, it is suggested that

Bcl11b may play a role in regulating the T-versus-NK cell lineage choice in DN1 and DN2 thymocytes.

4.1.4. Purposes of this chapter

In this chapter, I initially used microarray analysis to study the changes of global gene expression profile upon loss of Bcl11b in thymocytes using a Bcl11b conditional knockout mouse strain. Subsequently, I induced deletion of *Bcl11b* in early, committed and mature T cells in vitro to reveal function of Bcl11b in early T cell development and the maintenance of T cell identity. Then, I confirmed the function of Bcl11b in different T cell subsets using an in vivo tumor model. Finally, I showed that Notch signaling directly regulated Bcl11b.

4.2. Results

4.2.1. Bcl11b transcription regulation in T cells

To study Bcl11b functions in T cells, I used a *Bcl11b* conditional knockout mouse strain generated in the lab where exon 4 was floxed (Fig. 4.1). Exon 4 encodes three-quarters of the Bcl11b protein. *Bcl11b*^{lox/lox} mice were then crossed to the *Rosa26-Cre-ERT2* mice (Hameyer et al., 2007; He et al., 2010). *Rosa26*, which was originally identified in a gene-trap screen in murine ES cells, is a mouse genomic locus commonly used to knock-in cDNA constructs in transgenic mice because it is ubiquitously expressed during embryonic development and in adult mouse tissues (Nagy et al., 1993). Controlled by the regulatory elements of the *Rosa26* locus, the Cre-ERT2 fusion protein combines Cre recombinase and estrogen receptor (ER) and is retained in the cytoplasm but translocates to the nucleus upon addition of Tamoxifen or OHT (Brocard et al., 1997). Consequently, *Bcl11b* was ablated in all

the cells from *Cre-ERT2; Bcl11b^{flox/flox}* mice (referred to *flox/flox* in this study) after expression of Cre recombinase was induced by either Tamoxifen or OHT.

We cultured thymocytes from *flox/flox* mice and added OHT to the culture media. 48 hours after OHT treatment, Bcl11b protein was barely detectable on Western blot (Fig. 4.2). Deletion of *Bcl11b* was efficient in cells from the *flox/flox* mice. To probe gene expression changes immediately following *Bcl11b* deletion in T cells, we performed expression array analysis in whole thymocytes from *flox/flox* mice 24 and 48 hours following *in vitro* OHT treatment. Table 2 lists genes that exhibit at least a two-fold change in expression after *Bcl11b* deletion. 24 hours after OHT treatment, expression of T cell genes such as *Bcl11b*, *Tcrb* and *Cd3e*, had already downregulated. Within 48 hours after OHT treatment, expression of NK-cell-associated genes, such as *Id2*, *Nfil3*, *Klrd1*, *Lta*, *Plcg2*, *Ifng* (IFN- γ), and *Nkg7* that is expressed in activated T cell and NK cells (Cook et al., 2005; Turman et al., 1993), was significantly increased. The microarray results suggest that Bcl11b might suppress expression of NK cell-associated genes in T cells and might also induce or maintain the expression of T cell genes in T cells. Furthermore, Bcl11b expression became undetectable once DN2 thymocytes commit to NKPs while remained being at high level through T cell development. Taken together, I speculated that Bcl11b regulated the T-versus-NK cell lineage choice in NK/T progenitors.

4.2.2. *Bcl11b* is required for early T cell development

To investigate the function of Bcl11b in NK/T progenitors, we treated whole thymocytes from *flox/flox* and control (*CreERT2; Bcl11b^{flox/+}*, referred to *flox/+*) mice with OHT for 48 hours. Subsequently, DN1 thymocytes that have both T cell and NK cell potentials were sorted and cultured on OP9-DL1 stromal cells in T cell media (5.0 ng/ml IL-7 and 5.0 ng/ml Flt-3) for 2 weeks (Fig. 4.3). OP9-DL1 stromal cells

express Delta-Like-1 Notch ligand and support robust T cell development (Schmitt and Zuniga-Pflucker, 2002) while normally do not support NK cell development in the absence of IL-2 or IL-15 (Carotta et al., 2006; Rolink et al., 2006). 10 days after OHT treatment, all OP9-DL1 stromal cells were killed in the OHT-treated culture of the *flox/flox* DN1 thymocytes without IL-2 or IL-15 in T cell media. Similar killing activities are also observed when OP9-DL1 stromal cells are co-cultured with NK cells (Rolink et al., 2006). Therefore we speculated that these killer cells were similar to NK cells. Strikingly, I detected expression of NK cell surface markers such as NK1.1 and DX5 on these killer cells. I also checked cell surface expression of NKp46, which is primarily expressed on NK cells (Walzer et al., 2007). Flow cytometry analysis showed that 24% of the OHT-treated cultured thymocytes from *flox/flox* mice expressed NKp46 (Fig. 4.4A). These NKp46⁺ cells did not express T cell surface markers like CD3 or TCR β (Fig. 4.4A and 4.4B), indicating that they did not acquire or had lost T cell features despite being co-cultured with OP9-DL1 stromal cells for 14 days. Based on NKp46 and CD3 expression, it was clear that these OHT-treated cultures of DN1 thymocytes were heterogeneous, including NKp46⁺CD3⁻, NKp46⁻CD3⁻ and NKp46⁻CD3⁺ populations. As *Bcl11b* deletion efficiency usually cannot reach 100%, I checked the *Bcl11b* deletion efficiency in these populations by genomic PCR to investigate whether *Bcl11b* deletion was related to expression of NKp46 and CD3. The genotyping results showed that both alleles of the *Bcl11b* exon 4 had been deleted in these NKp46⁺CD3⁻ cells, whereas at least one copy of the *flox* allele was intact in the NKp46⁻CD3⁺ population (Fig. 4.5). In contrast to the OHT-treated *flox/flox* DN1 cells, the untreated *flox/flox* DN1 cells (Fig. 4.4C) or the OHT-treated control *flox/+* DN1 cells (Fig. 4.4A) proliferated rapidly on OP9-DL1 stromal cells, and many acquired CD3 expression but none were NKp46⁺. These

data thus demonstrated that the *Bcl11b* deficiency abolished T cell development at the early stage and produced NKp46⁺CD3⁻ cells from DN1 thymocytes.

Similarly, the OHT-treated DN2 thymocytes from the *flox/flox* mice produced NKp46⁺CD3⁻TCRβ⁻ cells in the T cell culture (Fig. 4.6A and 4.6B). OP9-DL1 stromal cells were also destroyed. In contrast, the control *flox/flox* DN2 thymocytes without OHT treatment (Fig. 4.6C) and the OHT-treated *flox/+* DN2 thymocytes (Fig. 4.6A) proliferated extensively on OP9-DL1 cells and gave rise to CD3⁺ cells but not NKp46⁺CD3⁻ cells. These results again demonstrated that *Bcl11b* was also required for DN2 thymocytes to differentiate towards T cells. During early T cell development, *Bcl11b* is thus an essential regulator to promote T cell development and/or to suppress NK cell development in NK/T progenitors.

4.2.3. *Bcl11b* is required for committed T cells

DN3 thymocytes lose NK cell and myeloid cell potentials, when they commit to the αβ-T cell lineage at this stage (Bell and Bhandoola, 2008; Huang et al., 2005; Wada et al., 2008). To determine whether committed DN3 thymocytes regain NK or other lineage potentials following the loss of *Bcl11b*, we repeated the *Bcl11b* deletion experiments using purified DN3 thymocytes and cultured them on OP9-DL1 stromal cells in T cell media. Within 14 days, 13% of the OHT-treated *flox/flox* DN3 cells became NKp46⁺TCRβ⁻ (Fig. 4.7, right), while the OHT-treated *flox/+* DN3 cells (Fig. 4.7, left) and the OHT-non-treated *flox/flox* DN3 cells proliferated and differentiated towards TCRβ⁺ T cells (Fig. 4.8). The cells from the culture of OHT-treated *flox/flox* DN3 cells in the culture with IL-2 or IL-15 grew faster than the ones in T cell media only. Also, with IL-2 or IL-15, the percentages of NKp46⁺ cells increased and these cells started to kill stromal cells within 10 days after OHT treatment (Fig. 4.8A and 4.8B). Therefore supplementation of IL-2 or IL-15 in the culture media greatly

promoted proliferation and/or differentiation of the NKp46⁺TCRβ⁻ cells. These results show that even committed DN3 T thymocytes exhibited NK cell properties upon loss of Bcl11b.

To confirm that these NKp46⁺CD3⁻ cells were directly reprogrammed from thymocytes rather than due to the presence of contaminating NK cells, we examined their TCRβ locus for the DNA rearrangements. These NKp46⁺CD3⁻ cells retained the TCRβ V(D)J recombination even though the TCRβ was not expressed, thus genetically confirming the thymocyte origin of NKp46⁺CD3⁻ cells (Fig. 4.9). We thus named these killer cells that were reprogrammed from T cells as Induced T-to-Natural-Killer (ITNK) cells.

Because loss of Bcl11b enables DN3 thymocytes to acquire NK cell potential, which is lost together with B cell and myeloid cell potentials during T cell commitment, I speculated that *Bcl11b*-deficient T cells might also possess potentials to differentiate to B cells or myeloid cells in proper conditions. To test these possibilities, I co-cultured the OHT-treated *flox/flox* DN3 thymocytes with OP9 stromal cells that support B cell proliferation and differentiation in B cell media (Nakano et al., 1994). After three weeks, NKp46⁺ ITNK cells, but not B cells (CD19⁺), were detected in the cultures. In contrast, the OHT-treated *flox/+* control DN3 thymocytes expressed neither CD19 nor NKp46 and eventually died, as B cell potential was lost in DN3 thymocytes (Fig. 4.10). Similarly, the development of ITNK cells from *Bcl11b*-deficient thymocytes was an intrinsic property of the mutant thymocytes as ITNK cells were readily produced, but no myeloid cells were detected, from the OHT-treated *flox/flox* DN3 thymocytes culture in myeloid cell culture condition (Fig. 4.11). While the OHT-treated *flox/+* control DN3 thymocytes expressed neither CD11b nor NKp46 in myeloid culture. These results demonstrated

that *Bcl11b*-deficient DN3 cells reacquired NK-, but not B- or myeloid-cell properties, and suggested that *Bcl11b* maintains the T cell identity and specifically suppresses NK potentials in committed T cells.

4.2.4. Reprogramming efficiency from T cells to ITNKs upon *Bcl11b* ablation

To estimate the reprogramming efficiency of the *Bcl11b*-deficient DN3 thymocytes, I sorted single DN3 T cells from the OHT-treated whole thymocytes from *flox/flox* mice into individual wells of 96-well plates that were pre-seeded with OP9-DL1 stromal cells. These DN3 cells were cultured in T cell media with or without IL-2 supplementation (Fig. 4.12). Out of the 79 wells that had cells growing, 36 wells had many fast-proliferating T cells (Fig. 4.13). PCR genotyping confirmed that these T cells had deleted only one *flox* allele of *Bcl11b*, while the other conditional knockout allele remained intact (Fig. 4.14 Lanes T1 and T2). These cells, nevertheless, served as excellent controls for Cre toxicity because they had activated Cre recombinase but retained expression of *Bcl11b* for robust T cell development. In the other 43 wells, stromal cells were killed and most live cells were NKp46⁺CD3⁻, again demonstrating reprogramming of DN3 thymocytes to ITNKs (Fig. 4.13). The DN3-derived ITNKs had great proliferation potential, since up to 0.5 million ITNK cells were readily produced from a single DN3 thymocyte in 2-3 weeks post OHT treatment in the presence of IL-2. IL-2 or IL-15 was clearly able to promote proliferation of ITNKs substantially because, in absence of IL-2 or IL-15, only about 50,000 cells that also killed stromal cells were obtained from a single DN3 thymocyte under otherwise identical culture conditions. This result again demonstrated that the IL-2/15 signaling, which is essential for normal NK cell development (Waldmann, 2006), was dispensable for the generation and function of ITNKs. As expected, the

PCR genotyping results showed that the cells from all the 43 wells containing ITNKs had lost both *Bcl11b* alleles (Fig. 4.14 Lanes I1 and I2). Moreover, ITNKs of individual wells possessed unique rearranged TCR β loci, thus confirming their independent thymocyte origins (Fig. 4.15). Therefore, once *Bcl11b* was deleted, the reprogramming efficiency of DN3 thymocytes to ITNKs could reach 100%.

4.2.5. *Bcl11b* is required in mature T cells

We next investigated whether *Bcl11b* was required for the maintenance of T cell identity in mature T cell subsets. The OHT-treated DP thymocytes, CD4⁺, CD8⁺ splenic T cells, and $\gamma\delta$ T cells from *flox/flox* mice were sorted and co-cultured with OP9-DL1 in T cell media plus IL-2. ITNKs (NKp46⁺) that effectively killed the stromal cells were found growing in the DP thymocytes cultures within 10 days after *Bcl11b* deletion (Fig. 4.16). These ITNKs, in contrast to those reprogrammed from early T cells, retained TCR β expression. While the OHT-treated *flox/+* control DP thymocytes as control died eventually in the culture within 2 weeks. ITNKs that were NKp46⁺CD8⁺ could also be derived from the OHT-treated *flox/flox* CD8⁺ T cells but not from the OHT-treated *flox/+* CD8⁺ T cells in cultures (Fig. 4.17). Thus, *Bcl11b* is required to sustain T cell identity in mature T cell subsets. Moreover, the fact that ITNKs derived from mature T cell subsets retained T cell surface markers even after the acquisition of NK markers suggested that T cells reprogrammed to ITNKs directly, instead of dedifferentiating towards progenitors at first, upon loss of *Bcl11b*.

Interestingly, I was unable to obtain consistent reprogramming results from *Bcl11b*-deficient splenic CD4⁺ T cells, or from thymic $\gamma\delta$ -T cells, using the same culture condition. These T cells appeared prone to cell death once *Bcl11b* was deleted. A possible reason could be that our in vitro culturing conditions were not yet optimized for the reprogramming of these T cell subsets.

4.2.6. ITNKs detected in Tamoxifen-treated *flox/flox* mice

To assess whether different T cell subsets including splenic CD4⁺ and thymic $\gamma\delta$ -T cells can reprogram to ITNKs in vivo, we treated the *flox/flox* mice with Tamoxifen to induce *Bcl11b* deletion and culled the mice for analysis two weeks later (Fig. 4.18). This experiment could also help us rule out the possibility that the reprogramming from T cells to ITNKs was an in vitro artifact rather than the direct consequence of *Bcl11b* ablation. Compared to Tamoxifen-treated *flox/+* mice as controls, thymi of the *flox/flox* mice were smaller and contained less thymocytes, suggesting the importance of Bcl11b in thymocyte homeostasis. The size and cellularity of the spleen were not affected by loss of Bcl11b. It was possible that other hematopoietic cells compensated for the space left by T cells in the spleen. Similar phenotypes with respect to cellularity were also observed in other studies using different Cre systems to induce deletion of *Bcl11b* in vivo (Albu et al., 2007; Kastner et al., 2010). By FACS, we detected ITNKs in both the spleen (NKp46⁺CD3⁺) and thymus (NKp46⁺CD3⁺ and NKp46⁺CD3⁻) from *flox/flox* mice but not from *flox/+* controls (Fig. 4.19). Similar to ITNKs that were derived from DP thymocytes or mature T cells in vitro, the majority of ITNKs in *flox/flox* mice maintained expression of their T cell surface markers, such as CD3 and TCR β . To confirm that the production of ITNK was caused by the loss of Bcl11b, we sorted different ITNK populations and examined whether the *Bcl11b* conditional knockout alleles had been deleted in ITNKs. PCR genotyping results showed that the in vivo reprogrammed ITNKs from the thymus had lost both copies of Bcl11b alleles, while the rest of the thymocytes from *flox/flox* mice retained at least one copy of *Bcl11b* allele (Fig. 4.20). Most of the NKp46⁺CD3⁺ cells in the spleen had Bcl11b deficiency, while analyzing the *Bcl11b*-deficiency in NKp46⁺CD3⁻ ITNKs was complicated due to the presence of

conventional NK cells (Fig. 4.20). Conventional NK cells constitute about 3% of splenocytes but cannot be distinguished from NKp46⁺CD3⁻ ITNKs that were reprogrammed from early T cells in the thymus and migrated out of the thymus to the periphery, thus these conventional NK cells might overshadow the presence of NKp46⁺CD3⁻ ITNKs in the spleen. Previously, we showed that CD8⁺, but not CD4⁺ splenocytes could reprogram to ITNKs after loss of Bcl11b in vitro. Here, ITNKs (NKp46⁺) expressing CD4, CD8 (Fig. 4.21) and TCR $\gamma\delta$ (Fig. 4.22) were found in the spleen of Tamoxifen-treated *flox/flox* mice, but not in *flox/+* controls, suggesting that CD4⁺ mature T cells and $\gamma\delta$ -T cells had the potential to be reprogrammed to ITNKs. Thus, the in vivo microenvironment facilitates the reprogramming from some T-cell subsets to ITNKs upon loss of Bcl11b better than the OP9-DL1 co-culture system.

Natural killer T (NKT) cells are a subgroup of T cells that share properties of both T and NK cells. However, ITNKs detected here were not NKT cells, because NKT cells do not express the cell surface marker NKp46 (Walzer et al., 2007). Additionally, ITNK cells did not recognize glycolipids presented by CD1d molecules. In fact, CD1d-restricted NKT cells decreased in *flox/flox* mice after being treated with Tamoxifen (Fig. 4.23), indicating that Bcl11b was required for both conventional T cells and CD1d-restricted NKT cells (Kastner et al., 2010).

The in vivo reprogrammed ITNKs could readily be expanded in NK culture conditions (100 ng/ml IL-2). The percentages of ITNKs (NKp46⁺CD3⁺) in splenocytes and thymocytes from *flox/flox* mice increased substantially after two weeks culture, whereas no ITNKs were detected in cultured splenocytes or thymocytes from *flox/+* mice (Fig. 4.24). In addition, we speculated that some NKp46⁺CD3⁻ cells in the culture of *flox/flox* splenocytes and thymocytes were ITNKs, which might be derived from early thymocytes. Furthermore, these ITNKs

stained negatively with CD1d dimer, further confirming that ITNKs were not NKT cells (Fig. 4.25).

4.2.7. Reprogramming from T cells to ITNKs in vivo

The above experiments in which *flox/flox* mice were treated with Tamoxifen showed the in vivo ITNK production from various T cell compartments. However, analyzing ITNKs in these mice was complicated by the presence of host T and NK cells. To address this problem, we transferred 2-4 million DP thymocytes from OHT-treated whole thymocytes of *flox/flox* mice (CD45.2⁺) into *Rag2^{-/-}Il2rγ^{-/-}* mice (CD45.1⁺) that have no B, T or NK cells (Fig. 4.26) (Colucci et al., 1999). These recipient mice thus enabled us to easily identify and analyze the reprogrammed ITNKs. I chose DP thymocytes because they usually account for more than 75% of total thymocytes and could be efficiently reprogrammed to ITNKs in vitro. Additionally, as committed T cells, DP thymocytes have lost NK cell potential. Two weeks post transplantation, we found that around 5% of splenocytes were from the donor cells (CD45.2⁺). Approximately 47% of the donor-derived splenocytes expressed NKp46 and CD3 (Fig. 4.27). Moreover, these NKp46⁺CD3⁺ cells had lost both copies of *Bcl11b* while the donor-derived NKp46⁻ cells still retained at least one copy of the *Bcl11b* allele (Fig. 4.28). Therefore the reprogramming from *Bcl11b*-deficient DP thymocytes to ITNKs in immune deficient mice was a cell-autonomous process.

In *Rag2^{-/-}Il2rγ^{-/-}* mice, the majority of NKp46⁺ ITNKs expressed CD8 and TCRβ, and no CD4⁺ ITNKs were detected (Fig. 4.29), suggesting the reprogramming from *Bcl11b*-deficient DP thymocytes to CD4⁺ ITNKs was not favored in this in vivo microenvironment. However, we did not know whether these CD8⁺NKp46⁺ ITNKs were derived directly from *Bcl11b* deficient DP thymocytes. Alternatively, these DP

thymocytes might have differentiated to CD8⁺ T cells before reprogramming to ITNKs. It was also possible that the differentiation and reprogramming processes could take place simultaneously.

Besides the spleen NKp46⁺ ITNK cells were also detected in the bone marrow and peripheral blood (Fig. 4.30). As there were about 5 million splenocytes in each recipient mouse, we estimated that there were 200,000 ITNK cells in the spleen alone. No NKp46⁺ cells were found in control mice transplanted with OHT-untreated DP thymocytes (Fig. 4.27). ITNK cells were maintained in the recipient mice for at least 3 months without changes to the cell number, perhaps reflecting a homeostasis of ITNKs. Importantly, the recipient mice did not show any noticeable abnormalities, indicating that ITNK cells did not indiscriminately kill normal host cells or exhibit any malignant transformation in the recipient mice.

4.2.8. *Bcl11b* is positively regulated by Notch signaling

During T cell specification and commitment, it is proposed that *Bcl11b* is regulated by Notch signaling (Rothenberg, 2007). The fact that ITNKs were readily produced from *Bcl11b*-deficient DN1, DN2 and DN3 thymocytes in co-culture with either OP9 or OP9-DL1 stromal cells (Fig. 4.31 and 4.10) demonstrated that T cells would reprogram to ITNKs upon loss of *Bcl11b* in vitro regardless of the presence of external Notch ligands. Thus *Bcl11b* might be one of the downstream genes regulated by Notch signaling in T cells.

To confirm this, we searched within the *Bcl11b* gene locus for the putative CSL (Rbpj)-binding sites (CGTGGGAA) (Tun et al., 1994). Several CSL sites were identified which were conserved between the mouse and human *Bcl11b* genes (Fig. 4.32). ChIP assays were subsequently performed using a CSL polyclonal antibody to pull down the genomic DNA fragments from T cells cultured on OP9-DL1 stromal

cells. The primers flanking the putative CSL binding regions were designed to amplify the ChIP pull-down genomic DNA. Three regions were greatly enriched in the T cell samples using the CSL antibody compared to the control (Fig. 4.33). The ChIP results thus strongly suggested that the canonical Notch signaling directly regulated *Bcl11b* at the transcription level. Moreover, it is reported that deletion of CSL (*Rbpj*) in Mx-Cre transgenic mice after injection of poly(I)-poly(C) results in a block of T cell development at the earliest stage and an increase of B cell development in the thymus (Han et al., 2002). This phenotype is very similar to that in a *Notch1* knockout mouse using the Mx1-Cre system (Radtke et al., 1999). However, we could not rule out the possibility that *Bcl11b* was regulated by other signaling pathways. Therefore, we proposed the following model to summarize the regulation and function of *Bcl11b* in T cells (Fig. 4.34).

4.3. Discussion

In this Chapter, I demonstrated that *Bcl11b* had essential roles in early T cell development and in the maintenance of T cell identity. Positively regulated by Notch signaling, *Bcl11b* suppressed key NK cell-associated genes expression and might positively regulate key T cell genes in T cells. Acute loss of *Bcl11b* made DN1 and DN2 thymocytes lose their T cell potential and differentiate to NK-like cells. Strikingly after *Bcl11b* ablation, DN3, DP thymocytes, and mature CD8⁺ T cells also lost T cell identity and reprogrammed to ITNKs in OP9-DL1 co-culture system. Similarly, ITNKs reprogrammed from various T cell subsets were also detected in vivo models. Additionally, transplantation experiments showed the reprogramming was a cell autonomous process. In summary, T cells at different developmental stages reprogrammed to ITNK upon loss of *Bcl11b*. Therefore *Bcl11b* was crucial to sustain T cell development in different T cell subsets (Fig. 4.35).

4.3.1. Deletion of *Bcl11b* using different Cre systems

T cell development is impaired beyond the DN3 stage, while DN1, DN2 and $\gamma\delta$ -T cells seems to be intact, in the fetal thymus of a *Bcl11b* germline knockout mouse (Wakabayashi et al., 2003b). However, a recent study using the same knockout strain shows that *Bcl11b*-deficient thymocytes are arrested at DN2 stages and acquired self-renewal properties in vitro (Ikawa et al., 2010). Our results, together with a study from Rothenberg's lab, show that *Bcl11b*-deficient DN1 and DN2 thymocytes stopped T cell development and acquired other cell potentials in the adult thymus (Li et al., 2010). Taken together, both fetal and adult early T cells needed *Bcl11b* to sustain T cell development and suppressed non-T cell potentials. However, unlike *Bcl11b*-deficient fetal $\gamma\delta$ -T cells, adult $\gamma\delta$ -T cells also reprogrammed to ITNKs upon loss of *Bcl11b*, suggesting that fetal and adult $\gamma\delta$ -T cells may require different transcription networks during development.

Using different Cre system to delete *Bcl11b* generates different phenotypes. For example, in *CD4-Cre; Bcl11b^{lox/lox}* mice, a reduction of $CD4^+$ and $CD8^+$ SP thymocytes is observed and *Bcl11b*-deficient DP thymocytes commit to apoptosis (Albu et al., 2007; Kastner et al., 2010). Additionally, $CD8^+$ T cells have reduced clonal expansion and cytolytic activity when *Bcl11b* ablation is induced by dLck-iCre (Zhang et al., 2010). Expression of both *CD4* and *Lck* is detected in early T cells (Lee et al., 2001; Wildin et al., 1995), thus DP thymocytes and mature T cells may have lost *Bcl11b* since they were early T cells in these two studies. In contrast, after acute loss of *Bcl11b*, we found that DP thymocytes and mature T cells reprogrammed to ITNKs both in vitro and in vivo. Thus deletion of *Bcl11b* in T cells at different stages may thus cause different phenotypes.

4.3.2. Possible factors affecting reprogramming efficiency

The efficiency of reprogramming from T cell to ITNK varies in different T cell subsets. For example, DN3, DP thymocytes, and CD8⁺ splenic T cells could be efficiently reprogrammed to ITNKs upon loss of Bcl11b in vitro, whereas *Bcl11b*-deficient CD4⁺ splenic and $\gamma\delta$ -T cells underwent apoptosis instead of reprogramming to ITNK in the same culture condition. Here are three possible reasons to explain why different T cell subsets had different abilities of reprogramming.

First, a suitable in vitro reprogramming condition has not been identified yet for *Bcl11b*-deficient CD4⁺ T cells and $\gamma\delta$ -T cells. It is possible that different T cells require different reprogram conditions. For example, OP9-DL1 stromal cells do not normally support CD4⁺ T cells for proliferation and differentiation because they do not express MHC-II molecules that are required for differentiation of CD4⁺ T cells (Schmitt and Zuniga-Pflucker, 2002). It is possible that MHC-II molecules are also required for *Bcl11b*-deficient CD4⁺ T cells to reprogram to ITNK cells. This may explain why CD4⁺ T cells failed to reprogram to ITNK in the OP9-DL1 co-culture system. In fact, *Bcl11b*-deficient CD4⁺ T cells were able to reprogram to ITNKs in vivo, where MHC-II molecules are available. However, this hypothesis cannot explain the blockage of reprogramming from $\gamma\delta$ -T cell to ITNK in vitro, because OP9-DL1 stromal cells support $\gamma\delta$ -T cells development.

The second explanation could be that *Bcl11b*-deficient mature CD4⁺ T cells and $\gamma\delta$ -T cells are more prone to apoptosis than other *Bcl11b*^{-/-} T cell subsets in vitro. In contrast, the apoptosis in these cells could be prevented in vivo, possibly because the in vivo microenvironment can provide suitable cytokines and cell-cell interactions at physiological conditions. This may explain why CD4⁺ and TCR $\gamma\delta$ ⁺ ITNKs were

detected in OHT-treated *flox/flox* mice but not in OP9-DL1 co-culture system. If this hypothesis is true, the addition of apoptosis inhibitors in culture should facilitate reprogramming from CD4⁺ and $\gamma\delta$ -T cell to ITNKs. The apoptosis caused by loss of Bcl11b could also depend on the cellular context. For example, Bcl11b might induce *Gata3* expression as loss of Bcl11b caused downregulation of Gata3 (shown in Chapter 5). Also, CHIP-seq experiments suggest that Bcl11b directly regulates *Zbtb7b*, which is essential for CD4⁺ T cells and $\gamma\delta$ -T cells but not for other T cell subsets (He et al., 2008; Park et al., 2010). Consequently, a decrease of Gata3 or *Zbtb7b* might specifically cause apoptosis of *Bcl11b*-deficient CD4⁺ T cells and $\gamma\delta$ -T cells.

Thirdly, I believe that the more similar two cell types are, the less changes in cellular components, transcription networks, protein synthesis, and epigenetic modifications are required for the reprogramming from one to the other. Therefore the similarities between two types of cells affect the reprogramming feasibility upon genetic manipulation. For example, induced pluripotent stem (iPS) cells have been generated from human somatic cells by overexpression of Oct3/4, Sox2, Klf4, Nanog and other defined factors (Takahashi et al., 2007; Yu et al., 2007). However, compared to other stem cells, such as HSC, neural stem cells (NSC) exhibit more similar transcriptional profiles to ES cells. Overexpression of Oct4 alone thus is sufficient to facilitate their reprogramming to iPS cells (Kim et al., 2009; Ramalho-Santos et al., 2002). Compared to mature CD4⁺ T cells, cytotoxic CD8⁺ T cells are more similar to NK cells. Both CTLs and NK cells express Eomes and T-bet at higher levels than CD4⁺ cells (Intlekofer et al., 2005; Szabo et al., 2000), while CD4⁺ expressed higher level of *Zbtb7b* than CD8⁺ and NK cells (Setoguchi et al., 2008). In addition, CTLs and NK cells use polarized secretion of the cytotoxic granules

containing granzymes and perforin to destroy virus-infected and tumorigenic target cells. These molecules are usually absent in CD4⁺ T cells. They also use a novel secretory mechanism, with the centrosome polarizing to the precise site of secretion within the immunological synapse (Blott and Griffiths, 2002; Griffiths et al., 2010; Stinchcombe et al., 2006). Taken together, it is not difficult to conceive that it may be easier for CD8⁺ T cells, especially activated ones assembling with more NK features, to reprogram to ITNKs than CD4⁺ T cells.

4.3.3. “Unconventional NKT cells” in wild type mice

Previous studies show some mature CD8⁺ T cells can exhibit some NK features following activation, indicating the similarity between NK cells and activated CD8⁺ T cells. For example, it is reported that some NK1.1⁺TCR $\alpha\beta$ ⁺CD8⁺ cells can be derived from activated CD8⁺ T cells upon stimulation with IL-2, IL-4, or IL-15 in vitro. These ‘unconventional NKT’ cells express CD122 and most Ly49 receptors (Assarsson et al., 2000). Similar to CD8⁺NK1.1⁺ cells, these non-CD1d-restricted cells can also be derived from tumor-bearing mice (Stremmel et al., 2001). These “unconventional NKT” cells can produce large amount of IFN- γ following activation and have a potent NK-like cytotoxic activity against multiple tumor targets regardless to MHC-I or non-classical MHC-I molecules (Stremmel et al., 2001). However, these “unconventional NKT” cells need further characterization for their expression of Bcl11b, more NK cell surface markers, such as NKp46, and for their global gene expression profiles before claiming that they are regular NK cells or ITNKs.

4.3.4. Dynamic balance of ITNKs in vivo

It is interesting to note that the total number of ITNKs in *Rag2*^{-/-}*Il2r γ* ^{-/-} mice did not either correlate with the initial number of injected *Bcl11b*-deficient DP T cells or

change markedly overtime in the hosts. It was likely that the homeostasis of ITNK cells was well maintained in *Rag2^{-/-}Il2rγ^{-/-}* mice. There are many factors likely to contribute the dynamic balance of ITNK cells *in vivo*. Due to the similarity between NK cells and ITNKs, the cytokines and cell-cell interactions that are important for NK cells may play a role for the homeostasis of ITNKs *in vivo*. For example, signals from IL-2 receptors provide essential positive homeostatic functions for NK cells and promoted proliferation of ITNKs as shown in the chapter 4 (Lodolce et al., 1998). Thus the availability of IL-15 and IL-2 can be one of the limiting factors. Other cytokines like IL-12, IL-18, IL-21 and TGFβ might also regulate ITNK cell homeostasis, as they are important for NK cell homeostasis (Laouar et al., 2005; Zwirner and Domaica, 2010). The expansion of ITNKs might also be affected by limited chemokines such as CCL19 and CCL21, of which co-stimulation can promote the proliferation of CD56^{lo}CD16⁺ NK cells in human (Robertson, 2002). The total number of ITNKs in *Rag2^{-/-}Il2rγ^{-/-}* mice might also be determined by the availability of adhesion molecules on the cell surface of stromal cells in the BM and spleen, as these adhesion molecules are known to affect NK cell homeostasis (Huntington et al., 2007). Additionally, the cross-talks between NK cells and other lymphocytes may also regulate the homeostasis of NK cells (Ferlazzo and Munz, 2009). Although adaptive immunity is absent in the *Rag2^{-/-}Il2rγ^{-/-}* host mice, it is possible that some dendritic cells participated to control the total number of ITNKs in host (Degli-Esposti and Smyth, 2005; Di Santo, 2008).

Chapter 5

CHARACTERIZATION AND APPLICATION OF ITNKs

5.1. Introduction

5.1.1. Cancer immunotherapy

The immune system is alert to not only external biological invasion from virus infection but also transformed tumor cells within the host. Many groups in the area of cellular therapy have exploited the application of cancer immunosurveillance to treat cancer (Rosenberg et al., 2004; Zitvogel et al., 2006). There are three main approaches in cancer immunotherapy: non-specific immunomodulation, cancer vaccines, and adoptive cell transfer (ACT) (Rosenberg and Dudley, 2009). In non-specific immunomodulation, cancer patients are administrated with IL-2 that can activate endogenous tumour-reactive cells, mainly T cells and NK cells in vivo (Rosenberg et al., 1985; Rosenberg et al., 1998). Thanks to the identification of a large number of human cancer antigens, cancer vaccines that are based on immunizing cancer patients against their autologous cancers using either whole cells, proteins and peptides, have been developed since 1990s (Rosenberg and Dudley, 2009; van der Bruggen et al., 1991). However, these two approaches are not as effective or promising as strategies using ACT of anti-tumor lymphocytes that are grown ex vivo and then infused into the cancer patient. ACT has the following advantages (Rosenberg et al., 2008). Firstly, a small number of anti-tumour lymphocytes with the appropriate properties can be identified and then expanded to

large numbers *ex vivo* for treatment (Rosenberg and Dudley, 2009). Secondly, the lymphocytes can be activated *in vitro* to avoid endogenous inhibitory factors, such as T regulatory cells and TGF β . In addition, ACT can often be combined with vaccines or growth factors that can augment the *in vivo* impact of the transferred lymphocytes. Finally, it is possible to manipulate the host before cell transfer to provide an optimal environment for the transferred cells (Rosenberg and Dudley, 2009). For example, prior to ACT, radiotherapy and chemotherapy are usually used to reduce tumor burden and deplete endogenous lymphocytes that compete with transferred lymphocytes for homeostatic cytokines (Hogan and Rothenberg, 2008; Rosenwasser and Rothenberg, 2010).

Cytotoxic T lymphocytes (CTLs) are the main source of cells in ACT (Rothenberg et al., 2008). However, in T cell-based therapy, direct immunological pressure from T cells on tumour cells can lead to the outgrowth of tumour clones which express low or no human leukocyte antigens (HLA) (Chang and Ferrone, 2007; Dunn et al., 2004; Smyth et al., 2006) or that have lost the targeted antigen (Yee et al., 2002). The development of ACT using tumour-infiltrating lymphocytes (TIL), which are mainly CD8⁺ T cells and can be expanded in IL-2, improves the tumour-specific activity in transferred cells and the immunization of lymphocyte donors (Muul et al., 1987; Rosenberg et al., 1986). However, the persistence of the transferred TILs *in vivo* is short (Rosenberg et al., 2008).

Evading tumour cells which have way low or no HLA antigens are nevertheless ideal targets for NK cells, because NK cells detect and kill tumor variants which lack MHC class I expression (Karre, 2008). In some trials, it was more effective to use alloreactive NK cells in cancer immunotherapy due to the mismatch between inhibitory receptors on NK cells and HLA on tumour cell surface (Ruggeri et al.,

2002). However, there are at least two hurdles to overcome before successful application of NK cells in ACT. Adoptive NK cell therapy requires large numbers of cells with a well-defined phenotype and high purity to be produced. This is difficult to achieve practically because the isolation, culture, and expansion of clinical NK cell products has been hampered by their relatively low representation in the blood. The other reason for this difficulty is that the in vitro proliferation potential of NK cells in IL-2 and IL-15 is limited (Carlens et al., 2001), despite some recent advances (Alici et al., 2008). In addition, the transferred NK cells must persist long enough to affect tumor killing (Robbins et al., 2004). Even with IL-2, however, transferred NK cells gradually lose killing ability in about 2 weeks (Miller et al., 2005) (Yee et al., 2002). Therefore, neither T cells nor NK cells are ideal sources for ACT.

5.1.2. Purposes of this chapter

In this chapter, I will characterize gene expression features of ITNKs and examine their capacity for killing tumour cells both in vitro and in vivo. The results from these experiments implicated ITNKs as a potentially new cellular product for ACT in cancer immunotherapy.

5.2. Results

5.2.1. Gene expression profile in ITNKs

In previous chapters, I showed that ITNKs (NKp46⁺CD3⁻) that were derived from *Bcl11b*-deficient DN3 thymocytes in vitro resembled NK cells, as they expressed NK cell surface markers, killed stromal cells, and grew in NK culture conditions. Another important criteria to judge the similarity between the two types of cells is to compare their gene expression profiles. Studies on gene expression profiles of ITNK cells could also help us dissect the molecular mechanisms involved in the

reprogramming from T cells to ITNKs. Therefore, I performed gene expression microarray using mRNA from DN3 thymocytes, normal splenic NK cells that were expanded in vitro after enrichment (lymphokine-activated killer, or LAK cells, composed of >90% NK cells), and DN3-derived ITNKs in microarray analysis. The heat map showed that the global expression profile of these ITNKs was much more similar to that of LAKs than to that of their parental DN3 thymocytes (Fig. 5.1). To quantify the similarity between ITNKs and LAKs, we conducted further analysis from the array data and identified 504 genes that were expressed at least two-fold higher in LAKs vs. DN3 thymocytes, and 366 genes in ITNKs vs. their parental DN3 thymocytes. 70% of these 366 genes in ITNKs were also found to be overexpressed in LAKs (Fig. 5.2).

Genes with differential expression levels between the parental DN3 thymocytes and ITNK cells were listed in Table 3. I selected some key T and NK genes from the list and validated their expression by performing qRT-PCR. The qRT-PCR results showed that the expression of many T lineage genes, such as *Notch1*, *Est1*, *Hes1*, *Gata3*, *Dtx1* and *Tcf1*, was decreased, while the expression of genes important in NK cells such as *Id2* (Boos et al., 2007), *Il2rb* (CD122), *Zfp105* (Chambers et al., 2007) and *Nfil3* (Gascoyne et al., 2009) was greatly upregulated in ITNKs, compared to their parental DN3 thymocytes (Fig. 5.3A). Among the upregulated genes in ITNKs, *Zbtb32* (Rog, Repressor of GATA), which prevents GATA3 from binding to DNA and regulates T cell activation, was highly expressed in ITNKs but absent in DN3 cells (Miaw et al., 2000; Omori et al., 2003). Expression of *Cdkn1c* (p57KIP2), a putative direct downstream target gene of Bcl11b (Topark-Ngarm et al., 2006), was barely detectable in DN3 thymocytes but drastically increased in ITNKs, confirming that Bcl11b suppresses its expression (Fig. 5.3B). These results thus collectively

demonstrated that Bcl11b was essential for maintaining the T cell expression profile and for suppressing NK cell-associated gene expression.

5.2.2. Characterization of ITNKs derived in vitro

Besides analysis of gene expression profiles, we found that ITNKs reprogrammed from single DN3 thymocytes were morphologically similar to LAK cells. ITNKs were larger in size and had larger cytoplasm than thymocytes (Fig. 5.4). Moreover, images from transmission electronic microscopy show that ITNKs had enlarged granules and showed evidence of high protein synthesis activity with abundant endoplasmic reticulum (Fig. 5.5).

To further examine NK features in ITNK cells, I examined the expression of more cell surface markers and genes that are expressed in NK cells. Flow cytometry analysis showed that ITNK cells derived from DN3 thymocytes in vitro expressed other NK genes such as NKG2A/C/E, Trail, perforin and IFN- γ , (Fig. 5.6, Table 4), but not some other key NK function genes, such as members of the Ly49 family (Fig. 5.7). Similarly, ITNK cells that were reprogrammed from DP thymocytes also expressed NKG2A/C/E, but did not express members of the Ly49 family (Fig. 5.8).

Recently, thymic NK cells that originate in the thymus were identified by expression of Gata3 and CD127 (Vosshenrich et al., 2006). DN3 thymocyte-derived ITNKs, however, did not express CD127 and were therefore unlikely to be related to thymic NK cells (Fig. 5.9). Interestingly, unlike conventional mature NK cells that are CD27⁻CD11b⁺, most DN3-derived ITNKs expressed CD27 but not CD11b, both of which are used to define maturity of NK cells (Colucci et al., 2003) (Fig. 5.10). These results showed the distinctions between ITNKs and normal NK cells.

5.2.3. Characterization of ITNKs derived in vivo

As I showed in Chapter 4, different T cell subsets reprogrammed to ITNKs in vivo in a cell-autonomous manner upon loss of Bcl11b. Flow cytometry analysis showed that these ITNKs expressed NK surface receptors such as members of Ly49 family including Ly49C/I and Ly49G2 (Fig. 5.11) (Table 4), which were absent on the in vitro reprogrammed ITNKs (Fig. 5.7 and Fig. 5.8). These results suggested that in vivo microenvironment could facilitate reprogrammed ITNK cells to acquire inhibitory NK-cell receptors.

The majority of ITNKs from the spleen and thymus of Tamoxifen-treated *flox/flox* mice retained expression of CD3 and TCR β , suggesting that T cell identity was not completely lost after Bcl11b ablation. To further define the T cell identity of the in vivo DP thymocyte-derived ITNK cells, I analyzed the expression of several key T cell and NK cell-associated genes. Compared to wild type CD8⁺ mature T cells, ITNK cells had lower expression of *Il7r*, *Tbx21* and *Cd8a*, which are all important for CD8⁺ T cells (Fig. 5.12). For example, IL-7 receptor signaling is indispensable for survival of CD8⁺ memory T cells (Carrio et al., 2007; Kaech et al., 2003). *Tbx21* is essential for effector and memory CD8⁺ T cells (Intlekofer et al., 2005; Szabo et al., 2002). In contrast, *Zfp105* (Fig. 5.12), the NK-associated gene (Chambers et al., 2007) was upregulated in ITNK cells. These results showed that ITNK cells lost or decreased some key T cell genes expression and acquired expression of some NK specific gene, indicating a loss of T cell identity.

TCR signaling is a unique hallmark of T cells, which leads to increased intracellular calcium (Lewis, 2001). Therefore we measured TCR-mediated calcium signaling to assess whether TCR signaling was functional or not in ITNK cells derived in vivo. The results of intracellular calcium flux assays showed that the

calcium response in ITNKs was not as robust as T cells from the controls (cells from Tamoxifen-treated *flox/flox* or *flox/+* mice) (Fig. 5.13). Moreover, we noticed that even calcium response of T cells that did not express NKp46 but had lost Bcl11b from Tamoxifen-treated *flox/flox* was lower than that in Tamoxifen-treated *flox/+* mice (Fig. 5.13), further suggesting that Bcl11b was required for full TCR signaling. Taken together, these results indicate that TCR signaling was impaired, at least partially, in ITNK cells.

Besides the calcium flux assays, we also performed a proliferation assay to further analyze the TCR signaling in ITNKs as wide-type CD8⁺ T cells blast and proliferate after being activated by CD3 and CD28 antibodies. Unlike wild-type CD8⁺ T cells, in vivo derived ITNKs died rather than proliferated upon activation by CD3 and CD28 antibodies in vitro. Although more investigation is needed to fully address to the observed loss of T cell identity in ITNKs, we can conclude that ITNKs from mature T cells did not simply acquire expression of NK associated genes, rather reprogramming was also accompanied by loss of T cell genes and functions.

Primary NK cells can be expanded for up to 7-10 days as LAKs with supplement of IL-2 or IL-15. Beyond this time, LAKs gradually lose proliferation and killing abilities. When 10 million whole splenocytes from Tamoxifen-treated *flox/flox* mice were cultured in NK culture conditions, most splenocytes died in the first 3 days, reflecting the low percentages of ITNKs in splenocytes initially (Fig. 5.14). However, within 7 days, about 12 million NKp46⁺TCRβ⁺ ITNKs were obtained, most of which also expressed NK1.1 and NKG2D (Fig. 5.15). The ex vivo expanded ITNKs continued proliferating for at least 3 weeks while still retaining their killing ability (Fig. 5.14). ITNKs thus have a longer lifespan and greater proliferation ability than normal NK cells. Because T cells normally have longer lifespan than NK

cells in culture, it is possible that some retained T cell features made the ITNKs have long lifespan in culture.

5.2.4. Killing ability of ITNK derived in vitro

As important cellular mediators of innate defense, NK cells efficiently kill some viral-infected and transformed tumor cells in a serial manner by releasing perforin, granzymes and IFN- γ to targets, and by expressing Fas ligand (CD178) and Trail on their cell surface (Colucci et al., 2003). Perforin and granzymes are major weapons of NK cells, and their killing ability by these means can be quantified using standard ^{51}Cr -release assays in which ^{51}Cr released by lysed targets is measured and correlated to killing activities of effectors. To measure the killing ability of reprogrammed ITNKs from DN3 thymocytes in vitro, Dr. Burke helped me to perform standard ^{51}Cr -release assays with three cell lines as targets: B16F10 melanoma (MHC-I low or negative) (Taniguchi et al., 1986), RMA lymphoma, which express MHC class I molecules, and RMA-S lymphoma (TAP-1-deficient variant), which have much reduced MHC class I presentation (Karre et al., 1986; Ljunggren and Karre, 1985). LAKs discriminate between MHC-class I positive and negative cells, sparing the former and killing the latter (Fig. 5.16). Similar to LAK cells, ITNKs selectively killed MHC-I negative B16F10 and RMA-S cells, but did not kill MHC-I positive RMA lymphoma cells (Fig. 5.16). Compared to LAKs, ITNKs derived in vitro appeared to have slightly lower killing potency.

5.2.5. Killing ability of ITNK derived in vivo

To assess the killing ability of in vivo reprogrammed ITNK cells, we expanded ex vivo ITNK cells that were reprogrammed from *Bcl11b*-deficient DP thymocytes in *Rag2^{-/-}Il2r γ ^{-/-}* mice in LAK culture conditions as described in Chapter 4 and

performed standard ^{51}Cr -release assays with three cell lines as targets: B16F10 melanoma, RMA lymphoma, and RMA-S lymphoma. Strikingly, these ITNK cells exhibited greatly elevated cytotoxic potential compared to in vitro reprogrammed ITNKs and LAKs against each of the target cells (Fig. 5.17). Moreover, unlike LAKs, these ITNKs killed RMA cells with almost the same efficiency as killing RMA-S cells (Fig. 5.17), despite expression of some inhibitory Ly49 receptors that recognize MHC-I. ITNK cells maintained their capacity to kill tumours even after extensive ex vivo expansion. Taken together, these results show that in vivo reprogrammed ITNK cells were potent killers of tumour cells regardless of MHC-I molecules expression on targets.

5.2.6. ITNKs prevent tumour expansion in vivo

Transplantable murine melanoma B16 cell lines are well-established models for studying experimental cancer therapies and NK cell tumour surveillance function (Gorelik et al., 1982). Intravenous injection of B16 cells into $Rag2^{-/-}Il2r\gamma^{-/-}$ mice leads to rapid formation of ‘metastatic’ foci on the lungs (Lakshmikanth et al., 2009). To investigate the tumour-killing ability of ITNK cells in vivo, we injected two million OHT-treated or -untreated DP thymocytes from $flox/flox$ mice into $Rag2^{-/-}Il2r\gamma^{-/-}$ recipients to allow reprogramming of thymocytes to ITNKs in vivo. Two weeks later, each recipient was injected with 50,000 B16F10 melanoma cells (Fig. 5.18). Four weeks after the initial thymocyte transplantation, recipients were sacrificed and analyzed. Mice injected with PBS or with untreated DP thymocytes had about 200 metastatic foci in the lungs. In sharp contrast, mice injected with OHT-treated DP thymocytes had only about 20 tumour colonies on the lung (Fig. 5.19 and Fig. 5.20). Therefore ITNKs were potent killers of tumour cells in vivo and prevented cancer outgrowth.

5.3. Discussion

In this chapter, I demonstrated that the gene expression profiles of ITNKs were similar to that of LAKs, with upregulation of NK cell-associated genes and downregulation of T cell genes. Also, I reported that in vivo reprogrammed ITNK cells had more features of NK cell surface markers expression than in vitro derived ones. ITNKs that were derived from DP thymocytes in vivo showed more potent killing ability than LAKs and eliminated MHC-I positive tumour cells. Moreover, these ITNKs were capable of preventing progression of B16 melanoma tumour cell in vivo.

5.3.1. Potential targets of *Bcl11b*

The microarray analysis showed that ITNKs shared similar gene expression profiles with LAKs instead of their parental DN3 T cells. For example, NK-associated genes such as *Id2*, *Zfp105* and *Nfil3* were highly expressed while key T cell genes like *Notch1*, *Hes1* and *Gata3* were suppressed in ITNK cells. Among these genes, some are critical for T-cell or NK-cell transcription program. Thus expression changes of these genes (drivers) might result in the reprogramming from T cells to ITNKs. In contrast, expression changes of other genes (passengers) may simply be the outcome of the reprogramming. We do not know which genes are the drivers of this reprogramming from T cells to ITNKs, nor which are the passengers. *Nfil3*, which promotes the expressions of other NK-associated genes thus drives T cells to NK lineage (Gascoyne et al., 2009), might be one of the drivers of reprogramming after *Bcl11b* ablation. In contrast, the decrease of CD8 and CD3 expressions in ITNKs shown in qRT-PCR results might simply be caused by the loss of the T cell identity. To identify the drivers of the reprogramming from T cells to ITNKs here, we need to

probe the direct targets of Bcl11b by ChIP-seq experiments in the future (Kastner et al., 2010).

5.3.2. Differences between ITNKs derived in vitro and in vivo

There are at least three key differences between ITNK cells derived from in vitro and in vivo. Firstly, in vivo derived ITNK cells expressed several NK cell-associated surface markers such as Ly49C/I and Ly49G2, which were absent in ITNK cells reprogrammed from the same type of T cells in vitro. A lack of Ly49 family expression is also observed in regular NK cells that are derived from BM or thymic progenitors in OP9 stromal cell co-cultured system (Rolink et al., 2006; Vegh et al., 2010). Interestingly, NK cells produced from the same progenitors in vivo do express Ly49 family (Carotta et al., 2006). It was possible that in vivo microenvironment provided some cytokines and cell-cell interactions that are required for the induction of Ly49 family expression in NK cells to ITNKs derived in vivo and made them express members of Ly49 family.

In addition, in vivo ITNKs efficiently killed targets expressing MHC-I molecules, while in vitro derived ones did not. These results demonstrate that in vitro ITNKs lacking inhibitory Ly49 family could use other inhibitory receptors to recognize MHC-I molecules. In contrast, in vivo derived ITNKs killed target regardless to MHC-I molecules expression, though the killing activities for RMA line was lower than that for RMA-s. We thus predict that inhibitory receptors were functional but was overshadowed by activating signals triggered by tumour cells in the in vivo derived ITNK cells. Alternatively, the retained T cell recognition elements in these ITNKs might trigger the killing machinery to eliminate MHC-I positive tumor targets. In this case, however, we do not know whether T cell and NK cell

recognition elements triggered T cell and NK cell killing machinery separately or integrate the signals simultaneously in ITNKs at first.

The third difference is that *in vivo* derived ITNK cells had stronger killing ability than *in vitro* derived ITNKs did, possibly due to more activating receptors expression or stronger killing machinery in ITNKs derived *in vivo*.

Overall, *in vivo* derived ITNK did not lose self-tolerance, as *Rag2^{-/-}Il2rγ^{-/-}* host mice that had been transplanted with *Bcl11b*-deficient DP T thymocytes did not show any abnormality such as autoimmune syndrome or inflammation, suggesting that reprogrammed ITNK cells were able to recognize host cells. Taken together, the *in vivo* microenvironment might condition ITNK cells to express functional inhibitory receptors and activating receptors, shaping them into potent killers with ‘self-recognition’ ability.

5.3.3. Application of ITNKs for tumor killing

We showed that ITNK cells could efficiently kill B16 melanoma cells and prevent cancer progression *in vivo*. However, several preliminary experiments must be performed before claiming that ITNKs have clinical potential to treat cancer. Firstly, due to the limitation of our current animal license, *Rag2^{-/-}Il2rγ^{-/-}* mice with ITNK cells had to be killed within 14 days post injection of tumour cells in this study. Therefore we did not have the opportunity to know how long these ITNKs can protect hosts from tumour cells, which depends on two factors. One is the persistence of ITNKs in the host. The data presented in this study indicate that ITNKs derived from different types of T cells under different microenvironment had various lifetimes and proliferation potentials. The longer ITNKs can live in host, the better they can protect host from tumour attacks. The other factor is the ratio of ITNKs to tumour cells. The

killing assays show that effective clearance of tumour cells could be achieved when this ratio was high enough.

To demonstrate the clinical potential of ITNKs for cancer immunotherapy, we also need to better mimic the reality of cancer treatment. Unlike cancer vaccines, ITNKs will be transferred to cancer patients and be expected to kill tumour cells that have grown in situ. In this thesis, ITNK were already present before injection and establishment of B16 tumour cells, making them kill tumor cells more easily than in a therapeutic situation. Therefore we need to inject tumour cells into mice before transferring ITNKs into host mice.

Thirdly, we need to study whether ITNKs are able to kill other tumour cell lines in vivo besides B16 melanoma cells, to further explore the clinical application of ITNKs for different types of cancer.

Finally, to apply ITNKs to treat human cancer, we need to develop a platform to modulate BCL11B or its downstream targets in human T cells to enable the production of human ITNKs. These ITNKs have to be carefully characterized in vitro and in vivo for its safety and efficiency in different animal models before entering clinical trials. In summary, although the application of ITNK cells for cancer therapy is very promising, a lot of basic research is required.

Chapter 6

GENERAL DISCUSSION

6.1. Summary

This chapter summarizes the thesis on *Bcl11b* expression and function in T cells, its regulatory networks, and its potential application in cancer immunotherapy. I will also evaluate the contribution of this thesis to the knowledge of T cell development and immunotherapy. Then, future experiments on the identification of upstream and downstream genes of *Bcl11b*, the gain-of-function studies, and approaches to reprogram human T cells to iTNKS will be discussed. Finally, I will make the conclusions of my study in this thesis.

6.1.1. *Bcl11b* expression in T cells

In Chapter 3, I characterized *Bcl11b* expression at the single cell level in a *Bcl11b-tdTomato* knock-in mouse, where the *tdTomato* cassette was inserted into the 3' UTR of the *Bcl11b* locus. In hematopoietic lineages, *Bcl11b* expression was restricted to T cell compartments including almost all DN2-DN4 and DP thymocytes, CD4⁺ and CD8⁺ mature T cells, $\gamma\delta$ -T cells, and NKT cells. Some immature NK cells also transiently expressed *Bcl11b* at low levels. However, neither ETPs nor CD117⁺⁺DN2 thymocytes expressed *Bcl11b*, suggesting that *Bcl11b* expression might be suppressed by c-Kit signaling, which often has important roles in progenitors (Kondo et al., 1997). A recent study from Kawamoto's lab showed that IL-7 signaling, which is essential for common lymphoid progenitors and early T cell

progenitors, suppresses induction of *Bcl11b* expression in early T cells (Akashi et al., 1998; Ikawa et al., 2010). Interestingly, Kit and IL-7 pathways directly interact with each other (Jahn et al., 2007). In T cells, activation of Kit induces strong tyrosine phosphorylation of γ and IL-7R α in the absence of IL-7 (Jahn et al., 2007). Taken together, I speculate that *Bcl11b* expression marks that early T cell progenitors start to lose multipotency and differentiate towards T cell lineage.

I further described that *Bcl11b* was expressed in CD4⁺ and CD8⁺ mature T cells at different levels. Its expression in CD8⁺ T cells was lower than that in CD4⁺ T cells, as measured by RNA samples from T cell pools. Interestingly, at a single cell level, some activated T cells expressed *Bcl11b* at very low levels, suggesting that *Bcl11b* might suppress some T-cell-activation-associated genes thus inhibit T cell activation (Li et al., 2010).

6.1.2. *Bcl11b* functions in early T cells

Early T cell progenitors retain myeloid- and NK-cell potentials (Bell and Bhandoola, 2008) (Wada et al., 2008). In Chapter 4, I demonstrated that acute deletion of *Bcl11b* in T cell progenitors stopped T cell development at DN1-2 stages, as these *Bcl11b*-deficient T cell progenitors differentiated to NK-like cells instead of T cells in T cell culture conditions. Further studies from Rothenberg's lab shows that *Bcl11b*-deficient T cell progenitors initiates T cell specification normally, as indicated by upregulation of *Cd3e*, *Cd3g*, *Ptcra*, and *Rag1* (Li et al., 2010). Thus the blockage of T cell development is not due to a failure of initiation of T cell program, but rather a likely failure to repress alternative cell-lineage development. This is supported by the fact that *Bcl11b*-deficient thymocytes also express genes such as *Id2*, *Il2rb* and *Nifl3* that normally promote NK cell development (Li et al., 2010). However, it is possible that some *Bcl11b*-deficient DN2 thymocytes are able to differentiate further

to the DN3 stage before undergoing apoptosis. Indeed, DN3 thymocytes are detected in the *Bcl1b*-deficient fetal thymus (Wakabayashi et al., 2003b).

Recently, the block of T cell differentiation was observed in the DN2 fetal thymocytes from *Bcl11b* conventional knockout embryos (Ikawa et al., 2010). These *Bcl11b*-deficient DN2 thymocytes proliferated extensively and were able to differentiate to NK cells, dendritic cells and myeloid cells, but not T cells (Ikawa et al., 2010). However, once Bcl11b is reintroduced to the *Bcl11b*-deficient DN2 thymocytes, T cell development resumed (Ikawa et al., 2010). These results thus suggest that Bcl11b terminates non-T-cell-lineage potentials in T cell progenitors thus essential for early T cell development.

6.1.3. *Bcl11b* functions in committed and mature T cells

In Chapter 4, I described that Bcl11b was not only required for early T cell development, but also essential for the maintenance of T cell identity in committed and mature T cells. Upon loss of Bcl11b, committed and mature T cells reprogrammed to ITNKs both in vitro and in vivo (Fig. 6.1) (Pentao Liu, 2010). *Bcl11b*-deficient DN3 thymocytes aborted T cell development and were reprogrammed to ITNK cells. These ITNK cells expressed other NK-cell-associated genes besides NKp46 and were similar to NK cells in morphology. In the single-cell-assay experiments, I demonstrated that every single *Bcl11b*-deficient DN3 thymocyte reprogrammed to ITNKs. And these ITNKs, similar to *Bcl11b*-deficient DN2 thymocytes, showed extensive in vitro expansion potentials. Besides DN3 thymocytes, ITNKs were also produced from DP thymocytes and CD8⁺ mature T cells upon loss of Bcl11b in vitro. These ITNKs retained TCR β and CD3 on the cell surface. However, I do not know the reprogramming efficiency of these ITNKs.

I also demonstrated that ITNKs from *Bcl11b*-deficient T cells was not an in vitro culture artifact, because the results from Chapter 4 showed that ITNK cells were detected in the spleen and thymus of Tamoxifen-treated *flox/flox* mice. Interestingly, these in vivo-derived ITNKs had higher proliferation potential than NK cells in NK culture condition. Moreover, similar to ITNKs reprogrammed from mature T cells in vitro, ITNKs that were reprogrammed from mature T cells in vivo also expressed TCR β and CD3, although their TCR signaling appeared to be compromised.

I further demonstrated that reprogramming from T cells to ITNKs upon loss of *Bcl11b* was a cell-autonomous process, because ITNKs were present in *Rag2^{-/-}Il2r γ ^{-/-}* mice after being transferred with *Bcl11b*-deficient DP thymocytes. These ITNKs expressed TCR β , CD3, CD8 and some members of Ly49 family receptors. The total number of ITNK cells did not vary substantially for at least 3 months, perhaps representing the homeostasis of ITNKs in the in vivo microenvironment.

In summary, acute loss of *Bcl11b* in T cells led to a failure of T-cell-lineage commitment and T-cell-identity maintenance. Possibly, *Bcl11b* maintains T cell identity by suppressing non-T cell potentials and sustains the T cell program in T cells. My results are different from the previous studies using constitutive expression of Cre recombinase in T cells. For example, in DP thymocytes, *Bcl11b* deletion using CD4-Cre causes defects in the initiation of positive selection (Albu et al., 2007). In another study, deletion of *Bcl11b* in early DP thymocytes using CD4-Cre causes expression of some genes that are found in mature SP T cells like *Zbtb7b* and *Runx3* (Kastner et al., 2010). Neither study revealed cells similar to ITNKs in these mutant mice.

6.1.4. *Bcl11b* transcription regulatory networks

Despite its importance in T cells, *Bcl11b* regulatory networks in T cells are not clear. Previous studies propose that *Bcl11b* is regulated by Notch signaling during T cell specification and commitment based on gene expression changes (Rothenberg, 2007). In Chapter 4, I showed NK-like cells instead of T cells grew out from *Bcl11b*-deficient DN1 and DN2 thymocytes on either OP9 or OP9-DL1 stromal cells. Therefore the lineage switch from T- to NK-cell upon loss of *Bcl11b* was independent of Notch signaling, suggesting that *Bcl11b* perhaps acted downstream of Notch signaling in T cells. Our ChIP analysis using antibodies to CSL confirmed that the canonical Notch signaling pathways directly regulated *Bcl11b* at the transcription level. Although *Bcl11b* expression is induced by Notch signaling, it is likely to be also regulated by other factors or signaling pathways in T cells. For example, the *Bcl11b* expression profile in early T cell progenitors from a *Bcl11b-tdTomato* knock-in mouse suggested that c-Kit signaling might suppress *Bcl11b* expression. IL-7 signaling is another candidate. In the stromal-free culture system higher concentration of IL-7 blocks DN2 thymocytes further differentiation into T cells. This block can be overcome by either lowering the concentration of IL-7 or by forcibly expressing *Bcl11b*, implicating that IL-7 signaling represses *Bcl11b* expression in early T cells (Ikawa et al., 2010).

Compared to upstream genes of *Bcl11b*, even less is known about its downstream genes. In Chapter 6, the microarray analysis showed that the global gene expression profile of ITNKs exhibited many NK cell features. Compared to their parental DN3 thymocytes, ITNKs had lower expression of many T-cell-lineage genes like *Gata3*, *Notch1*, *Dtx1* and *Hes1* and higher expression of NK cell-associated genes such as *E4bp4*, *Zfp105*, and *Id2*. Similar gene expression changes are also reported in

Bcl11b-deficient early T cells (Ikawa et al., 2010) (Li et al., 2010). In the future, ChIP assays will be required to determine whether these genes are the direct targets of Bcl11b.

6.1.5. Potentials of ITNKs in immunotherapy

Both T cells and NK cells have been used to treat cancer in adoptive cell transfer (ACT) therapy (Rosenberg et al., 2004). However, due to the limitations of T cells and NK cells, new cell sources are required to further explore the potential of cancer immunotherapy. The unique properties of ITNKs shown in Chapter 5 made them an attractive cell source for this purpose. In contrast to limited availability of NK cells for ACT, a large quantity of T cells could be readily obtained from either peripheral blood or thymus to produce ITNKs. Every *Bcl11b*-deficient DN3 T cell could be reprogrammed to ITNK cells, according to our single cell assay results. Furthermore, ITNKs could be expanded extensively *in vitro* and exhibited potent killing ability on various tumour cell lines, regardless of MHC-I molecules expression status. Finally, ITNKs appeared to be able to distinguish normal cells from the tumour cells, and were not malignantly transformed, because host mice with ITNKs did not show any abnormalities.

6.2. Significance

6.2.1. Novel roles of *Bcl11b* in the maintenance of T cell identity

This study demonstrates for the first time that ablation of a single transcription factor, Bcl11b, abolished maintenance of T cell identity, resulting in reprogramming of T cells at different developmental stages to ITNKs. IL-2 and IL-15 were

dispensable for, but could stimulate the growth of ITNKs. ITNKs share similar gene expression profiles with NK cells, and were potent killers for three tested tumour cell lines. However, ITNKs were not NK cells. They could be produced from DN1 and DN2 thymocytes in the presence of Notch signaling and are independent of cytokines such as IL-2 or IL-15 for survival and proliferation. Moreover, ITNKs from DP thymocytes or mature T cells retained some signatures of their T cell origin, such as expression of some T cell genes and compromised TCR function.

6.2.2. Clinical potential of ITNKs

NK-cell-based therapies hold promise in cancer and virus infection, such as hepatitis C virus infection, treatment (Barrett and Le Blanc, 2010; Rosenberg et al., 2008; Salem et al., 2010). We are now able to reprogram T cells to ITNKs, which could be extensively expanded but were not malignantly transformed. Moreover, they effectively killed tumor cells in vitro and eliminate metastatic cells in mice but did not appear to attack normal cells from hosts. Because *Bcl11b* sequence is highly conserved in both the mouse and human, we expect that ITNKs can also be produced from human T cells, where BCL11B is inactivated by genetic and non-genetic approaches such as RNAi, zinc finger nuclease (Urnov et al., 2005), and small molecule inhibitors. These ITNK cells may serve as a new cell source for cancer immunotherapy and other cell-based therapies (Fig. 6.2).

6.3. Future experiments

The results presented in this thesis demonstrate that *Bcl11b* was essential for early T cell development and the maintenance of the T cell identity in committed and mature T cells. Future work is required to probe the regulators of *Bcl11b* and its downstream genes and pathways. ITNKs that were produced from *Bcl11b*-deficient T

cells could efficiently kill tumor cells both in vitro and in vivo, regardless of MHC-I expression. To further explore the clinical application of ITNKs in cancer immunotherapy, future experiments are required to demonstrate whether human T cells can be reprogrammed to ITNK cells through genetic or non-genetic modification. Furthermore, it is necessary to test whether these human ITNKs are capable of eliminating human cancer cells efficiently in vitro and in tumor bearing animal models.

6.3.1. Upstream genes of *Bcl11b*

In Chapter 4, I showed that Notch1 induces *Bcl11b* expression through CSL in T cells, as CSL directly bind to the *Bcl11b* locus. Luciferase assays can be performed to examine whether enforced expression of CSL or Notch1 can induce *Bcl11b* expression at the cellular levels, or assess whether overexpression of a dominant negative form of NICD inhibits *Bcl11b* expression.

Besides Notch signaling, other signal pathways may regulate *Bcl11b* expression positively and negatively in different T cell compartments. *Bcl11b* was absent or expressed at undetectable levels in ETP and CD117⁺DN2 thymocytes. There are several candidates that may suppress *Bcl11b* expression in these populations. I propose that IL-2R β and its downstream JAK/STAT signaling pathways (Benczik and Gaffen, 2004), are candidates to repress *Bcl11b* expression in early T cell progenitors based on the following evidence. Wild type DN1 and DN2 thymocytes differentiate to T cells upon co-culture with OP9-DL1 stromal cells that provide Delta-like 1, the Notch ligand, to activate Notch signaling in these thymocytes. However, supplementation of IL-15 (30 ng/ml) or IL-2 (100 ng/ml) in this culture forces the early T cell progenitors to differentiate to NK cells instead of T cells, suggesting that the activation of IL-2R β signaling by its ligands can abolish T cell development in the

presence of Notch signaling. Mutual antagonism between the Notch and JAK/STAT signaling pathways is reported in drosophila. Notch signaling inhibits JAK/STAT signaling by preventing STAT nuclear translocation, while signaling by JAK/STAT reduces Notch signaling (Assa-Kunik et al., 2007; Gutierrez-Avino et al., 2009; Sotillos et al., 2008). Moreover, Bcl11b was induced by Notch signaling and was essential for T cell development. Therefore we speculate that IL-2R β signaling and JAK/STAT signaling may suppress *Bcl11b* expression through Notch signaling. In this case, extremely high concentrations of IL-2, IL-7, and IL-15 in culture, which all activate JAK/STAT pathways (Waldmann, 2006), may suppress Bcl11b expression in T cells and produce ITNKs. Nevertheless it is also possible that IL-2R β signaling repressed downstream genes of Bcl11b rather than Bcl11b expression directly. To investigate these possibilities, we can use flow cytometry or RT-PCR to measure *Bcl11b* expression changes in early T cell progenitors from *Bcl11b-tdTomato* knock-in mice when IL-2R β signaling is activated or inhibited. Similarly, we can examine the effect of IL-7R α and c-Kit signaling on Bcl11b expression in gain- and loss-of-function studies. For example, we can measure Bcl11b expression in early T cells expressing both CD127 and CD117 with high concentration of IL-7 or SCF. We can also block receptors of IL-7 and c-Kit with antibodies and then assess Bcl11b expression in the T cells.

Furthermore, it was shown that Bcl11b expression in activated T cells is lower than that in naïve T cells in the Chapter 3. Consistent with this, induction of T cell activation using anti-CD3 antibodies promoted expansion of the Bcl11b^{low} activated T cells (Shannon Burke, observation). Taken together, these results suggested that TCR signaling might suppress Bcl11b expression during T cell activation. Thus further

experiments are required to validate whether TCR signaling antagonizes Bcl11b in mature T cells.

6.3.2. Downstream genes of Bcl11b

Because Bcl11b is a transcription factor, ChIP-seq experiments using Bcl11b antibodies are the most straightforward method to study its downstream targets. The ChIP-seq results from Gross's laboratory showed that Bcl11b bound to several regions within the *Zbtb7b* locus, including the distal regulatory element (Kastner et al., 2010). However, NK-cell-associated genes are not found in the list of Bcl11b putative binding sites. To refine the list of Bcl11b downstream genes, we can combine the microarray analysis of gene expression profiles that were obtained from loss- and gain-of-function studies on Bcl11b in T cells and the ChIP-seq results together to probe overlapping candidates. Moreover, we should focus on the known NK-cell- and myeloid-cell-associated genes and T-cell genes from the Bcl11b downstream candidates listed in the Chapter 5 and two other recent publications (Ikawa et al., 2010; Li et al., 2010). For example, IL-2R β signaling, the prospect upstream of Bcl11b, may also be regulated by Bcl11b. *Bcl11b*-deficient DN1 or DN2 thymocytes differentiated to ITNKs that were IL-2 or IL-15 independent, suggesting that IL-2R β signaling is constitutively activated without the stimulation of its ligands after Bcl11b ablation. Therefore Bcl11b may suppress IL-2R β signaling in early T cell progenitors. And this repression cannot be bypassed in committed T cells by stimulation through IL-2R β , as DN3 thymocytes fail to switch to NK-cell lineage despite of high concentration of IL-2. This suggests that IL-2R β signaling cannot suppress Bcl11b expression once T cell program, possibly including Bcl11b self-sustain feedback loop, has been established in committed T cells.

6.3.3. Overexpression of *Bcl11b* in ITNKs and NK cells

In this thesis, I have used a loss of function approach (acute loss of *Bcl11b*) to identify *Bcl11b* function in T cells. However, it remains unknown whether overexpression of *Bcl11b* in NK cells would reprogram them to T cells. Therefore future experiments can include construction of a *Bcl11b* overexpression vector with a GFP marker in the *piggyBac* (PB) transposon, which can carry a large DNA cassette and integrate into mammalian genome efficiently with the help of transposase (Ding et al., 2005; Wang et al., 2008b). Additionally, the PB transposon can jump between genomic sites by a “cut and paste” mechanism, and can excise itself precisely, leaving no footprint behind (Thibault et al., 2004). Thus we can use the amaxa nuclear transfection technology to deliver this vector into the genome of NK cells efficiently. These transfected NK cells that overexpress *Bcl11b* can be sorted and cultured in T cell condition, or injected into *Rag2^{-/-}Il2r γ ^{-/-}* mice. T cells may result from these NK cells if *Bcl11b* expression disrupts the NK-cell transcription program and establishes the T-cell transcription program.

6.3.4. Reprogramming human T cells to ITNKs

To use ITNKs as a source of cell-based therapy for human cancer, we need to derive ITNKs from human T cells by inactivating *BCL11B*. Because the conditional knockout technology is not available for human cells, we have to explore alternative methods to ablate *BCL11B* in human T cells. With zinc finger nuclease (ZFN) technology (Klug, 2010), it is possible to design ZFNs that specifically bind to and introduce mutations at the *BCL11B* locus, thus abolishing *BCL11B* transcription completely in human T cells. Additionally, single cell assays can be conducted to assess the efficiency of reprogramming from human $CD8^+$ T cells to ITNKs. However, due to the low mutation efficiency and high undesired-mutation rate in ZFN

technology, it is more practical to use non-genetic approaches to inactivate BCL11B in human T cells. Though small molecules have been widely used to inhibit protein function, there are only few successful examples for transcription factors (Lee et al., 2010). Compared to the two approaches discussed above, it is more feasible to choose another approach, such as RNAi technology, at least in the short term. BCL11B can be knockdown efficiently in both normal human T cells and human T cell leukemia by expressing *BCL11B*-specific shRNAs (Grabarczyk et al., 2007). We plan to use the similar approach to knockdown BCL11B in human T cells and examine whether these T cells can be reprogrammed to ITNK cells. Since the knockdown efficiency normally does not achieve 100%, and if a complete loss of BCL11B is a prerequisite for T cells to be reprogrammed to ITNKs, we may not obtain ITNKs from human T cells using RNAi, or at least not very efficiently. Moreover, in some T cells, knockdown efficiency could be around 50%. It is known that mice heterozygous for *Bcl11b* deletion develop T cell leukemia. Thus it is very important to test whether these BCL11B knockdown cells have cancer potential as a population or as single cells in humanized mouse models.

6.3.5. Testing the tumor-killing ability of human ITNKs

Once we successfully obtain human ITNK cells, we will next need to investigate the persistence of human ITNKs in animal models and determine how long human ITNKs are able to survive and remain functional in vivo. For safety reasons, it is also required to examine whether human ITNKs have cancer or oncogenic potential, as described above.

Another important factor for consideration is from which human T cell compartments are best production of ITNKs for cancer therapy. In the mouse, ITNKs can be obtained from various T-cell subsets, and these ITNKs have distinct gene

expression profiles. For example, DN3 thymocytes-derived ITNKs did not express TCR, while those derived from CD8⁺ mature T cells retained a functional but compromised TCR complex. TCR signaling in CD8⁺ ITNKs may still be used for targeting ITNKs to tumour cells expressing specific antigens. In this case, using a tumor-specific chimeric receptor or transgenic TCR may enhance the killing potency of ITNKs. Alternatively, this could be achieved by deriving ITNKs from T cells enriched for tumor-specific CD8⁺ T cells or tumor infiltrating T cells (Fig. 6.2).

In addition, it is important to know whether ITNKs are suitable to a variety of tumor types. Thus we need to perform killing assays to measure how efficiently human ITNKs kill various human tumor cells. We also need to inject these ITNKs into humanized mice that are engrafted with human tumors and to examine whether ITNKs eliminate these tumors in vivo.

6.4. Conclusions

Bcl11b has now been identified as a critical transcription factor for T cell lineage commitment. Loss of Bcl11b in T cell progenitors allowed expression of genes of alternative lineages. Moreover, deletion of *Bcl11b* in committed or mature T cells caused loss, or decreased expression, of T-cell genes with concomitant expression of genes usually associated with NK cells. These ITNKs reprogrammed from T cells had enormous proliferation potential in vitro and potent killing ability that is MHC-independent, and yet killed normal cells. Therefore this thesis uncovered a critical transcription factor, Bcl11b, in T cells. ITNKs described in this study may provide a new cell source for cell-based therapies. Since ITNKs were a new type of killer cells, many exciting questions remain unanswered.

REFERENCES

- Abe, K., Hashiyama, M., Macgregor, G., and Yamamura, K. (1996). Purification of primordial germ cells from TNAPbeta-geo mouse embryos using FACS-gal. *Dev Biol* *180*, 468-472.
- Adolfsson, J., Mansson, R., Buza-Vidas, N., Hultquist, A., Liuba, K., Jensen, C.T., Bryder, D., Yang, L., Borge, O.J., Thoren, L.A., *et al.* (2005). Identification of Flt3+ lympho-myeloid stem cells lacking erythro-megakaryocytic potential a revised road map for adult blood lineage commitment. *Cell* *121*, 295-306.
- Akashi, K., Kondo, M., Cheshier, S., Shizuru, J., Gandy, K., Domen, J., Mebius, R., Traver, D., and Weissman, I.L. (1999). Lymphoid development from stem cells and the common lymphocyte progenitors. *Cold Spring Harb Symp Quant Biol* *64*, 1-12.
- Akashi, K., Kondo, M., and Weissman, I.L. (1998). Role of interleukin-7 in T-cell development from hematopoietic stem cells. *Immunol Rev* *165*, 13-28.
- Albu, D.I., Feng, D., Bhattacharya, D., Jenkins, N.A., Copeland, N.G., Liu, P., and Avram, D. (2007). BCL11B is required for positive selection and survival of double-positive thymocytes. *J Exp Med* *204*, 3003-3015.
- Alici, E., Sutlu, T., Bjorkstrand, B., Gilljam, M., Stellan, B., Nahi, H., Quezada, H.C., Gahrton, G., Ljunggren, H.G., and Dilber, M.S. (2008). Autologous antitumor activity by NK cells expanded from myeloma patients using GMP-compliant components. *Blood* *111*, 3155-3162.
- Allman, D., Sambandam, A., Kim, S., Miller, J.P., Pagan, A., Well, D., Meraz, A., and Bhandoola, A. (2003). Thymopoiesis independent of common lymphoid progenitors. *Nat Immunol* *4*, 168-174.

Amsen, D., Antov, A., and Flavell, R.A. (2009). The different faces of Notch in T-helper-cell differentiation. *Nat Rev Immunol* 9, 116-124.

Anderson, G., Jenkinson, W.E., Jones, T., Parnell, S.M., Kinsella, F.A., White, A.J., Pongrac'z, J.E., Rossi, S.W., and Jenkinson, E.J. (2006). Establishment and functioning of intrathymic microenvironments. *Immunol Rev* 209, 10-27.

Anderson, G., Moore, N.C., Owen, J.J., and Jenkinson, E.J. (1996). Cellular interactions in thymocyte development. *Annu Rev Immunol* 14, 73-99.

Antoch, M.P., Song, E.J., Chang, A.M., Vitaterna, M.H., Zhao, Y., Wilsbacher, L.D., Sangoram, A.M., King, D.P., Pinto, L.H., and Takahashi, J.S. (1997). Functional identification of the mouse circadian Clock gene by transgenic BAC rescue. *Cell* 89, 655-667.

Arlotta, P., Molyneaux, B.J., Chen, J., Inoue, J., Kominami, R., and Macklis, J.D. (2005). Neuronal subtype-specific genes that control corticospinal motor neuron development in vivo. *Neuron* 45, 207-221.

Arlotta, P., Molyneaux, B.J., Jabaudon, D., Yoshida, Y., and Macklis, J.D. (2008). Ctip2 controls the differentiation of medium spiny neurons and the establishment of the cellular architecture of the striatum. *J Neurosci* 28, 622-632.

Assa-Kunik, E., Torres, I.L., Schejter, E.D., Johnston, D.S., and Shilo, B.Z. (2007). *Drosophila* follicle cells are patterned by multiple levels of Notch signaling and antagonism between the Notch and JAK/STAT pathways. *Development* 134, 1161-1169.

Assarsson, E., Kambayashi, T., Sandberg, J.K., Hong, S., Taniguchi, M., Van Kaer, L., Ljunggren, H.G., and Chambers, B.J. (2000). CD8⁺ T cells rapidly acquire NK1.1 and NK cell-associated molecules upon stimulation in vitro and in vivo. *J Immunol* 165, 3673-3679.

Avram, D., Fields, A., Pretty On Top, K., Nevriy, D.J., Ishmael, J.E., and Leid, M. (2000). Isolation of a novel family of C(2)H(2) zinc finger proteins implicated in transcriptional repression mediated by chicken ovalbumin upstream promoter transcription factor (COUP-TF) orphan nuclear receptors. *J Biol Chem* 275, 10315-10322.

Bain, G., Maandag, E.C., Izon, D.J., Amsen, D., Kruisbeek, A.M., Weintraub, B.C., Krop, I., Schlissel, M.S., Feeney, A.J., van Roon, M., *et al.* (1994). E2A proteins are required for proper B cell development and initiation of immunoglobulin gene rearrangements. *Cell* 79, 885-892.

Bajoghli, B., Aghaallaei, N., Hess, I., Rode, I., Netuschil, N., Tay, B.H., Venkatesh, B., Yu, J.K., Kaltenbach, S.L., Holland, N.D., *et al.* (2009). Evolution of genetic networks underlying the emergence of thymopoiesis in vertebrates. *Cell* 138, 186-197.

Barrett, A.J., and Le Blanc, K. (2010). Immunotherapy prospects for acute myeloid leukaemia. *Clin Exp Immunol* 161, 223-232.

Barton, K., Muthusamy, N., Fischer, C., Ting, C.N., Walunas, T.L., Lanier, L.L., and Leiden, J.M. (1998). The Ets-1 transcription factor is required for the development of natural killer cells in mice. *Immunity* 9, 555-563.

Bell, J.J., and Bhandoola, A. (2008). The earliest thymic progenitors for T cells possess myeloid lineage potential. *Nature* 452, 764-767.

Benczik, M., and Gaffen, S.L. (2004). The interleukin (IL)-2 family cytokines: survival and proliferation signaling pathways in T lymphocytes. *Immunol Invest* 33, 109-142.

Bendelac, A. (1995). Positive selection of mouse NK1+ T cells by CD1-expressing cortical thymocytes. *J Exp Med* 182, 2091-2096.

Benlagha, K., Kyin, T., Beavis, A., Teyton, L., and Bendelac, A. (2002). A thymic precursor to the NK T cell lineage. *Science* 296, 553-555.

Benlagha, K., Wei, D.G., Veiga, J., Teyton, L., and Bendelac, A. (2005). Characterization of the early stages of thymic NKT cell development. *J Exp Med* 202, 485-492.

Bernard, O.A., Busson-LeConiat, M., Ballerini, P., Mauchauffe, M., Della Valle, V., Monni, R., Nguyen Khac, F., Mercher, T., Penard-Lacronique, V., Pasturaud, P., *et al.* (2001). A new recurrent and specific cryptic translocation, t(5;14)(q35;q32), is associated with expression of the Hox11L2 gene in T acute lymphoblastic leukemia. *Leukemia* 15, 1495-1504.

Betz, U.A., Vosshenrich, C.A., Rajewsky, K., and Muller, W. (1996). Bypass of lethality with mosaic mice generated by Cre-loxP-mediated recombination. *Curr Biol* 6, 1307-1316.

Blott, E.J., and Griffiths, G.M. (2002). Secretory lysosomes. *Nat Rev Mol Cell Biol* 3, 122-131.

Boos, M.D., Yokota, Y., Eberl, G., and Kee, B.L. (2007). Mature natural killer cell and lymphoid tissue-inducing cell development requires Id2-mediated suppression of E protein activity. *J Exp Med* 204, 1119-1130.

Borrego, F., Masilamani, M., Marusina, A.I., Tang, X., and Coligan, J.E. (2006). The CD94/NKG2 family of receptors: from molecules and cells to clinical relevance. *Immunol Res* 35, 263-278.

Bradley, A., Evans, M., Kaufman, M.H., and Robertson, E. (1984). Formation of germ-line chimaeras from embryo-derived teratocarcinoma cell lines. *Nature* 309, 255-256.

Brinster, R.L., Chen, H.Y., Trumbauer, M., Senechal, A.W., Warren, R., and Palmiter, R.D. (1981). Somatic expression of herpes thymidine kinase in mice following injection of a fusion gene into eggs. *Cell* 27, 223-231.

Brocard, J., Warot, X., Wendling, O., Messaddeq, N., Vonesch, J.L., Chambon, P., and Metzger, D. (1997). Spatio-temporally controlled site-specific somatic mutagenesis in the mouse. *Proc Natl Acad Sci U S A* 94, 14559-14563.

Bunz, F., Dutriaux, A., Lengauer, C., Waldman, T., Zhou, S., Brown, J.P., Sedivy, J.M., Kinzler, K.W., and Vogelstein, B. (1998). Requirement for p53 and p21 to sustain G2 arrest after DNA damage. *Science* 282, 1497-1501.

Burbach, B.J., Medeiros, R.B., Mueller, K.L., and Shimizu, Y. (2007). T-cell receptor signaling to integrins. *Immunol Rev* 218, 65-81.

Busslinger, M. (2004). Transcriptional control of early B cell development. *Annu Rev Immunol* 22, 55-79.

Capecchi, M.R. (1989). Altering the genome by homologous recombination. *Science* 244, 1288-1292.

Caraux, A., Kim, N., Bell, S.E., Zompi, S., Ranson, T., Lesjean-Pottier, S., Garcia-Ojeda, M.E., Turner, M., and Colucci, F. (2006). Phospholipase C-gamma2 is essential for NK cell cytotoxicity and innate immunity to malignant and virally infected cells. *Blood* 107, 994-1002.

Carlens, S., Gilljam, M., Chambers, B.J., Aschan, J., Guven, H., Ljunggren, H.G., Christensson, B., and Dilber, M.S. (2001). A new method for in vitro expansion of cytotoxic human CD3-CD56+ natural killer cells. *Hum Immunol* 62, 1092-1098.

Carotta, S., Brady, J., Wu, L., and Nutt, S.L. (2006). Transient Notch signaling induces NK cell potential in Pax5-deficient pro-B cells. *Eur J Immunol* 36, 3294-3304.

Carpenter, A.C., and Bosselut, R. (2010). Decision checkpoints in the thymus. *Nat Immunol* 11, 666-673.

Carrio, R., Rolle, C.E., and Malek, T.R. (2007). Non-redundant role for IL-7R signaling for the survival of CD8⁺ memory T cells. *Eur J Immunol* 37, 3078-3088.

Casey, T.P. (1966). Autoimmunity in strains of New Zealand mice. *NZ Med J* 65, 105-110.

Chambers, S.M., Boles, N.C., Lin, K.Y., Tierney, M.P., Bowman, T.V., Bradfute, S.B., Chen, A.J., Merchant, A.A., Sirin, O., Weksberg, D.C., *et al.* (2007). Hematopoietic fingerprints: an expression database of stem cells and their progeny. *Cell Stem Cell* 1, 578-591.

Chan, W., Costantino, N., Li, R., Lee, S.C., Su, Q., Melvin, D., Court, D.L., and Liu, P. (2007). A recombineering based approach for high-throughput conditional knockout targeting vector construction. *Nucleic Acids Res* 35, e64.

Chang, C., Rodriguez, A., Carretero, M., Lopez-Botet, M., Phillips, J.H., and Lanier, L.L. (1995). Molecular characterization of human CD94: a type II membrane glycoprotein related to the C-type lectin superfamily. *Eur J Immunol* 25, 2433-2437.

Chang, C.C., and Ferrone, S. (2007). Immune selective pressure and HLA class I antigen defects in malignant lesions. *Cancer Immunol Immunother* 56, 227-236.

Cherrier, T., Suzanne, S., Redel, L., Calao, M., Marban, C., Samah, B., Mukerjee, R., Schwartz, C., Gras, G., Sawaya, B.E., *et al.* (2009). p21(WAF1) gene promoter is epigenetically silenced by CTIP2 and SUV39H1. *Oncogene* 28, 3380-3389.

Ciofani, M., and Zuniga-Pflucker, J.C. (2007). The thymus as an inductive site for T lymphopoiesis. *Annu Rev Cell Dev Biol* 23, 463-493.

Cismasiu, V.B., Adamo, K., Gecewicz, J., Duque, J., Lin, Q., and Avram, D. (2005). BCL11B functionally associates with the NuRD complex in T lymphocytes to repress targeted promoter. *Oncogene* 24, 6753-6764.

Cismasiu, V.B., Duque, J., Paskaleva, E., Califano, D., Ghanta, S., Young, H.A., and Avram, D. (2009). BCL11B enhances TCR/CD28-triggered NF-kappaB activation through up-regulation of Cot kinase gene expression in T-lymphocytes. *Biochem J* 417, 457-466.

Cismasiu, V.B., Ghanta, S., Duque, J., Albu, D.I., Chen, H.M., Kasturi, R., and Avram, D. (2006). BCL11B participates in the activation of IL2 gene expression in CD4+ T lymphocytes. *Blood* 108, 2695-2702.

Cobaleda, C., Jochum, W., and Busslinger, M. (2007). Conversion of mature B cells into T cells by dedifferentiation to uncommitted progenitors. *Nature* 449, 473-477.

Colucci, F., Caligiuri, M.A., and Di Santo, J.P. (2003). What does it take to make a natural killer? *Nat Rev Immunol* 3, 413-425.

Colucci, F., Samson, S.I., DeKoter, R.P., Lantz, O., Singh, H., and Di Santo, J.P. (2001). Differential requirement for the transcription factor PU.1 in the generation of natural killer cells versus B and T cells. *Blood* 97, 2625-2632.

Colucci, F., Soudais, C., Rosmaraki, E., Vanes, L., Tybulewicz, V.L., and Di Santo, J.P. (1999). Dissecting NK cell development using a novel alymphoid mouse model: investigating the role of the c-abl proto-oncogene in murine NK cell differentiation. *J Immunol* 162, 2761-2765.

Cook, H.L., Lytle, J.R., Mischo, H.E., Li, M.J., Rossi, J.J., Silva, D.P., Desrosiers, R.C., and Steitz, J.A. (2005). Small nuclear RNAs encoded by Herpesvirus saimiri upregulate the expression of genes linked to T cell activation in virally transformed T cells. *Curr Biol* 15, 974-979.

Cronin, S.J., and Penninger, J.M. (2007). From T-cell activation signals to signaling control of anti-cancer immunity. *Immunol Rev* 220, 151-168.

Cunningham, J.J., and Roussel, M.F. (2001). Cyclin-dependent kinase inhibitors in the development of the central nervous system. *Cell Growth Differ* 12, 387-396.

Dave, V.P., Allman, D., Keefe, R., Hardy, R.R., and Kappes, D.J. (1998). HD mice: a novel mouse mutant with a specific defect in the generation of CD4(+) T cells. *Proc Natl Acad Sci U S A* 95, 8187-8192.

David-Fung, E.S., Butler, R., Buzi, G., Yui, M.A., Diamond, R.A., Anderson, M.K., Rowen, L., and Rothenberg, E.V. (2009). Transcription factor expression dynamics of early T-lymphocyte specification and commitment. *Dev Biol* 325, 444-467.

de Alboran, I.M., O'Hagan, R.C., Gartner, F., Malynn, B., Davidson, L., Rickert, R., Rajewsky, K., DePinho, R.A., and Alt, F.W. (2001). Analysis of C-MYC function in normal cells via conditional gene-targeted mutation. *Immunity* 14, 45-55.

Degli-Esposti, M.A., and Smyth, M.J. (2005). Close encounters of different kinds: dendritic cells and NK cells take centre stage. *Nat Rev Immunol* 5, 112-124.

Desplats, P.A., Lambert, J.R., and Thomas, E.A. (2008). Functional roles for the striatal-enriched transcription factor, Bcl11b, in the control of striatal gene expression and transcriptional dysregulation in Huntington's disease. *Neurobiol Dis* 31, 298-308.

Di Santo, J.P. (2006). Natural killer cell developmental pathways: a question of balance. *Annu Rev Immunol* 24, 257-286.

Di Santo, J.P. (2008). Natural killer cells: diversity in search of a niche. *Nat Immunol* 9, 473-475.

Di Santo, J.P., and Vosshenrich, C.A. (2006). Bone marrow versus thymic pathways of natural killer cell development. *Immunol Rev* 214, 35-46.

Ding, S., Wu, X., Li, G., Han, M., Zhuang, Y., and Xu, T. (2005). Efficient transposition of the piggyBac (PB) transposon in mammalian cells and mice. *Cell* *122*, 473-483.

Dudley, E.C., Petrie, H.T., Shah, L.M., Owen, M.J., and Hayday, A.C. (1994). T cell receptor beta chain gene rearrangement and selection during thymocyte development in adult mice. *Immunity* *1*, 83-93.

Dunn, G.P., Old, L.J., and Schreiber, R.D. (2004). The three Es of cancer immunoediting. *Annu Rev Immunol* *22*, 329-360.

Evans, M.J., and Kaufman, M.H. (1981). Establishment in culture of pluripotential cells from mouse embryos. *Nature* *292*, 154-156.

Feltri, M.L., D'Antonio, M., Quattrini, A., Numerato, R., Arona, M., Previtali, S., Chiu, S.Y., Messing, A., and Wrabetz, L. (1999). A novel P0 glycoprotein transgene activates expression of lacZ in myelin-forming Schwann cells. *Eur J Neurosci* *11*, 1577-1586.

Ferlazzo, G., and Munz, C. (2009). Dendritic cell interactions with NK cells from different tissues. *J Clin Immunol* *29*, 265-273.

Feyerabend, T.B., Terszowski, G., Tietz, A., Blum, C., Luche, H., Gossler, A., Gale, N.W., Radtke, F., Fehling, H.J., and Rodewald, H.R. (2009). Deletion of Notch1 converts pro-T cells to dendritic cells and promotes thymic B cells by cell-extrinsic and cell-intrinsic mechanisms. *Immunity* *30*, 67-79.

Forsberg, E.C., Downs, K.M., and Bresnick, E.H. (2000). Direct interaction of NF-E2 with hypersensitive site 2 of the beta-globin locus control region in living cells. *Blood* *96*, 334-339.

Fowlkes, B.J., and Robey, E.A. (2002). A reassessment of the effect of activated Notch1 on CD4 and CD8 T cell development. *J Immunol* *169*, 1817-1821.

Fujimoto, S., Ikawa, T., Kina, T., and Yokota, Y. (2007). Forced expression of Id2 in fetal thymic T cell progenitors allows some of their progeny to adopt NK cell fate. *Int Immunol* *19*, 1175-1182.

Fung-Leung, W.P., Schilham, M.W., Rahemtulla, A., Kundig, T.M., Vollenweider, M., Potter, J., van Ewijk, W., and Mak, T.W. (1991). CD8 is needed for development of cytotoxic T cells but not helper T cells. *Cell* *65*, 443-449.

Gadue, P., and Stein, P.L. (2002). NK T cell precursors exhibit differential cytokine regulation and require Itk for efficient maturation. *J Immunol* *169*, 2397-2406.

Ganguli-Indra, G., Liang, X., Hyter, S., Leid, M., Hanifin, J., and Indra, A.K. (2009). Expression of COUP-TF-interacting protein 2 (CTIP2) in human atopic dermatitis and allergic contact dermatitis skin. *Exp Dermatol* *18*, 994-996.

Gascoyne, D.M., Long, E., Veiga-Fernandes, H., de Boer, J., Williams, O., Seddon, B., Coles, M., Kioussis, D., and Brady, H.J. (2009). The basic leucine zipper transcription factor E4BP4 is essential for natural killer cell development. *Nat Immunol* *10*, 1118-1124.

Glaser, S., Anastassiadis, K., and Stewart, A.F. (2005). Current issues in mouse genome engineering. *Nat Genet* *37*, 1187-1193.

Glick, B. (1979). The Avian Immune System. *Avian Diseases* *23*, 282-289.

Go, R., Hirose, S., Morita, S., Yamamoto, T., Katsuragi, Y., Mishima, Y., and Kominami, R. (2010). Bcl11b heterozygosity promotes clonal expansion and differentiation arrest of thymocytes in gamma-irradiated mice. *Cancer Sci* *101*, 1347-1353.

Godfrey, D.I., Kennedy, J., Suda, T., and Zlotnik, A. (1993). A developmental pathway involving four phenotypically and functionally distinct subsets of CD3-CD4-CD8- triple-negative adult mouse thymocytes defined by CD44 and CD25 expression. *J Immunol* *150*, 4244-4252.

Godfrey, D.I., MacDonald, H.R., Kronenberg, M., Smyth, M.J., and Van Kaer, L. (2004). NKT cells: what's in a name? *Nat Rev Immunol* 4, 231-237.

Godin, I., and Cumano, A. (2002). The hare and the tortoise: an embryonic haematopoietic race. *Nat Rev Immunol* 2, 593-604.

Godin, I., Dieterlen-Lievre, F., and Cumano, A. (1995). Emergence of multipotent hemopoietic cells in the yolk sac and paraaortic splanchnopleura in mouse embryos, beginning at 8.5 days postcoitus. *Proc Natl Acad Sci U S A* 92, 773-777.

Golonzhka, O., Leid, M., Indra, G., and Indra, A.K. (2007). Expression of COUP-TF-interacting protein 2 (CTIP2) in mouse skin during development and in adulthood. *Gene Expr Patterns* 7, 754-760.

Golonzhka, O., Liang, X., Messaddeq, N., Bornert, J.M., Campbell, A.L., Metzger, D., Chambon, P., Ganguli-Indra, G., Leid, M., and Indra, A.K. (2009a). Dual role of COUP-TF-interacting protein 2 in epidermal homeostasis and permeability barrier formation. *J Invest Dermatol* 129, 1459-1470.

Golonzhka, O., Metzger, D., Bornert, J.M., Bay, B.K., Gross, M.K., Kioussi, C., and Leid, M. (2009b). *Ctip2/Bcl11b* controls ameloblast formation during mammalian odontogenesis. *Proc Natl Acad Sci U S A* 106, 4278-4283.

Gorelik, E., Wiltrot, R.H., Okumura, K., Habu, S., and Herberman, R.B. (1982). Role of NK cells in the control of metastatic spread and growth of tumor cells in mice. *Int J Cancer* 30, 107-112.

Gorer, P.A., Lyman, S., and Snell, G.D. (1948). Studies on the genetic and antigenic basis of tumour transplantation: linkage between a histocompatibility gene and 'Fused' in mice. *Proc R Soc Lond B* 135, 499-505.

Gossen, M., and Bujard, H. (1992). Tight control of gene expression in mammalian cells by tetracycline-responsive promoters. *Proc Natl Acad Sci U S A* 89, 5547-5551.

Grabarczyk, P., Przybylski, G.K., Depke, M., Volker, U., Bahr, J., Assmus, K., Broker, B.M., Walther, R., and Schmidt, C.A. (2007). Inhibition of BCL11B expression leads to apoptosis of malignant but not normal mature T cells. *Oncogene* 26, 3797-3810.

Graf, T., and Enver, T. (2009). Forcing cells to change lineages. *Nature* 462, 587-594.
Griffiths, G.M., Tsun, A., and Stinchcombe, J.C. (2010). The immunological synapse: a focal point for endocytosis and exocytosis. *J Cell Biol* 189, 399-406.

Guan, C., Ye, C., Yang, X., and Gao, J. (2010). A review of current large-scale mouse knockout efforts. *Genesis* 48, 73-85.

Guerra, N., Tan, Y.X., Joncker, N.T., Choy, A., Gallardo, F., Xiong, N., Knoblaugh, S., Cado, D., Greenberg, N.M., and Raulet, D.H. (2008). NKG2D-deficient mice are defective in tumor surveillance in models of spontaneous malignancy. *Immunity* 28, 571-580.

Guo, P., Hirano, M., Herrin, B.R., Li, J., Yu, C., Sadlonova, A., and Cooper, M.D. (2009). Dual nature of the adaptive immune system in lampreys. *Nature* 459, 796-801.

Guo, Y., Maillard, I., Chakraborti, S., Rothenberg, E.V., and Speck, N.A. (2008). Core binding factors are necessary for natural killer cell development and cooperate with Notch signaling during T-cell specification. *Blood* 112, 480-492.

Gutierrez-Avino, F.J., Ferres-Marco, D., and Dominguez, M. (2009). The position and function of the Notch-mediated eye growth organizer: the roles of JAK/STAT and four-jointed. *EMBO Rep* 10, 1051-1058.

Hadjantonakis, A.K., Gertsenstein, M., Ikawa, M., Okabe, M., and Nagy, A. (1998). Generating green fluorescent mice by germline transmission of green fluorescent ES cells. *Mech Dev* 76, 79-90.

Hameyer, D., Loonstra, A., Eshkind, L., Schmitt, S., Antunes, C., Groen, A., Bindels, E., Jonkers, J., Krimpenfort, P., Meuwissen, R., *et al.* (2007). Toxicity of ligand-dependent Cre recombinases and generation of a conditional Cre deleter mouse allowing mosaic recombination in peripheral tissues. *Physiol Genomics* 31, 32-41.

Han, H., Tanigaki, K., Yamamoto, N., Kuroda, K., Yoshimoto, M., Nakahata, T., Ikuta, K., and Honjo, T. (2002). Inducible gene knockout of transcription factor recombination signal binding protein-J reveals its essential role in T versus B lineage decision. *Int Immunol* 14, 637-645.

Hardy, R.R., and Hayakawa, K. (2001). B cell development pathways. *Annu Rev Immunol* 19, 595-621.

Harman, B.C., Jenkinson, E.J., and Anderson, G. (2003). Microenvironmental regulation of Notch signalling in T cell development. *Semin Immunol* 15, 91-97.

Harrison, P.R. (1976). Analysis of erythropoiesis at the molecular level. *Nature* 262, 353-356.

He, X., Park, K., and Kappes, D.J. (2010). The role of ThPOK in control of CD4/CD8 lineage commitment. *Annu Rev Immunol* 28, 295-320.

He, X., Park, K., Wang, H., Zhang, Y., Hua, X., Li, Y., and Kappes, D.J. (2008). CD4-CD8 lineage commitment is regulated by a silencer element at the ThPOK transcription-factor locus. *Immunity* 28, 346-358.

Herberman, R.B., Nunn, M.E., Holden, H.T., and Lavrin, D.H. (1975). Natural cytotoxic reactivity of mouse lymphoid cells against syngeneic and allogeneic tumors. II. Characterization of effector cells. *Int J Cancer* 16, 230-239.

Hickman-Davis, J.M., and Davis, I.C. (2006). Transgenic mice. *Paediatr Respir Rev* 7, 49-53.

Ho, I.C., Tai, T.S., and Pai, S.Y. (2009). GATA3 and the T-cell lineage: essential functions before and after T-helper-2-cell differentiation. *Nat Rev Immunol* 9, 125-135.

Hogan, S.P., and Rothenberg, M.E. (2008). Dietary allergenic proteins and intestinal immunity: a shift from oral tolerance to sensitization. *Clin Exp Allergy* 38, 229-232.

Huang, J., Garrett, K.P., Pelayo, R., Zuniga-Pflucker, J.C., Petrie, H.T., and Kincaid, P.W. (2005). Propensity of adult lymphoid progenitors to progress to DN2/3 stage thymocytes with Notch receptor ligation. *J Immunol* 175, 4858-4865.

Huang, W.Y., Aramburu, J., Douglas, P.S., and Izumo, S. (2000). Transgenic expression of green fluorescence protein can cause dilated cardiomyopathy. *Nat Med* 6, 482-483.

Huntington, N.D., Vosshenrich, C.A., and Di Santo, J.P. (2007). Developmental pathways that generate natural-killer-cell diversity in mice and humans. *Nat Rev Immunol* 7, 703-714.

Iguchi-Manaka, A., Kai, H., Yamashita, Y., Shibata, K., Tahara-Hanaoka, S., Honda, S., Yasui, T., Kikutani, H., Shibuya, K., and Shibuya, A. (2008). Accelerated tumor growth in mice deficient in DNAM-1 receptor. *J Exp Med* 205, 2959-2964.

Ikawa, T., Fujimoto, S., Kawamoto, H., Katsura, Y., and Yokota, Y. (2001). Commitment to natural killer cells requires the helix-loop-helix inhibitor Id2. *Proc Natl Acad Sci U S A* 98, 5164-5169.

Ikawa, T., Hirose, S., Masuda, K., Kakugawa, K., Satoh, R., Shibano-Satoh, A., Kominami, R., Katsura, Y., and Kawamoto, H. (2010). An essential developmental checkpoint for production of the T cell lineage. *Science* 329, 93-96.

Ikawa, T., Kawamoto, H., Fujimoto, S., and Katsura, Y. (1999). Commitment of common T/Natural killer (NK) progenitors to unipotent T and NK progenitors in the

murine fetal thymus revealed by a single progenitor assay. *J Exp Med* *190*, 1617-1626.

Intlekofer, A.M., Takemoto, N., Wherry, E.J., Longworth, S.A., Northrup, J.T., Palanivel, V.R., Mullen, A.C., Gasink, C.R., Kaech, S.M., Miller, J.D., *et al.* (2005). Effector and memory CD8⁺ T cell fate coupled by T-bet and eomesodermin. *Nat Immunol* *6*, 1236-1244.

Iwasaki, H., and Akashi, K. (2007). Myeloid lineage commitment from the hematopoietic stem cell. *Immunity* *26*, 726-740.

Izon, D.J., Aster, J.C., He, Y., Weng, A., Karnell, F.G., Patriub, V., Xu, L., Bakkour, S., Rodriguez, C., Allman, D., *et al.* (2002). Deltex1 redirects lymphoid progenitors to the B cell lineage by antagonizing Notch1. *Immunity* *16*, 231-243.

Jahn, T., Sindhu, S., Gooch, S., Seipel, P., Lavori, P., Leifheit, E., and Weinberg, K. (2007). Direct interaction between Kit and the interleukin-7 receptor. *Blood* *110*, 1840-1847.

Kaech, S.M., Tan, J.T., Wherry, E.J., Konieczny, B.T., Surh, C.D., and Ahmed, R. (2003). Selective expression of the interleukin 7 receptor identifies effector CD8 T cells that give rise to long-lived memory cells. *Nat Immunol* *4*, 1191-1198.

Kamimura, K., Mishima, Y., Obata, M., Endo, T., Aoyagi, Y., and Kominami, R. (2007a). Lack of Bcl11b tumor suppressor results in vulnerability to DNA replication stress and damages. *Oncogene* *26*, 5840-5850.

Kamimura, K., Ohi, H., Kubota, T., Okazuka, K., Yoshikai, Y., Wakabayashi, Y., Aoyagi, Y., Mishima, Y., and Kominami, R. (2007b). Haploinsufficiency of Bcl11b for suppression of lymphomagenesis and thymocyte development. *Biochem Biophys Res Commun* *355*, 538-542.

Kamizono, S., Duncan, G.S., Seidel, M.G., Morimoto, A., Hamada, K., Grosveld, G., Akashi, K., Lind, E.F., Haight, J.P., Ohashi, P.S., *et al.* (2009). Nfil3/E4bp4 is

required for the development and maturation of NK cells in vivo. *J Exp Med* 206, 2977-2986.

Karanam, N.K., Grabarczyk, P., Hammer, E., Scharf, C., Venz, S., Gesell-Salazar, M., Barthlen, W., Przybylski, G.K., Schmidt, C.A., and Volker, U. (2010). Proteome Analysis Reveals New Mechanisms of Bcl11b-loss Driven Apoptosis. *J Proteome Res* [Epub ahead of print].

Karasuyama, H., Kudo, A., and Melchers, F. (1990). The proteins encoded by the VpreB and lambda 5 pre-B cell-specific genes can associate with each other and with mu heavy chain. *J Exp Med* 172, 969-972.

Karasuyama, H., Rolink, A., and Melchers, F. (1993). A complex of glycoproteins is associated with VpreB/lambda 5 surrogate light chain on the surface of mu heavy chain-negative early precursor B cell lines. *J Exp Med* 178, 469-478.

Karre, K. (2008). Natural killer cell recognition of missing self. *Nat Immunol* 9, 477-480.

Karre, K., Ljunggren, H.G., Piontek, G., and Kiessling, R. (1986). Selective rejection of H-2-deficient lymphoma variants suggests alternative immune defence strategy. *Nature* 319, 675-678.

Kastner, P., Chan, S., Vogel, W.K., Zhang, L.J., Topark-Ngarm, A., Golonzhka, O., Jost, B., Le Gras, S., Gross, M.K., and Leid, M. (2010). Bcl11b represses a mature T-cell gene expression program in immature CD4(+)CD8(+) thymocytes. *Eur J Immunol*.

Kiessling, R., Haller, O., Fenyo, E.M., Steinitz, M., and Klein, G. (1978). Mouse natural killer (NK) cell activity against human cell lines is not influenced by superinfection of the target cell with xenotropic murine C-type virus. *Int J Cancer* 21, 460-465.

Kiessling, R., Klein, E., Pross, H., and Wigzell, H. (1975). "Natural" killer cells in the mouse. II. Cytotoxic cells with specificity for mouse Moloney leukemia cells. Characteristics of the killer cell. *Eur J Immunol* 5, 117-121.

Kiessling, R., Petrányi, G., Karre, K., Jondal, M., Tracey, D., and Wigzell, H. (1976). Killer cells: a functional comparison between natural, immune T-cell and antibody-dependent in vitro systems. *J Exp Med* 143, 772-780.

Kim, J.B., Greber, B., Arauzo-Bravo, M.J., Meyer, J., Park, K.I., Zaehres, H., and Scholer, H.R. (2009). Direct reprogramming of human neural stem cells by OCT4. *Nature* 461, 649-643.

Kim, S., Iizuka, K., Kang, H.S., Dokun, A., French, A.R., Greco, S., and Yokoyama, W.M. (2002). In vivo developmental stages in murine natural killer cell maturation. *Nat Immunol* 3, 523-528.

Kitamura, D., Roes, J., Kuhn, R., and Rajewsky, K. (1991). A B cell-deficient mouse by targeted disruption of the membrane exon of the immunoglobulin mu chain gene. *Nature* 350, 423-426.

Kleinjan, D.A., and van Heyningen, V. (2005). Long-range control of gene expression: emerging mechanisms and disruption in disease. *Am J Hum Genet* 76, 8-32.

Klug, A. (2010). The discovery of zinc fingers and their applications in gene regulation and genome manipulation. *Annu Rev Biochem* 79, 213-231.

Koller, B.H., Marrack, P., Kappler, J.W., and Smithies, O. (1990). Normal development of mice deficient in beta 2M, MHC class I proteins, and CD8⁺ T cells. *Science* 248, 1227-1230.

Koller, B.H., and Smithies, O. (1989). Inactivating the beta 2-microglobulin locus in mouse embryonic stem cells by homologous recombination. *Proc Natl Acad Sci U S A* 86, 8932-8935.

Kondo, M., Weissman, I.L., and Akashi, K. (1997). Identification of clonogenic common lymphoid progenitors in mouse bone marrow. *Cell* 91, 661-672.

Kopan, R., and Ilagan, M.X. (2009). The canonical Notch signaling pathway: unfolding the activation mechanism. *Cell* 137, 216-233.

Krejci, A., Bernard, F., Housden, B.E., Collins, S., and Bray, S.J. (2009). Direct response to Notch activation: signaling crosstalk and incoherent logic. *Sci Signal* 2, ra1.

Kuprash, D.V., Alimzhanov, M.B., Tumanov, A.V., Grivennikov, S.I., Shakhov, A.N., Drutskaya, L.N., Marino, M.W., Turetskaya, R.L., Anderson, A.O., Rajewsky, K., *et al.* (2002). Redundancy in tumor necrosis factor (TNF) and lymphotoxin (LT) signaling in vivo: mice with inactivation of the entire TNF/LT locus versus single-knockout mice. *Mol Cell Biol* 22, 8626-8634.

Lakshmikanth, T., Burke, S., Ali, T.H., Kimpfler, S., Ursini, F., Ruggeri, L., Capanni, M., Umansky, V., Paschen, A., Sucker, A., *et al.* (2009). NCRs and DNAM-1 mediate NK cell recognition and lysis of human and mouse melanoma cell lines in vitro and in vivo. *J Clin Invest* 119, 1251-1263.

Lander, E.S., Linton, L.M., Birren, B., Nusbaum, C., Zody, M.C., Baldwin, J., Devon, K., Dewar, K., Doyle, M., FitzHugh, W., *et al.* (2001). Initial sequencing and analysis of the human genome. *Nature* 409, 860-921.

Laouar, Y., Sutterwala, F.S., Gorelik, L., and Flavell, R.A. (2005). Transforming growth factor-beta controls T helper type 1 cell development through regulation of natural killer cell interferon-gamma. *Nat Immunol* 6, 600-607.

Lee, D.H., Iwanski, G.B., and Thoennissen, N.H. (2010). Cucurbitacin: ancient compound shedding new light on cancer treatment. *ScientificWorldJournal* 10, 413-418.

Lee, P.P., Fitzpatrick, D.R., Beard, C., Jessup, H.K., Lehar, S., Makar, K.W., Perez-Melgosa, M., Sweetser, M.T., Schlissel, M.S., Nguyen, S., *et al.* (2001). A critical role for Dnmt1 and DNA methylation in T cell development, function, and survival. *Immunity* 15, 763-774.

Lewis, R.S. (2001). Calcium signaling mechanisms in T lymphocytes. *Annu Rev Immunol* 19, 497-521.

Li, L., Leid, M., and Rothenberg, E.V. (2010). An early T cell lineage commitment checkpoint dependent on the transcription factor Bcl11b. *Science* 329, 89-93.

Lin, H., and Grosschedl, R. (1995). Failure of B-cell differentiation in mice lacking the transcription factor EBF. *Nature* 376, 263-267.

Liu, P., Keller, J.R., Ortiz, M., Tessarollo, L., Rachel, R.A., Nakamura, T., Jenkins, N.A., and Copeland, N.G. (2003). Bcl11a is essential for normal lymphoid development. *Nat Immunol* 4, 525-532.

Ljunggren, H.G., and Karre, K. (1985). Host resistance directed selectively against H-2-deficient lymphoma variants. Analysis of the mechanism. *J Exp Med* 162, 1745-1759.

Lodolce, J.P., Boone, D.L., Chai, S., Swain, R.E., Dassopoulos, T., Trettin, S., and Ma, A. (1998). IL-15 receptor maintains lymphoid homeostasis by supporting lymphocyte homing and proliferation. *Immunity* 9, 669-676.

M. Bielschowsky, B.J.H.a.J.H. (1959). Spontaneous haemolytic anaemia in mice of the NZB/B1 strain. *Proc Univ of Otago Med School* 37, 9-11.

MacLeod, R.A., Nagel, S., Kaufmann, M., Janssen, J.W., and Drexler, H.G. (2003). Activation of HOX11L2 by juxtaposition with 3'-BCL11B in an acute lymphoblastic leukemia cell line (HPB-ALL) with t(5;14)(q35;q32.2). *Genes Chromosomes Cancer* 37, 84-91.

Maillard, I., Fang, T., and Pear, W.S. (2005). Regulation of lymphoid development, differentiation, and function by the Notch pathway. *Annu Rev Immunol* 23, 945-974.

Mak, T.W., Hakem, A., McPherson, J.P., Shehabeldin, A., Zablocki, E., Migon, E., Duncan, G.S., Bouchard, D., Wakeham, A., Cheung, A., *et al.* (2000). Brcal required for T cell lineage development but not TCR loci rearrangement. *Nat Immunol* 1, 77-82.

Mak, T.W., Penninger, J.M., and Ohashi, P.S. (2001). Knockout mice: a paradigm shift in modern immunology. *Nat Rev Immunol* 1, 11-19.

Manz, M.G., Traver, D., Miyamoto, T., Weissman, I.L., and Akashi, K. (2001). Dendritic cell potentials of early lymphoid and myeloid progenitors. *Blood* 97, 3333-3341.

Marban, C., Suzanne, S., Dequiedt, F., de Walque, S., Redel, L., Van Lint, C., Aunis, D., and Rohr, O. (2007). Recruitment of chromatin-modifying enzymes by CTIP2 promotes HIV-1 transcriptional silencing. *EMBO J* 26, 412-423.

Mardis, E.R. (2008). The impact of next-generation sequencing technology on genetics. *Trends Genet* 24, 133-141.

Marsland, B.J., and Kopf, M. (2008). T-cell fate and function: PKC-theta and beyond. *Trends Immunol* 29, 179-185.

Martin, G.R. (1981). Isolation of a pluripotent cell line from early mouse embryos cultured in medium conditioned by teratocarcinoma stem cells. *Proc Natl Acad Sci U S A* 78, 7634-7638.

Masuda, K., Kakugawa, K., Nakayama, T., Minato, N., Katsura, Y., and Kawamoto, H. (2007). T cell lineage determination precedes the initiation of TCR beta gene rearrangement. *J Immunol* 179, 3699-3706.

Matsumoto, Y., Kosugi, S., Shinbo, T., Chou, D., Ohashi, M., Wakabayashi, Y., Sakai, K., Okumoto, M., Mori, N., Aizawa, S., *et al.* (1998). Allelic loss analysis of gamma-ray-induced mouse thymic lymphomas: two candidate tumor suppressor gene loci on chromosomes 12 and 16. *Oncogene* *16*, 2747-2754.

Menzel, S., Garner, C., Gut, I., Matsuda, F., Yamaguchi, M., Heath, S., Foglio, M., Zelenika, D., Boland, A., Rooks, H., *et al.* (2007). A QTL influencing F cell production maps to a gene encoding a zinc-finger protein on chromosome 2p15. *Nat Genet* *39*, 1197-1199.

Metzger, D., and Chambon, P. (2001). Site- and time-specific gene targeting in the mouse. *Methods* *24*, 71-80.

Miaw, S.C., Choi, A., Yu, E., Kishikawa, H., and Ho, I.C. (2000). ROG, repressor of GATA, regulates the expression of cytokine genes. *Immunity* *12*, 323-333.

Michie, A.M., Carlyle, J.R., Schmitt, T.M., Ljutic, B., Cho, S.K., Fong, Q., and Zuniga-Pflucker, J.C. (2000). Clonal characterization of a bipotent T cell and NK cell progenitor in the mouse fetal thymus. *J Immunol* *164*, 1730-1733.

Mikkola, I., Heavey, B., Horcher, M., and Busslinger, M. (2002). Reversion of B cell commitment upon loss of Pax5 expression. *Science* *297*, 110-113.

Miller, J.S., Soignier, Y., Panoskaltsis-Mortari, A., McNearney, S.A., Yun, G.H., Fautsch, S.K., McKenna, D., Le, C., Defor, T.E., Burns, L.J., *et al.* (2005). Successful adoptive transfer and in vivo expansion of human haploidentical NK cells in patients with cancer. *Blood* *105*, 3051-3057.

Mlodzik, M., Hiromi, Y., Weber, U., Goodman, C.S., and Rubin, G.M. (1990). The *Drosophila* seven-up gene, a member of the steroid receptor gene superfamily, controls photoreceptor cell fates. *Cell* *60*, 211-224.

Mohrs, M., Shinkai, K., Mohrs, K., and Locksley, R.M. (2001). Analysis of type 2 immunity in vivo with a bicistronic IL-4 reporter. *Immunity* *15*, 303-311.

Morris, L., Klanke, C., Lang, S., Lim, F.Y., and Crombleholme, T. (2010). TdTomato and EGFP identification in histological sections: insight and alternatives. *Biotech Histochem*.

Morrison, S.J., and Weissman, I.L. (1994). The long-term repopulating subset of hematopoietic stem cells is deterministic and isolatable by phenotype. *Immunity* *1*, 661-673.

Muul, L.M., Spiess, P.J., Director, E.P., and Rosenberg, S.A. (1987). Identification of specific cytolytic immune responses against autologous tumor in humans bearing malignant melanoma. *J Immunol* *138*, 989-995.

Nagel, S., Kaufmann, M., Drexler, H.G., and MacLeod, R.A. (2003). The cardiac homeobox gene NKX2-5 is deregulated by juxtaposition with BCL11B in pediatric T-ALL cell lines via a novel t(5;14)(q35.1;q32.2). *Cancer Res* *63*, 5329-5334.

Nagy, A. (2000). Cre recombinase: the universal reagent for genome tailoring. *Genesis* *26*, 99-109.

Nagy, A., Rossant, J., Nagy, R., Abramow-Newerly, W., and Roder, J.C. (1993). Derivation of completely cell culture-derived mice from early-passage embryonic stem cells. *Proc Natl Acad Sci U S A* *90*, 8424-8428.

Nakamura, T., Largaespada, D.A., Shaughnessy, J.D., Jr., Jenkins, N.A., and Copeland, N.G. (1996). Cooperative activation of Hoxa and Pbx1-related genes in murine myeloid leukaemias. *Nat Genet* *12*, 149-153.

Nakamura, T., Yamazaki, Y., Saiki, Y., Moriyama, M., Largaespada, D.A., Jenkins, N.A., and Copeland, N.G. (2000). Evi9 encodes a novel zinc finger protein that physically interacts with BCL6, a known human B-cell proto-oncogene product. *Mol Cell Biol* *20*, 3178-3186.

Nakano, T., Kodama, H., and Honjo, T. (1994). Generation of lymphohematopoietic cells from embryonic stem cells in culture. *Science* 265, 1098-1101.

Nelms, K.A., and Goodnow, C.C. (2001). Genome-wide ENU mutagenesis to reveal immune regulators. *Immunity* 15, 409-418.

Nikolic-Zugic, J., and Moore, M.W. (1989). T cell receptor expression on immature thymocytes with in vivo and in vitro precursor potential. *Eur J Immunol* 19, 1957-1960.

Nolan, G.P., Fiering, S., Nicolas, J.F., and Herzenberg, L.A. (1988). Fluorescence-activated cell analysis and sorting of viable mammalian cells based on beta-D-galactosidase activity after transduction of *Escherichia coli lacZ*. *Proc Natl Acad Sci U S A* 85, 2603-2607.

Northrup, D.L., and Allman, D. (2008). Transcriptional regulation of early B cell development. *Immunol Res* 42, 106-117.

Okazuka, K., Wakabayashi, Y., Kashihara, M., Inoue, J., Sato, T., Yokoyama, M., Aizawa, S., Aizawa, Y., Mishima, Y., and Kominami, R. (2005). p53 prevents maturation of T cell development to the immature CD4-CD8⁺ stage in *Bcl11b*^{-/-} mice. *Biochem Biophys Res Commun* 328, 545-549.

Oldham, R.K. (1983). Natural killer cells: artifact to reality: an odyssey in biology. *Cancer Metastasis Rev* 2, 323-336.

Omori, M., Yamashita, M., Inami, M., Ukai-Tadenuma, M., Kimura, M., Nigo, Y., Hosokawa, H., Hasegawa, A., Taniguchi, M., and Nakayama, T. (2003). CD8 T cell-specific downregulation of histone hyperacetylation and gene activation of the IL-4 gene locus by ROG, repressor of GATA. *Immunity* 19, 281-294.

Pai, S.Y., Truitt, M.L., Ting, C.N., Leiden, J.M., Glimcher, L.H., and Ho, I.C. (2003). Critical roles for transcription factor GATA-3 in thymocyte development. *Immunity* 19, 863-875.

Park, K., He, X., Lee, H.O., Hua, X., Li, Y., Wiest, D., and Kappes, D.J. (2010). TCR-mediated ThPOK induction promotes development of mature (CD24-) gammadelta thymocytes. *EMBO J* 29, 2329-2341.

Pearce, E.L., Mullen, A.C., Martins, G.A., Krawczyk, C.M., Hutchins, A.S., Zediak, V.P., Banica, M., DiCioccio, C.B., Gross, D.A., Mao, C.A., *et al.* (2003). Control of effector CD8+ T cell function by the transcription factor Eomesodermin. *Science* 302, 1041-1043.

Pellicci, D.G., Hammond, K.J., Uldrich, A.P., Baxter, A.G., Smyth, M.J., and Godfrey, D.I. (2002). A natural killer T (NKT) cell developmental pathway involving a thymus-dependent NK1.1(-)CD4(+) CD1d-dependent precursor stage. *J Exp Med* 195, 835-844.

Pentao Liu, P.L., Shannon Burke (2010). Critical Roles of Bcl11b in T Cell Development and Maintenance of T Cell Identity. *Immunological Reviews In press.*

Petrie, H.T., Hugo, P., Scollay, R., and Shortman, K. (1990). Lineage relationships and developmental kinetics of immature thymocytes: CD3, CD4, and CD8 acquisition in vivo and in vitro. *J Exp Med* 172, 1583-1588.

Przybylski, G.K., Dik, W.A., Wanzeck, J., Grabarczyk, P., Majunke, S., Martin-Subero, J.I., Siebert, R., Dolken, G., Ludwig, W.D., Verhaaf, B., *et al.* (2005). Disruption of the BCL11B gene through inv(14)(q11.2q32.31) results in the expression of BCL11B-TRDC fusion transcripts and is associated with the absence of wild-type BCL11B transcripts in T-ALL. *Leukemia* 19, 201-208.

Pui, J.C., Allman, D., Xu, L., DeRocco, S., Karnell, F.G., Bakkour, S., Lee, J.Y., Kadesch, T., Hardy, R.R., Aster, J.C., *et al.* (1999). Notch1 expression in early lymphopoiesis influences B versus T lineage determination. *Immunity* 11, 299-308.

Puzanov, I.J., Bennett, M., and Kumar, V. (1996). IL-15 can substitute for the marrow microenvironment in the differentiation of natural killer cells. *J Immunol* *157*, 4282-4285.

Qi, Q., and August, A. (2007). Keeping the (kinase) party going: SLP-76 and ITK dance to the beat. *Sci STKE* *2007*, pe39.

Radtke, F., Fasnacht, N., and Macdonald, H.R. (2010). Notch signaling in the immune system. *Immunity* *32*, 14-27.

Radtke, F., Wilson, A., Stark, G., Bauer, M., van Meerwijk, J., MacDonald, H.R., and Aguet, M. (1999). Deficient T cell fate specification in mice with an induced inactivation of Notch1. *Immunity* *10*, 547-558.

Rajewsky, K., Gu, H., Kuhn, R., Betz, U.A., Muller, W., Roes, J., and Schwenk, F. (1996). Conditional gene targeting. *J Clin Invest* *98*, 600-603.

Ramalho-Santos, M., Yoon, S., Matsuzaki, Y., Mulligan, R.C., and Melton, D.A. (2002). "Stemness": transcriptional profiling of embryonic and adult stem cells. *Science* *298*, 597-600.

Robbins, P.F., Dudley, M.E., Wunderlich, J., El-Gamil, M., Li, Y.F., Zhou, J., Huang, J., Powell, D.J., Jr., and Rosenberg, S.A. (2004). Cutting edge: persistence of transferred lymphocyte clonotypes correlates with cancer regression in patients receiving cell transfer therapy. *J Immunol* *173*, 7125-7130.

Robertson, E., Bradley, A., Kuehn, M., and Evans, M. (1986). Germ-line transmission of genes introduced into cultured pluripotential cells by retroviral vector. *Nature* *323*, 445-448.

Robertson, M.J. (2002). Role of chemokines in the biology of natural killer cells. *J Leukoc Biol* *71*, 173-183.

Rolink, A.G., Balciunaite, G., Demoliere, C., and Ceredig, R. (2006). The potential involvement of Notch signaling in NK cell development. *Immunol Lett* *107*, 50-57.

Rolink, A.G., Nutt, S.L., Melchers, F., and Busslinger, M. (1999). Long-term in vivo reconstitution of T-cell development by Pax5-deficient B-cell progenitors. *Nature* *401*, 603-606.

Rosenberg, S.A., and Dudley, M.E. (2009). Adoptive cell therapy for the treatment of patients with metastatic melanoma. *Curr Opin Immunol* *21*, 233-240.

Rosenberg, S.A., Lotze, M.T., Muul, L.M., Leitman, S., Chang, A.E., Ettinghausen, S.E., Matory, Y.L., Skibber, J.M., Shiloni, E., Vetto, J.T., *et al.* (1985). Observations on the systemic administration of autologous lymphokine-activated killer cells and recombinant interleukin-2 to patients with metastatic cancer. *N Engl J Med* *313*, 1485-1492.

Rosenberg, S.A., Restifo, N.P., Yang, J.C., Morgan, R.A., and Dudley, M.E. (2008). Adoptive cell transfer: a clinical path to effective cancer immunotherapy. *Nat Rev Cancer* *8*, 299-308.

Rosenberg, S.A., Spiess, P., and Lafreniere, R. (1986). A new approach to the adoptive immunotherapy of cancer with tumor-infiltrating lymphocytes. *Science* *233*, 1318-1321.

Rosenberg, S.A., Yang, J.C., and Restifo, N.P. (2004). Cancer immunotherapy: moving beyond current vaccines. *Nat Med* *10*, 909-915.

Rosenberg, S.A., Yang, J.C., White, D.E., and Steinberg, S.M. (1998). Durability of complete responses in patients with metastatic cancer treated with high-dose interleukin-2: identification of the antigens mediating response. *Ann Surg* *228*, 307-319.

Rosenwasser, L.J., and Rothenberg, M.E. (2010). IL-5 pathway inhibition in the treatment of asthma and Churg-Strauss syndrome. *J Allergy Clin Immunol* 125, 1245-1246.

Rothenberg, E.V. (2007). Negotiation of the T lineage fate decision by transcription-factor interplay and microenvironmental signals. *Immunity* 26, 690-702.

Rothenberg, E.V., Moore, J.E., and Yui, M.A. (2008). Launching the T-cell-lineage developmental programme. *Nat Rev Immunol* 8, 9-21.

Rothenberg, E.V., and Taghon, T. (2005). Molecular genetics of T cell development. *Annu Rev Immunol* 23, 601-649.

Ruggeri, L., Capanni, M., Urbani, E., Perruccio, K., Shlomchik, W.D., Tosti, A., Posati, S., Rogaia, D., Frassoni, F., Aversa, F., *et al.* (2002). Effectiveness of donor natural killer cell alloreactivity in mismatched hematopoietic transplants. *Science* 295, 2097-2100.

Russell, W.L., Kelly, E.M., Hunsicker, P.R., Bangham, J.W., Maddux, S.C., and Phipps, E.L. (1979). Specific-locus test shows ethylnitrosourea to be the most potent mutagen in the mouse. *Proc Natl Acad Sci U S A* 76, 5818-5819.

Salem, M.L., El-Demellawy, M., and El-Azm, A.R. (2010). The potential use of Toll-like receptor agonists to restore the dysfunctional immunity induced by hepatitis C virus. *Cell Immunol* 262, 96-104.

Sankaran, V.G., Menne, T.F., Xu, J., Akie, T.E., Lettre, G., Van Handel, B., Mikkola, H.K., Hirschhorn, J.N., Cantor, A.B., and Orkin, S.H. (2008). Human fetal hemoglobin expression is regulated by the developmental stage-specific repressor BCL11A. *Science* 322, 1839-1842.

Sankaran, V.G., Xu, J., Ragoczy, T., Ippolito, G.C., Walkley, C.R., Maika, S.D., Fujiwara, Y., Ito, M., Groudine, M., Bender, M.A., *et al.* (2009). Developmental and species-divergent globin switching are driven by BCL11A. *Nature* 460, 1093-1097.

Satterwhite, E., Sonoki, T., Willis, T.G., Harder, L., Nowak, R., Arriola, E.L., Liu, H., Price, H.P., Gesk, S., Steinemann, D., *et al.* (2001). The BCL11 gene family: involvement of BCL11A in lymphoid malignancies. *Blood* 98, 3413-3420.

Schmitt, T.M., and Zuniga-Pflucker, J.C. (2002). Induction of T cell development from hematopoietic progenitor cells by delta-like-1 in vitro. *Immunity* 17, 749-756.

Senawong, T., Peterson, V.J., Avram, D., Shepherd, D.M., Frye, R.A., Minucci, S., and Leid, M. (2003). Involvement of the histone deacetylase SIRT1 in chicken ovalbumin upstream promoter transcription factor (COUP-TF)-interacting protein 2-mediated transcriptional repression. *J Biol Chem* 278, 43041-43050.

Senawong, T., Peterson, V.J., and Leid, M. (2005). BCL11A-dependent recruitment of SIRT1 to a promoter template in mammalian cells results in histone deacetylation and transcriptional repression. *Arch Biochem Biophys* 434, 316-325.

Setoguchi, R., Tachibana, M., Naoe, Y., Muroi, S., Akiyama, K., Tezuka, C., Okuda, T., and Taniuchi, I. (2008). Repression of the transcription factor Th-POK by Runx complexes in cytotoxic T cell development. *Science* 319, 822-825.

Shaner, N.C., Campbell, R.E., Steinbach, P.A., Giepmans, B.N., Palmer, A.E., and Tsien, R.Y. (2004). Improved monomeric red, orange and yellow fluorescent proteins derived from *Discosoma* sp. red fluorescent protein. *Nat Biotechnol* 22, 1567-1572.

Shinbo, T., Matsuki, A., Matsumoto, Y., Kosugi, S., Takahashi, Y., Niwa, O., and Kominami, R. (1999). Allelic loss mapping and physical delineation of a region harboring a putative thymic lymphoma suppressor gene on mouse chromosome 12. *Oncogene* 18, 4131-4136.

Silver, L.M. (1985). *Mouse Genetics, Concepts and Applications*. Oxford University Press.

Smithies, O., Gregg, R.G., Boggs, S.S., Koralewski, M.A., and Kucherlapati, R.S. (1985). Insertion of DNA sequences into the human chromosomal beta-globin locus by homologous recombination. *Nature* 317, 230-234.

Smyth, M.J., Dunn, G.P., and Schreiber, R.D. (2006). Cancer immunosurveillance and immunoediting: the roles of immunity in suppressing tumor development and shaping tumor immunogenicity. *Adv Immunol* 90, 1-50.

Snell, G.D., and Reed, S. (1993). William Ernest Castle, pioneer mammalian geneticist. *Genetics* 133, 751-753.

Snell, G.D.a.H., G.F. (1951). Alleles at the histocompatibility-2 locus in the mouse as determined by tumor transplantation. *Genetics* 36, 306-310.

Sotillos, S., Diaz-Meco, M.T., Moscat, J., and Castelli-Gair Hombria, J. (2008). Polarized subcellular localization of Jak/STAT components is required for efficient signaling. *Curr Biol* 18, 624-629.

Spits, H., Couwenberg, F., Bakker, A.Q., Weijer, K., and Uittenbogaart, C.H. (2000). Id2 and Id3 inhibit development of CD34(+) stem cells into predendritic cell (pre-DC)2 but not into pre-DC1. Evidence for a lymphoid origin of pre-DC2. *J Exp Med* 192, 1775-1784.

Stinchcombe, J.C., Majorovits, E., Bossi, G., Fuller, S., and Griffiths, G.M. (2006). Centrosome polarization delivers secretory granules to the immunological synapse. *Nature* 443, 462-465.

Stremmel, C., Exley, M., Balk, S., Hohenberger, W., and Kuchroo, V.K. (2001). Characterization of the phenotype and function of CD8(+), alpha / beta(+) NKT cells from tumor-bearing mice that show a natural killer cell activity and lyse multiple tumor targets. *Eur J Immunol* 31, 2818-2828.

Suzuki, A., Yamaguchi, M.T., Ohteki, T., Sasaki, T., Kaisho, T., Kimura, Y., Yoshida, R., Wakeham, A., Higuchi, T., Fukumoto, M., *et al.* (2001). T cell-specific

loss of Pten leads to defects in central and peripheral tolerance. *Immunity* *14*, 523-534.

Suzuki, H., Duncan, G.S., Takimoto, H., and Mak, T.W. (1997). Abnormal development of intestinal intraepithelial lymphocytes and peripheral natural killer cells in mice lacking the IL-2 receptor beta chain. *J Exp Med* *185*, 499-505.

Szabo, S.J., Kim, S.T., Costa, G.L., Zhang, X., Fathman, C.G., and Glimcher, L.H. (2000). A novel transcription factor, T-bet, directs Th1 lineage commitment. *Cell* *100*, 655-669.

Szabo, S.J., Sullivan, B.M., Stemmann, C., Satoskar, A.R., Sleckman, B.P., and Glimcher, L.H. (2002). Distinct effects of T-bet in TH1 lineage commitment and IFN-gamma production in CD4 and CD8 T cells. *Science* *295*, 338-342.

Taghon, T., Yui, M.A., Pant, R., Diamond, R.A., and Rothenberg, E.V. (2006). Developmental and molecular characterization of emerging beta- and gammadelta-selected pre-T cells in the adult mouse thymus. *Immunity* *24*, 53-64.

Taghon, T.N., David, E.S., Zuniga-Pflucker, J.C., and Rothenberg, E.V. (2005). Delayed, asynchronous, and reversible T-lineage specification induced by Notch/Delta signaling. *Genes Dev* *19*, 965-978.

Takada, K., and Jameson, S.C. (2009). Naive T cell homeostasis: from awareness of space to a sense of place. *Nat Rev Immunol* *9*, 823-832.

Takahashi, K., Tanabe, K., Ohnuki, M., Narita, M., Ichisaka, T., Tomoda, K., and Yamanaka, S. (2007). Induction of pluripotent stem cells from adult human fibroblasts by defined factors. *Cell* *131*, 861-872.

Takahashi, M., Altschmied, L., and Hillen, W. (1986). Kinetic and equilibrium characterization of the Tet repressor-tetracycline complex by fluorescence measurements. Evidence for divalent metal ion requirement and energy transfer. *J Mol Biol* *187*, 341-348.

Takeda, K., Cretney, E., Hayakawa, Y., Ota, T., Akiba, H., Ogasawara, K., Yagita, H., Kinoshita, K., Okumura, K., and Smyth, M.J. (2005). TRAIL identifies immature natural killer cells in newborn mice and adult mouse liver. *Blood* *105*, 2082-2089.

Taniguchi, S., Kawano, T., Kakunaga, T., and Baba, T. (1986). Differences in expression of a variant actin between low and high metastatic B16 melanoma. *J Biol Chem* *261*, 6100-6106.

Taniuchi, I., Osato, M., Egawa, T., Sunshine, M.J., Bae, S.C., Komori, T., Ito, Y., and Littman, D.R. (2002). Differential requirements for Runx proteins in CD4 repression and epigenetic silencing during T lymphocyte development. *Cell* *111*, 621-633.

Telling, G.C., Tremblay, P., Torchia, M., Dearmond, S.J., Cohen, F.E., and Prusiner, S.B. (1997). N-terminally tagged prion protein supports prion propagation in transgenic mice. *Protein Sci* *6*, 825-833.

Thibault, S.T., Singer, M.A., Miyazaki, W.Y., Milash, B., Dompe, N.A., Singh, C.M., Buchholz, R., Demsky, M., Fawcett, R., Francis-Lang, H.L., *et al.* (2004). A complementary transposon tool kit for *Drosophila melanogaster* using P and piggyBac. *Nat Genet* *36*, 283-287.

Thomas, K.R., and Capecchi, M.R. (1986). Introduction of homologous DNA sequences into mammalian cells induces mutations in the cognate gene. *Nature* *324*, 34-38.

Topark-Ngarm, A., Golonzhka, O., Peterson, V.J., Barrett, B., Jr., Martinez, B., Crofoot, K., Filtz, T.M., and Leid, M. (2006). CTIP2 associates with the NuRD complex on the promoter of p57KIP2, a newly identified CTIP2 target gene. *J Biol Chem* *281*, 32272-32283.

Triezenberg, S.J., Kingsbury, R.C., and McKnight, S.L. (1988). Functional dissection of VP16, the trans-activator of herpes simplex virus immediate early gene expression. *Genes Dev* *2*, 718-729.

Trono, D., Van Lint, C., Rouzioux, C., Verdin, E., Barre-Sinoussi, F., Chun, T.W., and Chomont, N. (2010). HIV persistence and the prospect of long-term drug-free remissions for HIV-infected individuals. *Science* 329, 174-180.

Tun, T., Hamaguchi, Y., Matsunami, N., Furukawa, T., Honjo, T., and Kawaichi, M. (1994). Recognition sequence of a highly conserved DNA binding protein RBP-J kappa. *Nucleic Acids Res* 22, 965-971.

Turman, M.A., Yabe, T., McSherry, C., Bach, F.H., and Houchins, J.P. (1993). Characterization of a novel gene (NKG7) on human chromosome 19 that is expressed in natural killer cells and T cells. *Hum Immunol* 36, 34-40.

Tydell, C.C., David-Fung, E.S., Moore, J.E., Rowen, L., Taghon, T., and Rothenberg, E.V. (2007). Molecular dissection of prethymic progenitor entry into the T lymphocyte developmental pathway. *J Immunol* 179, 421-438.

Uda, M., Galanello, R., Sanna, S., Lettre, G., Sankaran, V.G., Chen, W., Usala, G., Busonero, F., Maschio, A., Albai, G., *et al.* (2008). Genome-wide association study shows BCL11A associated with persistent fetal hemoglobin and amelioration of the phenotype of beta-thalassemia. *Proc Natl Acad Sci U S A* 105, 1620-1625.

Urbanek, P., Wang, Z.Q., Fetka, I., Wagner, E.F., and Busslinger, M. (1994). Complete block of early B cell differentiation and altered patterning of the posterior midbrain in mice lacking Pax5/BSAP. *Cell* 79, 901-912.

Urnov, F.D., Miller, J.C., Lee, Y.L., Beausejour, C.M., Rock, J.M., Augustus, S., Jamieson, A.C., Porteus, M.H., Gregory, P.D., and Holmes, M.C. (2005). Highly efficient endogenous human gene correction using designed zinc-finger nucleases. *Nature* 435, 646-651.

van der Bruggen, P., Traversari, C., Chomez, P., Lurquin, C., De Plaen, E., Van den Eynde, B., Knuth, A., and Boon, T. (1991). A gene encoding an antigen recognized by cytolytic T lymphocytes on a human melanoma. *Science* 254, 1643-1647.

van der Wees, J., Matharu, P.J., de Roos, K., Destree, O.H., Godsave, S.F., Durston, A.J., and Sweeney, G.E. (1996). Developmental expression and differential regulation by retinoic acid of *Xenopus* COUP-TF-A and COUP-TF-B. *Mech Dev* 54, 173-184.

Vegh, P., Winckler, J., and Melchers, F. (2010). Long-term "in vitro" proliferating mouse hematopoietic progenitor cell lines. *Immunol Lett* 130, 32-35.

Venter, J.C., Adams, M.D., Myers, E.W., Li, P.W., Mural, R.J., Sutton, G.G., Smith, H.O., Yandell, M., Evans, C.A., Holt, R.A., *et al.* (2001). The sequence of the human genome. *Science* 291, 1304-1351.

Vosshenrich, C.A., Garcia-Ojeda, M.E., Samson-Villeger, S.I., Pasqualetto, V., Enault, L., Richard-Le Goff, O., Corcuff, E., Guy-Grand, D., Rocha, B., Cumano, A., *et al.* (2006). A thymic pathway of mouse natural killer cell development characterized by expression of GATA-3 and CD127. *Nat Immunol* 7, 1217-1224.

Wada, H., Masuda, K., Satoh, R., Kakugawa, K., Ikawa, T., Katsura, Y., and Kawamoto, H. (2008). Adult T-cell progenitors retain myeloid potential. *Nature* 452, 768-772.

Wagner, E.F., Stewart, T.A., and Mintz, B. (1981a). The human beta-globin gene and a functional viral thymidine kinase gene in developing mice. *Proc Natl Acad Sci U S A* 78, 5016-5020.

Wagner, T.E., Hoppe, P.C., Jollick, J.D., Scholl, D.R., Hodinka, R.L., and Gault, J.B. (1981b). Microinjection of a rabbit beta-globin gene into zygotes and its subsequent expression in adult mice and their offspring. *Proc Natl Acad Sci U S A* 78, 6376-6380.

Wakabayashi, Y., Inoue, J., Takahashi, Y., Matsuki, A., Kosugi-Okano, H., Shinbo, T., Mishima, Y., Niwa, O., and Kominami, R. (2003a). Homozygous deletions and point mutations of the *Rit1/Bcl11b* gene in gamma-ray induced mouse thymic lymphomas. *Biochem Biophys Res Commun* 301, 598-603.

Wakabayashi, Y., Watanabe, H., Inoue, J., Takeda, N., Sakata, J., Mishima, Y., Hitomi, J., Yamamoto, T., Utsuyama, M., Niwa, O., *et al.* (2003b). Bcl11b is required for differentiation and survival of alphabeta T lymphocytes. *Nat Immunol* 4, 533-539.

Waldmann, T.A. (2006). The biology of interleukin-2 and interleukin-15: implications for cancer therapy and vaccine design. *Nat Rev Immunol* 6, 595-601.

Waldmann, T.A., and Tagaya, Y. (1999). The multifaceted regulation of interleukin-15 expression and the role of this cytokine in NK cell differentiation and host response to intracellular pathogens. *Annu Rev Immunol* 17, 19-49.

Wallace, H.A., Marques-Kranc, F., Richardson, M., Luna-Crespo, F., Sharpe, J.A., Hughes, J., Wood, W.G., Higgs, D.R., and Smith, A.J. (2007). Manipulating the mouse genome to engineer precise functional syntenic replacements with human sequence. *Cell* 128, 197-209.

Walzer, T., Blery, M., Chaix, J., Fuseri, N., Chasson, L., Robbins, S.H., Jaeger, S., Andre, P., Gauthier, L., Daniel, L., *et al.* (2007). Identification, activation, and selective in vivo ablation of mouse NK cells via NKp46. *Proc Natl Acad Sci U S A* 104, 3384-3389.

Wang, D., Claus, C.L., Vaccarelli, G., Braunstein, M., Schmitt, T.M., Zuniga-Pflucker, J.C., Rothenberg, E.V., and Anderson, M.K. (2006). The basic helix-loop-helix transcription factor HEBAlt is expressed in pro-T cells and enhances the generation of T cell precursors. *J Immunol* 177, 109-119.

Wang, H., Feng, J., Qi, C., and Morse, H.C., 3rd (2008a). An ENU-induced mutation in the lymphotoxin alpha gene impairs organogenesis of lymphoid tissues in C57BL/6 mice. *Biochem Biophys Res Commun* 370, 461-467.

Wang, W., Lin, C., Lu, D., Ning, Z., Cox, T., Melvin, D., Wang, X., Bradley, A., and Liu, P. (2008b). Chromosomal transposition of PiggyBac in mouse embryonic stem cells. *Proc Natl Acad Sci U S A* 105, 9290-9295.

Ware, C.F., Crowe, P.D., Grayson, M.H., Androlewicz, M.J., and Browning, J.L. (1992). Expression of surface lymphotoxin and tumor necrosis factor on activated T, B, and natural killer cells. *J Immunol* *149*, 3881-3888.

Washburn, T., Schweighoffer, E., Gridley, T., Chang, D., Fowlkes, B.J., Cado, D., and Robey, E. (1997). Notch activity influences the alphabeta versus gammadelta T cell lineage decision. *Cell* *88*, 833-843.

Waterston, R.H., Lindblad-Toh, K., Birney, E., Rogers, J., Abril, J.F., Agarwal, P., Agarwala, R., Ainscough, R., Alexandersson, M., An, P., *et al.* (2002). Initial sequencing and comparative analysis of the mouse genome. *Nature* *420*, 520-562.

Wilde, J.I., and Watson, S.P. (2001). Regulation of phospholipase C gamma isoforms in haematopoietic cells: why one, not the other? *Cell Signal* *13*, 691-701.

Wildin, R.S., Wang, H.U., Forbush, K.A., and Perlmutter, R.M. (1995). Functional dissection of the murine lck distal promoter. *J Immunol* *155*, 1286-1295.

Winnard, P.T., Jr., Kluth, J.B., and Raman, V. (2006). Noninvasive optical tracking of red fluorescent protein-expressing cancer cells in a model of metastatic breast cancer. *Neoplasia* *8*, 796-806.

Wolfer, A., Wilson, A., Nemir, M., MacDonald, H.R., and Radtke, F. (2002). Inactivation of Notch1 impairs VDJbeta rearrangement and allows pre-TCR-independent survival of early alpha beta Lineage Thymocytes. *Immunity* *16*, 869-879.

Yee, C., Thompson, J.A., Byrd, D., Riddell, S.R., Roche, P., Celis, E., and Greenberg, P.D. (2002). Adoptive T cell therapy using antigen-specific CD8+ T cell clones for the treatment of patients with metastatic melanoma: in vivo persistence, migration, and antitumor effect of transferred T cells. *Proc Natl Acad Sci U S A* *99*, 16168-16173.

Yokota, Y., Mansouri, A., Mori, S., Sugawara, S., Adachi, S., Nishikawa, S., and Gruss, P. (1999). Development of peripheral lymphoid organs and natural killer cells depends on the helix-loop-helix inhibitor Id2. *Nature* 397, 702-706.

Yoshida, T., Ng, S.Y., Zuniga-Pflucker, J.C., and Georgopoulos, K. (2006). Early hematopoietic lineage restrictions directed by Ikaros. *Nat Immunol* 7, 382-391.

Young, D.C., Kingsley, S.D., Ryan, K.A., and Dutko, F.J. (1993). Selective inactivation of eukaryotic beta-galactosidase in assays for inhibitors of HIV-1 TAT using bacterial beta-galactosidase as a reporter enzyme. *Anal Biochem* 215, 24-30.

Yu, J., Vodyanik, M.A., Smuga-Otto, K., Antosiewicz-Bourget, J., Frane, J.L., Tian, S., Nie, J., Jonsdottir, G.A., Ruotti, V., Stewart, R., *et al.* (2007). Induced pluripotent stem cell lines derived from human somatic cells. *Science* 318, 1917-1920.

Yucel, R., Karsunky, H., Klein-Hitpass, L., and Moroy, T. (2003). The transcriptional repressor Gfi1 affects development of early, uncommitted c-Kit⁺ T cell progenitors and CD4/CD8 lineage decision in the thymus. *J Exp Med* 197, 831-844.

Yui, M.A., and Rothenberg, E.V. (2004). Deranged early T cell development in immunodeficient strains of nonobese diabetic mice. *J Immunol* 173, 5381-5391.

Zhang, S., Rozell, M., Verma, R.K., Albu, D.I., Califano, D., Vanvalkenburgh, J., Merchant, A., Rangel-Moreno, J., Randall, T.D., Jenkins, N.A., *et al.* (2010). Antigen-specific clonal expansion and cytolytic effector function of CD8⁺ T lymphocytes depend on the transcription factor Bcl11b. *J Exp Med* 207, 1687-1699.

Zheng, W., and Flavell, R.A. (1997). The transcription factor GATA-3 is necessary and sufficient for Th2 cytokine gene expression in CD4 T cells. *Cell* 89, 587-596.

Zhuang, Y., Soriano, P., and Weintraub, H. (1994). The helix-loop-helix gene E2A is required for B cell formation. *Cell* 79, 875-884.

Zijlstra, M., Bix, M., Simister, N.E., Loring, J.M., Raulet, D.H., and Jaenisch, R. (1990). Beta 2-microglobulin deficient mice lack CD4-8+ cytolytic T cells. *Nature* 344, 742-746.

Zitvogel, L., Tesniere, A., and Kroemer, G. (2006). Cancer despite immunosurveillance: immunoselection and immunosubversion. *Nat Rev Immunol* 6, 715-727.

Zwirner, N.W., and Domaica, C.I. (2010). Cytokine regulation of natural killer cell effector functions. *Biofactors*.

Figure 1.1

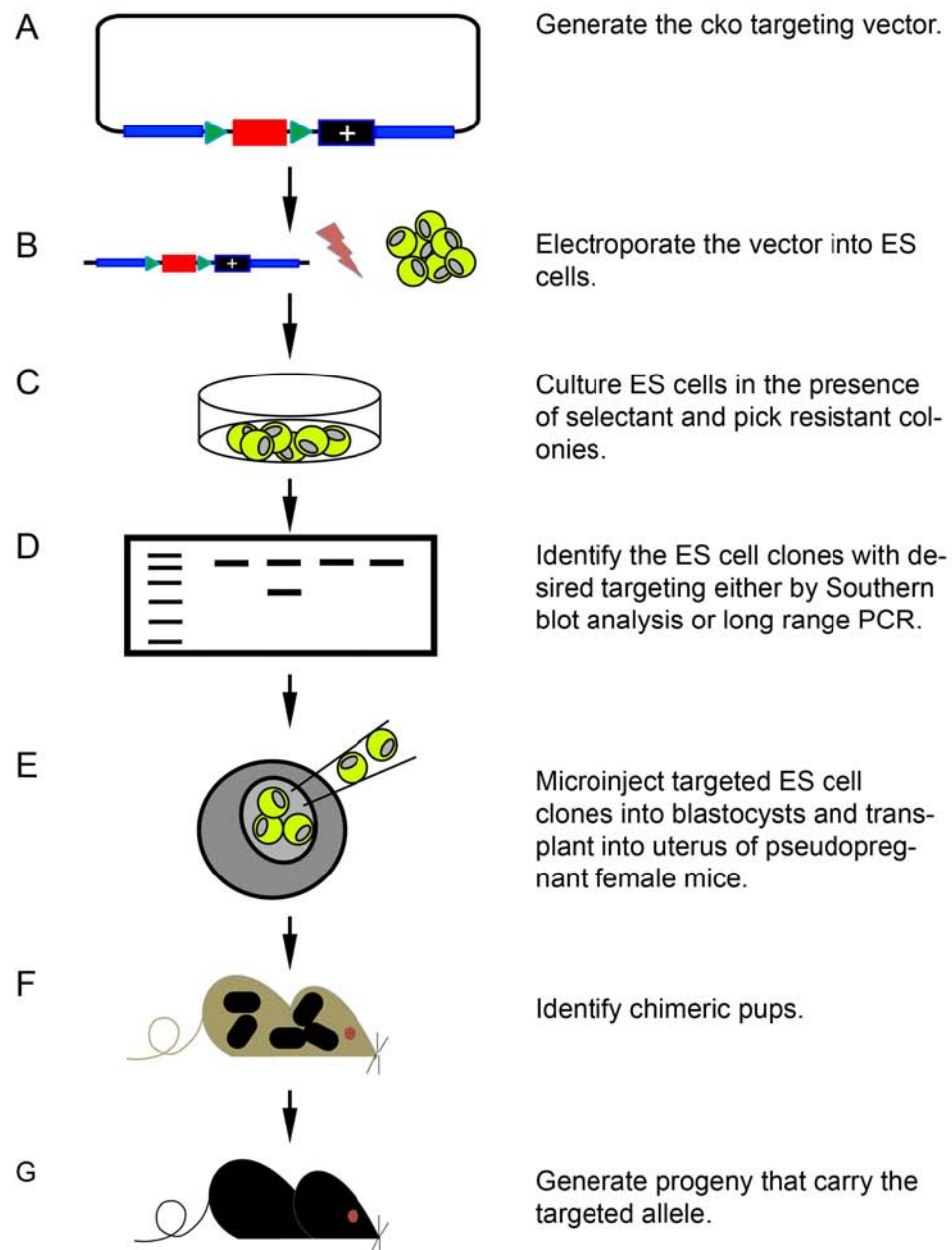


Figure 1.1 General procedure for generation of a conditional knockout mouse strain by gene targeting strategies.

(A) Generation of a targeting vector containing critical exon of targeted genes (red rectangle), two loxP site (green triangle), a positive (+) selection cassette and sequences of homology with the target locus (blue line). (B) The vector is linearized and electroporated into ES cells. (C) Correct transformants are selected for in the presence of a selectant (eg. G418 if a neomycin resistance cassette is present in the

targeting vector). (D) Correctly targeted ES cell clones are then identified and genetically characterized using long range PCR or Southern blot analysis. (E) The selected ES cell clones are then microinjected into 3.5 dpc blastocysts and transplanted into the uteri of pseudopregnant females. (F) Chimeras obtained from the microinjections are mated with wild-type mice to establish germ-line transmission of the modified allele. (G) Progeny derived from the chimeras are characterized using long range PCR or Southern blot analysis, and a mutant mouse line that carries the desired targeted allele is established.

Figure 1.2

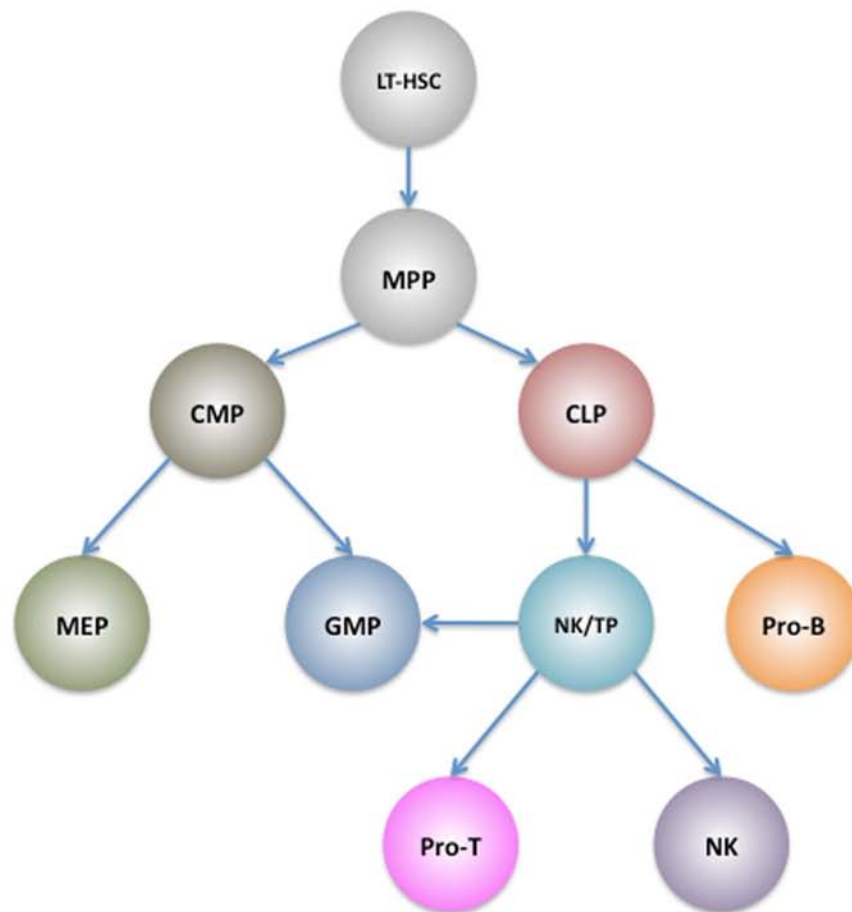


Figure 1.2 Current scheme of haematopoiesis.

LT-HSC, long-term hematopoietic stem cell; MPP, Multipotent progenitor; CMP, common myeloid progenitor; CLP, common lymphoid progenitor; MEP, megakaryocyte erythroid progenitor; GMP, granulocyte macrophage progenitor; NK/TP, NK/T progenitor, which have NK, T, and myeloid cell potentials. Pro-T and Pro-B are progenitor cells that go through several stages to eventually produce T and B cells. Arrows indicate cell differentiation.

Figure 1.3

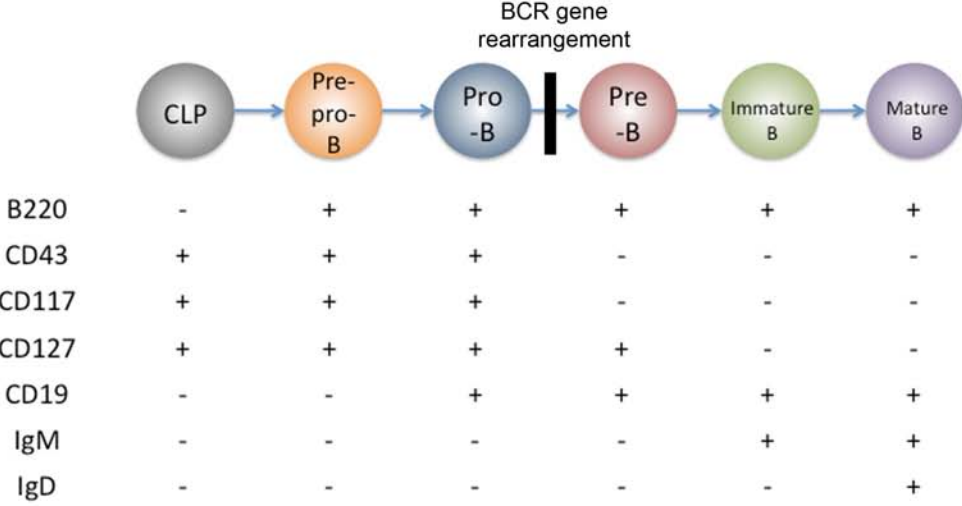


Figure 1.3 Stages in mouse bone marrow B lymphopoiesis from common lymphoid progenitors.

Diagram of B cell development from common lymphoid progenitors (CLPs) in mouse bone marrow (BM) through Pre-pro-B and Pro-B to mature B cell stages showing cell surface phenotype.

Figure 1.4

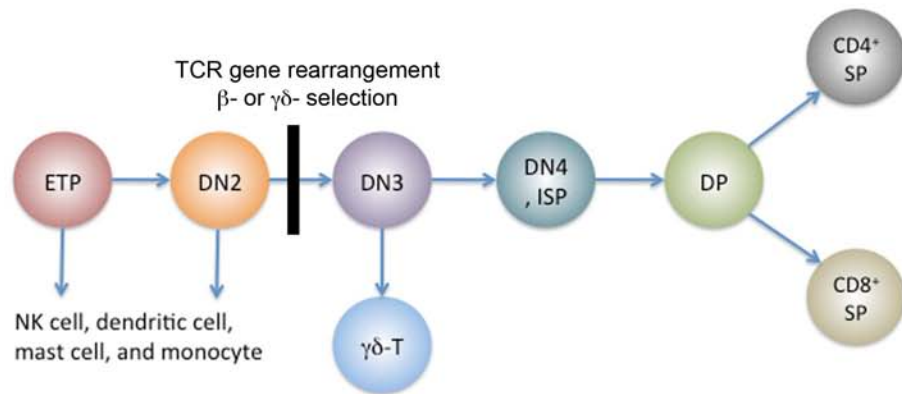


Figure 1.4 Stages in T cell development.

Early T cell precursors (ETPs) differentiate from double negative (DN) to double positive (DP) to single positive (SP) stages. Arrows indicate cell differentiation. Note that ETP and DN2 thymocytes contain non-T-cell options. β - and $\gamma\delta$ - selection occurs during the accumulation of the DN3 T cells.

Figure 3.1

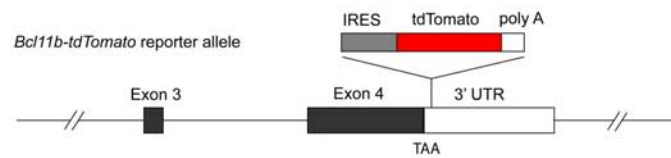


Figure 3.1 Targeting of the *IRES-tdTomato* reporter into the mouse *Bcl11b* locus. The 3' *UTR* of *Bcl11b* locus was mutated by the introduction of an internal ribosomal entry site (*IRES*) element followed by Tandem dimer Tomato (*tdTomato*) and a polyadenylation signal (*polyA*).

Figure 3.2

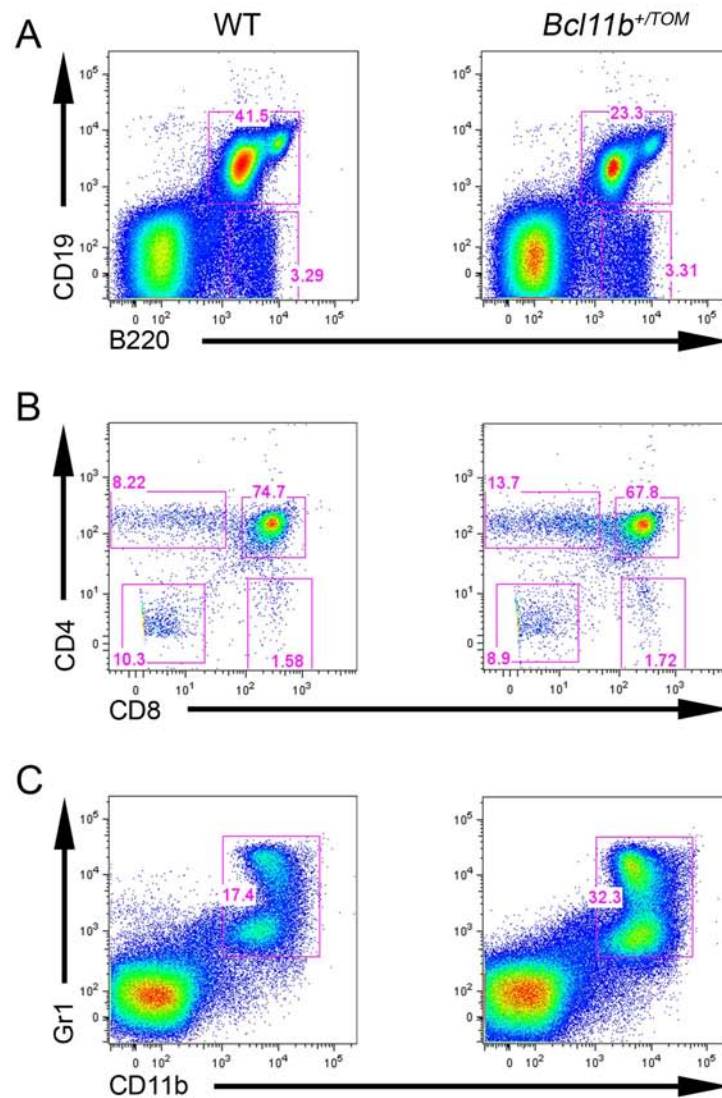


Figure 3.2 *Bcl11b*^{+TOM} mice have normal haematopoiesis.

(A) Flow cytometry analysis shows the percentages of B cells that were defined as B220⁺CD19⁻ and B220⁺CD19⁺ in BM from wild type (left panel) and *Bcl11b*^{+TOM} (right panel) mice. (B) Flow cytometry analysis shows the percentages of DP (CD4⁺CD8⁺), CD4 SP (CD4⁺CD8⁻), CD8 SP (CD4⁻CD8⁺) and DN (CD4⁻CD8⁻) T thymocytes from wild type (left panel) and *Bcl11b*^{+TOM} (right panel) mice. (C) Flow cytometry analysis shows the percentages of myeloid cells (CD11b⁺Gr1⁺) in BM from wild type (left panel) and *Bcl11b*^{+TOM} (right panel) mice. Numbers beside or in

outlined areas indicate the percentages of positive cells in each. Data are representative of two experiments.

Figure 3.3

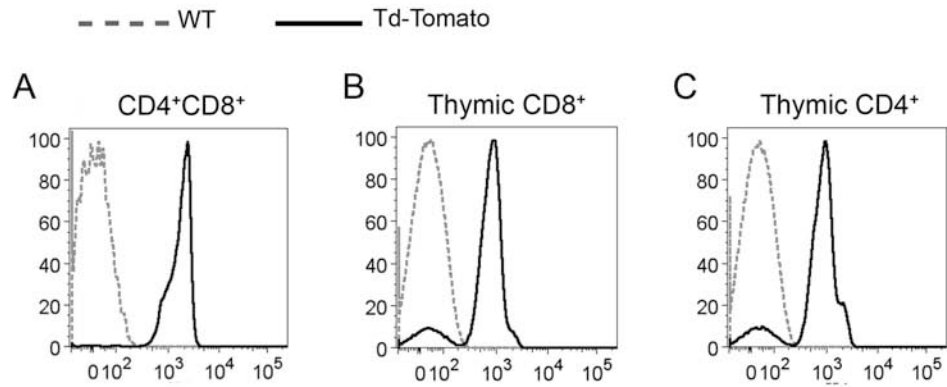


Figure 3.3 Expression of Bcl11b in thymocytes.

Flow cytometry analysis of single-cell suspensions from thymocytes of *Bcl11b*^{+/*TOM*} (solid black line) and wild type (dash grey line) mice, stained with antibodies to CD4 and CD8. (A) Bcl11b expression in CD4⁺CD8⁺ DP thymocytes, which were defined in Fig. 3.2B, was assessed indirectly with tdTomato signal. (B) Bcl11b expression in CD8⁺ thymocytes that were defined in Fig. 3.2B, was assessed indirectly with tdTomato signal. (C) Bcl11b expression in CD4⁺ thymocytes that were defined in Fig. 3.2B, was assessed indirectly with tdTomato signal. Data are representative of two experiments.

Figure 3.4

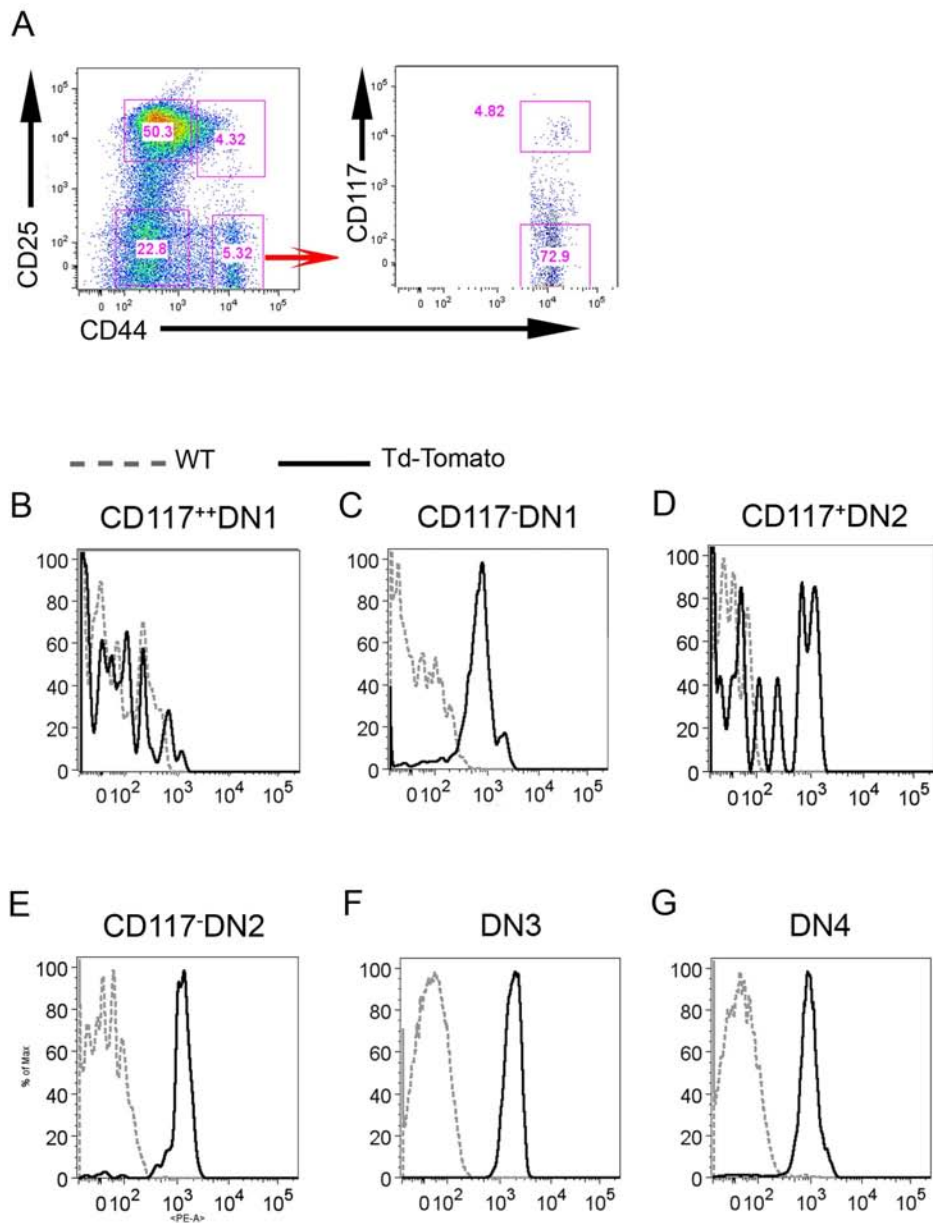


Figure 3.4 Expression of *Bcl11b* in subsets of DN thymocytes.

Flow cytometry analysis of single-cell suspensions from Lin^- thymocytes of *Bcl11b*^{+TOM} (solid black line) and wild type (dash grey line) mice, stained with antibodies to Lineage cocktail, CD44, CD25 and CD117. (A) Different subsets of DN thymocytes were defined by expression of CD25, CD44 and CD117 in Lin^- thymocytes as follows: DN1 ($\text{CD44}^+\text{CD25}^-$), DN2 ($\text{CD44}^+\text{CD25}^+$), DN3 ($\text{CD44}^-\text{CD25}^+$) and DN4 ($\text{CD44}^-\text{CD25}^-$). The DN1 subset was further divided into two

groups by expression of CD117. Numbers beside or in outlined areas indicated the percentages of positive cells in each. (B) Bcl11b expression in CD117⁺⁺DN1 thymocytes that are defined from flow cytometry in (A) was assessed indirectly with tdTomato signal. (C) Bcl11b expression in CD117⁻DN1 thymocytes that were defined from flow cytometry in (A) was assessed indirectly with tdTomato signal. (D) Bcl11b expression in CD117⁺DN2 thymocytes that are defined from flow cytometry in (A) was assessed indirectly with tdTomato signal. (E) Bcl11b expression in CD117⁻DN2 thymocytes that are defined from flow cytometry in (A) was assessed indirectly with tdTomato signal. (F) Bcl11b expression in DN3 thymocytes that are defined from flow cytometry in (A) was assessed indirectly with tdTomato signal. (G) Bcl11b expression in DN4 thymocytes that are defined from flow cytometry in (A) was assessed indirectly with tdTomato signal. Data are representative of four experiments.

Figure 3.5

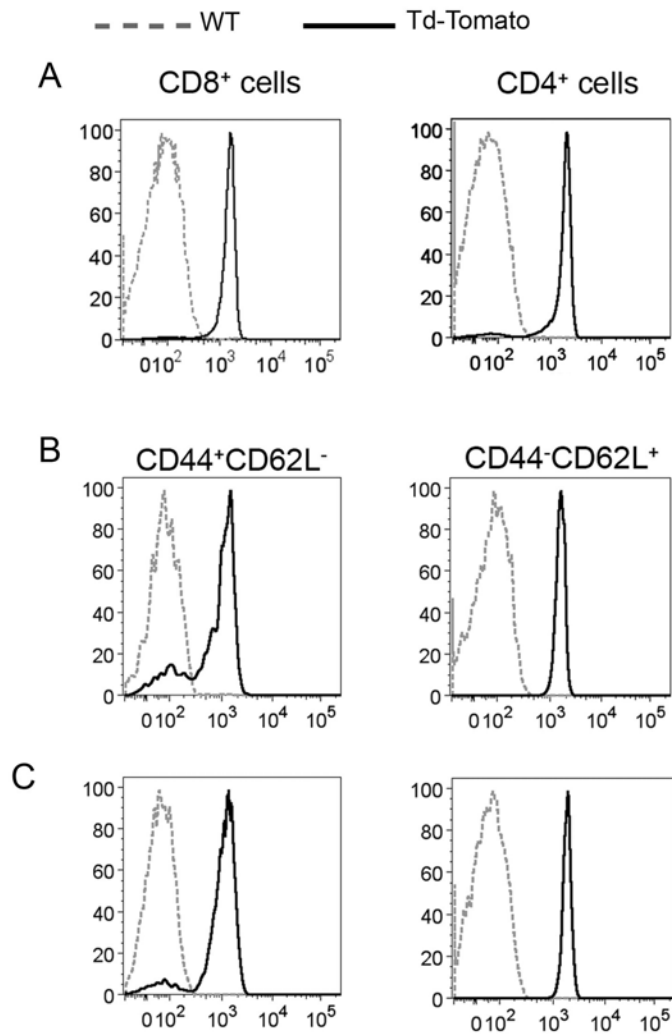


Figure 3.5 Detection of *Bcl11b* expressions in mature T cell subsets using *Bcl11b-tdTomato* knock-in reporter mice.

Flow cytometry analysis of single-cell suspensions from splenocytes of *Bcl11b*^{+/*TOM*} (solid black line) and wild type (dash grey line) mice, stained with antibodies to CD4, CD8, CD44 and CD62L. (A) *Bcl11b* expression in CD8⁺ (left panel) and CD4⁺ (right panel) splenic T cells that are defined from flow cytometry in Fig. 3.6A was assessed indirectly with tdTomato signal. (B) *Bcl11b* expression in activated (CD44⁺CD62L⁻, left panel) and naïve (CD44⁻CD62L⁺, right panel) CD8⁺ splenic T cells that are defined from flow cytometry in Fig. 3.6A (right panel) was assessed indirectly with

tdTomato signal. (C) Bcl11b expression in activated ($CD44^+CD62L^-$, left panel) and naïve ($CD44^-CD62L^+$, right panel) $CD4^+$ splenic T cells that are defined from flow cytometry in Fig. 3.6A (left panel) was assessed indirectly with tdTomato signal. Data are representative of four experiments.

Figure 3.6

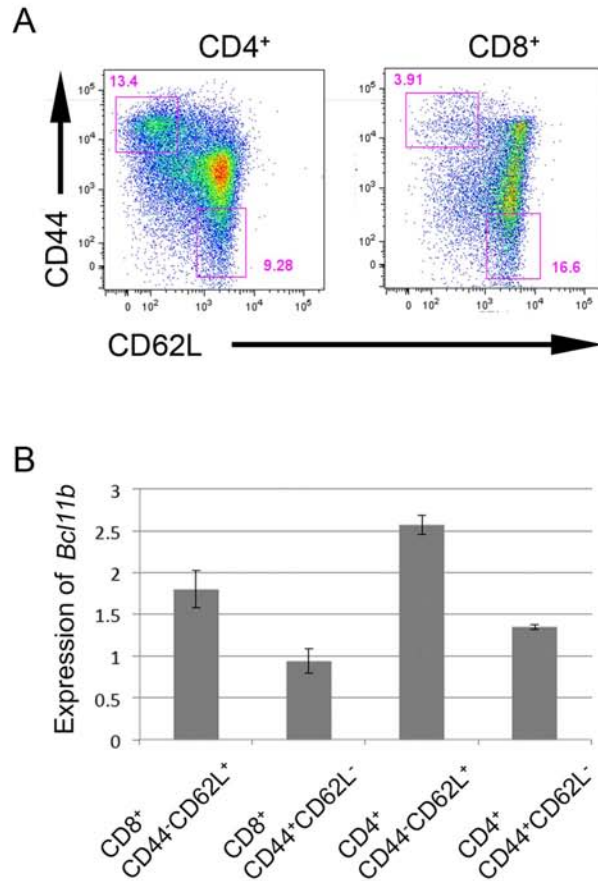


Figure 3.6 Detection of *Bcl11b* expressions in mature T cell subsets using qRT-PCR.

Flow cytometry analysis of single-cell suspensions from splenocytes of wild type mice, stained with antibodies to CD4, CD8, CD44 and CD62L. (A) Naïve (CD44⁻CD62L⁺) and activated (CD44⁺CD62L⁻) T cell subsets were defined and sorted from CD4⁺ (left panel) and CD8⁺ (right panel) splenic T cells by flow cytometry. Numbers beside or in outlined areas indicated the percentages of positive cells in each. (B) qRT-PCR was performed to measure *Bcl11b* expressions in sorted splenic naïve (CD44⁻CD62L⁺) and activated (CD44⁺CD62L⁻) T cells population. *Bcl11b* expression

was calculated relative to that in $CD8^+CD44^+CD62L^-$ (set to 1). Bars are mean \pm SEM of 3 samples.

Figure 3.7

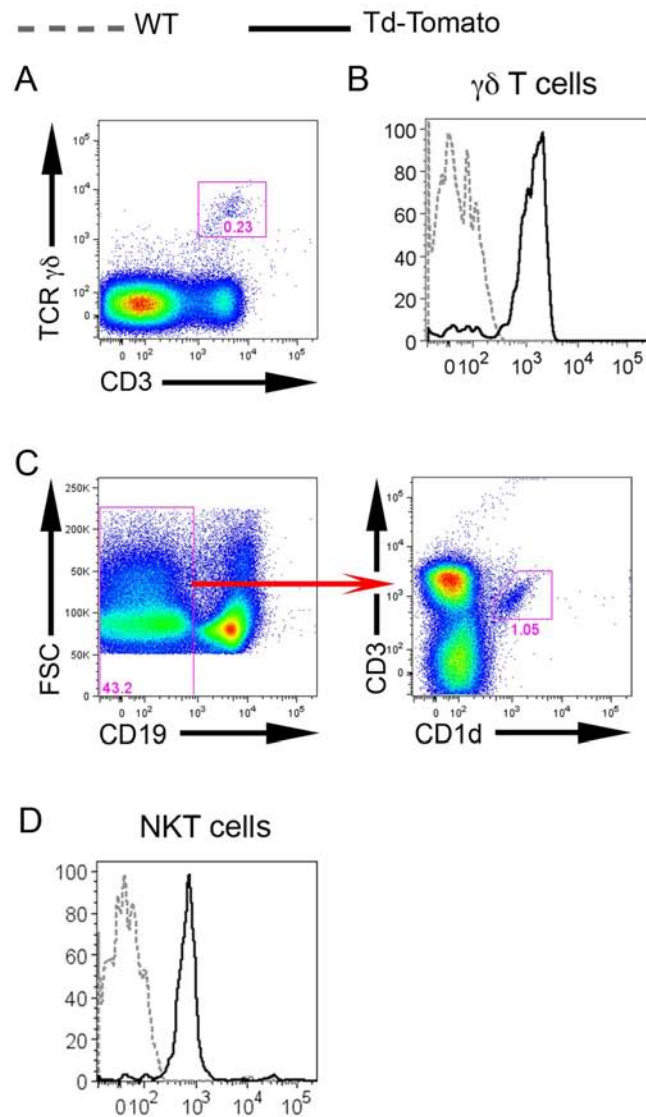


Figure 3.7 Expression of *Bcl11b* in $\gamma\delta$ -T cells and NKT cells.

(A) Flow cytometry analysis of single-cell suspensions from thymocytes of *Bcl11b*^{+TOM} (solid black line) and wild type (dash grey line) mice, stained with antibodies to TCR $\gamma\delta$ and CD3. $\gamma\delta$ T cells were defined as TCR $\gamma\delta$ ⁺CD3⁺. Numbers beside or in outlined areas indicated the percentages of positive cells in each. (B) *Bcl11b* expression in $\gamma\delta$ T cells defined in (A) was assessed indirectly with tdTomato signal. (C) Flow cytometry analysis of single-cell suspensions from splenocytes of *Bcl11b*^{+TOM} (solid black line) and wild type (dash grey line) mice, stained with

antibodies to CD19, CD3 and dimmer CD1d. NKT cells were defined as CD19⁻CD3⁺CD1d⁺. Numbers beside or in outlined areas indicated the percentages of positive cells in each. (D) Bcl11b expression in NKT cells defined in (C) was assessed indirectly with tdTomato signal. Data are representative of four experiments.

Figure 3.8

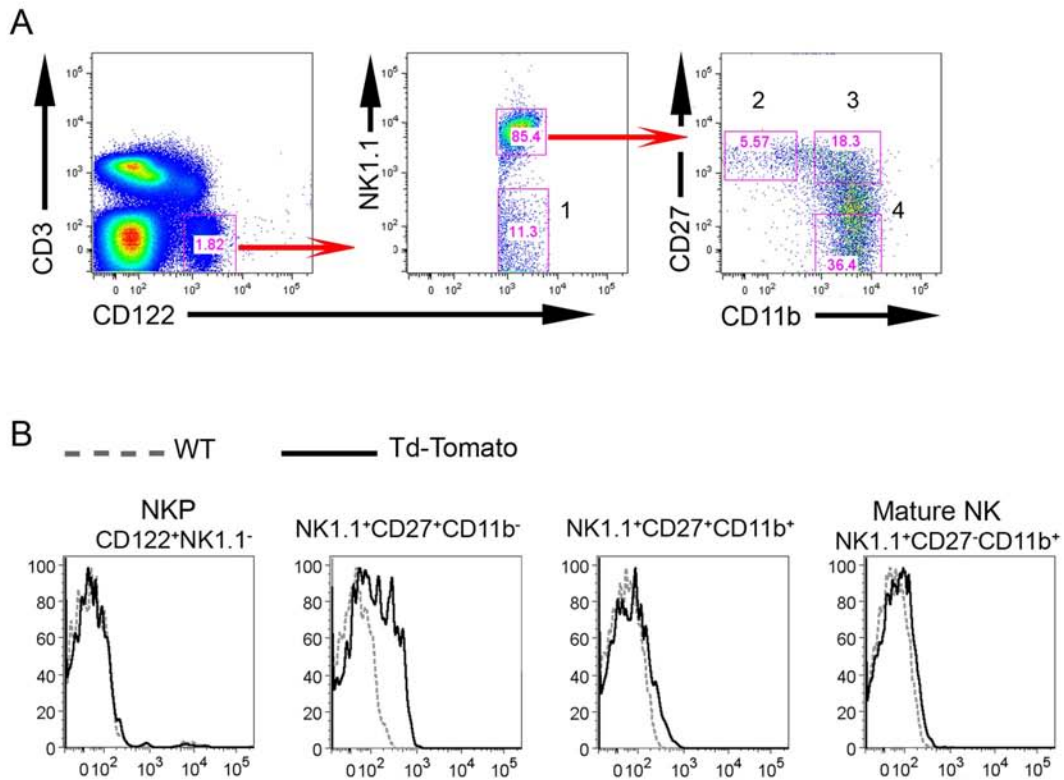


Figure 3.8 Expression of Bcl11b in NK cells.

Flow cytometry analysis of single-cell suspensions from splenocytes of *Bcl11b*^{+/*TOM*} (solid black line) and wild type (dash grey line) mice, stained with antibodies to CD3, CD122, NK1.1, CD27 and CD11b. (A) Different subsets of NK cells were defined by expression of NK1.1, CD122, CD11b and CD27. Numbers beside or in outlined areas indicated the percentages of positive cells in each. (B) Bcl11b expression in different NK cell subsets defined in (A) was assessed indirectly with tdTomato signal. Data are representative of four experiments.

Figure 3.9

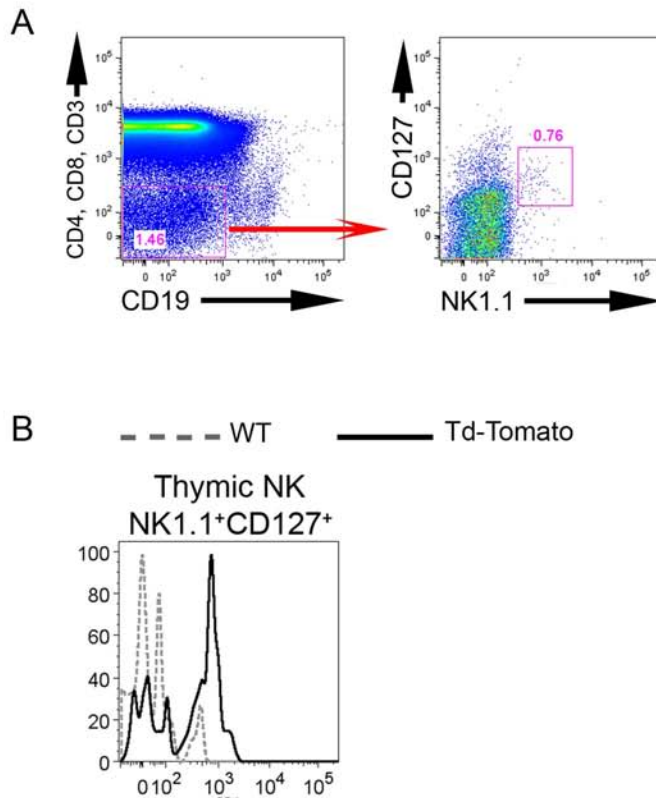


Figure 3.9 Expression of *Bcl11b* in thymic NK cells.

Flow cytometry analysis of single-cell suspensions from thymocytes of *Bcl11b*^{+/*TOM*} (solid black line) and wild type (dash grey line) mice, stained with antibodies to CD4, CD8, CD3, NK1.1, CD19 and CD127. (A) Thymic NK cells were defined as NK1.1⁺CD127⁺ thymocytes. Numbers beside or in outlined areas indicated the percentages of positive cells in each. (B) *Bcl11b* expression in thymic NK cells defined in (A) was assessed indirectly with tdTomato signal. Data are representative of four experiments.

Figure 3.10

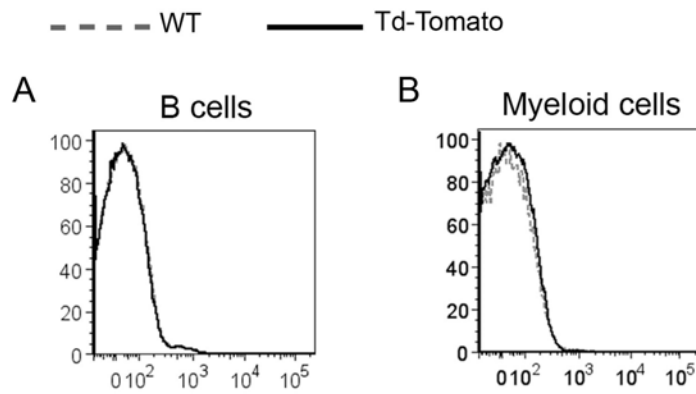


Figure 3.10 Expression of Bcl11b in B and myeloid cells.

Flow cytometry analysis of single-cell suspensions from BM of *Bcl11b*^{+TOM} (solid black line) and wild type (dash grey line) mice, stained with antibodies to CD19, B220, CD11b and Gr1. (A) Bcl11b expression in B cells defined in Fig. 3.2A was assessed indirectly with tdTomato signal. (B) Bcl11b expression in myeloid cells defined in Fig. 3.2C was assessed indirectly with tdTomato signal. Data are representative of four experiments.

Figure 4.1

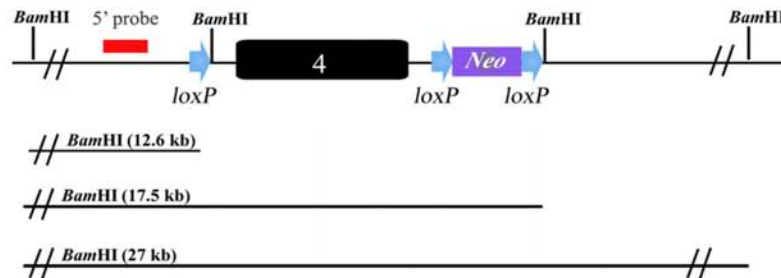


Figure 4.1 Schematic diagram of the *Bcl11b* conditional knockout allele.

Bcl11b exon 4 was flanked by *loxP* sites. Indicated DNA fragments were detected by the 5' probe in Southern blot analysis of targeted ES cells.

Figure 4.2

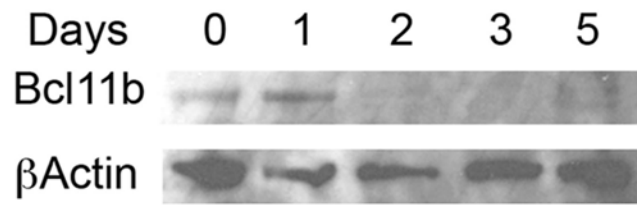


Figure 4.2 Loss of Bcl11b after OHT treatment.

Western blot analysis of Bcl11b levels from whole cell lysates of thymocytes from *flox/flox* mice at different time points after OHT treatment.

Figure 4.3

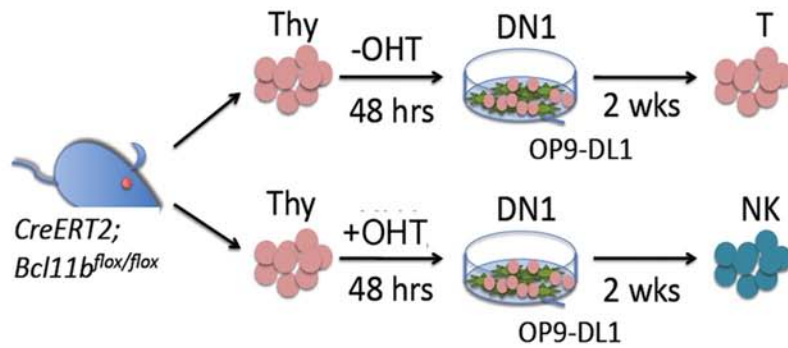


Figure 4.3 Experimental design for the analysis of *Bcl11b*-deficient DN thymocytes.

Whole thymocytes from (*flox/flox*) mice were treated with OHT (+OHT) or left untreated (-OHT) for 48 hr then sorted into the indicated subset and co-cultured with OP9-DL1 stromal cells in T cell culture condition. Two weeks later, T cells grew out from (-OHT) culture, while NK-like cells were produced from (+OHT) culture.

Figure 4.4

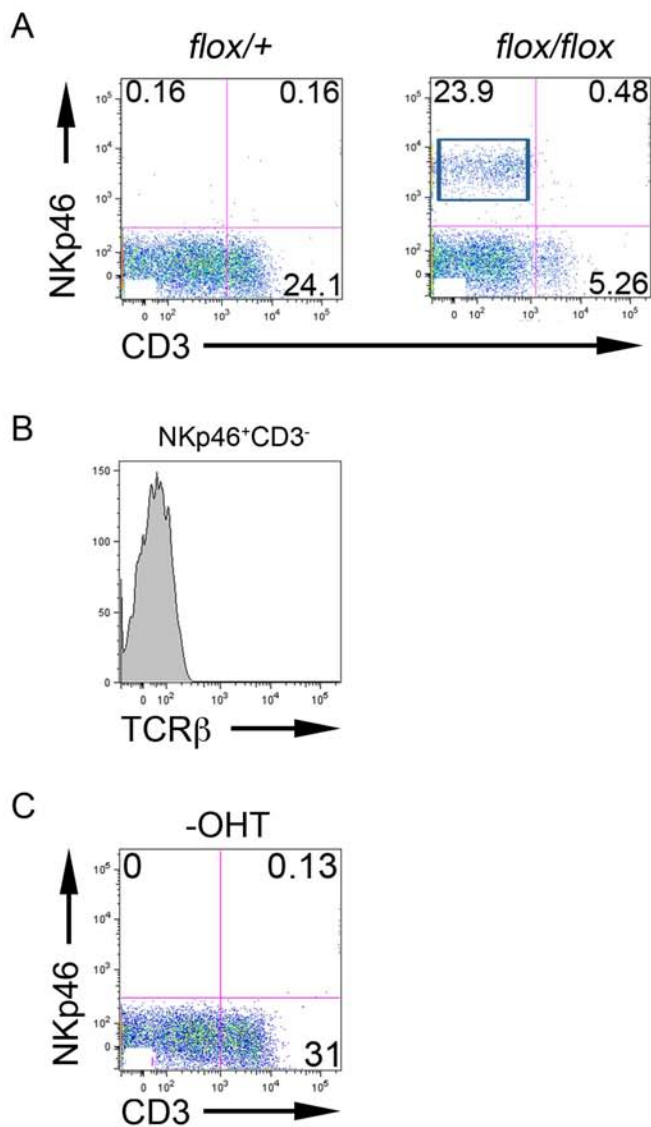


Figure 4.4 Bcl11b is essential for DN1 thymocytes to differentiate to T cells.

Thymocytes from *flox/flox* or *flox/+* control mice were treated, or not, with OHT then sorted into DN1 subsets, and co-cultured on OP9-DL1 stromal cells in T cell media.

(A) Flow cytometry profiles of cultured DN1 thymocytes from *flox/+* (left panel) and *flox/flox* (right panel) after OHT treatment in T cell culture condition without IL-2 supplement. Numbers refer to percentage of cells in the gate. Data are representative

of three experiments. (B) Flow cytometry analysis shows that NKp46⁺CD3⁻ cells

(gated in (A)) from DN1 OHT-treated *flox/flox* thymocytes did not express TCR β . Data are representative of two experiments. (C) Flow cytometry profiles of cultured DN1 thymocytes from *flox/flox* without OHT treatment in T cell culture condition. Numbers refer to percentage of cells in the gate. Data are representative of three experiments.

Figure 4.5

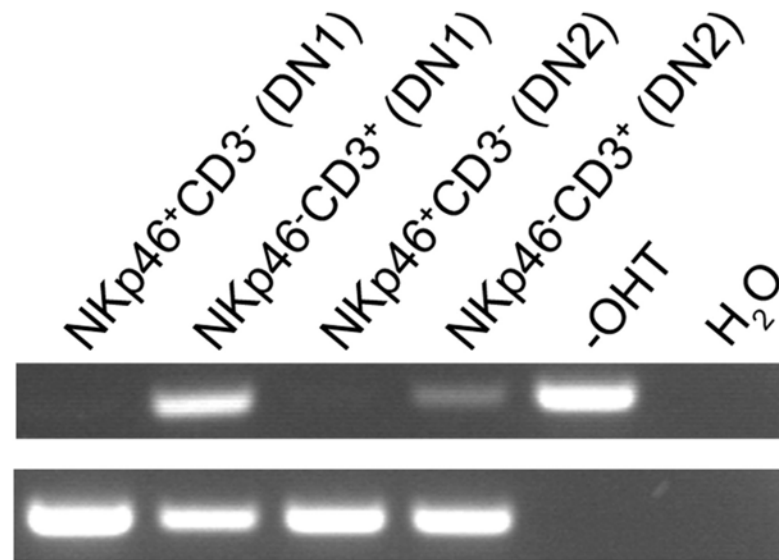


Figure 4.5 *Bcl11b* was deleted in NK-like cells.

Genotyping results show that homozygous *Bcl11b* deletion in NK-like cells (NKp46⁺CD3⁻) but not in T (NKp46⁻CD3⁺) cell populations from DN1 and DN2 cultures. *flox*: conditional knockout allele; *del*: deletion allele. H₂O: no DNA template control.

Figure 4.6

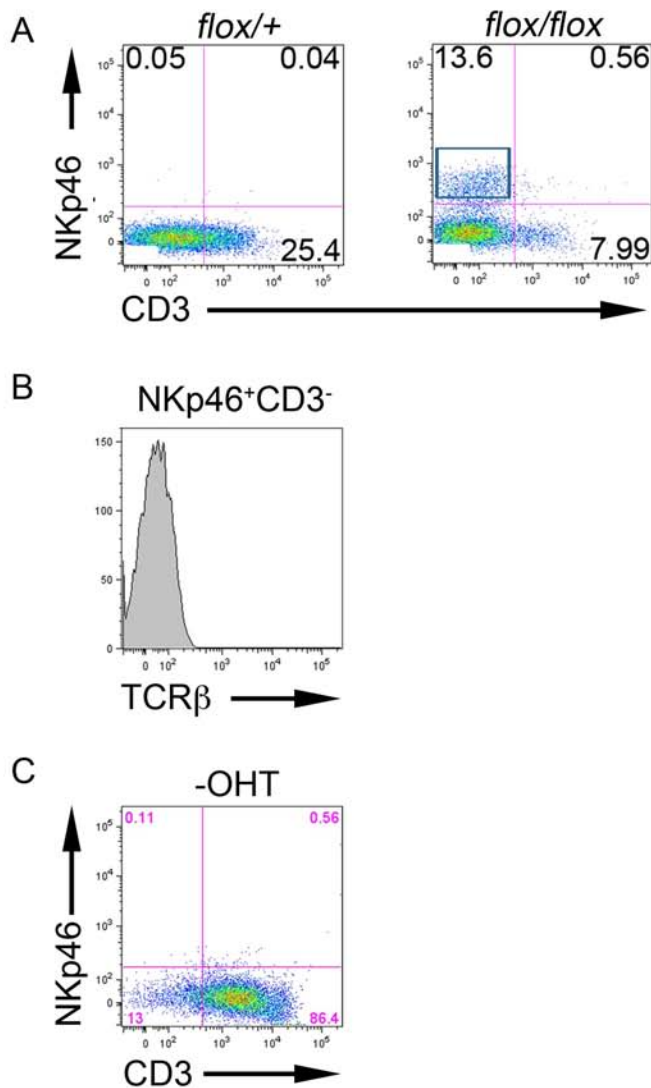


Figure 4.6 Bcl11b is essential for DN2 thymocytes to differentiate to T cells.

Thymocytes from *flox/flox* or *flox/+* control mice were treated, or not, with OHT then sorted into DN2 subsets, and co-cultured on OP9-DL1 stromal cells in T cell media.

(A) Flow cytometry profiles of cultured DN2 thymocytes from *flox/+* (left panel) and *flox/flox* (right panel) after OHT treatment in T cell culture condition without IL-2 supplement. Numbers refer to percentage of cells in the gate. Data are representative of three experiments.

(B) Flow cytometry analysis shows that NKp46⁺CD3⁻ cells

(gated in (A)) from DN2 OHT-treated *flox/flox* thymocytes did not express TCR β . Data are representative of two experiments. (C) Flow cytometry profiles of cultured DN1 thymocytes from *flox/flox* without OHT treatment in T cell culture condition. Numbers refer to percentage of cells in the gate. Data are representative of three experiments.

Figure 4.7

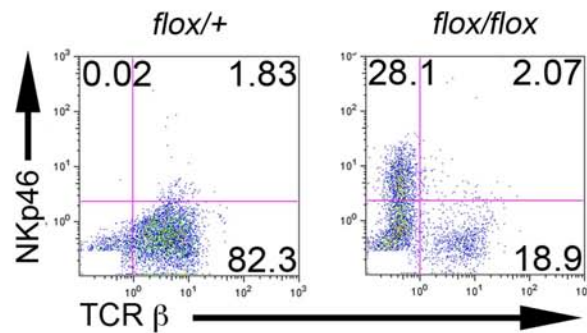


Figure 4.7 Bcl11b is essential to maintain T cell identity in committed DN3 thymocytes.

Thymocytes from *flox/flox* or *flox/+* control mice were treated, or not, with OHT then sorted into DN3 subsets, and co-cultured on OP9-DL1 stromal cells in T cell media. Flow cytometry profiles of cultured DN3 thymocytes from *flox/+* (left panel) and *flox/flox* (right panel) after OHT treatment in T cell culture condition without IL-2 supplement. Numbers refer to percentage of cells in the gate. Data are representative of three experiments.

Figure 4.8

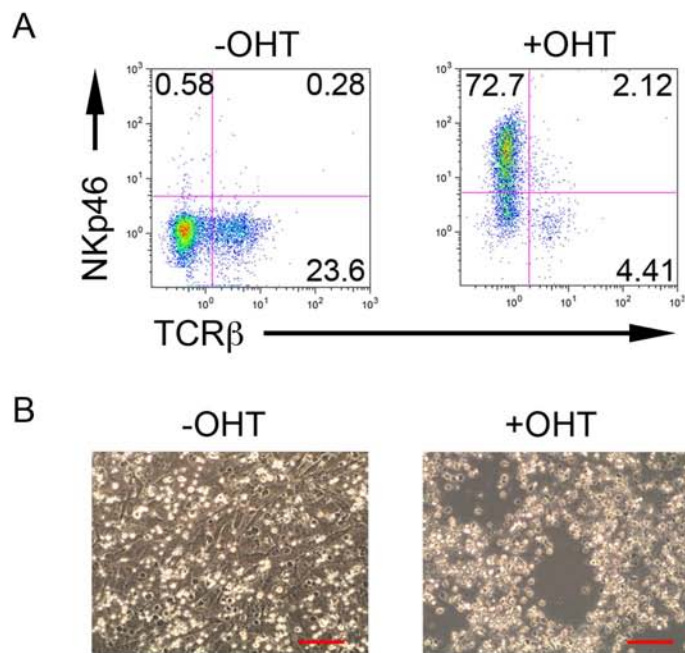


Figure 4.8 NK-like cells produced from *Bcl11b*-deficient DN3 thymocytes in T cell culture condition killed OP9-DL1 stromal cells.

(A) Flow cytometry profiles of cultured *flox/flox* DN3 thymocytes (\pm OHT) supplemented with IL-2. Data are representative of three experiments. (B) Killing of OP9-DLI stromal cells by OHT-treated *flox/flox* DN3 thymocytes. Scale bar, 40 μ m.

Figure 4.9

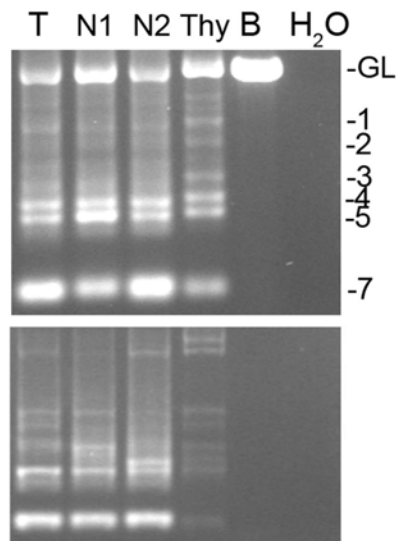


Figure 4.9 NK-like cells produced from *Bcl11b*-deficient DN3 thymocytes contain TCR DNA rearrangements.

DNA from purified NKp46⁺ cells was prepared and subjected to PCR to detect DJ (top) and V(D)J (bottom) recombination at the TCR β locus. T, T cells growing from untreated DN3 thymocytes; N1 and N2, sorted NKp46⁺ cells growing from OHT-treated *flox/flox* DN3 thymocytes; Thy, wild-type whole thymocytes; B, B cells; and GL, germline band. H₂O: no DNA template in PCR. Numbers indicate DJ recombination products.

Figure 4.10

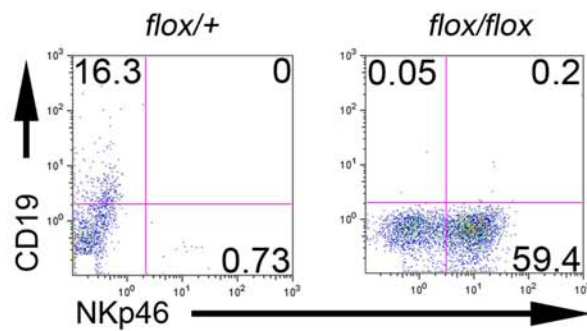


Figure 4.10 Reprogramming of *Bcl11b*-deficient DN3 thymocytes to ITNK cells in B cell culture condition.

Thymocytes from *flox/flox* or *flox/+* control mice were treated, or not, with OHT then sorted into DN3 subsets, and co-cultured on OP9 stromal cells in B cell media. Flow cytometry profiles of cultured DN3 thymocytes from *flox/+* (left panel) and *flox/flox* (right panel) after OHT treatment in B cell culture condition. Numbers refer to percentage of cells in the gate. Data are representative of three experiments.

Figure. 4.11

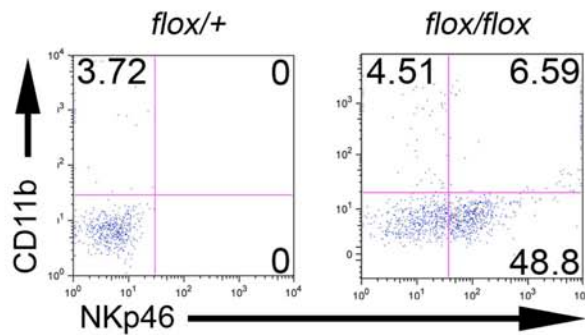


Figure 4.11 Reprogramming of *Bcl11b*-deficient DN3 thymocytes to ITNK cells in myeloid cell culture condition.

Thymocytes from *flox/flox* or *flox/+* control mice were treated, or not, with OHT then sorted into DN3 subsets, and co-cultured on OP9 stromal cells in myeloid cell media. Flow cytometry profiles of cultured DN3 thymocytes from *flox/+* (left panel) and *flox/flox* (right panel) after OHT treatment in myeloid cell culture condition. Numbers refer to percentage of cells in the gate. Data are representative of three experiments.

Figure 4.12

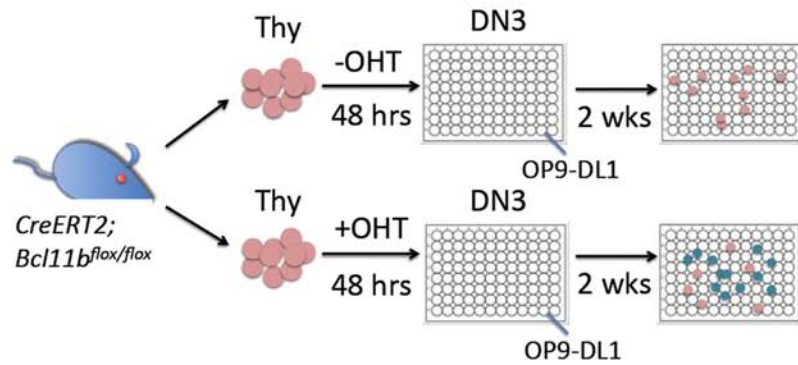


Figure 4.12 Experiment designs for single cell assay.

Experimental design for reprogramming of single DN3 thymocytes to ITNK. Whole thymocytes from *flox/flox* mice were treated with OHT (+OHT) or left untreated (-OHT) and 48-hours later single DN3 cells were sorted and seeded on OP9-DL1 stromal cells in 96-well plates for 10-14 days supplemented with IL-2.

Figure 4.13

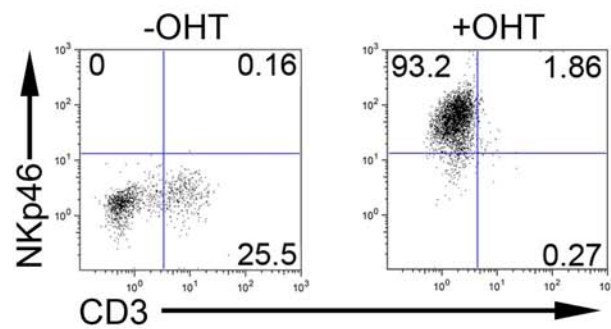


Figure 4.13 Production of ITNK cells from a single *Bcl11b*-deficient DN3 thymocytes.

Flow cytometry profiles of cells produced from a single DN3 thymocyte from *flox/flox* (right panel) treated with OHT (+OHT, right panel) or left untreated (-OHT, left panel) in T cell culture condition supplemented with IL-2. Numbers refer to percentage of cells in the gate. Data are representative of more than 200 wells.

Figure 4.14

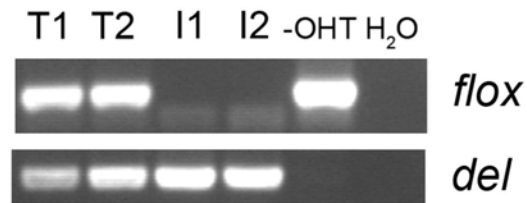


Figure 4.14 ITNK cells were produced from single *Bcl11b*-deficient DN3 thymocytes.

PCR genotyping of *Bcl11b* deletion in two representative T cell (T1 and T2) and ITNK (I1 and I2) wells. *flox*, floxed allele; *del*, deletion allele. -OHT: no OHT treatment; H₂O: no template control.

Figure 4.15

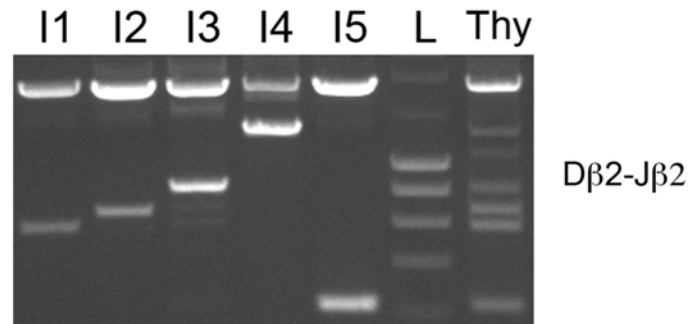


Figure 4.15 Each ITNK colony was derived from individual *Bcl11b*-deficient DN3 thymocytes.

Genotyping results show DJ recombination at the TCR β locus of five ITNK wells (I1 to I5) showing unique DJ recombination. L, DNA ladder; Thy, wild-type thymocytes.

Figure 4.16

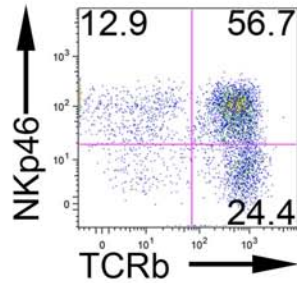


Figure 4.16 Production of ITNK cells from *Bcl11b*-deficient DP thymocytes.

Flow cytometry analysis shows that NKp46⁺TCRβ⁺ ITNK cells were reprogrammed from DP *flox/flox* thymocytes treated with OHT and cultured on OP9-DL1 in the presence of IL-2. Untreated cells died rapidly under this condition. Numbers refer to percentage of cells in the gate. Data are representative of four experiments.

Figure 4.17

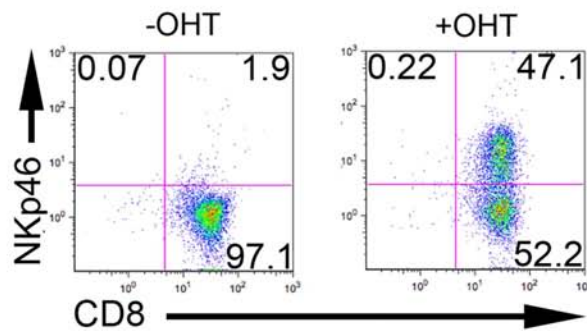


Figure 4.17 Production of ITNK cells from *Bcl11b*-deficient CD8⁺ mature T cells. Flow cytometry analysis shows that NKp46⁺CD8⁺ ITNK cells were reprogrammed from OHT-treated CD8 SP *lox/lox* splenocytes and cultured on OP9-DL1 in the presence of IL-2. Untreated cells died rapidly under this condition. Numbers refer to percentage of cells in the gate. Data are representative of four experiments.

Figure 4.18

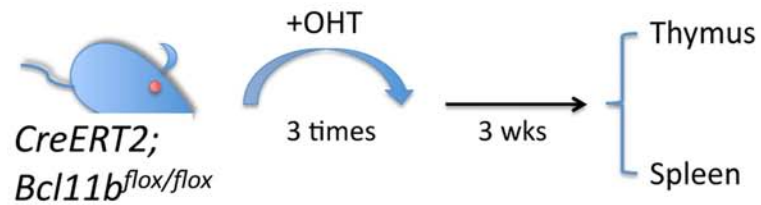


Figure 4.18 Experimental design for the analysis of *in vivo* reprogrammed ITNK cells.

flox/flox or *flox/+* mice were treated with Tamoxifen by oral gavage on three consecutive days, and the thymi and spleens were analyzed 2-3 weeks later. We observed a 5-10 fold reduction in total thymocytes and about 2-fold reduction in splenocytes in the treated *flox/flox* mice compared to treated *flox/+* control mice.

Figure 4.19

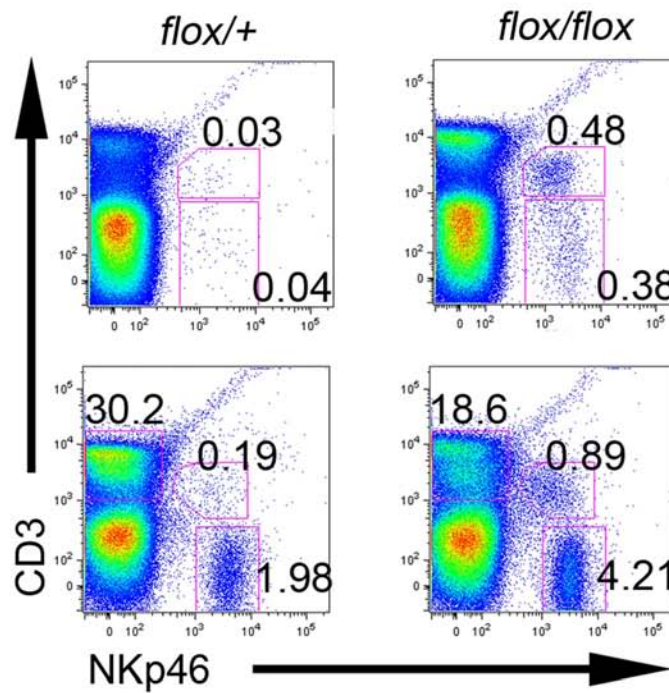


Figure 4.19 Analysis of *in vivo* reprogrammed ITNK cells in the *flox/flox* mouse. Flow cytometric analysis of thymocytes and splenocytes from OHT-treated *flox/flox* and *flox/+* mice. Numbers refer to the percentage in the lymphocyte gate. Data are representative of four mice.

Figure 4.20

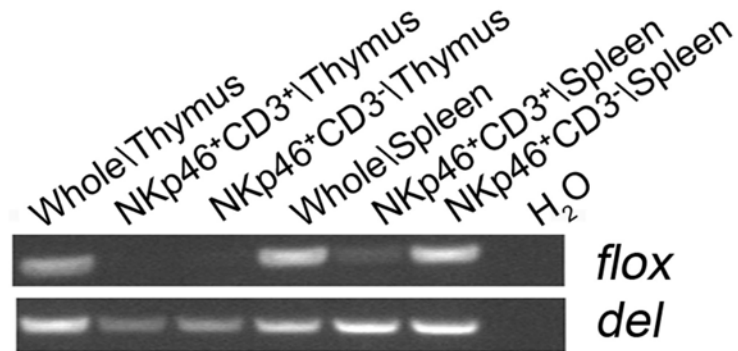


Figure 4.20 ITNK cells have *Bcl11b* deleted.

PCR results show that *Bcl11b* was deleted in ITNK (NKp46⁺CD3⁺ and NKp46⁺CD3⁻) cell populations in *flox/flox* mice. *flox*: conditional knockout allele; *del*: deletion allele. H₂O: no DNA template control. All the NKp46⁺CD3⁺ and NKp46⁺CD3⁻ cells in the thymus were ITNKs. Analyzing ITNKs in the spleen was more complicated due to the presence of many NKp46⁺ conventional NK cells. However, most of the NKp46⁺CD3⁺ cells in the spleen had *Bcl11b*-deficiency and thus were ITNKs. PCR data are representative of three experiments.

Figure 4.21

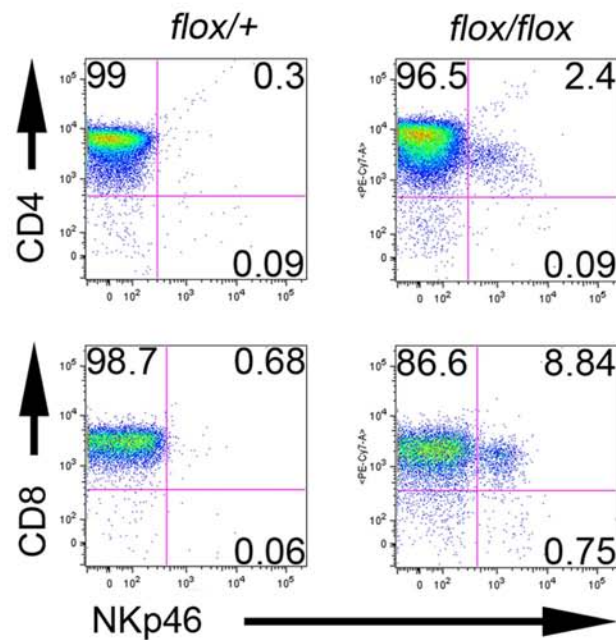


Figure 4.21 CD4 and CD8 T cells reprogram to ITNK upon loss of Bcl11b in vivo.

Flow cytometric analysis of CD4 and CD8 expression in NKp46⁺ ITNKs. Numbers refer to percentage of cells in the gate. Note that both CD4 and CD8 expression was down in ITNKs (CD4⁺NKp46⁺ or CD8⁺NKp46⁺) compared to CD4⁺NKp46⁻ or CD8⁺NKp46⁻ T cells. Numbers refer to percentage of cells in the gate. Data are representative of two mice.

Figure 4.22

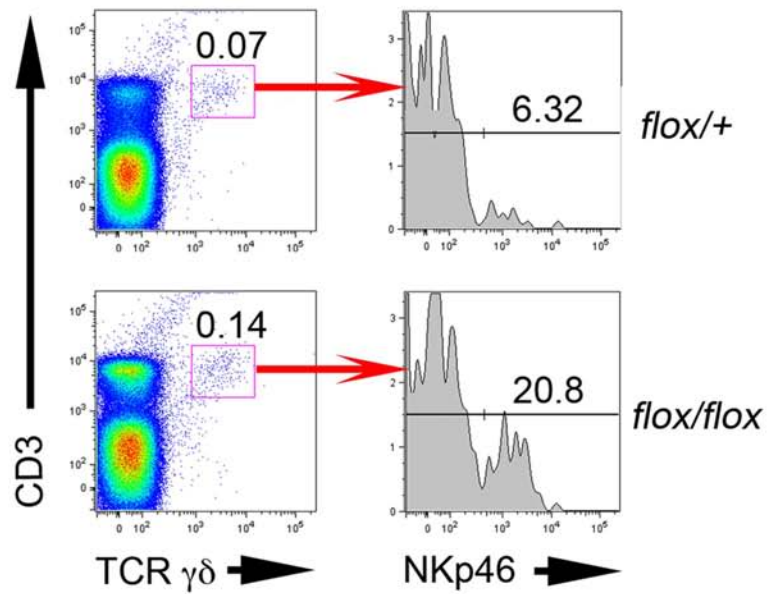


Figure 4.22 $\gamma\delta$ -T cells reprogram to ITNK cells upon loss of Bcl11b in vivo.

Flow cytometry analysis of ITNKs from thymic $\gamma\delta$ -T cells in OHT-treated *flox/flox* mice. Numbers refer to percentage of cells in the gate. Data are representative of two mice.

Figure 4.23

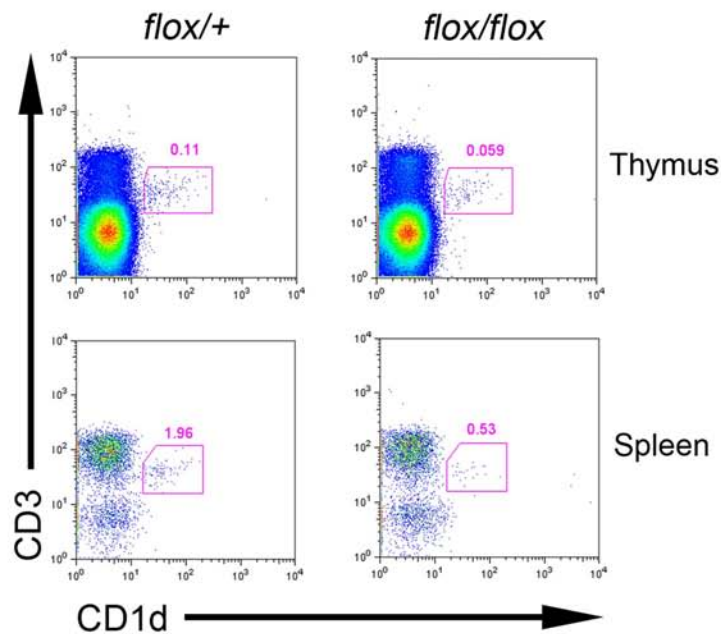


Figure 4.23 ITNKs are not NKT cells.

Flow cytometric analysis of CD1d-restricted NKT cells in thymus and spleen. Total lymphocytes and CD19⁻ splenocytes were gated in the thymus and spleen, respectively. Note the reduction of NKT cells in the OHT-treated *flox/flox* mice. Data are representative of two mice.

Figure 4.24

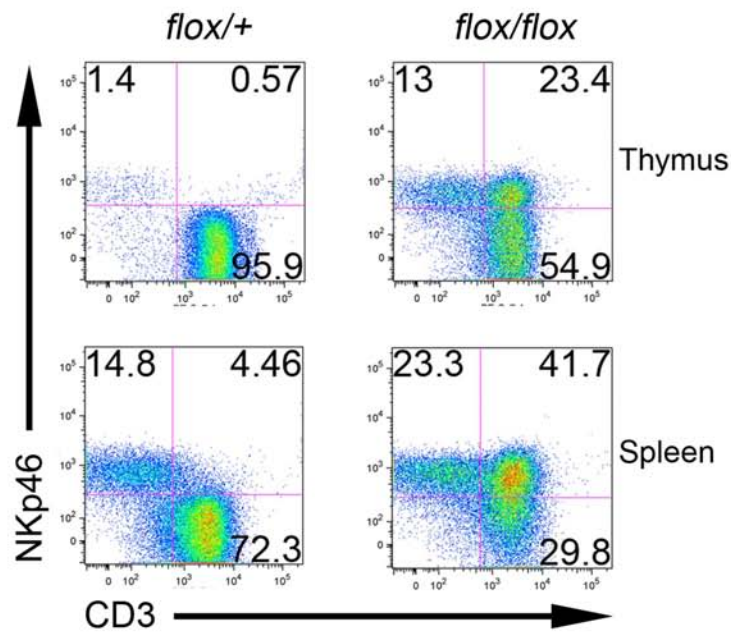


Figure 4.24 ITNK cells can be expanded in NK culture condition.

Flow cytometric analysis of cells following *ex vivo* expansion of whole thymocytes or splenocytes from OHT treated mice. Numbers refer to percentage of cells in the gate.

Data are representative of four experiments.

Figure 4.25

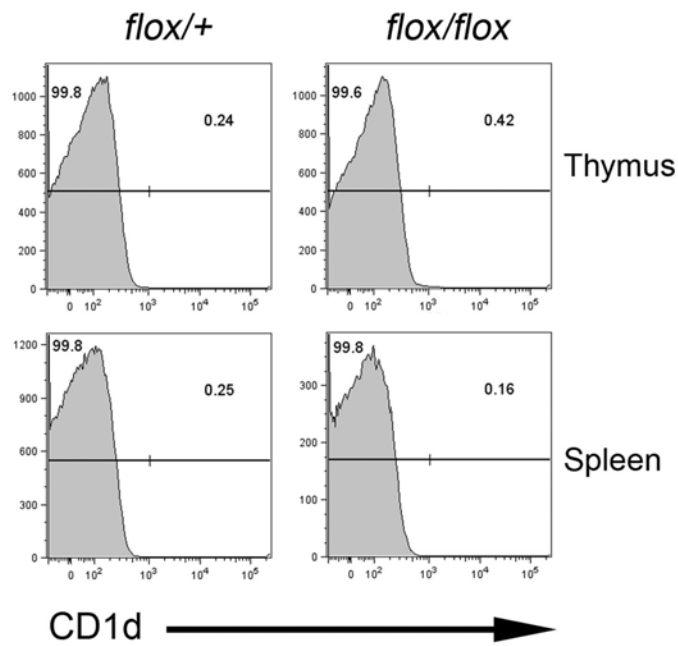


Figure 4.25 Ex vivo expanded ITNKs are not NKT cells.

Flow cytometry analysis of CD1d-restricted cells in the ex vivo expanded ITNK culture. Numbers refer to percentages in lymphocyte gate. Data are representative of four experiments.

Figure 4.26

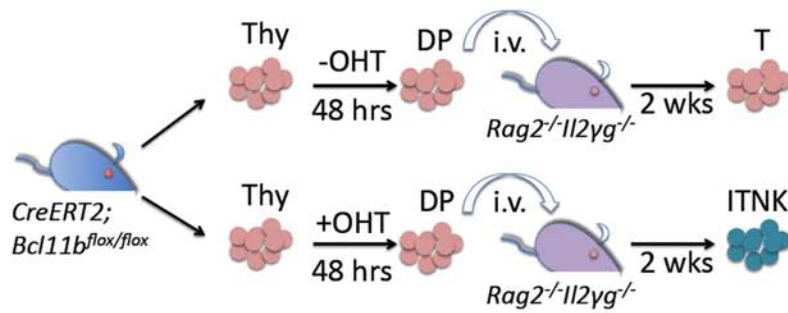


Figure 4.26 Experimental design for the analysis of in vivo reprogramming of DP thymocytes to ITNKs.

Whole thymocytes from *flox/flox* mice were treated with OHT (+OHT) or left untreated (-OHT) and 48-hours later DP cells were sorted and injected intravenously into *Rag2^{-/-}Il2rγ^{-/-}* mice. Two weeks later, splenocytes, bone marrow (BM) and peripheral blood cells (PB) were analyzed by flow cytometry.

Figure 4.27

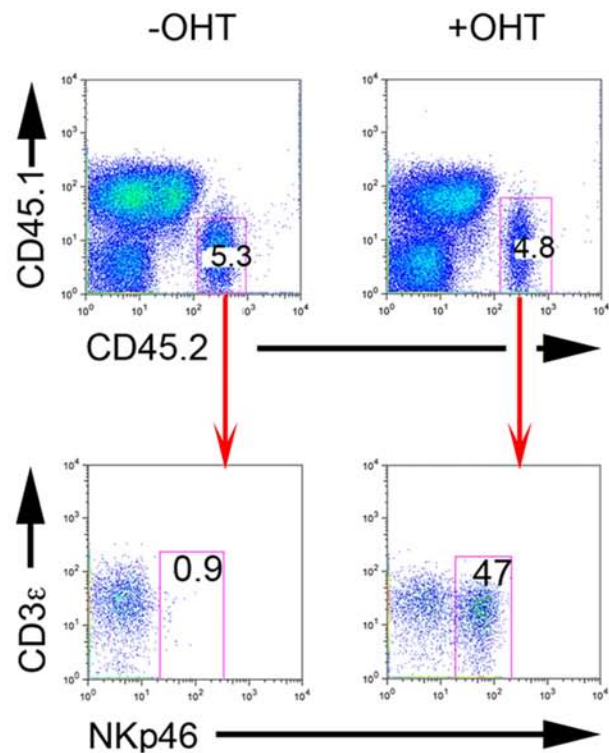


Figure 4.27 DP thymocytes reprogram to ITNKs upon loss of Bcl11b in vivo.

ITNKs production in *Rag2*^{-/-}*Il2ry*^{-/-} recipients injected with *flox/flox* DP thymocytes.

Two weeks after injection, donor (CD45.2⁺) and host (CD45.1⁺) splenocytes were analyzed by flow cytometry. Numbers refer to the percentage of lymphocyte gate.

Plots are representative of 15 mice from three independent experiments.

Figure 4.28

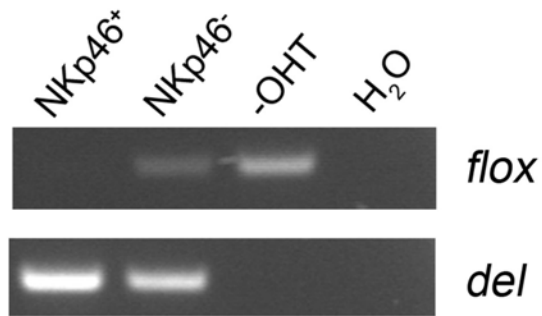


Figure 4.28 *Bcl11b* deletion in ITNKs.

PCR results show that ITNKs had complete *Bcl11b* deletion whereas donor derived NKp46⁻ cells still retained at least one copy of the *flox* allele. PCR data are representative of two individual experiments.

Figure 4.29

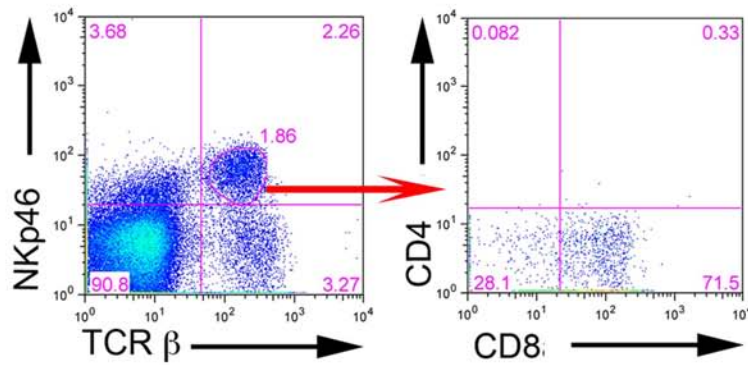


Figure 4.29 Most ITNKs in the spleen were CD8⁺.

Flow cytometry analysis shows that ITNKs derived from DP thymocytes in vivo did not express CD4 but CD8. Numbers in gates refer to percentages. Data are representative of three experiments.

Figure 4.30

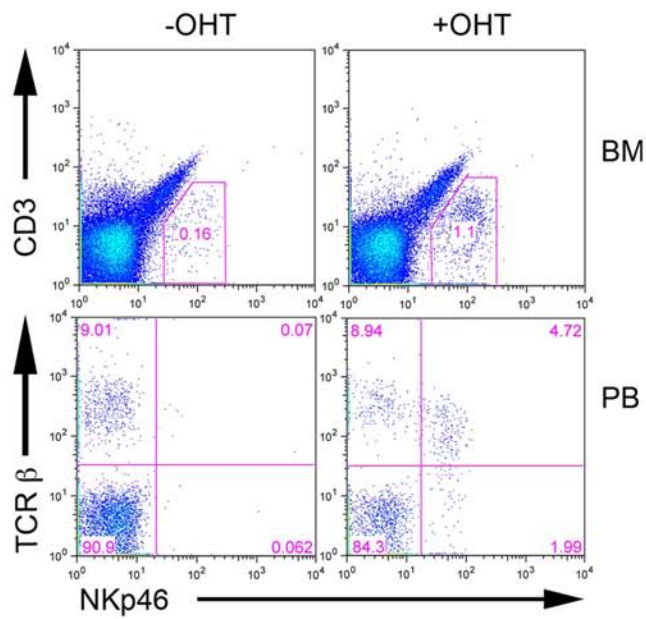


Figure 4.30 ITNKs in bone marrow and peripheral blood.

Flow cytometry analysis shows the percentages of ITNKs in bone marrow and peripheral blood. Numbers in gates refer to percentages. Data are representative of three experiments.

Figure 4.31

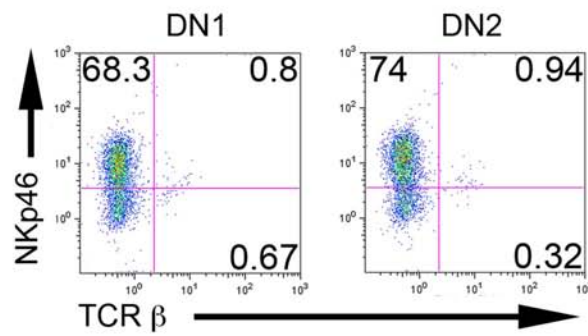


Figure 4.31 Production of NK-like cells from *Bcl11b*-deficient DN1 and DN2 thymocytes in absence of Notch signaling.

NKp46⁺TCRβ⁻ cells from OHT-treated DN1 (left panel) and DN2 (right panel) *flox/flox* thymocytes in the absence of IL-2 or IL-15 cultured on OP9 stromal cells.

Figure 4.32

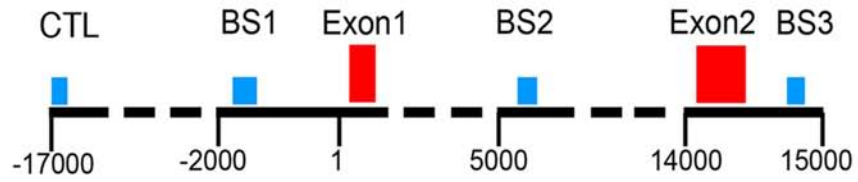


Figure 4.32 Putative CSL binding sites in *Bcl11b* locus.

Schematic of the *Bcl11b* locus showing three putative CSL binding sites (BS) and that of an irrelevant control binding site (CTL)

Figure 4.33

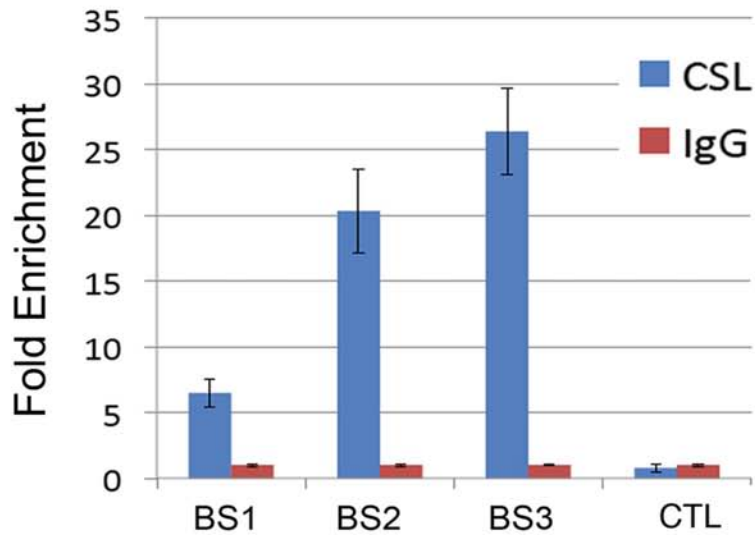


Figure 4.33 CSL directly binds to *Bcl11b* locus.

Genomic DNA was prepared from immunoprecipitation of thymocytes, by using CSL or control immunoglobulin G (IgG) antibodies, and was amplified by using primers flanking the putative CSL or the control binding sites at the *Bcl11b* locus. Three *Bcl11b*-binding regions: Region 1, about 1.8 kb from start of the transcription; region 2, 5.4 kb downstream of exon 1; region 3, about 600 base pairs downstream of exon 2. CSL, CSL antibody; IgG, control IgG. Fold-enrichment was calculated relative to the IgG control (set to 1). Bars are means \pm SD of triplicate samples.

Figure 4.34

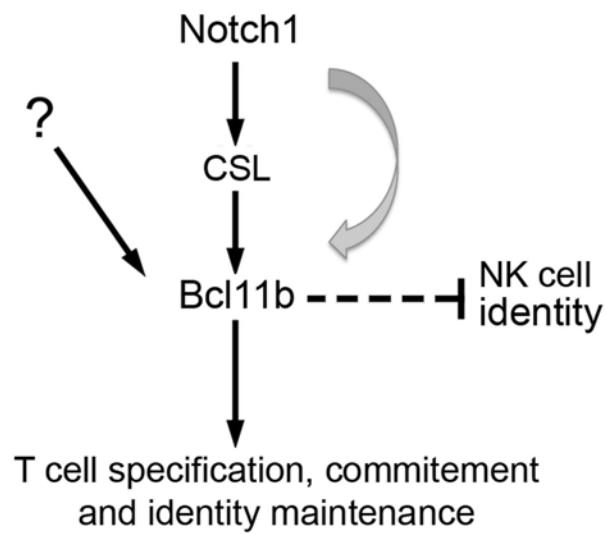


Figure 4.34 Bcl11b functions and networking in T cells.

A working model shows that Bcl11b acts downstream of Notch signaling and unknown pathways. Bcl11b promotes T cell development and maintains T cell identity and may also suppress NK cell identity.

Figure 4.35

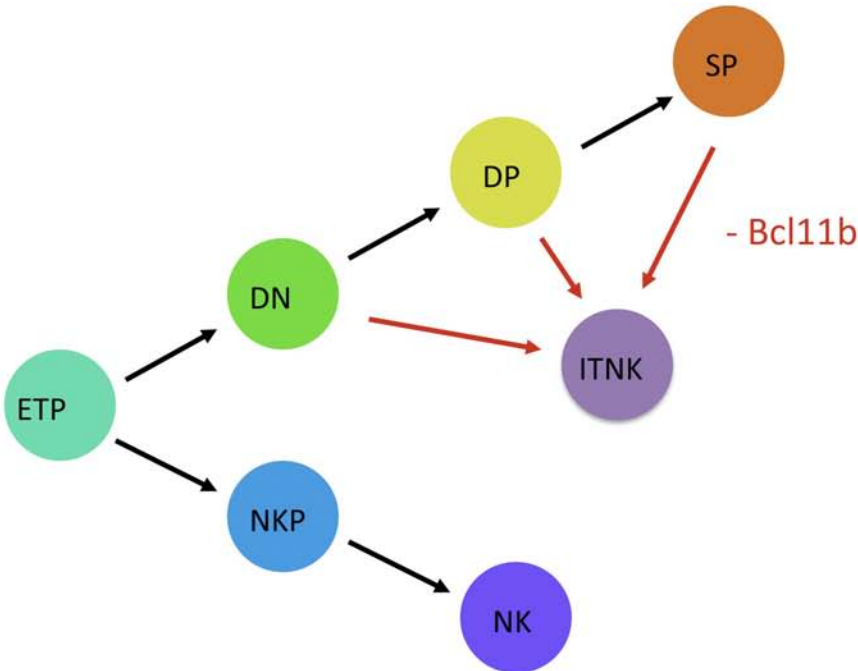


Figure 4.35 Summary of reprogram from various T cell subsets to ITNK cells. ETP, early T cell precursors; DN, double negative; DP, double positive; SP, single positive; ITNK, Induced T to natural killer cells; NKP, natural killer progenitors; NK, natural killer cells. Black arrows indicate differentiation and red arrows indicate reprogramming.

Figure 5.1

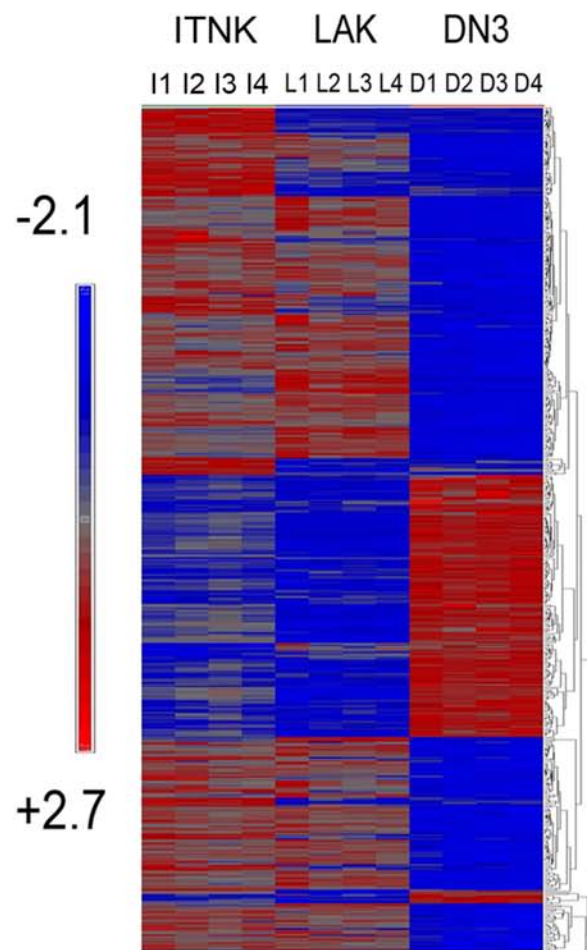


Figure 5.1 Comparison of gene expression profiles among ITNK, DN3 thymocytes and LAK.

Microarray analysis of gene expression in NKp46⁺CD3⁺ ITNK cells derived from DN3 thymocytes (columns I1 to I4), IL-2–expanded NK cells (LAK; L1 to L4) and sorted DN3 *flax/flax* thymocytes (DN3; D1 to D4) were subjected to expression. Two-way hierarchical cluster map of the array data. Column numbers (I1 to I4 for instance) refer to four independent RNA samples for each cell type, and rows represent individual transcripts. Scale indicates the log₂ value of normalized signal level.

Figure 5.2

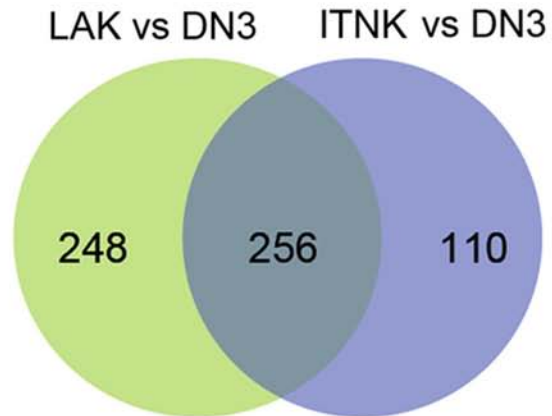


Figure 5.2 ITNKs were more similar to LAK than DN3 cells.

Venn diagram comparison of the upregulated (>2-fold) genes between LAK vs. DN3 (green) and ITNK vs. DN3 (purple) shows a significant overlapping between the two gene lists.

Figure 5.3

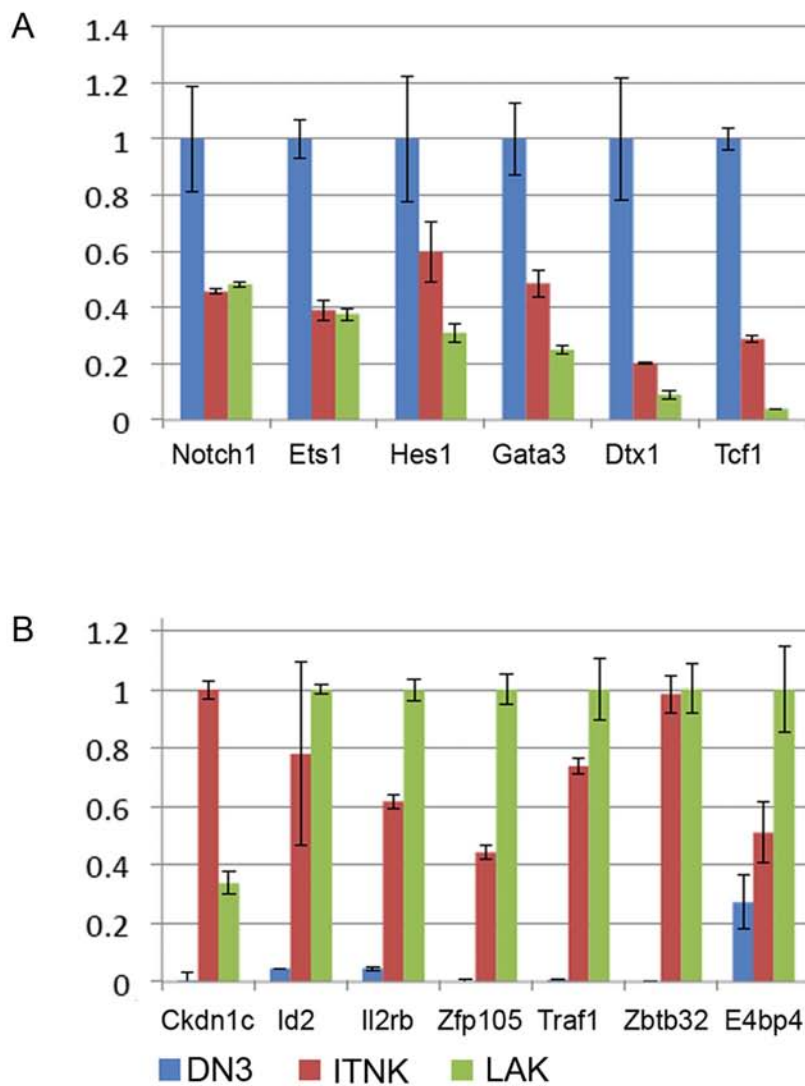


Figure 5.3 Validation of microarray analysis.

qRT-PCR was performed to validate gene expression of selected genes among ITNKs, LAKs, and DN3 cells. Bars are means \pm SD of three samples.

Figure 5.4

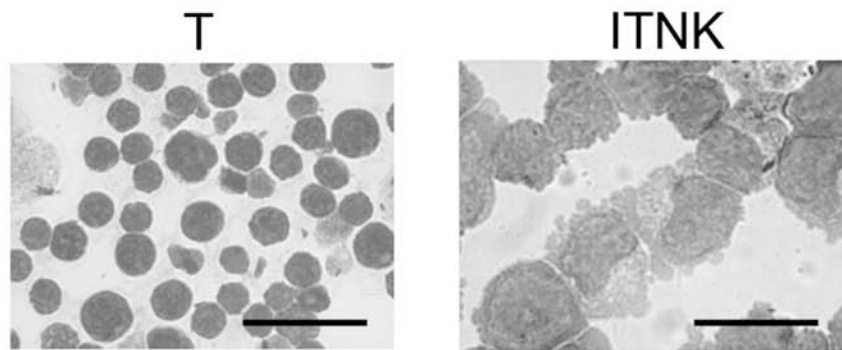


Figure 5.4 Comparison of ITNKs and T cells in morphology.

Giemsa stain of parental DN3 thymocytes (T) and ITNK cells. Scale bar, 20 μm .

Figure 5.5

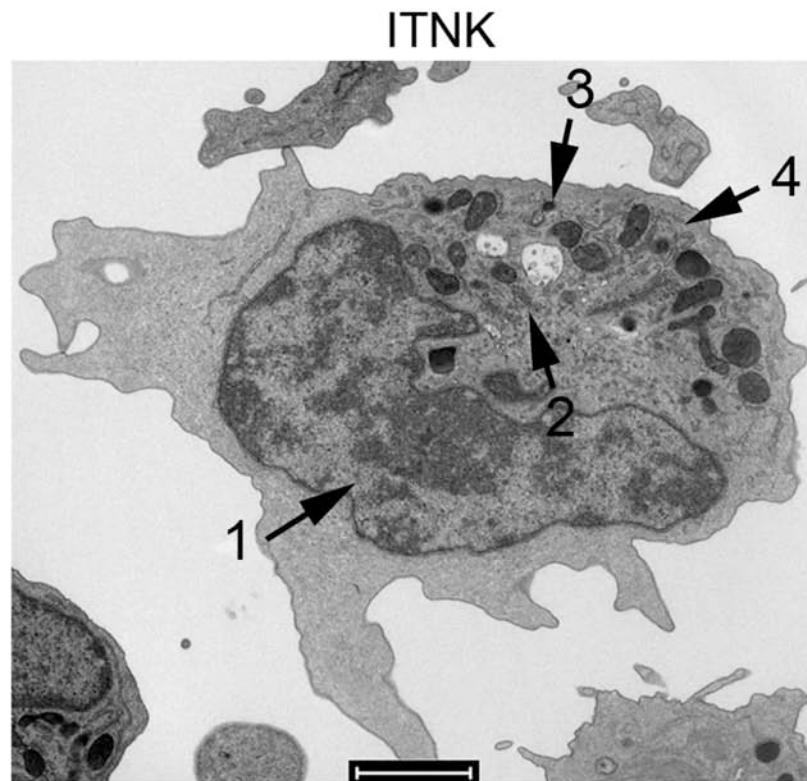


Figure 5.5 Morphology of ITNKs under electronic transmission microscopy. Transmission electron micrograph of an ITNK cell. 1, Nucleus; 2, Golgi body; 3, granule; 4, endoplasmic reticulum. Scale bar, 2 μm .

Figure 5.6

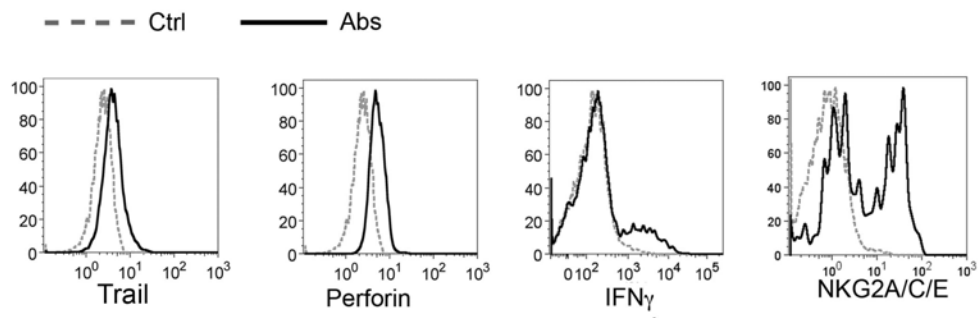


Figure 5.6 Expression of intracellular (TRAIL, perforin, IFN_γ) and NK cell surface markers in ITNKs.

Flow cytometry analysis shows that ITNKs from DN3 thymocytes in vitro expressed TRAIL, perforin, IFN_γ and NKG2A/C/E. Solid black lines represent experiments with antibody, while grey dash lines represent experiments with isotype control. Data are representative of three experiments.

Figure 5.7

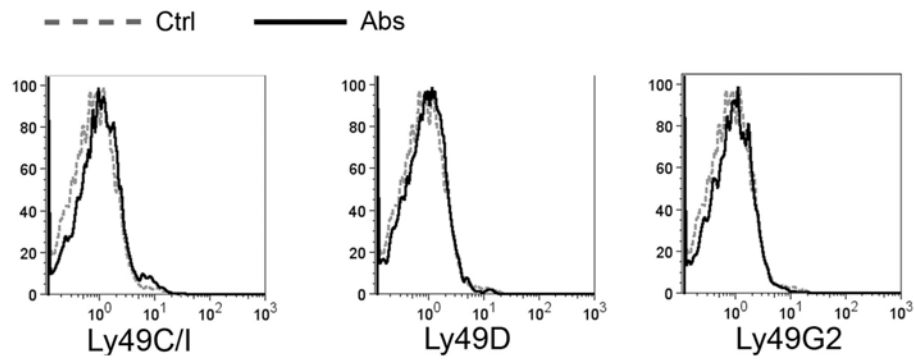


Figure 5.7 DN3-derived ITNKs did not express Ly49 family.

Flow cytometry analysis shows that ITNKs from DN3 thymocytes in vitro did not express some NK cell surface markers like Ly49C/I, Ly49D and Ly49G2. Solid black lines represent experiments with antibody, while grey dash lines represent experiments with appropriate isotype controls. Data are representative of three experiments.

Figure 5.8

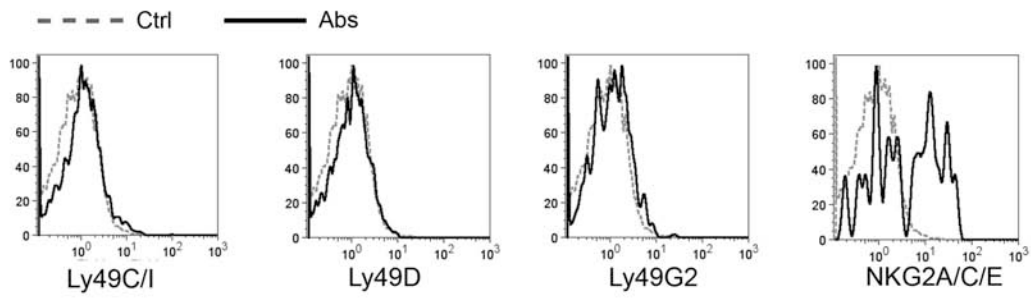


Figure 5.8 DP-derived ITNKs expressed NKG2A/C/E but not Ly49 family.

Flow cytometry analysis shows that ITNKs from DP thymocytes in vitro stained positively for NKG2A/C/E but not for Ly49C/I, Ly49D and Ly49G2. Solid black lines represent indicated antibody, while grey dash lines represent isotype control. Data are representative of three experiments.

Figure 5.9

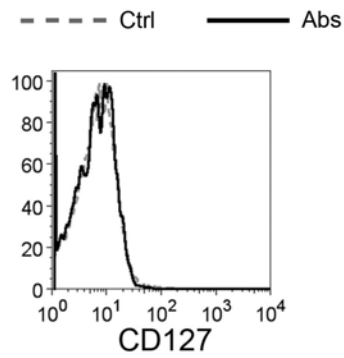


Figure 5.9 ITNKs were not thymic NK cells.

Flow cytometry analysis shows that ITNK cells did not express CD127. Solid black lines represent experiments with antibody, while grey dash lines represent experiments with isotype control. Data are representative of three experiments.

Figure 5.10

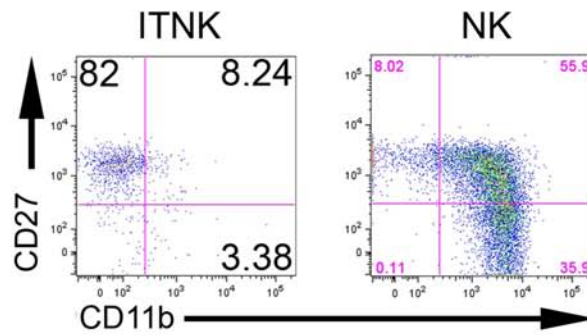


Figure 5.10 Expression of CD27 and CD11b on ITNK cells.

Flow cytometry analysis shows that ITNKs reprogrammed from DN3 thymocytes in vitro expressed CD27 but not CD11b. Numbers in gates refer to percentages. Data are representative of two experiments.

Figure 5.11

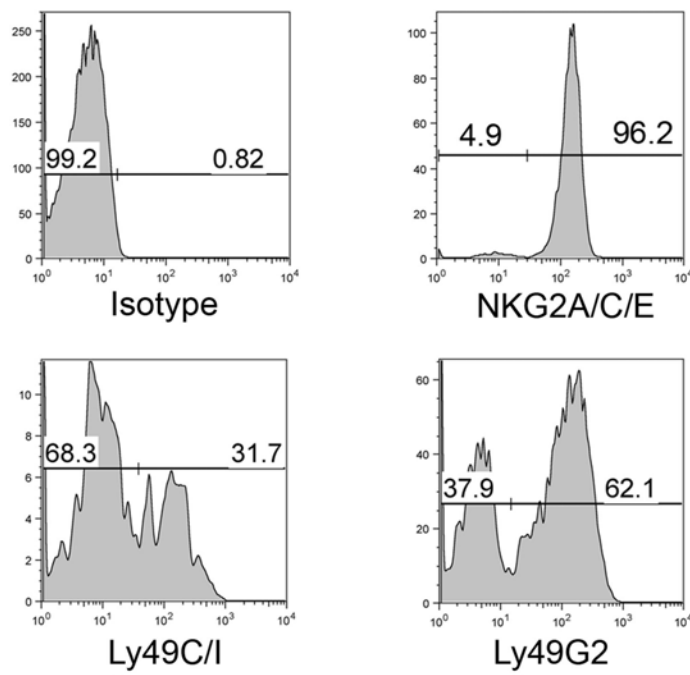


Figure 5.11 DP-derived ITNKs in vivo expressed NKG2A/C/E and Ly49 family. Flow cytometry analysis shows that ITNKs from DP thymocytes in vivo were stained positively for NKG2A/C/E, Ly49C/I, Ly49D and Ly49G2. Numbers in gates refer to percentages. Data are representative of three experiments.

Figure 5.12

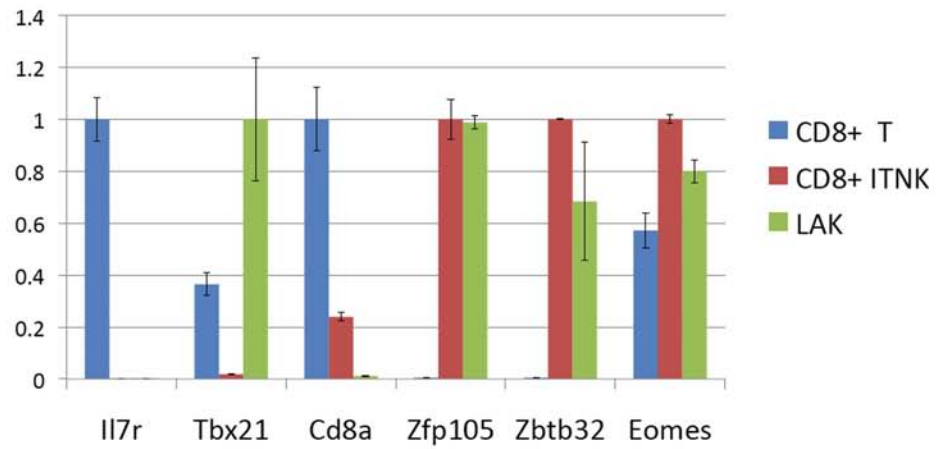


Figure 5.12 T cell associated genes decreased in ITNK cells.

qRT-PCR analysis of several key T or NK cell-associated genes in CD8⁺ T cells, CD8⁺ ITNKs and LAKs. Bars are mean \pm SEM of 3 samples. The highest expression level for each gene was chosen as 1.

Figure 5.13

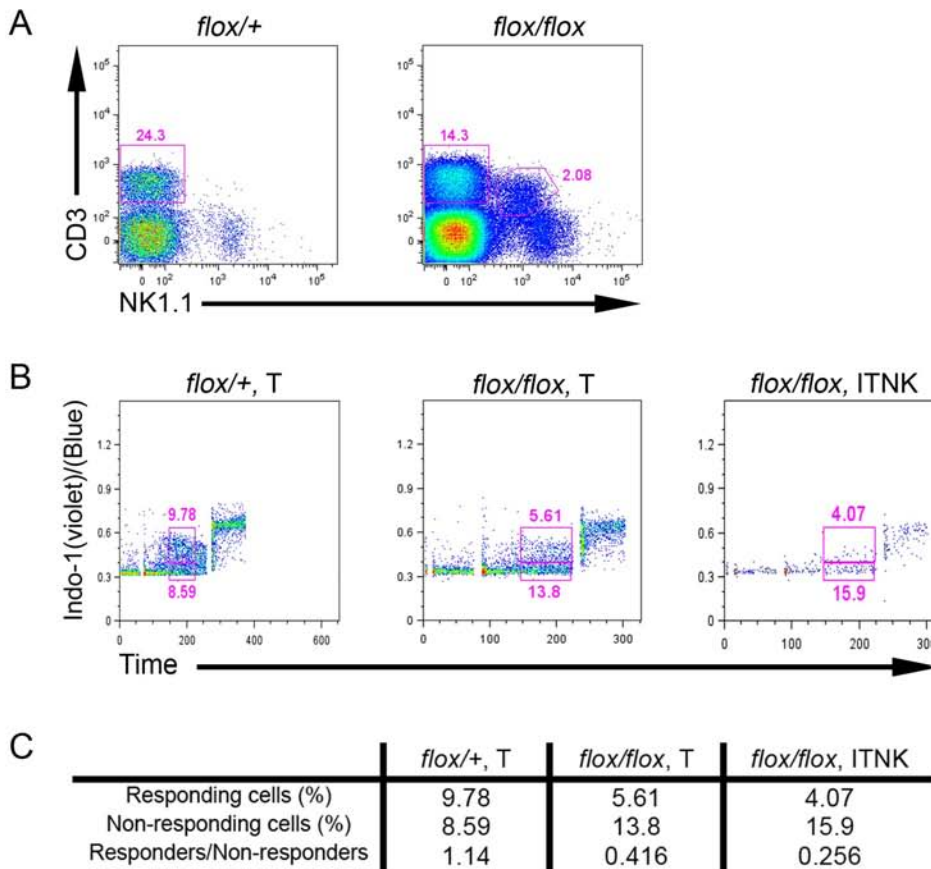


Figure 5.13 ITNK cells have compromised TCR signaling.

Splenocytes from *flox/flox* or *flox/+* mice treated with Tamoxifen were stained with NKp46, NK1.1, CD8 and CD3 to confirm expression of CD3 on ITNKs. A separate aliquot was loaded with Indo-1, stained with antibodies to NKp46, NK1.1 and CD8 and analyzed for calcium flux by flow cytometry. Top panel: Phenotype of splenocytes from *flox/flox* or *flox/+* mice indicating gated T cells ($CD3^+NKp46^-$) and ITNKs ($CD3^+NKp46^+$) cells. Numbers refer to percentages in gates of total lymphocytes. Lower panel: Calcium flux plots from the indicated cell subset. A baseline was established at the start of the assay, before acquisition was interrupted and anti-CD3 (145-2C11) was added (first arrow). CD3 was then cross-linked by

addition of anti-hamster secondary antibody (second arrow). Ionomycin was added (third arrow) as a positive control. Numbers in gates refer to responders (upper gate) and non-responders (lower gates) after addition of anti-hamster antibody. Data below calcium plots show ratio of responders to non-responders in gated area. Data are representative of two mice.

Figure 5.14

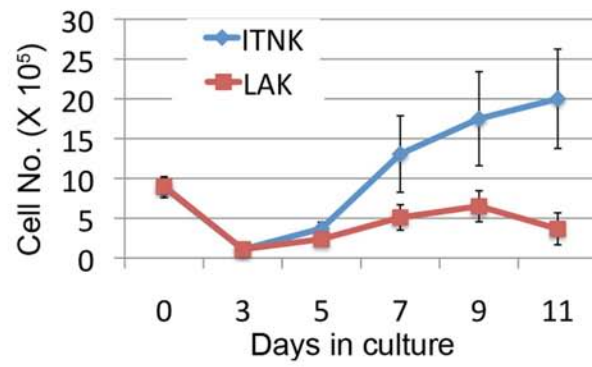


Figure 5.14 Splenocytes of the recipient mice can be expanded ex vivo.

Growth curved was drew based on numbers of viable cells that were counted at the indicated time points. Bars are means \pm SD of four samples.

Figure 5.15

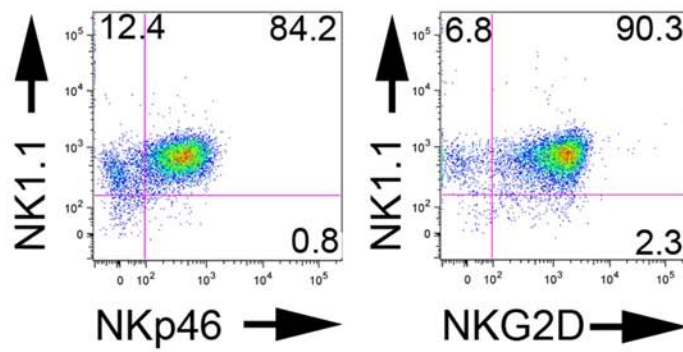


Figure 5.15 Ex vivo expansion of ITNKs.

Flow cytometry analysis shows that most cells in the culture were ITNKs because they expressed NKp46, Tcr β , NK1.1, and NKG2D. Numbers in gates refer to percentages. Data are representative of four experiments.

Figure 5.16

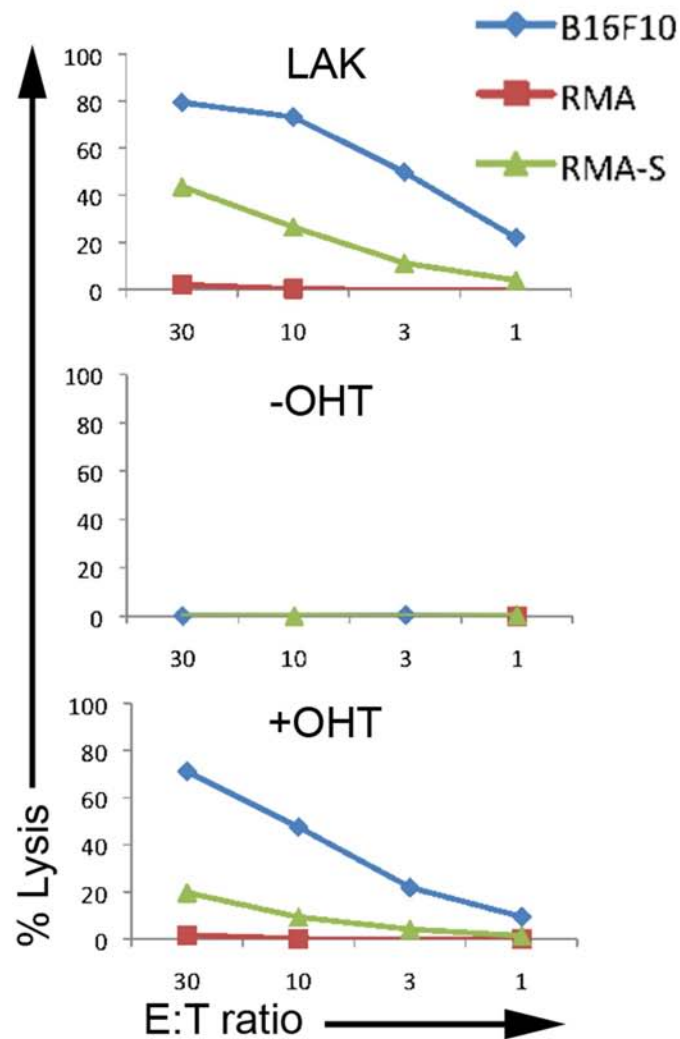


Figure 5.16 ITNK cells killed NK targets in killing assays.

The cytotoxicity of ITNKs (labeled as “+OHT”, bottom panel) and LAKs (top panel) was measured in standard ^{51}Cr -release assays with B16F10, RMA, and RMA-S tumor cell targets at the indicated effector-to-target (E:T) ratios. -OHT: *flx/flx* T cells (middle panel). Data are means of triplicate wells.

Figure 5.17

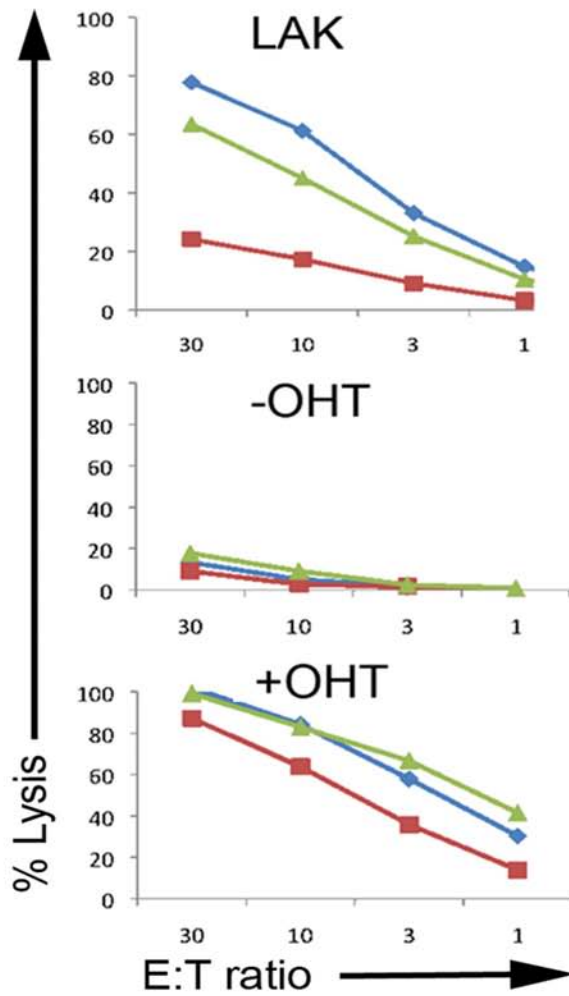


Figure 5.17 ITNK cells killed NK targets in killing assays.

The cytotoxicity of ex vivo expanded ITNKs (labeled as “+OHT”, bottom panel) and LAKs (top panel) was measured in standard ^{51}Cr -release assays with B16F10, RMA, and RMA-S tumor cell targets at the indicated effector-to-target (E:T) ratios. -OHT: *flox/flox* T cells (middle panel). Data are means of triplicate wells. Results are representative of three experiments.

Figure 5.18

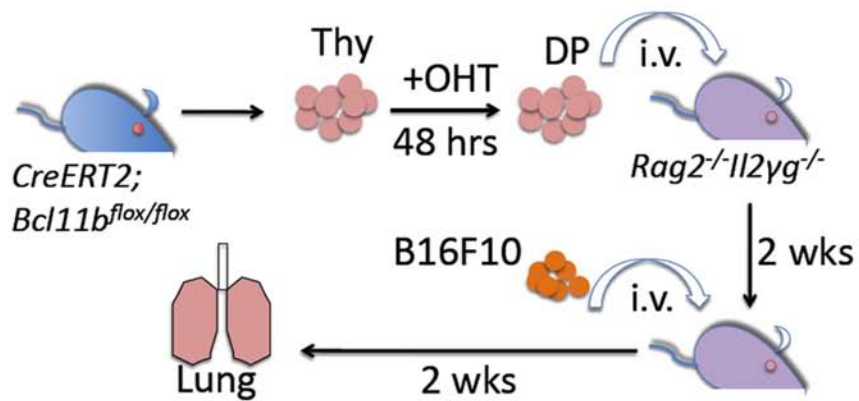


Figure 5.18 Experiment design for tumour killing assays in vivo.

Rag2^{-/-}Il2γ^{-/-} recipients were transplanted with treated (+OHT) or untreated (-OHT) *flox/flox* DP thymocytes or PBS. Recipients were subsequently injected intravenously with 5×10^4 B16F10 melanoma cells. Lung tumour colonies were enumerated two weeks after tumour challenge. Experiment was performed twice.

Figure 5.19

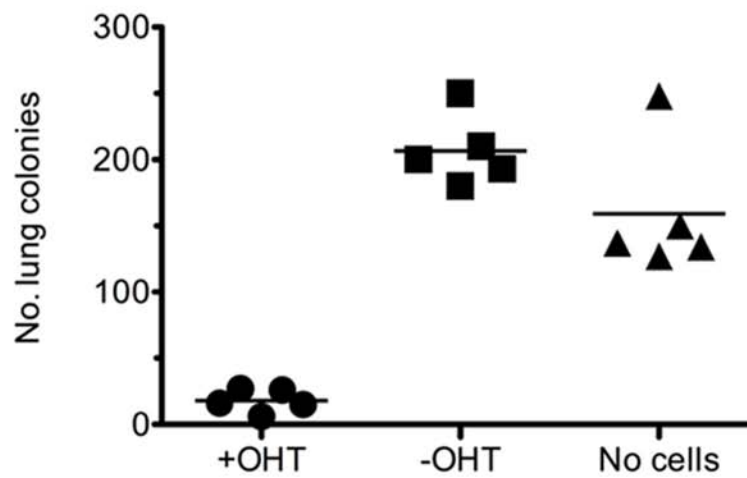


Figure 5.19 ITNKs prevented tumor metastasis.

Rag2^{-/-}*Il2rγ*^{-/-} recipients first transplanted with treated (+OHT) or untreated (-OHT) *flox/flox* DP thymocytes or phosphate-buffered saline. Recipients were subsequently injected intravenously with 50,000 B16F10 melanoma cells. Lung tumor colonies were enumerated 2 weeks after tumor challenge. Data are from individual mice, and bars represent the means.

Figure 5.20

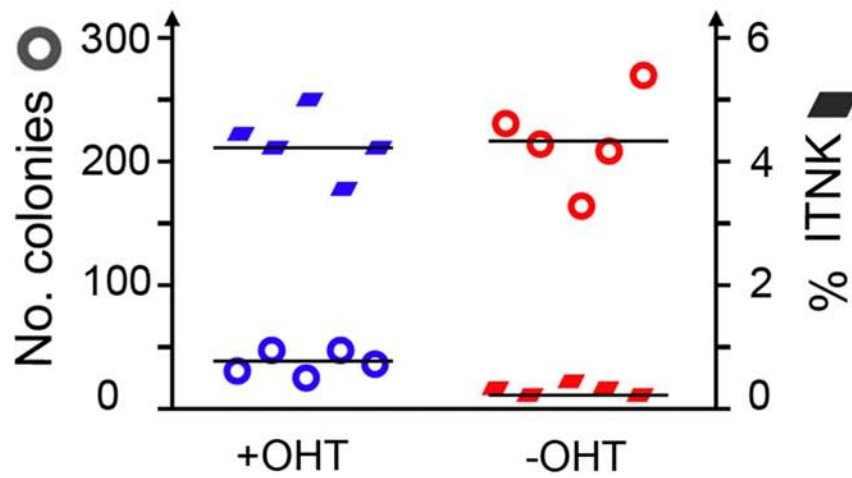


Figure 5.20 Killing ability was coordinated with numbers of ITNKs.

Plot shows inverse correlation between the percentage of ITNK cells (squares) obtained from recipient mice following *in vivo* reprogramming and tumor challenge and the number of lung colonies (circles) observed. Data are individual mice and are representative of two independent experiments, each with 5 mice per group.

Figure 6.1

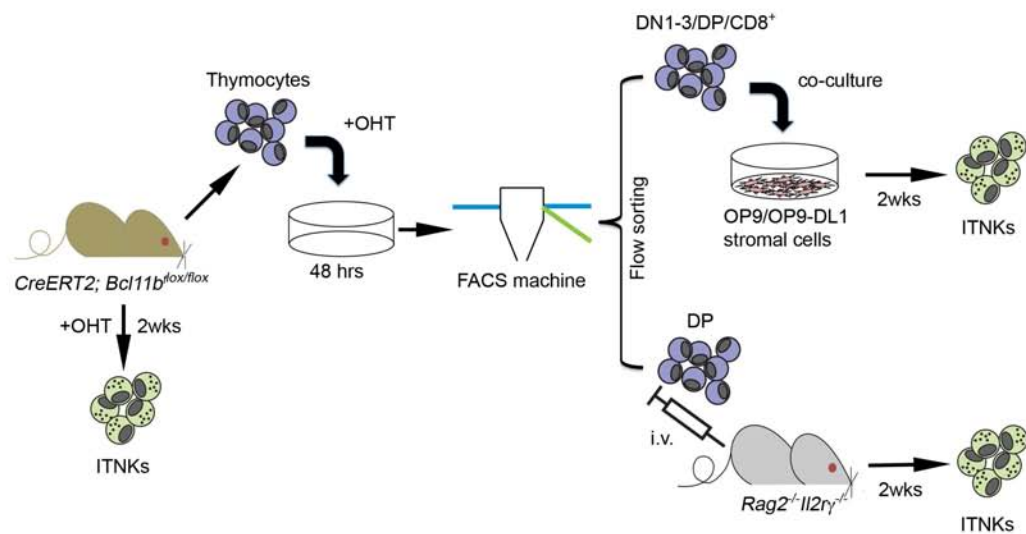


Figure 6.1 Reprogramming mouse T cells to ITNKs upon *Bcl11b* deletion (Pentao Liu, 2010).

ITNKs have been produced using three approaches. The flox/flox mice are treated with Tamoxifen to delete *Bcl11b*. ITNKs are found in peripheral blood, the spleen and thymus of the treated mice in a couple of weeks. Alternatively, *Bcl11b* are also deleted in vitro in thymocytes. Whole thymocytes from *flox/flox* mice are treated with Tamoxifen, which are then sorted into different subsets and cultured on stromal cells for ITNK production. DP thymocytes sorted from these whole thymocytes are also transferred into *Rag2^{-/-}Il2rγ^{-/-}* mice. ITNKs are detected in these recipient mice a couple of weeks after the injection.

Figure 6.2

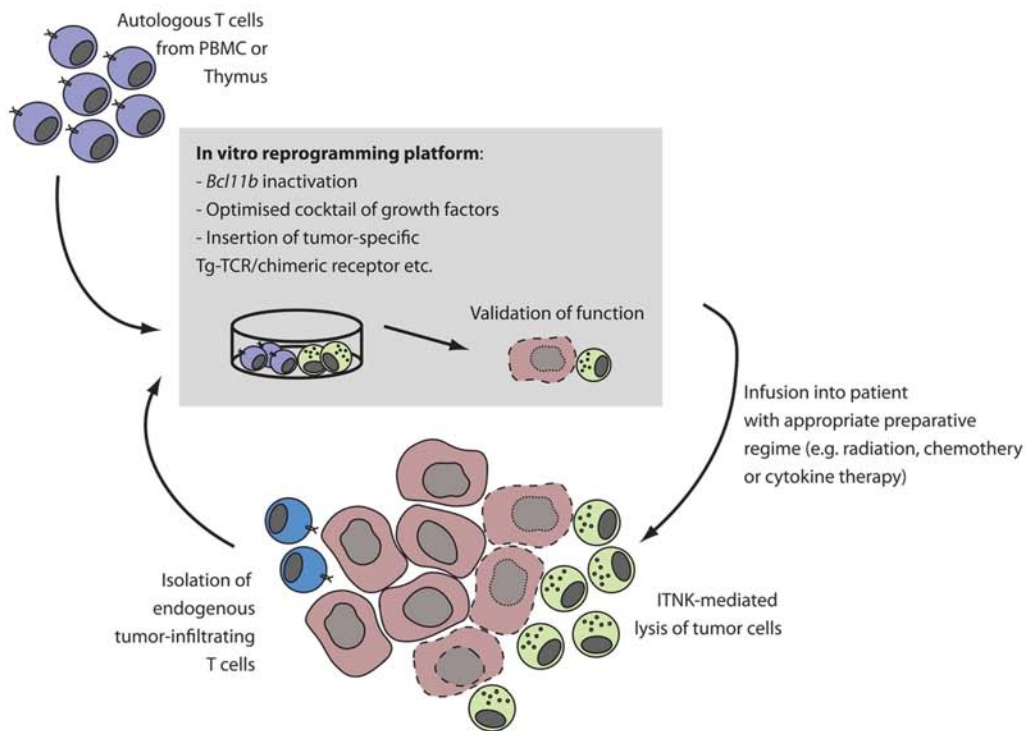


Figure 6.2 A potential platform for the production and application of human ITNKs (Pentao Liu, 2010).

Autologous T cells from PBMC or endogenous tumor-infiltrating T cells from the patient or allogeneic thymocytes are isolated and cultured in the in vitro reprogramming conditions. Several alternative approaches to modify the T cells, including *Bcl11b* inactivation, conditioning in optimized cocktails of growth factors, and insertion of tumor-specific Tg-TCR/chimeric receptors in this reprogramming platform. Then ITNKs are validated for their killing and self-tolerance capacities. Selected ITNKs are expanded and infused into patients where these ITNKs encounter and kill tumor cells. Reduction in the tumor volume by appropriate preparative regimes, including radiotherapy or chemotherapy and the co-administration of cytokine adjuncts may potentiate ITNK treatment efficacy.

Pentao Liu, P.L., Shannon Burke (2010). Critical Roles of Bcl11b in T Cell Development and Maintenance of T Cell Identity. *Immunological Reviews* *In press*.

Table 1. The list of primers in this study.

Genotyping primers.

Genotyping PCR primers	Primer sequences (5'-3')	Size of PCR products (bp)
Bcl11b-cko-FW	TGAGTCAATAAACCTGGGCGAC	243 (wild type);
Bcl11b-cko-RV	GGAATCCTTGGAGTCACTTGTGC	345 (<i>flox</i>);
Bcl11b-cko-DEL	TCCTGGTAACACACAATTGC	450 (<i>del</i>)

qRT-PCR primers.

qPCR primers	Primer sequences (5'-3')
Notch1-Fwd	CCCTTGCTCTGCCTAACGC
Notch1-Rev	GGAGTCCTGGCATCGTTGG
Ets1-Fwd	TTAGGAAAGGCTCGTTTGCTC
Ets1-Rev	CCAAAGCACAAGCATAGTTTGC
Hes1-Fwd	CCAGCCAGTGTCAACACGA
Hes1-Rev	AATGCCGGGAGCTATCTTTCT
Gata3-Fwd	CTCGGCCATTTCGTACATGGAA
Gata3-Rev	GGATACCTCTGCACCGTAGC
Deltax1-Fwd	TGTTCAAGGCTATACACGCATCAA
Deltax1-Rev	CCACCGCCCACTTTCAAG
Tcf1-Fwd	ATGGGCGGCAACTCTTTGAT
Tcf1-Rev	CGTAGCCGGGCTGATTCAT
Cdkn1c-Fwd	CGAGGAGCAGGACGAGAATC
Cdkn1c-Rev	GAAGAAGTCGTTTCGCATTGGC
Id2-Fwd	ATGAAAGCCTTCAGTCCGGTG
Id2-Rev	AGCAGACTCATCGGGTCGT
Il2rb-Fwd	TGGAGCCTGTCCCTCTACG
Il2rb-Rev	TCCACATGCAAGAGACATTGG
Zfp105-Fwd	GGCATCCAGCCAACAAGTGTA
Zfp105-Rev	CATTTCCCTGACCCTTTTCCTCAT
Traf1-Fwd	GGAGGCATCCTTTGATGGT A
Traf1-Rev	AGGGACAGGTGGGTCTTCTT
Zbtb32-Fwd	GCTCTGAGAGAGGACTTGGGA
Zbtb32-Rev	TGCTTTATGCTTGTGTGACATCT

Tcrb rearrangement PCR primers.

PCR primers	Primer sequences (5'-3')
TCRB_D β 2-Fwd	GTAGGCACCTGTGGGGAAGAACT
TCRB_V β 2-Fwd	GGGTCACTGATACGGAGCTG
TCRB_J β 2-Rev	TGAGAGCTGTCTCCTACTATCGATT

List of primers for ChIP assay qPCR.

PCR primers	Primer sequences (5'-3')
BS1-Fwd	CCGCTACGAGGCACCCTCCTTT
BS1-Rev	AGTCTCCTTGGGAAGCACGCGCTA
BS2-Fwd	GCTTGCTTGTTTTTAATTCAGTTTATGGG
BS2-Rev	TTGAATGTCTGTGTTGGTGTGTAATCAC
BS3-Fwd	GTGAAAAAAAGGGGGTAGGCCCTC
BS3-Rev	CAGCCCAAAGTCAAAGGCAAGATG
CTL-Fwd	GTTCTTAACTGAGAGTTCCTCCTCCC
CTL-Rev	TCACTCTGGGCCGGAGTCAGTT

Table 2. Changes of gene expression profiles in thymocytes at 24 and 48 hours after deletion of Bcl11b in microarray analysis.

24 hours		48 hours	
Column ID	Fold-Change (+OHT vs. -OHT)	Column ID	Fold-Change (+OHT vs. -OHT)
HMGCS1	27.1719	ROG	11.7941537
FCER1G	7.97969	FCER1G	11.6317801
CYBA	6.431	UPP1	9.00046788
LDH1	3.82439	IFITM1	8.6938789
CD52	3.81745	SCIN	8.6938789
1300002F13R1	3.6466	SERPINA3G	8.51496146
ATP5G3	3.54832	XCL1	7.62110398
UBL5	3.35851	AQP9	7.4127045
LAPTM5	2.8707	NKG7	7.01284577
RPA1	2.26914	IFITM2	6.40855902
LOC270037	2.16383	IFITM3	6.36429187
COX7C	2.11831	9130404D14R	5.69620078
TCRB-V8.2	-2.00629	GADD45G	5.6177795
RPS14	-2.0086	LGALS3	5.46416103
BCL11B	-2.011	CD160	5.31474326
4932414K18R	-2.01727	KLRD1	5.27803164
AA408556	-2.03945	VIM	4.9933222
VIM	-2.04688	TYROBP	4.89056111
MARCKS	-2.05494	LITAF	4.82323131
CD27	-2.07584	BC025206	4.78991482
COX6A2	-2.10037	AVIL	4.72397065
RNPEPL1	-2.11344	LMNA	4.72397065
RPL8	-2.11346	GLRX1	4.40762046
RPS27	-2.14844	NFIL3	4.40762046
CDCA7	-2.15035	LTA	4.1410597
E430002D04R	-2.15383	CCR5	4.0278222
HIBADH	-2.16873	WBSCR5	4
TRBV1_AE000	-2.17733	P2RY14	3.91768119
PSAP	-2.20351	1300002F13R1	3.83705648
CSTB	-2.21395	AMICA1	3.73213197
UPP1	-2.22963	LOC270152	3.70635225
HMG2	-2.2528	9130211I03RI	3.6553258

TCRB-V8.2	-2.2788	CDKN2B	3.6553258
HMGCS1	-2.30359	PLCG2	3.55537072
LOC382896	-2.35265	CTSW	3.53081199
PPIA	-2.37637	BC049975	3.50642289
LOC381808	-2.39227	LOC381140	3.36358566
TXNIP	-2.40294	LGALS1	3.34035168
MTDNA_ATP6	-2.41506	MT1	3.27160823
RPS17	-2.41723	SYTL2	3.27160823
LOC434197	-2.4265	GPR114	3.24900959
UBB	-2.45105	S100A1	3.24900959
TCRG-V4	-2.54552	2310067E08R	3.20427951
A130092J06R1	-2.55682	LRRK1	3.20427951
IGH-6	-2.5636	TNFRSF11B	3.18214594
AI481316	-2.62333	IDB2	3.16016525
HIST1H2AG	-2.64205	CCL4	3.11665832
G22P1	-2.74634	E030006K04R	3.11665832
LOC226574	-2.74888	OSBPL3	3.11665832
HIST1H2AF	-2.78505	LY6A	3.09512999
PRKACB	-2.90749	TNFRSF9	3.09512999
CD8B	-3.01933	S100A6	3.07375036
THY1	-3.11285	1500031H04R	3.05251842
TBCA	-3.1281	2210411K11R	3.05251842
PDLIM4	-3.15574	CTNNA1	3.03143313
EMP3	-3.22525	LOC381319	3.03143313
HIST1H2AO	-3.29719	EMILIN2	3.01049349
CD3E	-3.30996	1110018K11R	2.9896985
RPL23	-3.38327	ANXA2	2.9896985
CD160	-3.44386	SIAT10	2.96904714
EG668668	-3.46858	2310046K01R	2.94853843
CD3G	-3.49152	CISH	2.92817139
RPS27L	-3.63035	1110004P15R	2.90794503
RPL39	-3.69839	GOLPH2	2.88785839
ITGB7	-4.05052	HAVCR2	2.88785839
RPS11	-4.20813	PLSCR1	2.88785839

MYLC2PL	-4.32543
MT-CYTB	-4.34
HIST1H2AI	-4.60413
MTDNA_ND4	-4.61459
IFITM3	-4.86541
HIST2H2AC	-4.87534
18S_RRNA_XC	-5.08974
RPL41	-5.29871
RPS17	-5.30823
RPL13	-5.33629
IFITM2	-5.49522
CD3D	-5.74896
MYLC2PL	-6.76599
RPS14	-6.99771
MTDNA_COXII	-8.38116
RPS29	-9.27924
CD3D	-9.81142
PDLIM4	-10.206
CDCA7	-12.2615
IFITM1	-12.6519
MTDNA_CYTB	-13.7646
HIST1H2AO	-35.3085
TCRB-V13	-412.694
TCRB-V13	-14894.3

SLC2A6	2.8679105
CAPG	2.84810039
LAG3	2.84810039
F2R	2.82842712
LOC269941	2.82842712
1190002C06R	2.80888975
CD9	2.78948733
S100A11	2.78948733
GCNT1	2.75108364
CDKN1A	2.73208051
KLRE1	2.73208051
GPC1	2.71320865
SERPINE2	2.69446715
LRP12	2.67585511
MLKL	2.67585511
BC024955	2.65737163
BHLHB2	2.65737163
C330008K14R	2.65737163
F2RL2	2.63901582
GLRX	2.63901582
IFNG	2.62078681
PGLYRP1	2.62078681
1110007C02R	2.60268371
BC029169	2.60268371
TRAF1	2.60268371
CDKN2A	2.58470566
DUSP6	2.58470566
LY6G5B	2.58470566
RGS1	2.5668518
MYO1F	2.54912125
HBA-A1	2.53151319
2310047C17R	2.51402675
AIM1L	2.51402675
PILRB	2.4966611

2410008K03R	2.4794154
APOB48R	2.4794154
PDGFA	2.4794154
FURIN	2.46228883
SPP1	2.46228883
ROM1	2.44528056
SH3BP2	2.44528056
PPP3CC	2.42838977
B4GALNT4	2.41161566
IER3	2.41161566
OSM	2.41161566
DAPK2	2.39495741
LOC218482	2.39495741
MAPKAPK3	2.39495741
PLP2	2.37841423
BAG3	2.36198532
OSTF1	2.36198532
SERPINB6A	2.3456699
FXD4	2.32946717
LOC327957	2.32946717
AHNAK	2.29739671
CD69	2.28152743
HK2	2.28152743
FES	2.26576777
IL18R1	2.26576777
PPAP2C	2.26576777
SLC39A4	2.25011697
TES	2.25011697
TNF	2.25011697
HGFAC	2.23457428
CD244	2.21913894
6330414G02R	2.20381023
CD63	2.20381023
LOC383981	2.1885874

NAPSA	2.1885874
PKP3	2.1885874
EMP1	2.17346973
FOSL2	2.17346973
GLIPR1	2.17346973
NT5E	2.17346973
SLC24A3	2.17346973
2610009E16R	2.15845647
1110020C13R	2.14354693
D10BWG1379I	2.14354693
ID2	2.14354693
DOK2	2.12874036
LOC381924	2.12874036
2210008N01R	2.11403608
5330403J18RI	2.11403608
HIST1H1C	2.09943337
0610037M15R	2.08493152
7420404O03R	2.08493152
A430006M23R	2.07052985
D930046M13F	2.07052985
GNG2	2.07052985
GPR68	2.07052985
H2-Q8	2.07052985
IFI30	2.07052985
ZFP608	2.07052985
DCI	2.05622765
NFKB1	2.05622765
PIM3	2.05622765
SGK	2.05622765
CCNG1	2.04202425
CYP51	2.04202425
LOC385953	2.04202425
EGR1	2.02791896
HHEX	2.02791896

MYO1E	2.02791896
TMEM126A	2.02791896
NCF4	2.0139111
PDLIM7	2.0139111
CXCL9	2
GPR18	2
MVP	2
PRSS19	2
A130038J17R1	-2.0139111
A130093I21R1	-2.0139111
EPHX1	-2.0139111
NOTCH3	-2.0139111
MTF2	-2.02791896
TNFRSF7	-2.02791896
4932414K18R	-2.04202425
GFI1	-2.04202425
2410008J05R1	-2.05622765
2610019F03R1	-2.07052985
H2-OB	-2.07052985
SATB1	-2.07052985
TCF7	-2.07052985
2900060B14R	-2.08493152
TBXA2R	-2.08493152
NISCH	-2.09943337
LOC434197	-2.11403608
PARD6G	-2.11403608
DPP4	-2.14354693
H2-AB1	-2.14354693
LMAN2L	-2.14354693
BRD3	-2.15845647
CD27	-2.15845647
LOC386192	-2.15845647
H2-EB1	-2.17346973
NCK2	-2.17346973

RAMP1	-2.17346973
1110046J11RI	-2.1885874
AQP11	-2.23457428
SLA	-2.23457428
MARCKS	-2.25011697
IGH-6	-2.26576777
SH2D1A	-2.26576777
F730003H07R	-2.29739671
H2-T10	-2.29739671
DGKA	-2.31337637
DNTT	-2.31337637
ETS1	-2.32946717
LOC268393	-2.32946717
LOC386360	-2.32946717
TMEM108	-2.32946717
C230098O21R	-2.36198532
RNPEPL1	-2.36198532
G22P1	-2.37841423
TRBV31_X032	-2.37841423
ALDH2	-2.42838977
CDCA7	-2.46228883
NRP	-2.46228883
TXNIP	-2.46228883
SLC16A5	-2.4966611
ACAS2L	-2.51402675
FRAT2	-2.54912125
CD81	-2.63901582
PRKCB	-2.65737163
PDLIM4	-2.67585511
H2-BL	-2.71320865
PP11R	-2.73208051
ACTN1	-2.75108364
CD6	-2.75108364
CD2	-2.78948733

ST6GAL1	-2.80888975
TRBV1_AE000	-2.80888975
CD8B	-2.84810039
9430068D06R	-2.8679105
AI132321	-3.07375036
H19	-3.16016525
LY6D	-3.38698125
CTSE	-3.50642289
BCL11B	-3.58010028
LOC382896	-4.59479342
COX6A2	-6.27667278

Table 3. Comparison of gene expression profiles of ITNK, DN3 and LAK cells in microarray analysis.

ITNKs vs. DN3

Column ID	p-value (iTNK vs. DN3)	Ratio (iTNK vs. DN3)	Fold-Change (iTNK vs. DN3)
FCER1G	1.61E-08	38.85427	38.8542
ROG	3.56E-09	38.51902	38.519
UPP1	1.59E-11	27.95436	27.9543
IFITM1	3.53E-06	27.42649	27.4265
XCL1	1.21E-06	25.36912	25.3691
SERPINA3G	7.75E-08	21.14876	21.1487
SCIN	1.90E-08	20.78544	20.7854
NKG7	1.76E-08	20.18204	20.182
AQP9	1.71E-07	18.25221	18.2522
KLRD1	7.30E-09	17.17812	17.1781
LGALS3	7.17E-09	15.91703	15.917
AVIL	9.13E-07	13.61854	13.6185
IFITM3	1.54E-07	13.57143	13.5714
TYROBP	1.57E-09	13.52446	13.5245
GADD45G	4.52E-08	13.52446	13.5245
CD160	3.07E-07	12.64066	12.6407
IFITM2	4.83E-06	11.27457	11.2746
CTSW	3.28E-06	9.798062	9.79809
9130404D14RIK	6.12E-09	9.67998	9.67995
LOC270152	2.41E-07	9.530163	9.53016
BC025206	1.38E-08	9.063061	9.06307
VIM	3.49E-08	8.891971	8.89195
NFIL3	2.83E-06	8.426872	8.42689
AMICA1	9.38E-08	8.267811	8.26778
LTA	1.13E-11	8.210653	8.21067
GLRX1	2.07E-06	8.027744	8.02777
LITAF	1.96E-07	7.727498	7.72749
CCR5	6.07E-09	7.323325	7.32333
LMNA	5.83E-08	7.235052	7.23503
BC049975	2.32E-08	6.98856	6.98858
P2RY14	1.44E-07	6.797496	6.79748
WBSCR5	8.76E-08	6.486767	6.48677

LAKs vs. DN3

Column ID	p-value(LAK vs. DN3)	Ratio (LAK vs. DN3)	Fold-Change (LAK vs. DN3)
GZMD	2.97E-07	79.34115	79.3413
FCER1G	8.83E-09	50.30055	50.3005
ROG	3.50E-09	38.7869	38.787
CCL4	4.38E-08	38.5859	38.5858
KLRE1	6.58E-11	35.19986	35.1999
MT1	1.56E-07	35.01744	35.0174
SPP1	2.96E-08	32.50299	32.503
AVIL	8.90E-08	30.64326	30.6433
TYROBP	1.95E-10	26.86208	26.8621
GZME	6.58E-10	26.17287	26.1729
XCL1	1.12E-06	26.12753	26.1276
ASB2	4.61E-10	25.81251	25.8125
KLRA7	9.89E-11	22.70596	22.706
PRF1	9.89E-08	22.23868	22.2387
KLRD1	4.72E-09	19.83533	19.8353
LGALS3	4.28E-09	18.79791	18.7979
GZMG	6.92E-08	18.06342	18.0634
KLRA18	6.87E-08	16.67945	16.6795
SERPINA3	1.62E-07	16.50693	16.5069
NKG7	3.26E-08	16.47835	16.4784
LTB4R1	3.28E-07	16.13924	16.1392
GADD45G	2.57E-08	16.0834	16.0834
CTSG	5.88E-06	15.94464	15.9446
CCL3	2.43E-07	15.56248	15.5625
NFIL3	3.46E-07	15.34823	15.3482
AQP9	3.11E-07	15.03237	15.0324
1300002F1	2.22E-07	14.44502	14.445
KLRA4	9.74E-08	14.24615	14.2461
LITAF	2.42E-08	13.45435	13.4543
KLRA3	5.93E-09	13.26911	13.2691
LRRK1	1.90E-09	13.22321	13.2232
KLRG1	1.44E-07	13.20031	13.2003

LAG3	8.41E-08	6.190264	6.19026	EMILIN2	5.64E-06	12.83934	12.8393
LY6A	1.40E-05	5.989781	5.98977	1110007C0	3.19E-11	12.77278	12.7728
E030006K04RIK	6.54E-09	5.94838	5.94839	TNFRSF11	5.09E-06	12.77278	12.7728
9130211I03RIK	4.39E-06	5.876684	5.87667	LOC38114C	1.29E-08	12.46664	12.4666
1300002F13RIK	7.18E-06	5.866513	5.8665	HAVCR2	4.62E-07	12.02112	12.0211
LOC381140	2.90E-07	5.84621	5.8462	LOC32795	1.39E-07	12.00031	12.0003
GPR114	2.07E-05	5.785731	5.78573	PDGFA	2.78E-09	11.91742	11.9174
2310067E08RIK	3.25E-07	5.725901	5.72589	SCIN	1.18E-07	11.733	11.733
CDKN2B	6.18E-06	5.686341	5.68634	BC049975	2.96E-09	11.65196	11.652
IDB2	1.14E-08	5.637296	5.63728	PGLYRP1	1.73E-07	11.51147	11.5115
GOLPH2	4.35E-09	5.608053	5.60805	IFITM1	4.19E-05	11.47164	11.4716
PLCG2	2.95E-09	5.550036	5.55005	SPEER3	4.84E-05	10.74058	10.7406
1500031H04RIK	1.83E-07	5.492634	5.49264	1810044J0	3.59E-09	10.68489	10.6849
1110018K11RIK	7.30E-10	5.388947	5.38893	CCR5	1.38E-09	10.51954	10.5195
CD9	9.16E-09	5.388947	5.38893	WBSCR5	1.21E-08	10.42879	10.4288
LOC381319	6.47E-06	5.323963	5.32396	DAF1	3.14E-07	10.33882	10.3388
SYTL2	3.83E-10	5.250667	5.25066	2210411K1	1.18E-07	10.09102	10.091
SLC2A6	1.27E-07	5.223432	5.22344	P2RY14	3.12E-08	9.815084	9.81508
OSBPL3	3.09E-11	5.187368	5.18736	BCL2A1B	2.31E-08	9.781099	9.78112
2210411K11RIK	2.39E-06	5.080604	5.0806	F2R	5.12E-07	9.713547	9.71356
LRRK1	1.15E-07	5.045511	5.04551	LOC26828	1.40E-08	9.67998	9.67995
S100A6	3.80E-07	4.967438	4.96743	RGS1	1.42E-06	9.546722	9.54669
KLRE1	8.01E-08	4.933107	4.93312	2310057H1	5.56E-09	9.30172	9.30174
PGLYRP1	6.39E-06	4.933107	4.93312	BHLHB2	2.26E-07	9.30172	9.30174
GLRX	6.59E-06	4.873651	4.87364	CTSW	4.35E-06	9.078777	9.07879
MYO1F	8.46E-09	4.839967	4.83998	5330403J1	6.45E-09	9.063061	9.06307
LOC269941	9.61E-10	4.831595	4.8316	SH2D1B1	3.54E-07	8.891971	8.89195
TRAF1	1.82E-06	4.699469	4.69948	PLSCR1	1.15E-10	8.861163	8.86119
EMILIN2	0.000282473	4.691334	4.69134	1110018K1	7.85E-11	8.693913	8.69388
TNFRSF9	1.19E-07	4.675104	4.67511	ICSBP1	4.16E-07	8.589073	8.58906
CD52	9.20E-05	4.618746	4.61874	SPEER1-P	0.0001	8.296483	8.29648
PLSCR1	2.75E-09	4.602759	4.60276	RGS16	6.08E-08	8.224902	8.22491
BHLHB2	5.80E-06	4.570969	4.57097	EG433016	0.000987	8.210653	8.21067
S100A1	8.07E-08	4.555145	4.55515	DHRS6	2.02E-06	8.196453	8.19646
LGALS1	4.96E-07	4.5237	4.52369	2310067E0	7.56E-08	7.889858	7.88986
2310046K01RIK	3.01E-06	4.469154	4.46915	KLRA13	3.45E-10	7.876186	7.8762
CAPG	5.03E-09	4.453688	4.45369	TNFSF6	7.56E-09	7.700779	7.70076

C330008K14RIK	4.31E-07	4.430601	4.43059	CCL5	0.000148	7.387052	7.38706
TNFRSF11B	0.000351472	4.384773	4.38477	E030006KC	2.60E-09	7.235052	7.23503
CCL4	8.44E-05	4.362031	4.36203	CAR2	7.88E-11	6.904313	6.90432
SIAT10	6.50E-06	4.339411	4.33941	SERPINE2	1.33E-06	6.904313	6.90432
HBA-A1	1.28E-06	4.301982	4.30198	IER3	7.22E-06	6.844768	6.84476
ROM1	1.73E-08	4.272263	4.27226	TNFRSF9	1.74E-08	6.832888	6.83291
1190002C06RIK	2.57E-07	4.198876	4.19887	SIAT10	6.93E-07	6.797496	6.79748
F2R	2.39E-05	4.184346	4.18434	GLRX1	4.58E-06	6.646064	6.64606
RGS1	5.76E-05	4.184346	4.18434	DAPK2	7.72E-10	6.611614	6.6116
CD69	2.26E-05	4.177092	4.17709	F2RL2	5.36E-06	6.554583	6.55456
CISH	1.63E-06	4.15543	4.15544	IFITM3	2.68E-06	6.464333	6.46433
DAPK2	9.71E-09	4.133888	4.13389	MLKL	5.34E-09	6.309387	6.30939
SH3BP2	3.58E-08	4.098226	4.09823	SYTL2	1.70E-10	6.147491	6.1475
GCNT1	2.49E-08	4.069921	4.06992	TMEM119	0.000651	6.136852	6.13686
HAVCR2	5.18E-05	4.062877	4.06287	2810025M1	1.47E-08	6.041894	6.04189
DUSP6	3.27E-09	4.041808	4.04181	SEPN1	8.40E-07	6.041894	6.04189
CTNNA1	4.08E-08	3.993068	3.99307	TCRD-V1	7.87E-09	6.010555	6.01056
BC024955	6.91E-10	3.917682	3.91768	OSBPL3	1.46E-11	5.989781	5.98977
ITGB7	0.000152314	3.917682	3.91768	APOB48R	3.32E-07	5.989781	5.98977
MLKL	7.92E-08	3.877156	3.87716	CD52	2.73E-05	5.979395	5.9794
SERPINE2	2.49E-05	3.870448	3.87045	MYO1F	2.88E-09	5.938101	5.93809
LY6G5B	7.00E-06	3.863749	3.86375	SH3BP2	4.75E-09	5.897061	5.89708
PPP3CC	5.92E-09	3.850374	3.85038	RASD2	1.15E-06	5.856344	5.85634
LOC218482	1.61E-08	3.837063	3.83706	LOC26994	3.60E-10	5.805819	5.80582
A430006M23RIK	3.38E-06	3.777676	3.77768	IFITM2	6.30E-05	5.805819	5.80582
2410008K03RIK	3.43E-08	3.732137	3.73213	GPR87	1.21E-06	5.775706	5.77572
FURIN	1.27E-06	3.732137	3.73213	LOC27015	2.10E-06	5.745773	5.74577
F2RL2	9.14E-05	3.732137	3.73213	HIST1H1C	2.95E-05	5.715984	5.71598
GPR18	2.97E-06	3.712779	3.71278	AA467197	3.72E-05	5.706069	5.70608
HGFAC	7.05E-05	3.706353	3.70635	KLRA1	3.83E-07	5.637296	5.63728
S100A10	4.21E-06	3.693526	3.69353	IDB2	1.24E-08	5.550036	5.55005
APOB48R	4.85E-06	3.680747	3.68075	LY6A	2.01E-05	5.540442	5.54044
OSM	1.62E-05	3.680747	3.68075	FCGR3	2.61E-07	5.511707	5.51171
AIM1L	2.96E-06	3.674377	3.67438	GVIN1	3.28E-05	5.511707	5.51171
IL18R1	3.56E-07	3.661662	3.66167	A430038C1	2.04E-08	5.426407	5.42642
NT5E	2.59E-08	3.655331	3.65533	ID2	4.68E-09	5.379612	5.3796
IFNG	3.30E-06	3.636377	3.63637	S100A1	3.25E-08	5.379612	5.3796

H2-Q8	0.000127421	3.63008	3.63008	CAPG	1.77E-09	5.370281	5.37029
FXYD4	1.04E-07	3.617513	3.61752	PPP3CC	8.68E-10	5.333191	5.33319
PILRB	3.51E-05	3.592535	3.59253	1500031H0	2.19E-07	5.305546	5.30554
PLP2	3.87E-08	3.580098	3.5801	PLCG2	3.91E-09	5.259781	5.25977
MT1	0.000577989	3.580098	3.5801	NCF4	1.99E-07	5.241585	5.24157
DOK2	7.55E-08	3.567708	3.56771	AI115600	1.22E-09	5.142604	5.14261
0610037M15RIK	7.75E-06	3.549221	3.54922	DUSP6	8.20E-10	5.115953	5.11594
2310047C17RIK	4.43E-05	3.549221	3.54922	SERPINB6	9.97E-06	5.098243	5.09824
S100A11	2.00E-07	3.530812	3.53081	BCL2A1D	1.37E-08	4.899055	4.89904
FES	1.98E-08	3.518599	3.5186	UPP1	1.21E-08	4.856774	4.85678
BC029169	3.49E-07	3.500347	3.50035	PIM3	1.14E-06	4.856774	4.85678
TNF	5.66E-10	3.482197	3.4822	AMICA1	1.15E-06	4.848367	4.84837
LRP12	7.21E-05	3.482197	3.4822	SLC2A3	4.16E-06	4.814891	4.81488
IER3	0.000215344	3.476169	3.47617	5031436OC	2.13E-06	4.773338	4.77334
NAPSA	2.95E-05	3.47015	3.47015	CD160	1.84E-05	4.73216	4.73216
ANXA2	3.41E-06	3.434266	3.43426	A430084PC	2.72E-07	4.691334	4.69134
PRSS19	1.77E-05	3.428321	3.42832	GOLPH2	1.25E-08	4.618746	4.61874
OSTF1	5.84E-09	3.38112	3.38112	CD244	8.49E-09	4.618746	4.61874
GVIN1	0.000422456	3.36942	3.36942	DMWD	1.23E-06	4.578901	4.5789
1110007C02RIK	2.44E-08	3.340348	3.34035	AHNAK	1.67E-08	4.570969	4.57097
MAPKAPK3	1.77E-07	3.311532	3.31153	TRAF1	2.12E-06	4.570969	4.57097
CD244	7.87E-08	3.277281	3.27728	TES	1.82E-08	4.555145	4.55515
F630022B06RIK	4.89E-06	3.271609	3.27161	CDKN2B	1.88E-05	4.555145	4.55515
ID2	1.03E-07	3.265946	3.26594	1110004P1	6.74E-06	4.555145	4.55515
GPR68	6.05E-06	3.265946	3.26594	SRGAP2	1.33E-08	4.508038	4.50804
GLIPR1	4.48E-07	3.260292	3.26029	SULF2	3.60E-09	4.469154	4.46915
PDGFA	1.76E-06	3.254647	3.25464	HHEX	1.23E-08	4.384773	4.38477
PKP3	1.71E-08	3.254647	3.25464	LAG3	5.75E-07	4.301982	4.30198
D10BWG1379E	5.49E-08	3.254647	3.25464	ALDOA	1.30E-05	4.220745	4.22075
SLC39A4	4.73E-08	3.215403	3.2154	AI850995	5.34E-08	4.213436	4.21344
TES	1.92E-07	3.182149	3.18215	PTER	3.14E-06	4.206152	4.20615
EGR1	0.0012963	3.182149	3.18215	LOC21848	9.08E-09	4.198876	4.19887
1110004P15RIK	5.91E-05	3.17664	3.17664	1190002C0	2.68E-07	4.169864	4.16986
B4GALNT4	4.86E-07	3.149229	3.14923	CTNNA1	3.18E-08	4.15543	4.15544
CDKN1A	0.000553492	3.149229	3.14923	CDKN1A	0.000117	4.141061	4.14106
D2ERTD217E	7.91E-08	3.079083	3.07908	2310016C1	9.43E-06	4.12674	4.12673
NCF4	5.37E-06	3.073755	3.07375	A530050EC	2.79E-07	4.08405	4.08405

LOC381924	1.33E-06	3.047229	3.04723	LMNA	1.14E-06	4.062877	4.06287
1700025G04RIK	2.02E-06	3.041955	3.04196	GLIPR1	1.07E-07	4.034812	4.03481
AA467197	0.00100238	3.036689	3.03669	9830144J0	4.06E-09	4.020844	4.02085
SGK	5.37E-08	3.020947	3.02095	PPAP2C	3.54E-07	3.958624	3.95863
BC021614	5.58E-05	3.015718	3.01571	SAT1	1.91E-05	3.958624	3.95863
LOC385953	1.27E-10	3.005277	3.00528	SLC2A1	5.83E-05	3.958624	3.95863
CDKN2A	8.87E-06	2.989698	2.9897	HAK	4.36E-08	3.938093	3.9381
2610009E16RIK	2.28E-05	2.953651	2.95365	SCL00031E	6.01E-07	3.917682	3.91768
HIST1H1C	0.00103646	2.928172	2.92817	2310046K0	7.02E-06	3.863749	3.86375
DCI	1.02E-08	2.912989	2.91299	RHOF	3.34E-07	3.843715	3.84371
NFKB1	1.21E-07	2.902909	2.90291	LOC21239E	4.55E-08	3.823785	3.82378
TPST2	2.16E-06	2.902909	2.90291	CD69	3.83E-05	3.810554	3.81055
TRF	2.76E-06	2.897887	2.89788	B230343A1	1.49E-08	3.803959	3.80395
HK2	3.64E-06	2.887861	2.88786	BC022224	7.94E-08	3.777676	3.77768
PDZK1	5.44E-10	2.882858	2.88286	KLRB1C	9.87E-09	3.745094	3.74509
GNG2	6.86E-09	2.872886	2.87288	MYO1E	8.79E-09	3.719214	3.71922
S100A4	8.62E-08	2.848102	2.8481	KLRA33	3.61E-06	3.693526	3.69353
ZFP608	8.21E-08	2.838248	2.83825	WDFY1	5.95E-08	3.680747	3.68075
2210008N01RIK	6.64E-08	2.833335	2.83333	GCNT1	5.12E-08	3.642682	3.64268
SH3BGR13	4.55E-05	2.82843	2.82843	C80638	3.80E-05	3.642682	3.64268
MYO1G	2.01E-06	2.823527	2.82353	HGFAC	7.89E-05	3.636377	3.63637
1110019C08RIK	1.34E-05	2.81864	2.81864	RASL12	4.28E-07	3.611256	3.61125
S100A13	8.29E-05	2.81864	2.81864	GNG2	1.28E-09	3.580098	3.5801
PPAP2C	3.95E-06	2.813763	2.81376	SH2D2A	1.04E-06	3.567708	3.56771
MYO1E	7.25E-08	2.808886	2.80889	GPR141	1.94E-05	3.567708	3.56771
IFI30	1.07E-06	2.799168	2.79917	DCI	2.41E-09	3.518599	3.5186
LTB4R1	0.000868775	2.784654	2.78466	GLRX	4.20E-05	3.518599	3.5186
TMEM126A	3.48E-08	2.775026	2.77502	LOC38569E	9.48E-07	3.512506	3.5125
1110020C13RIK	7.24E-08	2.775026	2.77502	CD72	8.84E-05	3.488246	3.48824
CD7	7.40E-06	2.775026	2.77502	EGR1	0.000779	3.488246	3.48824
4933439K08RIK	1.06E-08	2.751085	2.75108	2210008N0	1.43E-08	3.458149	3.45815
E030003N15RIK	2.16E-05	2.732084	2.73208	ADORA2B	6.64E-07	3.446184	3.44618
CCL5	0.0117888	2.732084	2.73208	KLRA10	4.19E-08	3.434266	3.43426
7420404O03RIK	1.10E-05	2.722629	2.72263	S100A11	2.42E-07	3.434266	3.43426
4930486L24RIK	1.95E-06	2.717916	2.71791	F730045P1	3.27E-05	3.434266	3.43426
BC022224	9.36E-07	2.713211	2.71321	PILRB	4.70E-05	3.428321	3.42832
5330403J18RIK	5.98E-06	2.708508	2.70851	LGALS1	2.90E-06	3.404638	3.40463

FXYD5	4.01E-06	2.703821	2.70382	S100A10	7.33E-06	3.392855	3.39286
A430038C16RIK	2.01E-06	2.699143	2.69914	NQO2	4.88E-08	3.386983	3.38698
GPC1	0.00472373	2.675857	2.67586	CD9	1.56E-07	3.38112	3.38112
AHNAK	7.45E-07	2.666596	2.6666	PLP2	5.92E-08	3.36942	3.36942
EMP1	0.000268268	2.666596	2.6666	SLC39A4	3.49E-08	3.351948	3.35195
CX3CR1	3.25E-09	2.661982	2.66198	7420404OC	2.40E-06	3.334567	3.33457
2810032E02RIK	4.29E-07	2.661982	2.66198	NEDD9	3.25E-07	3.311532	3.31153
LOC327957	0.000272484	2.657369	2.65737	BSPRY	1.11E-06	3.288662	3.28866
FCGR3	3.00E-05	2.625333	2.62533	STX11	2.41E-06	3.288662	3.28866
CLNK	1.01E-08	2.620785	2.62079	NFKBIZ	5.41E-07	3.277281	3.27728
HVCN1	0.000222656	2.620785	2.62079	ADAM8	1.09E-06	3.277281	3.27728
BSCL2	5.79E-06	2.616246	2.61625	PPP1R3B	1.39E-06	3.277281	3.27728
LGALS3BP	6.49E-06	2.616246	2.61625	SEC61B	1.17E-10	3.265946	3.26594
CYP51	7.38E-07	2.607195	2.6072	S100A6	4.92E-06	3.265946	3.26594
PIM3	6.98E-05	2.593677	2.59368	ANXA2	4.93E-06	3.254647	3.25464
BC038881	7.63E-09	2.584707	2.58471	HK2	1.70E-06	3.193195	3.19319
LOC383981	0.00132323	2.584707	2.58471	PDLIM7	9.37E-08	3.187668	3.18766
PDLIM7	5.33E-07	2.580232	2.58023	TRIO	4.54E-07	3.17664	3.17664
SLC24A3	6.09E-05	2.580232	2.58023	ENO1	2.54E-07	3.160167	3.16017
HHEX	5.95E-07	2.575766	2.57576	LOC38398	0.000359	3.154694	3.15469
D930046M13RIK	1.74E-05	2.575766	2.57576	N4WBP5-P	5.19E-09	3.149229	3.14923
BC087945	7.68E-07	2.571302	2.5713	LOC32870	2.98E-07	3.143784	3.14378
9830144J08RIK	1.24E-07	2.566854	2.56685	HIC1	5.07E-06	3.116663	3.11666
DP1	1.29E-06	2.566854	2.56685	AOAH	2.89E-09	3.111262	3.11126
E130012A19RIK	1.31E-05	2.562407	2.56241	1110020C1	2.86E-08	3.111262	3.11126
4631423F02RIK	7.66E-05	2.540302	2.5403	MAPKAPK	2.85E-07	3.105879	3.10588
4930555L03RIK	4.40E-08	2.535902	2.5359	FTL1	8.72E-06	3.095132	3.09513
FOSL2	6.92E-06	2.535902	2.5359	BC046404	6.62E-07	3.079083	3.07908
ZFP296	2.68E-09	2.518384	2.51839	E030003N1	8.70E-06	3.079083	3.07908
F730045P10RIK	0.000293728	2.518384	2.51839	VIM	1.02E-05	3.068426	3.06843
PEA15	5.59E-08	2.509675	2.50967	CISH	1.19E-05	3.068426	3.06843
ITGAE	0.000534865	2.50533	2.50533	C230043G	1.82E-07	3.052522	3.05252
A530050E01RIK	1.01E-05	2.50533	2.50533	GPR97	4.15E-06	3.041955	3.04196
SCL0001419.1_32	1.67E-07	2.500994	2.50099	LASP1	1.17E-07	3.036689	3.03669
SPP1	0.00129868	2.496661	2.49666	9930117H0	6.85E-06	3.036689	3.03669
ASB2	2.54E-05	2.492336	2.49234	CASP1	0.000297	3.000075	3.00008
CCNG1	4.25E-05	2.492336	2.49234	D10ERTD4	3.40E-07	2.979356	2.97935

TUBA6	1.47E-06	2.483713	2.48372
SDF2L1	7.56E-05	2.483713	2.48372
RHOF	9.16E-06	2.479415	2.47942
1110030J09RIK	2.72E-10	2.458023	2.45803
EGR3	0.00128127	2.458023	2.45803
CXCR3	5.82E-05	2.453771	2.45377
ALDOA	0.000483723	2.449521	2.44952
GCNT2	3.22E-08	2.445281	2.44528
MVP	4.37E-07	2.445281	2.44528
C130027E04RIK	5.53E-07	2.445281	2.44528
SEC61B	1.47E-09	2.436819	2.43682
E430036I04RIK	2.87E-07	2.432599	2.4326
AI481100	9.30E-05	2.424184	2.42419
CD63	0.000436295	2.419989	2.41999
DEGS	4.85E-07	2.415797	2.4158
LOC385699	1.78E-05	2.415797	2.4158
EG331493	3.45E-06	2.415797	2.4158
A930008A22RIK	6.04E-07	2.411614	2.41162
4930504E06RIK	0.000436715	2.411614	2.41162
LOC212399	1.73E-06	2.40744	2.40744
AI850995	3.62E-06	2.40744	2.40744
CTGF	0.000743838	2.40744	2.40744
KIRL2	3.13E-06	2.394957	2.39496
1700017I11RIK	6.32E-08	2.390812	2.39081
2310037P21RIK	2.51E-06	2.386669	2.38667
UAP1L1	3.29E-06	2.382541	2.38254
D14ERTD449E	0.000867516	2.382541	2.38254
BC023892	4.42E-09	2.378415	2.37841
AA175286	0.000409847	2.361983	2.36199
PPIB	5.05E-09	2.357896	2.3579
GPR34	1.68E-07	2.357896	2.3579
IRAK2	7.34E-05	2.357896	2.3579
SH2D1B1	0.000605208	2.353811	2.35381
HSD11B1	6.66E-05	2.353811	2.35381
LOC328703	3.58E-06	2.34974	2.34974
BC004728	5.49E-07	2.34974	2.34974
LOC215405	4.47E-05	2.34974	2.34974

TBC1D2B	7.23E-09	2.974199	2.9742
1700129I1E	2.83E-05	2.963903	2.96391
NDFIP1	1.87E-07	2.958772	2.95878
5730469M1	9.16E-05	2.958772	2.95878
JUNB	0.000169	2.958772	2.95878
PGK1	2.49E-06	2.953651	2.95365
LOC24067A	1.77E-07	2.948539	2.94854
BSCL2	2.21E-06	2.943436	2.94343
IFNG	1.45E-05	2.938333	2.93834
S100A13	6.20E-05	2.933248	2.93325
CHN2	1.49E-07	2.928172	2.92817
CST7	1.31E-07	2.923105	2.9231
POLD4	1.30E-05	2.912989	2.91299
BC087945	2.69E-07	2.907949	2.90794
4631423F0	2.76E-05	2.892866	2.89287
2310061N2	0.002866	2.872886	2.87288
GIPC2	3.20E-05	2.862942	2.86295
AA175286	9.62E-05	2.848102	2.8481
TUBA6	4.58E-07	2.838248	2.83825
KLRB1D	7.14E-11	2.833335	2.83333
HRMT1L1	2.71E-07	2.833335	2.83333
TMEM126A	2.96E-08	2.82843	2.82843
TRF	3.44E-06	2.81864	2.81864
LOC38318E	2.82E-08	2.813763	2.81376
AW536289	4.33E-07	2.813763	2.81376
CCNG1	1.58E-05	2.813763	2.81376
HAAO	5.90E-06	2.799168	2.79917
6720467C0	2.29E-11	2.794326	2.79433
SLC24A3	3.28E-05	2.789486	2.78949
PSTPIP1	5.32E-06	2.775026	2.77502
TBX21	4.36E-06	2.765426	2.76542
PRDX5	7.28E-05	2.765426	2.76542
EGR3	0.000564	2.760631	2.76063
TFF1	0.008643	2.760631	2.76063
E130012A1	7.32E-06	2.746317	2.74632
BCAP29	8.13E-06	2.746317	2.74632
IRAK2	2.06E-05	2.741566	2.74157

RAB3D	1.16E-05	2.337552	2.33755	2310016C0	0.000898	2.741566	2.74157
SULT2B1	0.000164735	2.337552	2.33755	E430036I0	9.77E-08	2.736817	2.73682
EVI2A	2.55E-07	2.33351	2.33351	FES	1.41E-07	2.732084	2.73208
TSPO	2.22E-06	2.33351	2.33351	C330023F1	1.27E-07	2.717916	2.71791
TNFRSF18	2.31E-05	2.33351	2.33351	FKBP11	0.000164	2.713211	2.71321
EG630499	0.000147665	2.329466	2.32947	GP49A	8.69E-07	2.708508	2.70851
SERPINB6A	0.00133703	2.325435	2.32543	FHL2	3.43E-08	2.703821	2.70382
SYPL	6.57E-07	2.321408	2.32141	PRMT2	5.08E-07	2.694466	2.69447
8030402P03RIK	0.000483123	2.321408	2.32141	3300005D0	5.96E-05	2.685148	2.68514
HAAO	3.04E-05	2.31739	2.31739	RPS6KA1	5.06E-08	2.666596	2.6666
NRGN	5.54E-05	2.313374	2.31338	GPD2	2.77E-08	2.661982	2.66198
TAF9B	1.33E-06	2.309373	2.30937	SNAG1	8.24E-08	2.661982	2.66198
9930117H01RIK	6.56E-05	2.309373	2.30937	CLN3	2.04E-05	2.652773	2.65277
GBP2	0.000466109	2.309373	2.30937	TMPIT	4.29E-07	2.648179	2.64818
AW212394	7.13E-06	2.305375	2.30537	1810011E0	4.07E-06	2.648179	2.64818
KIT	0.000138895	2.301379	2.30138	BIN1	6.15E-08	2.643593	2.64359
A630086H07RIK	3.07E-05	2.297398	2.2974	PEA15	3.62E-08	2.629883	2.62989
ANK	1.14E-07	2.29342	2.29342	SDF2L1	4.71E-05	2.629883	2.62989
BATF	6.24E-06	2.29342	2.29342	LOC38309	3.70E-05	2.629883	2.62989
TIAM1	1.13E-07	2.289451	2.28945	4930486L2	2.78E-06	2.607195	2.6072
TCRD-V1	6.14E-06	2.285484	2.28548	CAMK2N1	2.06E-06	2.602682	2.60268
ARL6IP5	2.09E-07	2.285484	2.28548	IFI30	2.03E-06	2.598179	2.59818
EHD4	3.43E-05	2.285484	2.28548	4930513E2	0.000993	2.593677	2.59368
N4WBP5-PENDING	9.39E-08	2.281527	2.28153	0610037M1	7.56E-05	2.589191	2.58919
B3GNT8	1.44E-07	2.281527	2.28153	PFKP	1.61E-05	2.584707	2.58471
BLR1	8.56E-06	2.281527	2.28153	A630024B1	2.56E-06	2.580232	2.58023
NDFIP1	2.11E-06	2.261845	2.26184	SPIN2	4.24E-07	2.575766	2.57576
PRDX4	1.09E-05	2.261845	2.26184	MMD	1.33E-06	2.575766	2.57576
SNAG1	4.20E-07	2.250119	2.25012	MGC18837	1.51E-06	2.562407	2.56241
B4GALNT2	0.000956597	2.250119	2.25012	C130027E0	3.69E-07	2.553541	2.55354
TRPM6	9.96E-08	2.238448	2.23845	IL18R1	5.54E-06	2.553541	2.55354
CXCL9	0.00820156	2.230704	2.23071	GALGT1	1.55E-05	2.553541	2.55354
0610009O03RIK	8.23E-09	2.222988	2.22299	STK39	3.36E-08	2.549122	2.54912
PRR7	1.26E-06	2.207632	2.20763	OBFC2A	8.44E-06	2.549122	2.54912
A630077B13RIK	3.14E-05	2.207632	2.20763	D930046M	1.92E-05	2.544711	2.54471
SLC19A2	4.63E-05	2.207632	2.20763	ALDOC	0.001341	2.544711	2.54471
2810440J20RIK	7.67E-07	2.192381	2.19238	IL2RB	4.01E-07	2.540302	2.5403

MED10	3.04E-06	2.192381	2.19238
COMT	8.15E-09	2.188586	2.18859
PLTP	6.19E-07	2.188586	2.18859
2310010I15RIK	1.21E-08	2.181016	2.18102
0610039P13RIK	0.000646447	2.181016	2.18102
VPS29	1.09E-07	2.17724	2.17724
AI847670	1.60E-06	2.165951	2.16595
ASAH1	3.80E-08	2.1622	2.1622
B830021E24RIK	1.42E-05	2.1622	2.1622
SRGAP2	4.27E-06	2.158457	2.15846
IQGAP2	0.000141764	2.158457	2.15846
LASP1	2.73E-06	2.154717	2.15472
CORO1C	7.53E-07	2.150991	2.15099
H2-Q6	3.02E-06	2.150991	2.15099
9130604K18RIK	4.57E-06	2.147264	2.14726
FNBP1	2.88E-08	2.143549	2.14355
TMPIT	3.47E-06	2.139834	2.13984
H2-Q7	5.84E-05	2.136131	2.13613
0610007H07RIK	2.48E-06	2.132433	2.13243
CCND2	3.28E-06	2.125055	2.12505
SERTAD1	0.000141861	2.121377	2.12138
RAB19	7.99E-06	2.114035	2.11404
BAG3	0.00480518	2.110377	2.11038
VTI1B	1.30E-05	2.106722	2.10672
CAPN2	2.23E-06	2.103076	2.10307
2310057H16RIK	6.11E-05	2.099433	2.09943
STX11	0.000109261	2.095799	2.0958
FTL1	0.00023523	2.095799	2.0958
ARF6	3.80E-07	2.092168	2.09217
2900026A02RIK	2.85E-07	2.088546	2.08855
CSTB	3.81E-05	2.088546	2.08855
LOC383189	5.48E-07	2.084932	2.08493
CCL3	0.00511685	2.084932	2.08493
GLIPR2	6.01E-05	2.084932	2.08493
C330023F11RIK	1.81E-06	2.081321	2.08132
SIRT3	2.69E-06	2.081321	2.08132
CAPNS1	3.44E-08	2.077719	2.07772

LOC381319	0.000587	2.531511	2.53151
BAG3	0.001254	2.531511	2.53151
DOK2	1.17E-06	2.522755	2.52275
UGCG	8.13E-05	2.522755	2.52275
ARRDC4	0.000487	2.518384	2.51839
ATF4	0.002253	2.518384	2.51839
IL12RB1	6.73E-07	2.514028	2.51403
9130211I03	0.000664	2.514028	2.51403
1810061M1	7.55E-08	2.50533	2.50533
KLRA21	1.66E-06	2.500994	2.50099
MVP	3.59E-07	2.496661	2.49666
CYBA	1.03E-06	2.492336	2.49234
BATF	2.83E-06	2.492336	2.49234
NENF	1.16E-05	2.492336	2.49234
TNFSF13	2.10E-08	2.48802	2.48802
EHD4	1.57E-05	2.48802	2.48802
CSDA	3.96E-08	2.479415	2.47942
CRELD2	1.86E-05	2.475125	2.47512
LOC238943	2.92E-06	2.470838	2.47084
1110019C0	3.97E-05	2.470838	2.47084
OSTF1	8.10E-08	2.46656	2.46656
2510048K0	4.28E-07	2.46656	2.46656
1700025GC	1.15E-05	2.46229	2.46229
PADI2	1.20E-08	2.458023	2.45803
A530060O	9.89E-07	2.458023	2.45803
FXVD5	9.20E-06	2.458023	2.45803
MYO1G	6.72E-06	2.453771	2.45377
ECH1	1.99E-05	2.453771	2.45377
GABARAPI	5.14E-09	2.445281	2.44528
AI847670	4.70E-07	2.441049	2.44105
PPIB	3.62E-09	2.436819	2.43682
FOSL2	1.02E-05	2.428393	2.42839
BC023892	3.65E-09	2.424184	2.42419
STX7	1.05E-06	2.424184	2.42419
NUCB1	1.57E-05	2.424184	2.42419
KLF7	1.89E-05	2.424184	2.42419
TAF9B	8.39E-07	2.419989	2.41999

RBMS1	1.72E-07	2.077719	2.07772	LOC38168	4.83E-07	2.419989	2.41999
1110008P14RIK	2.41E-07	2.077719	2.07772	LOC38640	0.004194	2.419989	2.41999
MINA	1.96E-08	2.074121	2.07412	H47	6.51E-07	2.415797	2.4158
CCDC132	2.24E-06	2.074121	2.07412	GPR34	1.34E-07	2.411614	2.41162
LOC234582	1.09E-06	2.066944	2.06695	1110006I15	1.08E-07	2.40744	2.40744
KCTD10	9.73E-05	2.066944	2.06695	MYL6	2.17E-08	2.403274	2.40327
LOC240672	5.49E-06	2.05623	2.05623	SOAT2	1.66E-05	2.403274	2.40327
A230057G18RIK	9.28E-07	2.05623	2.05623	HIP1	1.04E-10	2.399111	2.39911
ELOVL1	3.81E-06	2.05623	2.05623	DEGS	5.19E-07	2.399111	2.39911
STX7	5.97E-06	2.052667	2.05267	2810032E0	1.12E-06	2.399111	2.39911
BC017612	5.16E-06	2.052667	2.05267	SH3BGRL3	0.000169	2.399111	2.39911
ZBTB32	3.61E-05	2.052667	2.05267	DTR	4.75E-06	2.386669	2.38667
H47	3.72E-06	2.049113	2.04911	SLK	1.18E-08	2.382541	2.38254
TNFRSF22	7.52E-05	2.049113	2.04911	EOMES	8.89E-07	2.378415	2.37841
AI115600	1.65E-06	2.045567	2.04557	GMDS	2.61E-06	2.378415	2.37841
MYL6	1.28E-07	2.045567	2.04557	DCXR	3.22E-05	2.370185	2.37019
H2-GS17	0.000428176	2.042025	2.04202	H2-Q8	0.002068	2.370185	2.37019
CAPZB	5.20E-07	2.038491	2.03849	HIP-1	1.62E-10	2.36608	2.36608
SC4MOL	3.38E-06	2.038491	2.03849	DAB2IP	5.55E-08	2.36608	2.36608
FHL2	6.33E-07	2.034961	2.03496	KLRK1	3.04E-08	2.36608	2.36608
3010031K01RIK	4.37E-08	2.034961	2.03496	OLFM1	7.39E-08	2.361983	2.36199
A330042I21RIK	1.18E-06	2.034961	2.03496	CABLES1	2.23E-06	2.361983	2.36199
D15MGI27	2.70E-05	2.034961	2.03496	AI840980	0.000111	2.361983	2.36199
RAB4A	4.71E-08	2.024406	2.02441	BC024955	4.20E-08	2.357896	2.3579
DCXR	0.000151877	2.024406	2.02441	MINA	4.70E-09	2.357896	2.3579
AIM1	0.000114024	2.024406	2.02441	A530090PC	6.45E-06	2.357896	2.3579
SEMA4A	7.97E-05	2.017402	2.0174	NRGN	4.73E-05	2.353811	2.35381
XBP1	0.000154152	2.017402	2.0174	ZFP52	0.000839	2.353811	2.35381
LOC383099	0.000417017	2.013912	2.01391	TSPO	2.07E-06	2.34974	2.34974
JUNB	0.00325781	2.013912	2.01391	TDRD7	2.88E-06	2.345672	2.34567
HRMT1L1	7.88E-06	2.010426	2.01042	TMEM38B	6.08E-08	2.341608	2.34161
GPR97	0.000165473	2.010426	2.01042	SAMSN1	1.16E-06	2.341608	2.34161
COTL1	0.000539041	2.010426	2.01042	IAN4	0.000116	2.341608	2.34161
2310061N23RIK	0.025362	2.006944	2.00694	IMPA2	0.000465	2.337552	2.33755
9130227C08RIK	4.47E-06	2.00347	2.00347	2310056P0	0.000375	2.337552	2.33755
AI840980	0.000521047	2.00347	2.00347	ETFB	8.23E-07	2.33351	2.33351
DYRK3	0.000241993	2.00347	2.00347	GZMK	0.000515	2.321408	2.32141

CASP1	0.00573828	2.00347	2.00347	5730438N1	1.67E-05	2.31739	2.31739
TRBV11_AE000663_T	0.000105474	0.5	-2	LOC215678	4.32E-05	2.313374	2.31338
C920004C08RIK	0.0113298	0.5	-2	LOC269358	1.94E-05	2.309373	2.30937
A930023F05RIK	1.93E-06	0.499134	-2.00347	STK32C	4.69E-07	2.305375	2.30537
PLEKHG2	1.52E-05	0.499134	-2.00347	SLAMF7	1.11E-06	2.305375	2.30537
ABHD8	7.47E-05	0.499134	-2.00347	ABCB1B	1.12E-06	2.301379	2.30138
3110013H01RIK	0.00068445	0.499134	-2.00347	4930539E0	3.24E-05	2.301379	2.30138
E030007N04RIK	3.23E-07	0.496547	-2.01391	CLNK	3.67E-08	2.297398	2.2974
PRKCD	1.24E-06	0.495688	-2.0174	TEX9	1.16E-06	2.297398	2.2974
9130430L19RIK	1.04E-05	0.494829	-2.0209	LOC218617	6.06E-08	2.29342	2.29342
6030443O07RIK	1.78E-05	0.494829	-2.0209	PALD	8.48E-07	2.29342	2.29342
A130062D16RIK	1.86E-06	0.493971	-2.02441	GPR114	0.004116	2.29342	2.29342
5930416I19RIK	2.26E-06	0.493971	-2.02441	GOLGA7	1.77E-06	2.289451	2.28945
FYB	9.40E-06	0.493971	-2.02441	GPR160	5.41E-06	2.289451	2.28945
AA408556	0.000447224	0.49141	-2.03496	KIT	0.000146	2.289451	2.28945
TRBV31_X03277_T_C	0.00870127	0.49141	-2.03496	SQSTM1	0.000722	2.289451	2.28945
A130038J17RIK	8.99E-05	0.490559	-2.03849	KLRA16	3.18E-07	2.285484	2.28548
AJ237586	1.68E-05	0.490559	-2.03849	ZBTB32	1.19E-05	2.285484	2.28548
ZFP260	3.69E-06	0.490559	-2.03849	1110030J08	5.87E-10	2.281527	2.28153
0710008K08RIK	9.80E-06	0.489711	-2.04202	CYP51	2.62E-06	2.281527	2.28153
ANP32E	0.000183335	0.485486	-2.05979	3110054C0	1.87E-06	2.281527	2.28153
4921518A06RIK	8.35E-06	0.484644	-2.06337	C730026J1	4.19E-05	2.269699	2.2697
4933421G18RIK	1.04E-05	0.484644	-2.06337	SERTAD1	7.39E-05	2.269699	2.2697
3110018A08RIK	0.00338526	0.484644	-2.06337	2310004N1	8.08E-05	2.269699	2.2697
C730009F21RIK	1.18E-07	0.483805	-2.06695	VEGFC	1.79E-07	2.265765	2.26577
OLFML3	1.61E-05	0.482132	-2.07412	LOC114607	7.89E-06	2.265765	2.26577
A330103N21RIK	9.39E-05	0.481297	-2.07772	A930008A2	1.15E-06	2.261845	2.26184
H2-T9	0.000542267	0.481297	-2.07772	GFOD1	6.22E-07	2.261845	2.26184
LOC386360	0.00269607	0.481297	-2.07772	STK2	7.89E-09	2.250119	2.25012
ILVBL	4.13E-05	0.478801	-2.08855	BC036961	4.29E-06	2.250119	2.25012
SBK	5.91E-07	0.477973	-2.09217	1810006K2	4.62E-06	2.250119	2.25012
6330403M23RIK	6.88E-08	0.47632	-2.09943	2310047C1	0.001134	2.250119	2.25012
C230075L19RIK	4.42E-07	0.475495	-2.10307	CAI	2.16E-07	2.238448	2.23845
MSH6	0.00037102	0.475495	-2.10307	CAPNS1	1.49E-08	2.234572	2.23457
CXCL12	0.00745872	0.475495	-2.10307	RPL36	3.70E-05	2.234572	2.23457
BC035291	1.11E-05	0.474672	-2.10672	2310043N1	7.41E-05	2.230704	2.23071
MMP2	0.000824671	0.473848	-2.11038	SYPL	1.01E-06	2.226844	2.22684

GM525	0.000141229	0.473028	-2.11404	GZMN	0.002202	2.226844	2.22684
STK4	2.73E-05	0.47221	-2.1177	COMT	6.85E-09	2.222988	2.22299
A130093I21RIK	7.45E-05	0.471391	-2.12138	SCL00041E	1.60E-08	2.222988	2.22299
A230013K13RIK	3.45E-06	0.471391	-2.12138	LOC38212I	0.000239	2.222988	2.22299
0610041G09RIK	0.00831324	0.471391	-2.12138	2610009E1	0.000239	2.21914	2.21914
TRIM28	3.45E-05	0.470577	-2.12505	GPC1	0.01453	2.21914	2.21914
B230342M21RIK	7.67E-06	0.468949	-2.13243	ASAH1	2.95E-08	2.21146	2.21146
1190002H23RIK	5.23E-05	0.464902	-2.15099	HADH2	7.87E-06	2.21146	2.21146
TSPAN32	9.87E-06	0.462492	-2.1622	XDH	1.37E-06	2.207632	2.20763
2610019F03RIK	3.67E-05	0.462492	-2.1622	DP1	5.63E-06	2.203808	2.20381
H2-OB	1.61E-05	0.461691	-2.16595	TGFBR2	3.17E-07	2.199993	2.19999
4732481H14RIK	1.72E-05	0.460891	-2.16971	SC4MOL	1.44E-06	2.199993	2.19999
COL5A1	0.00288136	0.460891	-2.16971	XAB1	1.99E-06	2.199993	2.19999
LDH2	8.49E-05	0.459297	-2.17724	PTPN8	3.84E-06	2.192381	2.19238
6720418B01RIK	7.62E-06	0.458501	-2.18102	DIP3B	3.01E-06	2.184799	2.1848
6430510M02RIK	1.62E-06	0.458501	-2.18102	VTI1B	8.79E-06	2.184799	2.1848
TNFRSF7	0.000102955	0.458501	-2.18102	STK17B	1.46E-05	2.184799	2.1848
CRYL1	8.89E-07	0.458501	-2.18102	GNS	0.000893	2.184799	2.1848
B230345P09RIK	5.94E-05	0.458501	-2.18102	MTMR9	0.001715	2.184799	2.1848
CTLA4	0.000629703	0.456915	-2.18859	ALAD	2.13E-08	2.181016	2.18102
RGL2	2.61E-06	0.455334	-2.19619	ARPC1B	3.71E-07	2.181016	2.18102
1810015C11RIK	3.91E-09	0.452974	-2.20763	2600010E0	1.17E-05	2.181016	2.18102
F730003H07RIK	0.00244488	0.452974	-2.20763	LOC23736	1.67E-05	2.158457	2.15846
CD97	0.000238915	0.45219	-2.21146	MPP6	2.77E-06	2.154717	2.15472
LLGL1	1.90E-06	0.450625	-2.21914	PDCD1LG2	8.02E-06	2.154717	2.15472
LOX	0.000702165	0.450625	-2.21914	SERPINB6	2.58E-05	2.154717	2.15472
PDXP	3.27E-05	0.449845	-2.22299	CAPN2	1.74E-06	2.150991	2.15099
TRIB2	4.12E-06	0.449067	-2.22684	ELOVL1	2.29E-06	2.150991	2.15099
2210008I11RIK	0.000393721	0.449067	-2.22684	RAB3D	2.65E-05	2.150991	2.15099
H2-AB1	0.00426068	0.449067	-2.22684	HINT2	0.00035	2.147264	2.14726
SLC29A1	8.67E-06	0.448288	-2.23071	FIGF	4.55E-05	2.143549	2.14355
ITPR2	5.30E-06	0.446738	-2.23845	OSM	0.000888	2.143549	2.14355
TPST1	9.65E-06	0.445965	-2.24233	ACATE3	1.20E-06	2.139834	2.13984
RPS6KL1	9.39E-07	0.442884	-2.25793	5430427O1	3.35E-06	2.139834	2.13984
RIL-PENDING	1.64E-06	0.441351	-2.26577	EG630499	0.000337	2.128742	2.12874
TTC3	8.83E-09	0.439825	-2.27363	KLK1B11	0.003666	2.128742	2.12874
MAPK1	2.50E-07	0.439063	-2.27758	FNBP1	3.25E-08	2.121377	2.12138

H2-EB1	0.00320736	0.438302	-2.28153	SRI	2.09E-08	2.121377	2.12138
CD3D	0.000186864	0.435275	-2.2974	2610529H0	2.11E-07	2.121377	2.12138
TRBV8_AE000663_T_	0.000766092	0.435275	-2.2974	ANXA5	0.000191	2.121377	2.12138
PPP1R1C	6.89E-07	0.434522	-2.30138	RPIA	2.24E-08	2.114035	2.11404
PITPNM2	5.21E-07	0.432268	-2.31338	LCP1	1.15E-05	2.114035	2.11404
2210419D22RIK	1.12E-07	0.43152	-2.31739	LOC233526	3.13E-05	2.110377	2.11038
RAPGEF3	1.11E-07	0.430773	-2.32141	UGALT2	1.37E-05	2.106722	2.10672
SATB1	5.66E-06	0.427057	-2.34161	ANXA3	0.005884	2.103076	2.10307
C530015C18	9.54E-09	0.426317	-2.34567	JAM4	2.28E-07	2.099433	2.09943
5830496L11RIK	1.02E-06	0.424843	-2.35381	CHST12	6.51E-07	2.099433	2.09943
BCL7A	3.37E-07	0.424843	-2.35381	SCL000126	3.97E-05	2.099433	2.09943
GLDC	0.000448781	0.424106	-2.3579	PYGL	9.38E-05	2.099433	2.09943
CD27	0.000101099	0.423372	-2.36199	MREG	1.19E-07	2.095799	2.0958
A830080H07RIK	1.99E-05	0.423372	-2.36199	1810003N2	2.62E-06	2.095799	2.0958
ART4	9.75E-06	0.42264	-2.36608	HRC	0.000101	2.095799	2.0958
SCL000121.1_106	6.92E-06	0.41972	-2.38254	DDIT4	0.010118	2.092168	2.09217
4932414K18RIK	2.36E-06	0.418994	-2.38667	FBXO4	2.51E-07	2.084932	2.08493
ACVR2B	4.27E-08	0.417544	-2.39496	2010007E0	5.45E-06	2.084932	2.08493
AI481316	4.04E-07	0.417544	-2.39496	ZFP296	2.06E-08	2.081321	2.08132
POU6F1	8.86E-07	0.417544	-2.39496	0610039D0	7.86E-07	2.081321	2.08132
NCK2	0.000270785	0.412509	-2.42419	COTL1	0.000383	2.081321	2.08132
1110046J11RIK	5.70E-05	0.411083	-2.4326	KLRI1	1.30E-08	2.077719	2.07772
ETS2	1.91E-06	0.408243	-2.44952	UBL4	2.81E-07	2.077719	2.07772
FBP1	0.00205479	0.408243	-2.44952	ARHGAP16	3.33E-07	2.077719	2.07772
TPCN1	3.56E-08	0.407536	-2.45377	SNX9	1.75E-07	2.074121	2.07412
TBXA2R	3.11E-06	0.405423	-2.46656	PFN1	3.03E-07	2.074121	2.07412
5430417L22RIK	5.18E-07	0.404021	-2.47512	9130227C0	2.98E-06	2.074121	2.07412
PPARGC1B	1.79E-07	0.404021	-2.47512	DAP	2.54E-05	2.074121	2.07412
TCF7	1.40E-05	0.398459	-2.50967	9030611O1	7.73E-05	2.074121	2.07412
DNTT	0.00027177	0.397768	-2.51403	D8ERTD35	0.000214	2.074121	2.07412
LOC386545	0.00608272	0.394337	-2.5359	2900026A0	3.15E-07	2.070531	2.07053
SOX4	1.85E-07	0.390258	-2.56241	M6PR	1.54E-06	2.070531	2.07053
GPR83	1.40E-05	0.388908	-2.5713	MRPS6	1.82E-05	2.070531	2.07053
HIBADH	2.18E-08	0.387562	-2.58023	0610009OC	1.91E-08	2.066944	2.06695
IGH-6	2.87E-05	0.386221	-2.58919	CAPZB	4.50E-07	2.063366	2.06337
LOC381739	1.61E-06	0.382889	-2.61172	ARRB2	1.28E-06	2.063366	2.06337
DAP3	2.30E-08	0.380904	-2.62533	A430093BC	4.59E-07	2.059796	2.05979

DGKA	8.26E-05	0.378929	-2.63902	NIBAN	3.10E-05	2.059796	2.05979
SNAI3	4.51E-07	0.376964	-2.65277	2610036L1	0.001476	2.059796	2.05979
SLC5A9	2.33E-05	0.376964	-2.65277	DHRS7	1.18E-08	2.05623	2.05623
2410008J05RIK	1.24E-06	0.376312	-2.65737	LOC24162	3.38E-06	2.052667	2.05267
NAV1	2.19E-06	0.376312	-2.65737	COX7A1	0.0006	2.052667	2.05267
HDAC7A	2.22E-06	0.376312	-2.65737	RBMS1	2.03E-07	2.049113	2.04911
A130092J06RIK	6.62E-06	0.37566	-2.66198	CDKN2A	0.000238	2.049113	2.04911
SLA	2.73E-05	0.373065	-2.6805	BB220380	1.50E-07	2.038491	2.03849
MTF2	2.39E-06	0.371131	-2.69447	CMKBR2	3.22E-06	2.038491	2.03849
C230098O21RIK	6.12E-05	0.370488	-2.69914	AW212394	2.59E-05	2.038491	2.03849
GFI1	2.05E-06	0.368567	-2.71321	1110030C2	0.00017	2.034961	2.03496
EPHX1	2.39E-08	0.36793	-2.71791	SCL003196	8.06E-06	2.031434	2.03144
BRD3	2.92E-06	0.36793	-2.71791	LCN4	0.003078	2.031434	2.03144
AQP11	4.62E-07	0.364755	-2.74157	KDELR2	1.28E-06	2.02792	2.02792
IL17RB	2.04E-07	0.362236	-2.76063	CD59A	0.00082	2.024406	2.02441
RAMP1	0.000135079	0.361609	-2.76542	CAPN5	0.001239	2.017402	2.0174
NISCH	3.31E-07	0.361609	-2.76542	ZFP608	2.50E-06	2.013912	2.01391
BGN	0.0025721	0.360982	-2.77022	SLC2A6	0.000147	2.013912	2.01391
TXNIP	0.000742272	0.359733	-2.77984	CORO1C	1.61E-06	2.013912	2.01391
COL6A1	0.00166573	0.35911	-2.78466	GNPDA1	7.70E-07	2.013912	2.01391
CCL9	0.000264226	0.356013	-2.80889	CARD4	8.05E-06	2.010426	2.01042
DPP4	1.63E-06	0.354167	-2.82353	9-Sep	2.79E-06	2.006944	2.00694
MLL	1.54E-07	0.35233	-2.83825	2410012H2	8.81E-07	2.00347	2.00347
C3	0.0001376	0.350503	-2.85304	SKAP2	1.02E-06	2.00347	2.00347
MARCKS	4.55E-06	0.349896	-2.85799	IAN3	0.004387	2.00347	2.00347
TRBV1_AE000663_T_	0.00160689	0.348083	-2.87288	TPI1	0.000372	2.00347	2.00347
3830612M24	2.00E-06	0.344482	-2.90291	9130422GC	8.52E-08	2	2
PP11R	0.000186213	0.344482	-2.90291	2810004N2	1.13E-06	2	2
2510015F01RIK	0.000255295	0.342696	-2.91804	B4GALNT2	0.002623	2	2
PARD6G	1.26E-07	0.327598	-3.05252	DNMT3B	1.05E-06	0.5	-2
NOTCH3	3.24E-06	0.327598	-3.05252	SCL000548	2.96E-06	0.5	-2
H2-T10	0.000761011	0.327598	-3.05252	LYT-2	2.32E-05	0.5	-2
LMAN2L	1.87E-07	0.327031	-3.05781	LBR	1.18E-05	0.499134	-2.00347
DTX1	2.93E-07	0.324772	-3.07908	6330406L2	5.22E-05	0.499134	-2.00347
TMEM108	2.25E-05	0.32421	-3.08442	MIER1	1.68E-08	0.498271	-2.00694
ETS1	5.90E-07	0.322529	-3.1005	1810020D1	2.21E-07	0.498271	-2.00694
SH2D1A	2.22E-06	0.320856	-3.11666	SLC9A9	4.02E-05	0.498271	-2.00694

9626100_15	0.00161165	0.314253	-3.18215	TCRG-V5	0.001068	0.498271	-2.00694
CD8B	3.35E-05	0.313166	-3.19319	BC035295	8.94E-08	0.497409	-2.01042
ACAS2L	7.23E-06	0.309927	-3.22657	LOC386192	0.004528	0.497409	-2.01042
LOC434197	1.33E-06	0.30566	-3.27161	ARHGEF11	2.19E-08	0.496547	-2.01391
9626100_224	0.00113435	0.305131	-3.27728	B230114J0	6.30E-07	0.496547	-2.01391
FRAT2	2.01E-06	0.302499	-3.3058	ARID1A	2.03E-06	0.496547	-2.01391
NRP	8.11E-07	0.299889	-3.33457	C030002B1	3.75E-05	0.496547	-2.01391
G22P1	8.46E-08	0.296273	-3.37526	E430013K1	3.08E-06	0.495688	-2.0174
RNPEPL1	4.01E-09	0.29576	-3.38112	A130022AC	4.53E-06	0.495688	-2.0174
9626958_317	0.00188407	0.293718	-3.40463	LOC269407	5.58E-06	0.495688	-2.0174
H19	0.000268847	0.283221	-3.53081	2700007B1	3.11E-05	0.495688	-2.0174
ACTN1	2.58E-07	0.278838	-3.58631	DDAH1	0.000139	0.495688	-2.0174
SLC16A5	3.62E-09	0.275476	-3.63008	HP	0.001812	0.495688	-2.0174
CD2	1.50E-06	0.275	-3.63637	DNCHC1	5.02E-06	0.494829	-2.0209
PRKCB	2.18E-07	0.272155	-3.67438	SPEC1	1.46E-05	0.493971	-2.02441
ST6GAL1	7.38E-08	0.268874	-3.71922	KCNH3	5.03E-08	0.492262	-2.03144
PRELP	1.65E-05	0.268408	-3.72567	LRMP	3.72E-06	0.492262	-2.03144
CDCA7	4.57E-05	0.267944	-3.73213	CAMK4	5.35E-08	0.49141	-2.03496
PDLIM4	4.93E-06	0.267016	-3.74509	1110001P0	2.50E-06	0.49141	-2.03496
CD6	1.61E-09	0.264713	-3.77768	COL15A1	7.73E-05	0.490559	-2.03849
ALDH2	7.40E-07	0.248704	-4.02085	E130307M0	3.42E-05	0.489711	-2.04202
CD81	6.28E-06	0.247414	-4.04181	NFE2	3.74E-05	0.489711	-2.04202
9430068D06RIK	3.23E-10	0.239816	-4.16986	ASB13	4.76E-07	0.48717	-2.05267
H2-BL	9.51E-06	0.232854	-4.29453	XLR4A	0.000619	0.48717	-2.05267
AI132321	1.19E-06	0.208772	-4.78991	LOC382020	0.001199	0.48717	-2.05267
LY6D	2.50E-08	0.184924	-5.40764	3110018A0	0.003534	0.48717	-2.05267
COX6A2	0.000397718	0.15822	-6.32033	BC020108	0.00042	0.486327	-2.05623
BCL11B	1.64E-08	0.150205	-6.65759	SOX9	0.001197	0.486327	-2.05623
LOC382896	6.81E-09	0.112267	-8.90737	CD5	2.42E-06	0.485486	-2.05979
				ZFP96	2.60E-05	0.485486	-2.05979
				AKAP8L	8.62E-07	0.484644	-2.06337
				5530400P0	1.11E-06	0.483805	-2.06695
				A430107D2	2.94E-06	0.483805	-2.06695
				0610012D1	7.81E-08	0.482968	-2.07053
				GALNT2	5.48E-07	0.482968	-2.07053
				EPPB9	2.51E-05	0.482968	-2.07053
				NSG2	8.56E-08	0.482132	-2.07412

DUSP10	4.51E-08	0.481297	-2.07772
9430080K1	3.61E-08	0.481297	-2.07772
RNASEN	2.84E-06	0.481297	-2.07772
GAS6	0.000311	0.481297	-2.07772
1810015C1	7.75E-09	0.480464	-2.08132
SLITL2	0.00045	0.480464	-2.08132
LOC386330	0.00292	0.480464	-2.08132
FKBP9	0.000505	0.479632	-2.08493
ZFPN1A1	8.59E-07	0.478801	-2.08855
DDX6	3.03E-07	0.477973	-2.09217
BACH1	1.88E-06	0.477973	-2.09217
TNNT1	0.000227	0.477973	-2.09217
BLK	2.09E-08	0.477145	-2.0958
MSCP	3.61E-07	0.477145	-2.0958
2900060B1	0.018802	0.477145	-2.0958
CNN3	2.16E-06	0.475495	-2.10307
REEP1	3.13E-08	0.474672	-2.10672
SDH1	4.36E-08	0.473028	-2.11404
PPARGC1E	9.21E-07	0.473028	-2.11404
TLK1	5.15E-07	0.473028	-2.11404
A630097DC	3.46E-05	0.47221	-2.1177
3110078MC	8.46E-07	0.471391	-2.12138
1110015K0	2.05E-06	0.470577	-2.12505
EXT1	5.14E-06	0.468949	-2.13243
FBLN2	1.48E-07	0.468136	-2.13613
1810018P1	4.02E-05	0.466516	-2.14355
DCAMKL2	1.02E-06	0.46571	-2.14726
PPT1	1.66E-06	0.46571	-2.14726
2810036L1	3.90E-05	0.46571	-2.14726
H2-EB1	0.004956	0.464902	-2.15099
2810470K0	6.54E-06	0.464097	-2.15472
RAG1	2.91E-05	0.463293	-2.15846
2610020H1	1.83E-07	0.462492	-2.1622
D10UCLA1	4.00E-05	0.461691	-2.16595
1110003A1	7.74E-07	0.460891	-2.16971
KCTD2	2.52E-05	0.460891	-2.16971
G630024G1	3.72E-08	0.459297	-2.17724

1700026B2	3.84E-06	0.458501	-2.18102
FAS	7.68E-09	0.457708	-2.1848
4933424M2	1.76E-07	0.457708	-2.1848
4921518A0	4.47E-06	0.457708	-2.1848
IGTP	0.001511	0.457708	-2.1848
9430068D0	6.51E-08	0.456915	-2.18859
A930005H1	1.37E-07	0.456915	-2.18859
ABCA3	2.04E-07	0.455334	-2.19619
5330403D1	3.86E-07	0.455334	-2.19619
4631427C1	9.36E-07	0.455334	-2.19619
TRIM28	2.42E-05	0.454548	-2.19999
CERK	1.15E-05	0.454548	-2.19999
CRYL1	7.94E-07	0.45376	-2.20381
IL7R	1.25E-08	0.452974	-2.20763
IHPK1	4.52E-07	0.452974	-2.20763
RENBP	1.68E-08	0.45219	-2.21146
TPST1	1.05E-05	0.449845	-2.22299
9430029L2	9.20E-09	0.448288	-2.23071
5730593F1	3.51E-06	0.448288	-2.23071
C530015C	1.57E-08	0.446738	-2.23845
HMG2	0.000104	0.446738	-2.23845
TRAF4	8.39E-08	0.445965	-2.24233
AXIN2	2.23E-09	0.445192	-2.24622
BCL7A	5.46E-07	0.445192	-2.24622
A630082K2	7.65E-08	0.444421	-2.25012
TNRC6C	1.44E-07	0.444421	-2.25012
PCOLCE	0.00026	0.443652	-2.25402
PRICKLE1	6.89E-07	0.442884	-2.25793
BCL6	1.24E-05	0.442884	-2.25793
COL2A1	3.25E-05	0.442118	-2.26184
MRPL14	5.42E-07	0.441351	-2.26577
ZFP148	8.82E-07	0.440587	-2.2697
CNOT2	1.44E-07	0.439825	-2.27363
C230075L1	1.84E-07	0.439063	-2.27758
2700083E1	2.52E-07	0.439063	-2.27758
CCND1	1.92E-05	0.438302	-2.28153
CUTL1	8.66E-08	0.437545	-2.28548

AI467606	5.41E-07	0.43603	-2.29342
GMFG	7.47E-05	0.43603	-2.29342
GLDC	0.000565	0.43603	-2.29342
CNP1	1.01E-07	0.435275	-2.2974
RBM38	2.02E-08	0.434522	-2.30138
BC039093	2.61E-06	0.434522	-2.30138
6.33E+19	2.02E-05	0.434522	-2.30138
SCARA3	5.87E-05	0.434522	-2.30138
FKBP5	3.81E-07	0.43377	-2.30537
BC063749	1.34E-09	0.433019	-2.30937
LOC226131	0.000315	0.433019	-2.30937
AFF1	5.19E-07	0.432268	-2.31338
COL4A1	3.11E-05	0.430028	-2.32543
COL6A3	0.001678	0.430028	-2.32543
VAMP4	4.17E-07	0.429282	-2.32947
NUP210	0.0001	0.428539	-2.33351
ADCY6	1.78E-07	0.427798	-2.33755
UHRF1	0.000152	0.427798	-2.33755
PTPRS	3.83E-07	0.427057	-2.34161
LBH	5.98E-05	0.426317	-2.34567
SCML4	1.21E-07	0.425579	-2.34974
1700095N2	2.00E-07	0.425579	-2.34974
5930416I1C	4.45E-07	0.425579	-2.34974
SEMA4B	1.98E-06	0.425579	-2.34974
SCA2	6.05E-07	0.424843	-2.35381
5830431A1	2.60E-06	0.424843	-2.35381
MSH6	0.000132	0.424843	-2.35381
TTC3	5.71E-09	0.421907	-2.37019
KCTD1	1.30E-06	0.421907	-2.37019
BC028975	1.19E-08	0.421177	-2.3743
GPSM1	2.16E-06	0.421177	-2.3743
ERICH1	3.26E-08	0.420449	-2.37841
GATA3	6.03E-07	0.420449	-2.37841
TTYH3	4.09E-06	0.420449	-2.37841
H2-OB	6.36E-06	0.420449	-2.37841
BHLHB9	1.72E-05	0.420449	-2.37841
AW046396	0.001335	0.420449	-2.37841

4632417D2	5.33E-07	0.417544	-2.39496
PDLIM1	8.32E-07	0.417544	-2.39496
1810010N1	1.37E-06	0.416821	-2.39911
CHRNA9	1.78E-09	0.4161	-2.40327
GSTM2	0.0004	0.415379	-2.40744
SCL000121	6.07E-06	0.413942	-2.4158
MNS1	0.000532	0.413942	-2.4158
GABABRB1	3.45E-05	0.412509	-2.42419
ANP32E	3.77E-05	0.411083	-2.4326
SMARCD2	6.84E-06	0.404021	-2.47512
CASP6	6.84E-07	0.40332	-2.47942
LTAP	3.13E-08	0.400535	-2.49666
EFEMP2	8.18E-05	0.399842	-2.50099
4932408F1	3.03E-07	0.398459	-2.50967
CD1D1	9.54E-07	0.398459	-2.50967
SH2D1A	1.27E-05	0.398459	-2.50967
ADRB2	1.53E-08	0.397768	-2.51403
6330403E0	2.81E-07	0.397079	-2.51839
C230082I2	1.32E-09	0.396393	-2.52275
FBXL12	3.35E-06	0.395021	-2.53151
SMO	3.82E-09	0.394337	-2.5359
6720469N1	1.55E-07	0.393654	-2.5403
ZFPN1A2	1.20E-07	0.392972	-2.54471
PHF2	2.68E-07	0.392972	-2.54471
LIP1	8.34E-07	0.392972	-2.54471
IFNGR1	1.21E-07	0.392292	-2.54912
SPATA13	1.64E-07	0.391613	-2.55354
NEDD4L	4.00E-09	0.390935	-2.55797
SLA	4.00E-05	0.390935	-2.55797
ARHGEF18	2.56E-05	0.390935	-2.55797
RASGRP1	7.85E-08	0.390258	-2.56241
NOTCH1	2.02E-08	0.388235	-2.57576
2900016B0	6.34E-09	0.387562	-2.58023
PITPNM2	1.79E-07	0.386891	-2.58471
SMAD3	2.00E-06	0.385553	-2.59368
CHDH	1.11E-07	0.383553	-2.6072
C920011N1	5.34E-06	0.383553	-2.6072

NISCH	5.43E-07	0.382889	-2.61172
2310007GC	1.06E-06	0.382889	-2.61172
SIT1	3.76E-09	0.382226	-2.61625
SLC29A3	7.22E-07	0.380904	-2.62533
AEBP1	0.000162	0.380904	-2.62533
C730009F2	9.48E-09	0.379586	-2.63445
PLEKHG2	9.65E-07	0.379586	-2.63445
MBP	2.65E-08	0.378273	-2.64359
D8ERTD32	9.64E-06	0.378273	-2.64359
VPS54	4.16E-08	0.377618	-2.64818
MLL	2.80E-07	0.377618	-2.64818
LOC386144	4.21E-05	0.377618	-2.64818
LOC386360	0.000404	0.377618	-2.64818
BACH2	0.000136	0.376964	-2.65277
BDH	2.28E-10	0.375009	-2.6666
KLHL6	2.22E-08	0.375009	-2.6666
DAP3	1.93E-08	0.373712	-2.67586
TCRB-V8.2	8.04E-08	0.373712	-2.67586
A130062D1	1.07E-07	0.373712	-2.67586
SSBP3	1.03E-07	0.373712	-2.67586
MAPK1	5.13E-08	0.37242	-2.68514
FRMD6	3.31E-08	0.371775	-2.6898
TNFRSF13	6.85E-08	0.371775	-2.6898
MMP2	0.000109	0.371775	-2.6898
ECM1	1.84E-07	0.371131	-2.69447
CUL7	2.80E-07	0.366021	-2.73208
NOTCH3	7.70E-06	0.366021	-2.73208
D930015EC	2.19E-07	0.365388	-2.73682
A430106G7	1.00E-06	0.364755	-2.74157
5830468F0	5.09E-06	0.364124	-2.74632
HIBADH	1.23E-08	0.363494	-2.75108
TMEM9	4.73E-07	0.362236	-2.76063
TSPAN32	8.74E-07	0.35663	-2.80403
H2-T9	4.22E-05	0.35663	-2.80403
ESM1	0.001321	0.356013	-2.80889
ALOX5AP	1.28E-07	0.355396	-2.81376
RFX2	1.13E-06	0.355396	-2.81376

2610019F0	3.33E-06	0.354781	-2.81864
WHRN	4.89E-07	0.353553	-2.82843
5830496L1	1.90E-07	0.352942	-2.83333
GSTP1	7.09E-07	0.352942	-2.83333
3100002J2:	3.91E-07	0.35233	-2.83825
YPEL3	0.000133	0.351111	-2.8481
A130092J0	3.76E-06	0.350503	-2.85304
IGSF3	5.35E-07	0.34929	-2.86295
HDAC7A	1.07E-06	0.344482	-2.90291
IDB3	1.63E-07	0.343886	-2.90794
OLFML3	6.69E-07	0.34329	-2.91299
6430510MC	1.07E-07	0.342696	-2.91804
TRBV13-1_	1.50E-05	0.34151	-2.92817
CD97	2.26E-05	0.33974	-2.94343
MTF2	1.12E-06	0.337977	-2.95878
PLA2G12A	1.72E-08	0.336225	-2.9742
D15WSU7E	2.04E-06	0.336225	-2.9742
ETHE1	1.66E-08	0.334482	-2.9897
HIVEP3	3.41E-09	0.333903	-2.99488
CYB5	3.77E-08	0.333903	-2.99488
CTSE	0.149884	0.333324	-3.00008
ZFP219	2.26E-07	0.329877	-3.03143
ABHD8	1.69E-06	0.329877	-3.03143
4732481H1	8.63E-07	0.329306	-3.03669
PRNP	3.14E-05	0.328735	-3.04196
A630038E1	0.000216	0.328735	-3.04196
A930013B1	8.09E-08	0.325336	-3.07375
ETS1	5.90E-07	0.322529	-3.1005
LOC38508E	0.001044	0.322529	-3.1005
RNPEPL1	7.60E-09	0.32197	-3.10588
KLF13	6.51E-07	0.321413	-3.11126
KCNN4	1.98E-06	0.320856	-3.11666
NIPSNAP1	1.39E-06	0.320856	-3.11666
C920004C	0.000563	0.320856	-3.11666
TRBV7_AE	6.95E-05	0.319746	-3.12748
SLC43A1	3.64E-08	0.316439	-3.16017
STK4	7.89E-07	0.315891	-3.16565

WISP2	1.27E-05	0.312624	-3.19873
ACTN2	3.36E-07	0.310465	-3.22098
EPB4.1L4B	4.42E-07	0.310465	-3.22098
RNF144	2.74E-09	0.308855	-3.23777
SCL000184	1.73E-05	0.307786	-3.24901
ART4	6.83E-07	0.306191	-3.26594
18S_RRNA	0.00445	0.299889	-3.33457
A330103N2	1.65E-06	0.29937	-3.34035
TPCN1	2.60E-09	0.298851	-3.34615
AJ237586	1.97E-07	0.298334	-3.35195
BC026370	6.26E-09	0.29576	-3.38112
EPHX1	4.14E-09	0.295248	-3.38698
COL5A1	0.000124	0.293718	-3.40463
SNN	1.47E-08	0.292701	-3.41645
BCL9L	1.00E-08	0.292194	-3.42238
0710008K0	9.65E-08	0.291688	-3.42832
F730003HC	0.00011	0.289674	-3.45216
A1504432	2.49E-08	0.287175	-3.4822
OACT1	9.74E-09	0.286678	-3.48824
A130093I2	1.16E-06	0.285191	-3.50642
RGS10	2.26E-05	0.284698	-3.5125
1110046J11	3.46E-06	0.284204	-3.5186
E2F2	2.29E-06	0.278355	-3.59253
BRD3	3.58E-07	0.277873	-3.59876
AA408556	4.12E-06	0.272627	-3.66802
SATB1	1.49E-07	0.270744	-3.69353
ILVBL	3.59E-07	0.270744	-3.69353
TIAM1	1.97E-09	0.268874	-3.71922
POU6F1	2.59E-08	0.268874	-3.71922
MAGED1	1.17E-05	0.268874	-3.71922
1810055GC	1.69E-09	0.266554	-3.75158
0710001E1	6.72E-10	0.264713	-3.77768
LMAN2L	4.14E-08	0.264713	-3.77768
SLC29A1	1.20E-07	0.264255	-3.78423
3830612M2	2.98E-07	0.263797	-3.79079
H2-T10	0.000217	0.263797	-3.79079
CXCR4	4.41E-08	0.26334	-3.79737

RIL-PENDI	2.35E-08	0.262429	-3.81055
SERPINH1	3.41E-05	0.262429	-3.81055
PALM	2.59E-09	0.261975	-3.81716
CXCL12	0.000158	0.261069	-3.83041
5430417L2	1.68E-08	0.260616	-3.83706
TRIB2	4.82E-08	0.260165	-3.84371
ETS2	5.78E-08	0.260165	-3.84371
ALDH2	9.48E-07	0.258816	-3.86375
HMGN1	3.20E-05	0.257028	-3.89062
TRP53INP	4.08E-08	0.255696	-3.9109
ITPR2	5.70E-08	0.25393	-3.9381
TCRB	8.36E-06	0.25349	-3.94493
A930023F0	4.58E-09	0.247843	-4.03481
SLC5A9	1.20E-06	0.246986	-4.04882
ICAM2	2.53E-07	0.246558	-4.05584
H2-DMA	1.25E-05	0.246558	-4.05584
4932414K1	3.75E-08	0.244431	-4.09113
TAP2	9.85E-09	0.243585	-4.10534
TRBV12-2_	3.25E-05	0.243585	-4.10534
PRELP	8.99E-06	0.242323	-4.12673
TRBV12-1_	1.47E-06	0.241066	-4.14824
LOX	8.44E-06	0.240232	-4.16264
1500004A0	1.03E-07	0.239816	-4.16986
6720418B0	4.27E-08	0.238572	-4.1916
4930572J0	4.75E-07	0.236925	-4.22075
SCL00010	7.57E-06	0.236925	-4.22075
PSAP	4.23E-08	0.236105	-4.2354
ASS1	5.82E-08	0.235696	-4.24275
PAR6G	1.30E-08	0.235288	-4.25011
1500009L1	9.73E-07	0.232451	-4.30198
GM2A	2.89E-06	0.231246	-4.3244
LAT	5.46E-08	0.230846	-4.3319
C3	9.90E-06	0.230846	-4.3319
PPAP2B	1.69E-05	0.230446	-4.33941
CTLA4	5.06E-06	0.230446	-4.33941
FBP1	5.98E-05	0.228458	-4.37717
B3BP	1.28E-10	0.224533	-4.45369

PRKCB	6.59E-08	0.224533	-4.45369
PPP1R1C	3.85E-09	0.220676	-4.53154
RAPGEF3	6.21E-10	0.219532	-4.55515
BAMBI-PS	7.87E-08	0.219151	-4.56306
1700012H1	5.26E-09	0.218393	-4.5789
ACVR2B	3.12E-10	0.218015	-4.58684
18S_RRNA	0.000603	0.215386	-4.64282
SERPINF1	1.43E-05	0.214642	-4.65893
NAV1	4.40E-08	0.21427	-4.66701
TBXA2R	3.11E-08	0.213528	-4.68322
SCL000113	1.63E-05	0.20733	-4.82323
SOX4	1.93E-09	0.205541	-4.8652
E430021E2	3.57E-07	0.204476	-4.89056
LOC381736	2.02E-08	0.203063	-4.92458
CD6	3.02E-10	0.200963	-4.97605
H2-OA	1.09E-07	0.198884	-5.02805
LOC384370	7.41E-06	0.197853	-5.05426
ZDHHC8	3.73E-09	0.19751	-5.06303
AI481316	1.75E-09	0.196827	-5.0806
H2-BL	3.80E-06	0.196146	-5.09824
AA407270	7.17E-09	0.195467	-5.11594
ITGAE	6.39E-06	0.195129	-5.12482
GPR83	1.37E-07	0.194791	-5.1337
SBK	4.54E-10	0.18783	-5.32396
RPS6KL1	1.75E-09	0.187505	-5.33319
TCF7	8.08E-08	0.183965	-5.43583
NRP	4.24E-08	0.183646	-5.44526
DNAJC6	3.58E-11	0.182694	-5.47364
SCL000105	3.66E-09	0.182694	-5.47364
SCL000113	1.31E-06	0.179245	-5.57897
IL17RB	1.94E-09	0.178006	-5.61778
ACAS2L	2.63E-07	0.17647	-5.66667
AKR1C12	8.40E-09	0.176165	-5.67649
COL6A1	3.56E-05	0.174645	-5.72589
SOCS3	3.74E-08	0.172839	-5.78573
LDH2	1.01E-07	0.172839	-5.78573
DGKA	6.54E-07	0.172839	-5.78573

GM525	1.28E-07	0.17254	-5.79577
TIMP2	2.00E-08	0.172241	-5.80582
AQP11	3.40E-09	0.170459	-5.8665
TRBV6_AE	5.66E-08	0.166951	-5.98977
TNFRSF7	9.20E-08	0.161544	-6.19026
CD2	7.22E-08	0.15932	-6.27667
DTX1	3.94E-09	0.158769	-6.29846
AI875142	2.49E-07	0.157127	-6.36429
IGFBP4	1.57E-08	0.155771	-6.41967
SH3KBP1	2.13E-10	0.154964	-6.45313
2510015F0	3.11E-06	0.153627	-6.50929
TRBV11_AI	2.50E-08	0.151511	-6.60016
SLC16A5	1.12E-10	0.148651	-6.72717
TUBB2B	4.82E-08	0.148137	-6.75053
DNTT	7.39E-07	0.14534	-6.88044
SYTL1	6.70E-08	0.143091	-6.98858
2410008J0	2.59E-09	0.137262	-7.28536
0610041GC	9.40E-06	0.137024	-7.29799
2210408F1	2.70E-08	0.135138	-7.39987
LOC38654	2.77E-05	0.131215	-7.6211
TRBV31_X	4.97E-06	0.129184	-7.74089
TCRB-V8.3	1.15E-08	0.128292	-7.79473
KLF2	3.06E-06	0.125434	-7.97232
TCRB-V13	5.74E-08	0.124352	-8.0417
A130038J1	8.77E-09	0.117848	-8.4855
LOC38173	1.87E-09	0.117237	-8.52973
G22P1	5.44E-10	0.115823	-8.63383
CD27	4.55E-08	0.113834	-8.78474
TMEM108	8.61E-08	0.112656	-8.87656
ACTN1	2.20E-09	0.110913	-9.01608
ST6GAL1	6.69E-10	0.106579	-9.38268
9626100_1	1.11E-05	0.103485	-9.66319
9626100_2	8.13E-06	0.10118	-9.88335
C030046M	1.45E-12	0.101005	-9.90049
SELL	6.85E-09	0.099442	-10.0561
COX6A2	7.37E-05	0.098755	-10.1261
FRAT2	6.49E-09	0.098414	-10.1612

LY6D	1.48E-09	0.097903	-10.2142
9130430L1	2.71E-10	0.092782	-10.7779
CDCA7	3.37E-07	0.092142	-10.8528
LOC382896	3.09E-09	0.091506	-10.9283
CD8B	7.37E-08	0.089934	-11.1193
E430002DC	2.09E-10	0.089312	-11.1967
TRGV2_M1	2.57E-11	0.08657	-11.5514
PP11R	2.12E-07	0.086419	-11.5715
CD81	4.58E-08	0.083187	-12.0211
IGH-6	8.08E-09	0.082899	-12.0629
AI132321	2.09E-08	0.082042	-12.1889
9626958_3	8.03E-06	0.077214	-12.9511
TRBV8_AE	9.31E-08	0.076947	-12.996
MGST2	3.44E-09	0.074197	-13.4777
RAMP1	5.23E-08	0.072043	-13.8806
NCK2	3.02E-08	0.068631	-14.5707
MARCKS	1.18E-09	0.065721	-15.2158
DPP4	2.19E-10	0.056426	-17.7224
TRBV1_AE	6.96E-07	0.056036	-17.8456
H19	3.39E-07	0.055745	-17.9387
TCRG-V4	3.97E-09	0.051296	-19.4946
1190002H2	4.58E-10	0.050241	-19.9042
BCL11B	2.77E-10	0.049549	-20.182
CD3G	8.20E-11	0.046472	-21.5184
BGN	3.71E-07	0.039692	-25.1939
CD3D	1.53E-09	0.034976	-28.5912
CD3E	7.19E-10	0.031907	-31.3414
LOC434197	5.40E-11	0.02356	-42.4443
MYLC2PL	8.10E-10	0.017039	-58.6883
PDLIM4	8.76E-11	0.009786	-102.182

Table 4. Comparison of cell surface receptor repertoires of ITNKs and LAKs.

Cell Type	Ly49C/I	Ly49D	Ly49G2	NK1.1	NKp46	NKG2A/C/E	NKG2D	CD3
DN3-reprogrammed ITNK (in vitro)	-	-	-	+	+	+	-	-
DP-reprogrammed ITNK (in vitro)	-	-	-	+	+	+	ND	+
DP-reprogrammed ITNK (in vivo)	+	-	+	+	+	+	+	low
LAK	+	+	+	+	+	+	+	-

Note: N.D., not determined. +, present; -, absent; low, low levels.